

UC San Diego

UC San Diego Electronic Theses and Dissertations

Title

Topics in Effective Field Theory

Permalink

<https://escholarship.org/uc/item/4qx9x2f7>

Author

Chang, Hsi-Ming

Publication Date

2015

Peer reviewed|Thesis/dissertation

UNIVERSITY OF CALIFORNIA, SAN DIEGO

Topics in Effective Field Theory

A dissertation submitted in partial satisfaction of the requirements for the degree
Doctor of Philosophy

in

Physics

by

Hsi-Ming Chang

Committee in charge:

Professor Aneesh Manohar, Chair
Professor Benjamín Grinstein
Professor Jeffrey Rabin
Professor Justin Roberts
Professor Frank Wuerthwein

2015

Copyright
Hsi-Ming Chang, 2015
All rights reserved.

The Dissertation of Hsi-Ming Chang is approved, and
it is acceptable in quality and form for publication on
microfilm and electronically:

Chair

University of California, San Diego

2015

TABLE OF CONTENTS

Signature Page	iii
Table of Contents	iv
List of Figures	vi
List of Tables	ix
Acknowledgements	x
Vita	xii
Abstract of the Dissertation	xiii
Chapter 1 Introduction	1
1.1 Lightning Review of the Development of the Standard Model	2
1.2 Brief Introduction to Effective Field Theory	5
1.3 Outline of Dissertation	7
Chapter 2 Double Parton Correlations in the Bag Model	10
2.1 Introduction	10
2.2 Calculation	13
2.2.1 Single PDF	16
2.2.2 Double PDF	18
2.2.3 Spin Correlations	19
2.2.4 Rigid Bag	21
2.2.5 Normalization	22
2.3 Parton Correlations	25
2.4 Conclusions	28
Chapter 3 Calculating Track-Based Observables for the LHC	29
3.1 Introduction	30
3.2 Definition of Track Function	30
3.3 NLO Track Function	35
3.4 Application to Higgs Plus One Jet	38
3.5 Conclusions	39
Chapter 4 Calculating Track Thrust with Track Functions	41
4.1 Introduction	42
4.2 Summary of Results	44
4.3 Review of Track Function Formalism	50
4.4 Fixed Order Analysis of Track Thrust	56

4.5	Factorization and Resummation of Track Thrust	58
4.5.1	Hard Function	61
4.5.2	Soft Function	62
4.5.3	Leading Power Correction	63
4.5.4	Jet Function	66
4.5.5	Resummation	68
4.5.6	Non-Singular Contribution	70
4.6	Simplifications at NLL	71
4.7	Numerical Results	73
4.8	Discussion	77
Chapter 5 Renormalization Group Evolution of Dimension-Six Baryon Number Violating Operators		80
5.1	Introduction	80
5.2	Results	83
5.3	Discussion	89
5.3.1	Minimal Flavor Violation	89
5.3.2	Grand Unified Theories	90
5.3.3	Magnitude of Effects	92
5.4	Conclusions	93
Chapter 6 Non-Standard Semileptonic Hyperon Decays		95
6.1	Introduction	95
6.2	The SM Effective Field Theory	97
6.3	Semileptonic Hyperon Decays	98
6.4	Bounds on Scalar and Tensor Operators	101
6.5	Limits from LHC Data	104
6.6	Conclusions and Outlook	105
Appendix A Bag Model Wave Function in Momentum Space		107
Appendix B Relationship between the dPDFs \mathcal{F} and F		109
Appendix C Resummation		110
Appendix D Profile Functions		113
Appendix E Plus Distributions		115
Appendix F Operator Relations and Custodial Symmetry		116
Bibliography		118

LIST OF FIGURES

Figure 2.1: The proton PDFs u (solid red), Δu (dashed blue) and δu (dotted green).	17
Figure 2.2: Plot of the PY factors which enter the calculation of the single PDF (dotted blue) and double PDF (solid red). They suppress the PDFs in the unphysical regions $x > 1$ and $x < 0$	21
Figure 2.3: Plot of the bag model proton PDF $u(x)$ with (solid red) and without (dotted blue) PY factors.	22
Figure 2.4: The double PDF $uu(x_1, x_2, \mathbf{k}_\perp)$ as a function of x_1 and $ \mathbf{k}_\perp $ for fixed $x_2 = 0.4$. The right panel tests the ansatz in Eq. (2.2) that x_i and \mathbf{k}_\perp are uncorrelated. This holds reasonably well, since the different $ \mathbf{k}_\perp $ curves are nearly identical.	22
Figure 2.5: The double PDF $uu(x_1, x_2, \mathbf{k}_\perp)$ as a function of x_1 and x_2 for fixed $\mathbf{k}_\perp = 0$. In the right panel, we divide by $u(x_2)$ to test the often-used assumption in Eq. (2.3) that the x_i are uncorrelated. This clearly fails, since the ratio depends strongly on x_2	23
Figure 2.6: The correlation between the momentum fractions of two u quarks in the proton is shown by plotting the ratio of the double PDF $uu(x_1, x_2, \mathbf{k}_\perp = 0)$ to the product of two single PDFs $u(x_1)u(x_2)$	24
Figure 2.7: Comparison of the double PDF spin structures as functions of x_1 or $ \mathbf{k}_\perp $, keeping the other variables fixed. The left panels show the uu double PDFs, and the right panels show the ud double PDFs. The $u\delta u$, $\delta u\delta u$, $\delta u\delta u^t$, $\Delta u\Delta d$, $u\delta d$ and $\delta u\delta d^t$ distributions are negative, and we have changed their sign in these plots.	26
Figure 3.1: Schematic relationship between the partonic matrix element σ_3 and the matching coefficient $\bar{\sigma}_3$ for $e^+e^- \rightarrow q\bar{q}g$. Here, black (blue) dots represent the tree-level ($\mathcal{O}(\alpha_s)$) track functions. Diagrams with emissions from the other quark leg are elided for simplicity. Note the trivial matching condition $\sigma_2 = \bar{\sigma}_2$	32
Figure 3.2: LO (dotted) and NLO (solid) track functions extracted in PYTHIA from the fraction of the jet energy carried by charged particles.	33
Figure 3.3: The evolution of the NLO gluon (top) and d -quark (bottom) track functions compared to PYTHIA. Starting from $\mu = 100$ GeV (shown in Fig. 3.2), we evolve using Eq. (3.6) down to $\mu = 10$ GeV and up to $\mu = 1000$ GeV.	34
Figure 3.4: Normalized distribution of the energy fraction w of charged particles in e^+e^- at $Q = 91$ GeV, calculated at LO (green) and NLO (orange), compared with PYTHIA (blue). The uncertainty bands are obtained by varying μ between $Q/2$ and $2Q$, and do not include track function uncertainties.	37
Figure 3.5: Track mass distribution in $pp \rightarrow H + \text{jet}$ obtained from the PYTHIA parton shower matched onto either track functions or the Lund string model.	39
Figure 3.6: Comparison between track and calorimeter measurements of ratio of jet mass and jet p_T . Here the cuts are on \bar{p}_T^J and $\bar{\eta}_J$ from the tracks in the jet.	40

Figure 4.1: Illustration of the track thrust measurement in an e^+e^- event with jets initiated by a $q\bar{q}$ pair. Solid lines indicate charged particles and dashed lines indicate neutral particles. For track thrust, the thrust axis \hat{t} is determined by the charged particles alone.	45
Figure 4.2: ALEPH (top) and DELPHI (bottom) measurements of calorimeter and track thrust. Error bars correspond to the statistical and systematic uncertainties added in quadrature. The experimental uncertainties associated with the track-based measurements are noticeably smaller.	47
Figure 4.3: Top: NLL' distributions for calorimeter and track thrust including the leading non-perturbative correction Ω_1^τ . Bottom: comparing our analytic results to the DELPHI measurement. There is good quantitative agreement in the tail region where our NLL' calculation is most accurate.	48
Figure 4.4: Perturbative QCD calculation of the quark (top) and gluon (middle and bottom) track functions at NLO from Eqs. (4.11) and (4.12) with partonic intermediate states. The NLO track function gets contributions from both branches of the collinear splitting.	53
Figure 4.5: Distributions for calorimeter and track thrust from Eq. (4.21) at $\mathcal{O}(\alpha_s)$. The NLO track functions are extracted from PYTHIA 8.150 [1, 2] using the procedure in Ref. [3].	57
Figure 4.6: Distributions for calorimeter and track thrust using dummy track functions. Comparing to Fig. 4.5, we conclude that the similarity between τ and $\bar{\tau}$ is due to the specific form of the track function.	58
Figure 4.7: Non-singular contribution to the normalized cumulative thrust distribution at $\mathcal{O}(\alpha_s)$. The central value corresponds to $\mu = M_Z$, with the uncertainty bands from varying $\mu \in [M_Z/2, 2M_Z]$	70
Figure 4.8: Track thrust and calorimeter thrust at NLL. As explained in Sec. 4.6, these distributions are remarkably similar.	74
Figure 4.9: Track thrust distribution going from NLL to NLL'. The bands encode perturbative uncertainties from RG scale variations, but not uncertainties in α_s or the track functions themselves.	75
Figure 4.10: Track thrust distribution in the tail and far-tail regions, illustrating the effect of including the non-singular contribution at NLL' order. The full NLL' distribution interpolates between the resummed and fixed-order results.	75
Figure 4.11: Track thrust at NLL' adding the leading power correction.	76
Figure 4.12: Comparison of analytical predictions with DELPHI data for both track and calorimeter thrust distributions. There is good qualitative and quantitative agreement in the tail region, though as shown in Fig. 4.3, the theoretical uncertainties at NLL' are larger than the experimental ones.	77
Figure 4.13: Calorimeter and track thrust distributions obtained from PYTHIA 8. Apart from deviations in the peak region due to higher-order non-perturbative corrections, these agree well with our NLL' calculation after the leading power correction is included (compare to Fig. 4.3).	78

Figure 5.1: The one-loop Yukawa renormalization graph. 83

Figure 6.1: 90% CL constraints on $\epsilon_{S,T}$ at $\mu = 2$ GeV from the measurements of $R^{\mu e}$ in different channels (dot-dashed lines) and combined (filled ellipse). LHC bounds obtained from CMS data at $\sqrt{s} = 8$ TeV (7 TeV) are represented by the black solid (dashed) ellipse. 104

LIST OF TABLES

Table 5.1: Flavor representations of the BNV operators, and their dimensions. There are 273 operators in Eq. (5.1) and 135 in Eq. (5.2), for a total of 408 $\Delta B = 1$ operators with complex coefficients. One coefficient can be made real by a phase rotation of fields proportional to baryon number.	87
Table 6.1: Comparison between the predictions of $R^{\mu e}$ in the SM at NLO and experimental measurements for different SHD.	101
Table 6.2: SHD data for $g_1(0)/f_1(0)$ and theoretical determinations of $f_{S,T}(0)/f_1(0)$ at $\mu = 2$ GeV used in this work. The corresponding $r_{S,T}$ are shown in the last two lines.	103

ACKNOWLEDGEMENTS

I would not have been able to finish this dissertation without many people’s help and support. First and foremost, I would like to thank my advisor Aneesh for his continuous support. Aneesh is undoubtedly a great teacher, and I have learned a lot from him. Besides Aneesh, I would like to express my sincere gratitude to all my committee members: Professor Ben Grinstein, Professor Jeff Rabin, Professor Justin Roberts, and Professor Frank Wuerthwein, for their patience and encouragement. Thanks also go to the postdocs I have been working with: Dr. Wouter Waalewijn, Dr. Rodrigo Alonso, and Dr. Jorge Camalich. I learned a lot of interesting details in the advanced topics in particle physics from them. I thank my officemate, Brian Shotwell, for the enlightening discussions and all the fun we have had. I thank my family for supporting all my decisions and my life in general.

I must make some technical acknowledgements at this point regarding publications that have been used in this dissertation. Chapter 2, Appendix A and Appendix B are a reprint of the material as it appears in “Double Parton Correlations in the Bag Model,” H.-M. Chang, A. V. Manohar and W. J. Waalewijn, Phys. Rev. D **87**, no. 3, 034009 (2013) [arXiv:1211.3132 [hep-ph]]. Chapter 3 is a reprint of the material as it appears in “Calculating Track-Based Observables for the LHC,” H.-M. Chang, M. Procura, J. Thaler and W. J. Waalewijn, Phys. Rev. Lett. **111**, 102002 (2013) [arXiv:1303.6637 [hep-ph]]. Chapter 4, Appendix C, Appendix D, and Appendix E are a reprint of the material as it appears in “Calculating Track Thrust with Track Functions,” H.-M. Chang, M. Procura, J. Thaler and W. J. Waalewijn, Phys. Rev. D **88**, 034030 (2013) [arXiv:1306.6630 [hep-ph]]. Chapter 5 and Appendix F are a reprint of the material as it appears in “Renormalization Group Evolution of Dimension-Six Baryon Number Violating Operators,” R. Alonso, H.-M. Chang, E. E. Jenkins, A. V. Manohar and B. Shotwell, Phys. Lett. B **734**, 302 (2014) [arXiv:1405.0486 [hep-ph]]. Chapter 6 is a reprint of the material as it appears in “Nonstandard Semileptonic Hyperon Decays,” H.-M. Chang, M. González-Alonso and J. M. Camalich, Phys. Rev. Lett. **114**, no. 16, 161802 (2015) [arXiv:1412.8484 [hep-ph]].

I was a co-author in all of these papers. All work was supported in part by Department of Energy contracts DE-SC0009919.

VITA

2004	B. S. in Physics, National Tsing Hua University, Hsinchu, Taiwan
2006	M. S. in Physics, National Taiwan University, Taipei, Taiwan
2010-2015	Teaching and Research Assistant, University of California, San Diego
2014	Candidate in Philosophy in Physics, University of California, San Diego
2015	Ph.D. in Physics, University of California, San Diego

PUBLICATIONS

H.-M. Chang, A. V. Manohar and W. J. Waalewijn, “Double Parton Correlations in the Bag Model,” Phys. Rev. D **87**, no. 3, 034009 (2013) [arXiv:1211.3132 [hep-ph]].

H.-M. Chang, M. Procura, J. Thaler and W. J. Waalewijn, “Calculating Track-Based Observables for the LHC,” Phys. Rev. Lett. **111**, 102002 (2013) [arXiv:1303.6637 [hep-ph]].

H.-M. Chang, M. Procura, J. Thaler and W. J. Waalewijn, “Calculating Track Thrust with Track Functions,” Phys. Rev. D **88**, 034030 (2013) [arXiv:1306.6630 [hep-ph]].

R. Alonso, H.-M. Chang, E. E. Jenkins, A. V. Manohar and B. Shotwell, “Renormalization group evolution of dimension-six baryon number violating operators,” Phys. Lett. B **734**, 302 (2014) [arXiv:1405.0486 [hep-ph]].

H.-M. Chang, M. González-Alonso and J. M. Camalich, “Nonstandard Semileptonic Hyperon Decays,” Phys. Rev. Lett. **114**, 161802 (2015) [arXiv:1412.8484 [hep-ph]].

ABSTRACT OF THE DISSERTATION

Topics in Effective Field Theory

by

Hsi-Ming Chang

Doctor of Philosophy in Physics

University of California, San Diego, 2015

Professor Aneesh Manohar, Chair

This dissertation focuses on two aspects of high energy physics—quantum chromodynamics (QCD) and the effective field theory. On the QCD side, the double parton scattering has become an important background in new physics searches. Correlations in double parton distribution function including flavor, spin, momentum fractions, and transverse separation were studied using a proton bag model. Pile-up contamination also affects new physics searches. One way to suppress this effect is to use observables that depend only on charged particles. A non-perturbative object, the track function, was defined to deal with calculations that only involved charged particles. The track function formalism was applied to calculate the thrust with charged particles only. Then, the focus shifts to the effective field theory. Soft-collinear effective theory was used to resum the large logarithms in the thrust calculation. The one-loop anomalous dimension matrix for the dimension-six baryon number violating operators is computed. Lastly, the Standard Model effective theory was used to study the semileptonic hyperon decays.

Chapter 1

Introduction

Quantum electrodynamics (QED)¹ is a quantum field theory describing how light and matter interact at the subatomic level. The agreement between QED and experiments is within ten parts in a billion by comparing the measurement of the electron anomalous magnetic moment and the QED prediction. This beautiful theory has been the most precisely tested one in physics.

At the early development stage of QED in the 1930s, people encountered divergent quantities in perturbative calculations. Those divergences made QED lose its predictive power, thus rendering it unsatisfactory as a physical theory. In the late 1940s, Feynman, Schwinger, and Tomonaga independently discovered a method called “renormalization” to tame those infinities from QED computations. There are two steps in renormalization. First, we separate the infinite part and the finite remainder systematically by following some algorithm. Second, we redefine the parameters in the theory in such a way that the isolated infinite part gets absorbed by the redefined parameters. A theory is called renormalizable if only a finite number of parameters is needed for this task. Otherwise, the theory is called non-renormalizable.

Because of the huge success of QED, the renormalizability became a guiding principle for constructing any quantum field theory. People thought non-renormalizable

¹For the development history of QED, see Silvan Schweber, “QED and the Men Who Made It: Dyson, Feynman, Schwinger, and Tomonaga,” Princeton University Press (1994).

theories were internally inconsistent and had no predictive power, but this picture has changed dramatically thanks to the notion of effective field theory.

1.1 Lightning Review of the Development of the Standard Model

In 1932, Fermi—one of the co-founders of QED—published his “Quantum Theory of Radiation” in the *Review of Modern Physics* [4]. This article gave a transparent formulation of QED. It was very influential at the time. Fermi pointed out that for an electron to transit from one quantum state to another and emit a photon, it was better to think of the photon as being created right at the moment of the transition rather than pre-existing inside the electron. Quantum field theory is a suitable tool for studying processes such as electron transition where the particle number is not conserved. By applying the framework of quantum field theory to the weak interaction, Fermi proposed his theory for the β -decay. In his theory, the neutron was annihilated at some spacetime point, and a proton, electron, and neutrino were created at the same spacetime point. The neutrino was postulated by Pauli in 1930, and the neutron was just discovered by Chadwick in 1932. Fermi’s work “A Tentative Theory of Beta Rays” was rejected by the journal *Nature* in 1933, for it “contained speculations too remote from reality to be of interest to the reader.” Fermi then submitted the paper to Italian and German publications. Later the editors of *Nature* admitted this was the greatest blunder they had ever made [5]. Fermi’s theory worked well for energies much lower than $\mathcal{O}(100 \text{ GeV})$, but it was clear that the theory was incomplete. Due to unitarity, cross sections of the Fermi interaction should be no greater than $4\pi/E^2$, where E is the center-of-mass energy. However, calculations in Fermi’s theory show that the cross sections are proportional to E^2 . Thus, at a particular E , approximately 300 GeV, Fermi’s theory becomes inconsistent with unitarity. This is in addition to being a manifestly non-renormalizable theory, which, at the time, no one knew how to deal with the infinities present in such theories.

In search of a renormalizable theory for β -decay or the weak interaction, it would be nice to have a deeper understanding of why QED is renormalizable. The

renormalizability of QED is intimately tied to the principle of gauge invariance as we will explain. Ward showed with his famous identity that the infinities from QED were not completely independent of each other. Some of the infinities in QED are exactly the same, and this leads to the miracle of complete cancellation of ultraviolet divergences in QED. The Ward identity guarantees the renormalizability of QED, and this identity is rooted in the principle of gauge invariance. This principle of gauge invariance played an important role in the development of the Standard Model of particle physics.

As a graduate student, Chen-Ning Yang was fascinated by the beauty of gauge invariance. The $U(1)$ gauge group of QED implies not only the renormalizability as Ward had shown, but also the charge conservation and the existence of massless photons. Yang had been thinking about generalizing the principle of gauge invariance to describe isospin conservation in the strong interaction, but in vain.

In 1954, Yang and his colleague Mills proposed the idea of replacing the $U(1)$ gauge group in QED with $SU(2)$ for the strong interaction. With hindsight, we know that the importance of Yang-Mills theory cannot be overemphasized. It laid the foundation for modern theoretical particle physics. However, in the 1950s people did not pay much attention to the Yang-Mills theory because it predicted the existence of charged massless particles. Such particles were never found in nature.

The picture changed dramatically in the 1960s and 1970s. Physicists were able to overcome the obstacles Yang-Mills theory had presented. Glashow, Salam, and Weinberg were able to unify the weak interaction and electromagnetism with the $SU(2) \times U(1)$ type Yang-Mills theory. This work led them to the Nobel Prize in Physics in 1979. However, Weinberg's work "A Model of Leptons", published in 1967, did not initially pique many readers' interest. According to the INSPIRE database, Weinberg's paper had only 3 citations before 1971. In 1971, 't Hooft and Veltman proved the renormalizability of the massive Yang-Mills theory, and the Glashow-Weinberg-Salam electroweak theory is of this type. 't Hooft and Veltman shared the Nobel Prize in Physics in 1999 because of this work. Once the renormalizability of Glashow-Weinberg-Salam theory was proved, it caught everyone's attention.

On the strong interaction side, the gauge symmetry group is the color $SU(3)$ gauge group. This gauge theory is named quantum chromodynamics (QCD) with red, green, and blue color charges. The colors were initially introduced to solve the Fermi statistics problem in the Δ^{++} baryon. The Δ^{++} contains three up quarks in the quark model with their spins aligned in the same direction. This contradicts Pauli exclusion principle, which implies the three up quarks cannot be in the same quantum state. One way out is to assume there exists additional $SU(3)$ gauge degree of freedom, the color. The three up quarks in Δ^{++} then have different color charges, so they are no longer in the same quantum state. We need the color degree of freedom not only in the strong interaction, but also in the electroweak interaction. In order for the electroweak theory to be consistent, complete cancellation of anomalies between the lepton sector and the quark sector is required. This is only true when we have three differently-colored quark sectors.

In 1966, Bjorken proposed his famous scaling idea, later confirmed by experiments. It basically says that the high-energy hadron scattering experiment is scaled by the dimensionless scattering angle and some energy ratio, but not the absolute energy scale of the experiment. Since higher experiment energy implies higher experimental resolution, Bjorken scaling indicates there is no preferred scale for the experimental resolution. This in turn implies the structure inside the hadron is point-like. To explain this scaling behavior with quantum field theory, one requires the β -function to be negative. In quantum field theory, β -functions are functions that encode the information of how coupling parameters change when the energy scale changes. Back then, all the known theories, including QED, had positive β -functions. Gross was among those who thought it was impossible to have a negative β -function in any field theory. His original idea was to show that the β -function is positive in the $SU(3)$ Yang-Mills theory, so he could exclude the Yang-Mills theory from being the correct theory of the strong interaction. However, Politzer discovered that the β -function was indeed negative in the $SU(3)$ Yang-Mills theory. Gross and his student Wilczek also found this independently at around the same time. The 2004 Nobel Prize in Physics was awarded to Gross, Politzer, and Wilczek for

their contribution to the strong interaction theory.

The Glashow-Weinberg-Salam electroweak theory together with QCD is now known as the Standard Model of particle physics, with gauge symmetry group $SU(3) \times SU(2) \times U(1)$.

1.2 Brief Introduction to Effective Field Theory

Historically, Fermi's β -decay theory was proposed before the Glashow-Weinberg-Salam electroweak theory. With hindsight, we can treat Fermi's theory as a low-energy effective field theory derived from the more fundamental electroweak theory. The motivation of doing this is that sometimes we are only interested in the physics at low energy. If you use the complete theory, usually the calculation is cumbersome or even impossible. For example, if you want to study water as a fluid, you can start from water molecules and calculate the interactions among them. However, this is impractical. A more practical way is to use hydrodynamics, so you do not need to keep track of all the water molecules. In the Standard Model, the lowest order weak decay is through the exchange of W^\pm gauge boson between two left-handed currents. At low energy, the momentum transfer q is much smaller than M_W , the mass of the W^\pm gauge boson. The W^\pm boson propagator can be approximated as:

$$\frac{-g_{\mu\nu} + q_\mu q_\nu / M_W^2}{q^2 - M_W^2} \stackrel{q^2 \ll M_W^2}{\approx} \frac{g_{\mu\nu}}{M_W}. \quad (1.1)$$

Then for the muon decay $\mu \rightarrow e + \bar{\nu}_e + \nu_\mu$, the decay amplitude can be described by the local four-fermion effective Hamiltonian

$$H_W = \frac{4G_F}{\sqrt{2}} (\bar{\nu}_\mu \gamma_\alpha P_L \mu) (\bar{e} \gamma^\alpha P_L \nu_e), \quad (1.2)$$

where the Fermi coupling constant

$$G_F \equiv \frac{g^2}{8M_W^2}, \quad (1.3)$$

and g is the weak $SU(2)$ coupling constant. We can see that only the relevant light degrees of freedom, μ , ν_μ , e , and $\bar{\nu}_e$ appear in the effective Hamiltonian. The heavy degree of freedom W is “integrated out” from the underlying high energy theory. The remnants of the high-energy dynamics become the low-energy couplings and symmetries in the effective field theory. From this simple example, we know that in order to construct an effective theory, we need to identify the

- (i) relevant degrees of freedom,
- (ii) symmetries, which in turn determine the possible interactions,
- (iii) expansion parameters

at the low energy. The expansion parameter is q^2/M_W^2 in this case. By taking the low-energy limit of the fundamental theory, we obtain the effective theory. Nevertheless, even if we do not know the fundamental theory, we can still construct an effective theory by identifying (i) and (ii) based on the information we have. This is historically how people construct effective field theories, because the underlying theory is usually unknown.

Another feature of effective field theories is that they are often non-renormalizable as in the Fermi’s four-fermion theory. It is non-renormalizable in the sense that we need an infinite number of counterterms to absorb all the divergences. Thus people say non-renormalizable theories have no predictive power because we cannot deal with infinite counterterms. However, these infinite number of counterterms are weighted by powers of the expansion parameter in the effective theory. An effective theory is still renormalizable order by order in its expansion parameters—there are only a finite number of counterterms at each expansion order. As it turns out, effective field theories are predictive to a given accuracy in their expansion parameters. If we look at field theories

in this new perspective, we can abandon the renormalizability as a guiding principle of constructing a new quantum field theory. We can also think of the Standard Model as an effective field theory, then the Lagrangian becomes

$$\mathcal{L}_{EFT} = \mathcal{L}_{SM} + \sum_i \frac{1}{\Lambda^{d_i-4}} C_i \mathcal{O}_i , \quad (1.4)$$

where \mathcal{L}_{SM} includes the Standard Model terms up to mass dimension 4, Λ is the cutoff scale of the effective theory, \mathcal{O}_i are operators that respect the $SU(3) \times SU(2) \times U(1)$ gauge symmetry with mass dimension $d_i > 4$, and C_i are the Wilson coefficients. The second term, constrained by experiments, encodes new physics that is beyond the Standard Model. This provides a very general, model-independent framework for studying new physics.

1.3 Outline of Dissertation

In this dissertation, Chapter 2 and Chapter 3 are about topics in QCD. Starting from Chapter 4, we discuss various topics in effective field theories.

In Chapter 2, we provide a first estimate of the size of the various correlations in the double parton distribution function (PDF). These correlations can be used to guide the experimental analyses involving double parton scattering. Double parton scattering is a process in which two hard partonic collisions take place within a single hadronic collision. It has become an important background for new physics searches at the LHC. In the literature, it is commonly assumed in double parton scattering studies that the dependence on the transverse separation is uncorrelated with the momentum fractions or parton flavors. In addition, a factorized ansatz is often made: a double PDF can be factorized into multiplication of two single PDFs with kinematic constraint. We implement a bag model for the proton to calculate the non-perturbative matrix elements and find significant correlations between momentum fractions, spin and flavor, but negligible correlations with transverse separation between two partons inside the hadron.

We show the assumption of the transverse separation holds reasonably well, but the factorized ansatz is badly broken. The results provide quantitative descriptions for the diparton correlations, which will help in the experimental analysis of double parton scattering at the LHC.

Next in Chapter 3, we perform QCD calculations with charged particles only. Experimentally, one way to suppress pile-up contamination at the LHC is by using observables that only depend on charged particles (tracks). However, such measurements are not infrared safe in perturbation theory. We develop a formalism to perform these calculations in QCD, by matching partonic cross sections onto new non-perturbative objects called track functions which absorb infrared divergences. The track function is similar to a PDF in that it absorbs infrared divergences and has a well-defined QCD evolution equation known as the DGLAP equation ². We extract the leading order track functions from pure quark and gluon jet samples produced by Monte Carlo event generators—PYTHIA, and cluster using the anti- k_T algorithm in FASTJET package. We then compute the next-to-leading order track function in perturbation theory by convolving two leading order track functions. We find that the up- and down-quark track functions are very similar, with a peak at $x = 0.6$. This means that on average 60% of the energy of the initial quark is contained in charged hadrons, in agreement with a CMS study.

Then in Chapter 4, we perform the first calculation of the track (charged particle) thrust event shape with the framework developed in Chapter 3. In order to get reliable predictions, we have to include the effects of logarithmic resummation. By incorporating track functions into soft-collinear effective theory, we are able to calculate the distribution for track thrust with next-to-leading logarithmic resummation precision. The result is in good agreement with track thrust measurements performed at LEP by ALEPH and

²DGLAP stands for Dokshitzer, Gribov, Lipatov, Altarelli, and Parisi. The QED version of the evolution equation was originally derived by Gribov and Lipatov [6] in 1972, while the QCD version was obtained independently in 1977 by Altarelli and Parisi [7] and by Dokshitzer [8]. In the Mellin moment space, the QED version was derived by Christ, Hasslacher, and Mueller [9] in 1972, and the QCD version was derived by Georgi and Politzer [10] and by Gross and Wilczek [11] in 1974.

DELPHI collaborations.

In Chapter 5, we calculate the one-loop anomalous dimension matrix for the dimension-six baryon number violating operators. These operators are of the Standard Model effective field theory, including right-handed neutrino fields. Together with the previous computations [12, 13, 14], this last piece completes the anomalous dimension matrix for the totality of dimension-six operators of the Standard Model.

Finally, in Chapter 6 we investigate the discovery potential of semileptonic hyperon decays in terms of searches of new physics at teraelectronvolt scales using the Standard Model effective theory framework. These decays are controlled by a small $SU(3)$ -flavor breaking parameter that allows for systematic expansions and accurate predictions in terms of a reduced dependence on hadronic form factors. We find that muonic modes are very sensitive to non-standard scalar and tensor contributions and demonstrate that these could provide a powerful synergy with direct searches of new physics at the LHC.

Chapter 2

Double Parton Correlations in the Bag Model

Double parton scattering is sensitive to correlations between two partons in the hadron, including correlations in flavor, spin, color, momentum fractions and transverse separation. We obtain a first estimate of the size of these correlations by calculating the corresponding double parton distribution functions in a bag model of the proton. We find significant correlations between momentum fractions, spin and flavor, but negligible correlations with transverse separation. The model estimates of the relative importance of these correlations will help experimental studies disentangle them.

2.1 Introduction

High-energy scattering processes such as Drell-Yan production, $pp \rightarrow \ell^+ \ell^-$, are described by the scattering of two incoming partons, and the cross section is given by the convolution of a partonic scattering cross section $\hat{\sigma}$ and parton distribution functions (PDFs). Sometimes two hard partonic collisions take place within a single hadronic collision, a process which is known as double parton scattering (DPS). DPS is higher twist, i.e. it is suppressed by a power of $\Lambda_{\text{QCD}}^2/Q^2$, where Q is the partonic center-

of-mass energy of the collision. Despite this power suppression, the DPS scattering rate is still large enough that it has become a background for new physics searches at the LHC. For example, DPS contributes to same-sign WW and same-sign dilepton production [15, 16, 17, 18] and is a background for Higgs studies in the channel $pp \rightarrow WH \rightarrow \ell\nu b\bar{b}$ [19, 20, 21, 22]. DPS has been observed at the LHC; a preliminary study using 33 pb^{-1} of data found that 16% of the $W + 2$ jet events were due to DPS [23].

In the original work on DPS, the cross section was written as [24]

$$\begin{aligned} d\sigma = \frac{1}{S} \sum_{i,j,k,l} & \int d^2 \mathbf{z}_\perp F_{ij}(x_1, x_2, \mathbf{z}_\perp, \mu) F_{kl}(x_3, x_4, \mathbf{z}_\perp, \mu) \\ & \times \hat{\sigma}_{ik}(x_1 x_3 \sqrt{s}, \mu) \hat{\sigma}_{jl}(x_2 x_4 \sqrt{s}, \mu). \end{aligned} \quad (2.1)$$

The double parton distribution function (dPDF) $F_{ij}(x_1, x_2, \mathbf{z}_\perp)$ describes the probability of finding two partons with flavors $i, j = g, u, \bar{u}, d, \dots$, longitudinal momentum fractions x_1, x_2 and transverse separation \mathbf{z}_\perp inside the hadron. The partonic cross sections $\hat{\sigma}$ describe the short-distance processes, and S is a symmetry factor that arises for identical particles in the final state. Eq. (2.1) ignores additional contributions that are sensitive to diparton correlations in flavor, spin and color, as well as parton-exchange interference contributions [25, 26, 27, 28]. These correlations are present in QCD, and one of our goals is to estimate the size of these effects.

It is commonly assumed in DPS studies that the dependence on the transverse separation is uncorrelated with the momentum fractions or parton flavors,

$$F_{ij}(x_1, x_2, \mathbf{z}_\perp, \mu) = F_{ij}(x_1, x_2, \mu) G(\mathbf{z}_\perp, \mu). \quad (2.2)$$

In addition, a factorized ansatz is often made,

$$F_{ij}(x_1, x_2, \mu) = f_i(x_1, \mu) f_j(x_2, \mu) \theta(1 - x_1 - x_2)(1 - x_1 - x_2)^n, \quad (2.3)$$

where f denotes the usual (single) PDF. The factor $\theta(1 - x_1 - x_2)(1 - x_1 - x_2)^n$ smoothly

imposes the kinematic constraint $x_1 + x_2 \leq 1$, and different values of the parameter $n > 0$ have been considered.

The dPDF is a nonperturbative function, but once it is known at a certain scale μ , its renormalization group evolution can be used to evaluate it at a different scale. The evolution of $F_{ij}(x_1, x_2, \mu)$ was determined a long time ago [29, 30]. It has recently been extended to include the \mathbf{z}_\perp dependence and describe correlation and interference dPDFs [26, 27, 28, 31]. The color-correlated and interference dPDFs are all Sudakov suppressed at high energies [32, 28] and will, therefore, not be considered.

Eventually the dPDFs will be determined by fitting to experimental data, just as for the usual PDFs. Reference [33] goes a step in this direction, showing how angular correlations in double Drell-Yan production may be used to study spin correlations in dPDFs. In this chapter, we determine the dPDFs at a low scale $\mu \sim \Lambda_{\text{QCD}}$ using a bag model for the proton [34]. This model calculation provides an estimate of the importance of various diparton correlations, which can be used to guide the experimental analysis. It also provides an estimate of dPDF distributions in the absence of more accurate determinations directly from experiment.

We follow some of the existing structure function calculations in the bag model [35, 36, 37]. There are obvious limitations to this approach, just as for bag model calculations of the usual PDFs. First of all, the bag model only describes valence quarks. Bag model calculations are only meaningful when the fields in the dPDF act inside the bag, which restricts the momentum fractions $x \gtrsim 1/(2MR) \sim 0.1$, where M is the proton mass and R is the bag radius. Finally, the bag was treated as rigid in the early literature, Ref. [35]. A consequence is that momentum is not conserved, and parton distributions do not vanish outside the physical region ($x > 1$). Alternative treatments of the bag were proposed to alleviate this problem [36, 37, 38]. We emphasize that we are not attempting to use the most sophisticated bag model description of the proton. Rather, we simply want to provide a first estimate of the size of the various correlation effects. Bag model PDFs are usually chosen as the initial value of PDFs at a low scale $\mu \sim \Lambda_{\text{QCD}}$, which are then evolved to higher scales using their QCD evolution. Since in the bag model the valence

quarks carry all the momentum, this initial scale μ needs to be taken quite low [36].

We also investigate Eqs. (2.2) and (2.3) in this chapter, using our bag model results. We find that Eq. (2.2) holds reasonably well, but Eq. (2.3) is badly violated. Problems with Eq. (2.3) have already been pointed out in Ref. [39], using sum rules and the evolution of the dPDF. (Though Eq. (2.3) may still be approximately true when one of the momentum fractions x_i is small; see, e.g., Ref. [40].) In the simplest bag models of the type we consider, the color-correlated dPDFs F^T are given by $-2/3$ times the color-direct dPDFs F^1 , since diquarks are in a $\bar{\mathbf{3}}$ representation of color.

2.2 Calculation

We briefly summarize the ingredients of the bag model [34] that are needed to calculate the dPDFs. The bag model wave functions are the solutions of the massless Dirac equation in a spherical cavity of radius R . We only need the ground state, which is given by

$$\Psi_m(\mathbf{r}, t) = N \begin{pmatrix} j_0(\Omega|\mathbf{r}|/R) \chi_m \\ i \hat{\mathbf{r}} \cdot \boldsymbol{\sigma} j_1(\Omega|\mathbf{r}|/R) \chi_m \end{pmatrix} e^{-i\Omega t/R}, \quad (2.4)$$

for a bag centered at the origin. Here $\Omega = ER$, with E the energy of the particle,

$$N^2 = \frac{1}{R^3} \frac{\Omega^4}{\Omega^2 - \sin^2 \Omega}, \quad \chi_m = \frac{1}{\sqrt{4\pi}} \begin{pmatrix} \delta_{m,\uparrow} \\ \delta_{m,\downarrow} \end{pmatrix}, \quad (2.5)$$

j_i are spherical Bessel functions, and $m = \uparrow, \downarrow$. The condition that the color current does not flow through the boundary $r^\mu \Psi \gamma_\mu T^A \Psi|_{|\mathbf{r}|=R} = 0$ leads to

$$j_0(\Omega) = j_1(\Omega) \quad \Rightarrow \quad \Omega \approx 2.043, \quad (2.6)$$

and we will take $R = 1.6$ fm in our numerical analysis.

The quark field is expanded in terms of bag wave functions, quark creation and annihilation operators $a_i(\mathbf{a})$, $a_i^\dagger(\mathbf{a})$ and antiquark creation and annihilation operators $b_i(\mathbf{a})$, $b_i^\dagger(\mathbf{a})$. These operators create or annihilate quarks and antiquarks in a bag centered at $\mathbf{r} = \mathbf{a}$ [see Eq. (2.14)].

The spin-up proton wave function is given in terms of the standard quark model wave functions as

$$\frac{1}{\sqrt{6}} |uud\rangle (2 |\uparrow\uparrow\downarrow\rangle - |\uparrow\downarrow\uparrow\rangle - |\downarrow\uparrow\uparrow\rangle) . \quad (2.7)$$

As usual, the color indices are suppressed, and the wave function has to be symmetrized over permutations. Ignoring color, one can also write the wave function in terms of bosonic [41] creation operators,

$$|P \uparrow, \mathbf{r} = \mathbf{a}\rangle = \frac{1}{\sqrt{3}} \left[a_{u\uparrow}^\dagger(\mathbf{a}) a_{u\uparrow}^\dagger(\mathbf{a}) a_{d\downarrow}^\dagger(\mathbf{a}) - a_{u\uparrow}^\dagger(\mathbf{a}) a_{u\downarrow}^\dagger(\mathbf{a}) a_{d\uparrow}^\dagger(\mathbf{a}) \right] |0, \mathbf{r} = \mathbf{a}\rangle . \quad (2.8)$$

Here $|P \uparrow, \mathbf{r} = \mathbf{a}\rangle$ and $|0, \mathbf{r} = \mathbf{a}\rangle$ are the proton and empty bag state, respectively, both at position \mathbf{a} . The $a_{qm}^\dagger(\mathbf{a})$ denotes the creation operator for a quark of flavor q with spin m in a bag at position \mathbf{a} .

An important difference between various calculations in the literature is the treatment of the overlap between empty bags at different positions,

$$\begin{aligned} \langle 0, \mathbf{r} = \mathbf{a} | 0, \mathbf{r} = \mathbf{b} \rangle &= \delta^3(\mathbf{a} - \mathbf{b}) && \text{in Ref. [35],} \\ \langle 0, \mathbf{r} = \mathbf{a} | 0, \mathbf{r} = \mathbf{b} \rangle &= 1 && \text{in Refs. [36, 37].} \end{aligned} \quad (2.9)$$

These opposite limits treat the bags as either completely rigid or fully flexible, and the latter will be our default. We will return to the rigid bag in Sec. 2.2.4. To account for the

displacement between bags, we follow Ref. [36] in taking

$$\{a_i(\mathbf{a}), a_j^\dagger(\mathbf{b})\} = \delta_{ij} \int d^3x \Psi_j^\dagger(\mathbf{x} - \mathbf{b}) \Psi_i(\mathbf{x} - \mathbf{a}). \quad (2.10)$$

For the rigid bag these are replaced by the familiar anticommutation relations

$$\{a_i, a_j^\dagger\} = \delta_{ij}, \quad (2.11)$$

where we only need the relation when a and a^\dagger are at the same bag position, because of Eq. (2.9).

The proton state with momentum \mathbf{p} is constructed using the Peierls-Yoccoz (PY) projection [42],

$$|P, \mathbf{p}\rangle = \frac{1}{\phi_3(\mathbf{p})} \int d^3\mathbf{a} e^{i\mathbf{a}\cdot\mathbf{p}} |P, \mathbf{r} = \mathbf{a}\rangle, \quad (2.12)$$

where $\phi_3(\mathbf{p})$ fixes the (nonrelativistic) normalization of the state. The functions $\phi_n(\mathbf{p})$ are given by

$$|\phi_n(\mathbf{p})|^2 = \int d\mathbf{a} e^{-i\mathbf{p}\cdot\mathbf{a}} \left[\int d\mathbf{x} \Psi^\dagger(\mathbf{x} - \mathbf{a}) \Psi(\mathbf{x}) \right]^n, \quad (2.13)$$

which we will need for $n = 1, 2, 3$.

The final ingredient is the expression for quark fields acting in the bag. The field for a u quark relative to a bag at \mathbf{a} is given by [36]

$$u(\mathbf{x}, t) = \sum_{m=\uparrow, \downarrow} a_{um}(\mathbf{a}) \Psi_m(\mathbf{x} - \mathbf{a}) e^{-i\Omega t/R} + \dots \quad (2.14)$$

Here “ \dots ” denotes contributions from other bag states that will not be needed¹. The expression for d quarks is similar.

¹We will not consider the so-called z graph or four-quark intermediate state contribution [35, 37], where the field creates an antiquark. This only contributes at small x and is thus outside the range of validity of the calculation.

2.2.1 Single PDF

We first summarize the well-known calculation of the (single) PDF in the bag model. The light-cone vectors are

$$n^\mu = (1, 0, 0, 1), \quad \bar{n}^\mu = (1, 0, 0, -1), \quad (2.15)$$

and we assume the light-cone gauge $n \cdot A = 0$, where A is the gluon field. In the proton rest frame, where $p^\mu = (M, \mathbf{0})$,²

$$\begin{aligned} q(x) &= 2M \int \frac{dz^+}{4\pi} e^{-ixMz^+/2} \left\langle P, \mathbf{p} = \mathbf{0} \middle| \bar{q} \left(z^+ \frac{\bar{n}}{2} \right) \frac{\vec{\eta}}{2} q(0) \middle| P, \mathbf{p} = \mathbf{0} \right\rangle \\ &= \sum_{m_1, m_2 = \uparrow, \downarrow} \left\langle P, \mathbf{r} = \mathbf{0} \middle| a_{qm_1}^\dagger(\mathbf{0}) a_{qm_2}(\mathbf{0}) \middle| P, \mathbf{r} = \mathbf{0} \right\rangle \\ &\quad \times 2M \int \frac{dz^+}{4\pi} \frac{d\mathbf{k}_1}{(2\pi)^3} \frac{d\mathbf{k}_2}{(2\pi)^3} \frac{d\mathbf{k}_3}{(2\pi)^3} e^{-i(xM - \frac{\Omega}{R} + k_{1z})z^+/2} \\ &\quad \times (2\pi)^3 \delta(\mathbf{k}_1 - \mathbf{k}_3) (2\pi)^3 \delta(\mathbf{k}_2 - \mathbf{k}_3) \tilde{\Psi}_{m_1}(\mathbf{k}_1) \frac{\vec{\eta}}{2} \tilde{\Psi}_{m_2}(\mathbf{k}_2) \frac{|\phi_2(\mathbf{k}_3)|^2}{|\phi_3(0)|^2} \\ &= \sum_{m_1, m_2 = \uparrow, \downarrow} \left\langle P, \mathbf{r} = \mathbf{0} \middle| a_{qm_1}^\dagger(\mathbf{0}) a_{qm_2}(\mathbf{0}) \middle| P, \mathbf{r} = \mathbf{0} \right\rangle \\ &\quad \times 2M \int \frac{d\mathbf{k}}{(2\pi)^3} \tilde{\Psi}_{m_1}(\mathbf{k}) \frac{\vec{\eta}}{2} \tilde{\Psi}_{m_2}(\mathbf{k}) \frac{|\phi_2(\mathbf{k})|^2}{|\phi_3(0)|^2} \delta\left(xM - \frac{\Omega}{R} + k_z\right) \\ &= \sum_{m_1, m_2 = \uparrow, \downarrow} \left\langle P, \mathbf{r} = \mathbf{0} \middle| a_{qm_1}^\dagger(\mathbf{0}) a_{qm_2}(\mathbf{0}) \middle| P, \mathbf{r} = \mathbf{0} \right\rangle \\ &\quad \times \frac{2M}{(2\pi)^2} \int_{|\Omega/R - xM|}^\infty d|\mathbf{k}| |\mathbf{k}| \tilde{\Psi}_m(\mathbf{k}) \frac{\vec{\eta}}{2} \tilde{\Psi}_m(\mathbf{k}) \frac{|\phi_2(\mathbf{k})|^2}{|\phi_3(0)|^2}. \end{aligned} \quad (2.16)$$

Here $z^+ = n \cdot z$, $\tilde{\Psi}$ denotes the Fourier transform of Ψ , and ϕ_2 is given by Eq. (2.13). The overall factor of $2M$ is due to the nonrelativistic normalization of states. The delta function on the fourth line sets

$$k_z = \frac{\Omega}{R} - xM, \quad (2.17)$$

²We also use the notation q for the PDF f_q , and qq , $q\Delta q$, \dots for the dPDFs F_{qq} , $F_{q\Delta q}$, \dots .

implying that the peak of the PDF is at $x = \Omega/(MR)$, independent of the quark flavor. This disagreement with experimental measurements of u and d may be alleviated by refining the bag model; see, e.g., Ref. [43]. We will restrict ourselves to the simplest bag models in this chapter, so its limitations should be kept in mind while using the results.

In using Eq. (2.14) we assumed that the field \bar{q} acts at the position of the bag of the left state and q at the position of the bag of the right state [36]. The matrix element of Eq. (2.16) contains all the dependence on the spin-flavor wave function of Eq. (2.7), which is connected with the spin of the bag wave functions through the sum on $m_{1,2}$. For the unpolarized single PDF only $m_1 = m_2$ contributes, and the matrix element simply counts the number of quarks of a given flavor q in the proton,

$$n_q = \sum_{m=\uparrow,\downarrow} \langle P, \mathbf{r} = \mathbf{0} | a_{qm}^\dagger(\mathbf{0}) a_{qm}(\mathbf{0}) | P, \mathbf{r} = \mathbf{0} \rangle. \quad (2.18)$$

The extension of Eq. (2.16) to longitudinal and transversely polarized quark distributions is given by replacing $\frac{\not{q}}{2}$ by $\frac{\not{q}}{2}\gamma_5$ for Δq and $\frac{\not{q}}{2}\gamma_\perp^\mu\gamma_5$ for δq . Δq and δq only contribute in processes involving longitudinally and transversely polarized protons, respectively. The matrix elements required are evaluated in Sec. 2.2.3. To aid the evaluation of the remaining integral in Eq. (2.16), convenient expressions for the functions ϕ_i and the bag wave function in momentum space are given in Appendix A. The resulting PDFs are compared in Fig. 2.1.

The spatial distribution of partons inside the nucleon is also probed by the elec-

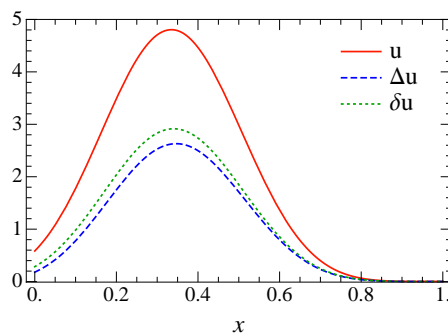


Figure 2.1: The proton PDFs u (solid red), Δu (dashed blue) and δu (dotted green).

tromagnetic form factors, which are independent of the renormalization scale. They have been calculated within the bag model that we are using, showing reasonable agreement with experiment [44]. Calculations of form factors for more sophisticated bag models can, for example, be found in Refs. [45, 46, 47].

2.2.2 Double PDF

We calculate the double PDF using the definitions in Ref. [28]. We will not consider color correlated or interference double PDFs, since these are Sudakov suppressed. The spin-averaged dPDF $F_{q_1 q_2}(x_1, x_2, \mathbf{z}_\perp)$ is defined as

$$\begin{aligned} F_{q_1 q_2}(x_1, x_2, \mathbf{z}_\perp) &= -8\pi M^2 \int \frac{dz_1^+}{4\pi} \frac{dz_2^+}{4\pi} \frac{dz_3^+}{4\pi} e^{-ix_1 M z_1^+/2} e^{-ix_2 M z_2^+/2} e^{ix_1 M z_3^+/2} \\ &\times \left\langle P, \mathbf{p} = \mathbf{0} \middle| \left[\bar{q}_1 \left(z_1^+ \frac{\bar{n}}{2} + z_\perp \right) \frac{\vec{\eta}}{2} \right]_c \left[\bar{q}_2 \left(z_2^+ \frac{\bar{n}}{2} \right) \frac{\vec{\eta}}{2} \right]_d q_{1,c} \left(z_3^+ \frac{\bar{n}}{2} + z_\perp \right) q_{2,d}(0) \middle| P, \mathbf{p} = \mathbf{0} \right\rangle. \end{aligned} \quad (2.19)$$

It is convenient to work in terms of the Fourier-transformed distribution $F_{q_1 q_2}(x_1, x_2, \mathbf{k}_\perp)$. Evaluated in the bag model,

$$\begin{aligned} F_{q_1 q_2}(x_1, x_2, \mathbf{k}_\perp) &= \int d^2 \mathbf{z}_\perp e^{i \mathbf{z}_\perp \cdot \mathbf{k}_\perp} F_{q_1 q_2}(x_1, x_2, \mathbf{z}_\perp) \quad (2.20) \\ &= \sum_{m_1, m_2, m_3, m_4} \left\langle P, \mathbf{r} = \mathbf{0} \middle| a_{q_1 m_1}^\dagger(\mathbf{0}) a_{q_2 m_2}^\dagger(\mathbf{0}) a_{q_2 m_4}(\mathbf{0}) a_{q_1 m_3}(\mathbf{0}) \middle| P, \mathbf{r} = \mathbf{0} \right\rangle \\ &\times 8\pi M^2 \int \frac{d\mathbf{k}_1}{(2\pi)^3} \frac{d\mathbf{k}_2}{(2\pi)^3} \frac{d\mathbf{k}_3}{(2\pi)^3} \\ &\times \delta\left(x_1 M - \frac{\Omega}{R} + \mathbf{k}_{1z}\right) \delta\left(x_2 M - \frac{\Omega}{R} + \mathbf{k}_{2z}\right) \delta\left(x_1 M - \frac{\Omega}{R} + \mathbf{k}_{3z}\right) \\ &\times (2\pi)^2 \delta^2(\mathbf{k}_{1\perp} - \mathbf{k}_{3\perp} - \mathbf{k}_\perp) \tilde{\Psi}_{m_1}(\mathbf{k}_1) \frac{\vec{\eta}}{2} \tilde{\Psi}_{m_3}(\mathbf{k}_3) \tilde{\Psi}_{m_2}(\mathbf{k}_2) \frac{\vec{\eta}}{2} \tilde{\Psi}_{m_4}(\mathbf{k}_1 + \mathbf{k}_2 - \mathbf{k}_3) \\ &\times \frac{|\phi_1(\mathbf{k}_1 + \mathbf{k}_2)|^2}{|\phi_3(0)|^2}, \end{aligned}$$

where ϕ_1 is given by Eq. (2.13). Results for the matrix elements on the second line of Eq. (2.20) are given in Sec. 2.2.3. The remaining integrals were numerically performed using the expressions in Appendix A and the CUBA integration package [48].

2.2.3 Spin Correlations

The computation of spin-correlated dPDFs is almost identical to Eq. (2.20). For $F(x_1, x_2, \mathbf{z}_\perp)$ the spinors $\frac{\vec{\eta}}{2} \otimes \frac{\vec{\eta}}{2}$ in Eq. (2.19) are replaced by [26, 27, 28]

$F_{\Delta q_1 \Delta q_2}$	$\frac{\vec{\eta}}{2} \gamma_5 \otimes \frac{\vec{\eta}}{2} \gamma_5$
$F_{\delta q_1 \delta q_2}$	$\frac{\vec{\eta}}{2} \gamma_\perp^\mu \gamma_5 \otimes \frac{\vec{\eta}}{2} \gamma_\mu^\perp \gamma_5$
$F_{q_1 \delta q_2}$	$-\frac{1}{M \mathbf{z}_\perp^2} \frac{\vec{\eta}}{2} \otimes \frac{\vec{\eta}}{2} \gamma_\perp^\mu \epsilon_{\mu\nu} z_\perp^\nu \gamma_5$
$F_{\Delta q_1 \delta q_2}$	$-\frac{1}{M \mathbf{z}_\perp^2} \frac{\vec{\eta}}{2} \gamma_5 \otimes \frac{\vec{\eta}}{2} \not{k}_\perp \gamma_5$
$F_{\delta q_1 \delta q_2}^t$	$\frac{2}{M^2 \mathbf{z}_\perp ^4} (z_\perp^\mu z_\perp^\nu + \frac{1}{2} \mathbf{z}_\perp^2 g_\perp^{\mu\nu}) \frac{\vec{\eta}}{2} \gamma_\mu \gamma_5 \otimes \frac{\vec{\eta}}{2} \gamma_\nu \gamma_5$

As in Eq. (2.20), we switch to momentum space, for which it is convenient to modify some of the spin structures:

$\mathcal{F}_{q_1 \delta q_2}$	$\frac{iM}{\mathbf{k}_\perp^2} \frac{\vec{\eta}}{2} \otimes \frac{\vec{\eta}}{2} \gamma_\perp^\mu \epsilon_{\mu\nu} k_\perp^\nu \gamma_5$
$\mathcal{F}_{\Delta q_1 \delta q_2}$	$\frac{iM}{\mathbf{k}_\perp^2} \frac{\vec{\eta}}{2} \gamma_5 \otimes \frac{\vec{\eta}}{2} \not{k}_\perp \gamma_5$
$\mathcal{F}_{\delta q_1 \delta q_2}^t$	$\frac{2M^2}{ \mathbf{k}_\perp ^4} (k_\perp^\mu k_\perp^\nu + \frac{1}{2} \mathbf{k}_\perp^2 g_\perp^{\mu\nu}) \frac{\vec{\eta}}{2} \gamma_\mu \gamma_5 \otimes \frac{\vec{\eta}}{2} \gamma_\nu \gamma_5$

We will always use these momentum-space spin structures in plots. The relationship between \mathcal{F} and F is not simply a Fourier transform, and is given in Appendix B. The additional factors of $-i$ in $\mathcal{F}_{q_1 \delta q_2}$ and $\mathcal{F}_{\Delta q_1 \delta q_2}$ ensure that these dPDFs are real. The spin structure $\Delta q_1 \delta q_2$ vanishes in our calculation. Assuming for simplicity that \mathbf{k} is along the x direction, this follows from the reflection $k_{1y} \rightarrow -k_{1y}$, $k_{2y} \rightarrow -k_{2y}$, under which the integrand in Eq. (2.20) is odd. Though this is due to the form of the bag model matrix elements, it suggests that the spin structure $\Delta q_1 \delta q_2$ is likely smaller than the others.

We now evaluate the spin-flavor matrix elements that enter in the single and double PDFs. Since we suppressed the *antisymmetric* color wave function of the proton, the creation and annihilation operators essentially satisfy *commutation* relations. For the unpolarized and longitudinally polarized single PDF, only $m_1 = m_2$ contributes, and we find the weighting:

q	m	$\langle P \uparrow a_{qm}^\dagger a_{qm} P \uparrow \rangle$
u	\uparrow	5/3
u	\downarrow	1/3
d	\uparrow	1/3
d	\downarrow	2/3

For δq we need a transversely polarized proton

$$|P \rightarrow\rangle = \frac{1}{\sqrt{2}}(|P \uparrow\rangle + |P \downarrow\rangle). \quad (2.21)$$

The nonvanishing matrix elements are

q	m_1	m_2	$\langle P \rightarrow a_{qm_1}^\dagger a_{qm_2} P \rightarrow \rangle$
u	\uparrow	\downarrow	2/3
u	\downarrow	\uparrow	2/3
d	\uparrow	\downarrow	-1/6
d	\downarrow	\uparrow	-1/6

The dPDFs we consider are invariant under spin flip (they are only sensitive to diparton spin correlations), so we can simply use a spin-up proton. The dPDF for dd in all spin combinations vanishes in the bag model since there is only one valance d quark in the proton. The nonvanishing matrix elements are

q_1	q_2	m_1	m_2	m_3	m_4	$\langle P \uparrow a_{q_1 m_1}^\dagger a_{q_2 m_2}^\dagger a_{q_2 m_4} a_{q_1 m_3} P \uparrow \rangle$
u	u	\uparrow	\uparrow	\uparrow	\uparrow	4/3
u	u	\uparrow	\downarrow	\uparrow	\downarrow	1/3
u	u	\downarrow	\uparrow	\downarrow	\uparrow	1/3
u	u	\uparrow	\downarrow	\downarrow	\uparrow	1/3
u	u	\downarrow	\uparrow	\uparrow	\downarrow	1/3
u	d	\uparrow	\uparrow	\uparrow	\uparrow	1/3
u	d	\uparrow	\downarrow	\uparrow	\downarrow	4/3
u	d	\downarrow	\uparrow	\downarrow	\uparrow	1/3
u	d	\uparrow	\downarrow	\downarrow	\uparrow	-2/3
u	d	\downarrow	\uparrow	\uparrow	\downarrow	-2/3

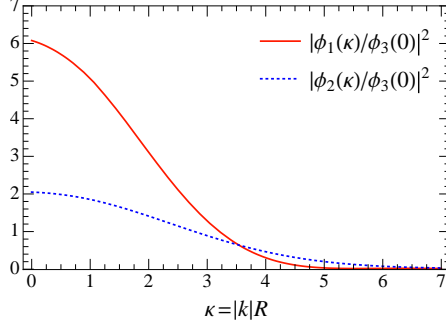


Figure 2.2: Plot of the PY factors which enter the calculation of the single PDF (dotted blue) and double PDF (solid red). They suppress the PDFs in the unphysical regions $x > 1$ and $x < 0$.

Note that due to these spin-flavor correlations, the dPDF for uu and ud do not simply differ by an overall factor, as is the case for the single PDF.

2.2.4 Rigid Bag

For a rigid bag, the overlap of empty bag states is

$$\langle 0, \mathbf{r} = \mathbf{a} | 0, \mathbf{r} = \mathbf{b} \rangle = \delta^3(\mathbf{a} - \mathbf{b}) . \quad (2.22)$$

The only change to the single PDF in Eq. (2.16) is that it removes the PY factor $|\phi_2(\mathbf{k})|^2/|\phi_3(\mathbf{0})|^2$. This factor suppresses the “leakage” of the PDF into the unphysical regions $x < 0$ and $x > 1$, without affecting the integral over all x , see Sec. 2.2.5. The PY factor is plotted in Fig. 2.2, and the PDF with and without the PY factor is shown in Fig. 2.3.

Similarly, the rigid bag overlap in Eq. (2.22) removes the factor $|\phi_1(\mathbf{k})|^2/|\phi_3(\mathbf{0})|^2$ (also plotted in Fig. 2.2) from the double PDF in Eq. (2.20). In this case, the dPDF factors, and there are no correlations between the momentum fractions x_1 and x_2 , which is a clear shortcoming of treating the bag as rigid. At $\mathbf{k}_\perp = \mathbf{0}$, the rigid bag dPDF takes a particularly simple form:

$$F_{q_1 q_2}(x_1, x_2, \mathbf{k}_\perp = \mathbf{0}) = \frac{c_{q_1 q_2}}{n_{q_1} n_{q_2}} q_1(x_1) q_2(x_2) , \quad (2.23)$$

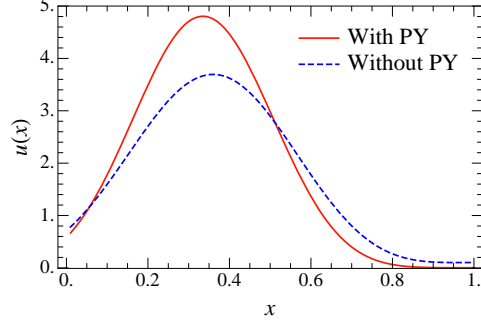


Figure 2.3: Plot of the bag model proton PDF $u(x)$ with (solid red) and without (dotted blue) PY factors.

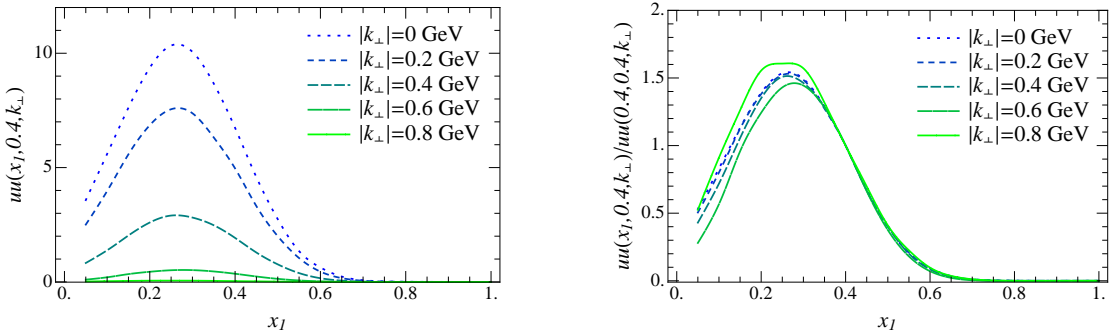


Figure 2.4: The double PDF $uu(x_1, x_2, \mathbf{k}_\perp)$ as a function of x_1 and $|\mathbf{k}_\perp|$ for fixed $x_2 = 0.4$. The right panel tests the ansatz in Eq. (2.2) that x_i and \mathbf{k}_\perp are uncorrelated. This holds reasonably well, since the different $|\mathbf{k}_\perp|$ curves are nearly identical.

where the coefficient $c_{q_1 q_2}$ is fixed by the spin-flavor wave function

$$c_{q_1 q_2} = \sum_{\substack{m_1=m_3 \\ m_2=m_4}} \left\langle P, \mathbf{r} = \mathbf{0} \middle| a_{q_1 m_1}^\dagger(\mathbf{0}) a_{q_2 m_2}^\dagger(\mathbf{0}) \right. \\ \times \left. a_{q_2 m_4}(\mathbf{0}) a_{q_1 m_3}(\mathbf{0}) \middle| P, \mathbf{r} = \mathbf{0} \right\rangle. \quad (2.24)$$

From the tables in Sec. 2.2.3, we find that $c_{uu} = c_{ud} = 2$.

2.2.5 Normalization

The normalization of the single PDF and dPDF is given by integrating over all x , including unphysical regions. Both treatments of the bag in Eq. (2.9) will be considered.

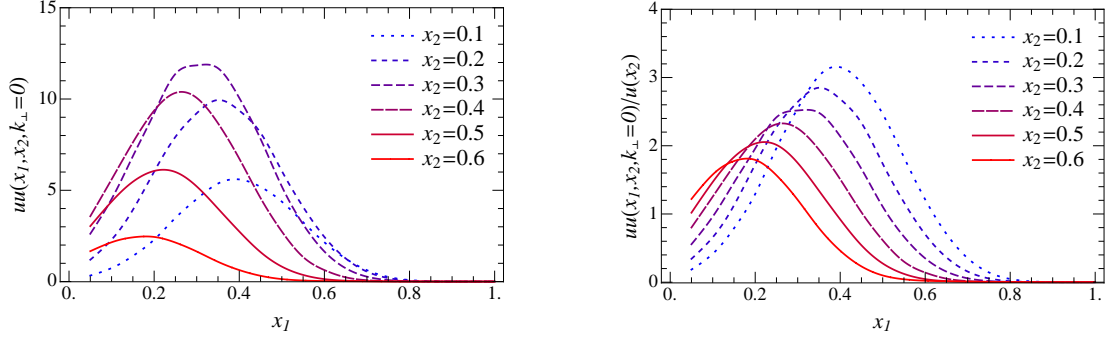


Figure 2.5: The double PDF $uu(x_1, x_2, \mathbf{k}_\perp = 0)$ as a function of x_1 and x_2 for fixed $\mathbf{k}_\perp = 0$. In the right panel, we divide by $u(x_2)$ to test the often-used assumption in Eq. (2.3) that the x_i are uncorrelated. This clearly fails, since the ratio depends strongly on x_2 .

The single PDF in a rigid bag gives

$$\begin{aligned}
 \int dx q(x) &= n_q \int dx \frac{2M}{(2\pi)^2} \int_{|xM-\Omega/R|}^{\infty} d|\mathbf{k}| |\mathbf{k}| \bar{\tilde{\Psi}}_m(\mathbf{k}) \frac{\vec{\eta}}{2} \tilde{\Psi}_m(\mathbf{k}) \\
 &= 2n_q \int \frac{d^3\mathbf{k}}{(2\pi)^3} \tilde{\Psi}^\dagger(\mathbf{k}) \frac{\vec{\eta}\vec{\eta}}{4} \tilde{\Psi}(\mathbf{k}) \\
 &= n_q \int d^3y |\Psi(y)|^2 \\
 &= n_q.
 \end{aligned} \tag{2.25}$$

Here we used that

$$\gamma^0 \frac{\vec{\eta}}{2} = \frac{\vec{\eta}\vec{\eta}}{4}, \quad \frac{\vec{\eta}\vec{\eta}}{4} + \frac{\vec{\eta}\vec{\eta}}{4} = 1. \tag{2.26}$$

This second equation and the symmetry between n and \bar{n} implies that we could replace $\vec{\eta}\vec{\eta}/4 \rightarrow 1/2$ in Eq. (2.25). The corresponding calculation with a flexible bag, i.e. including the PY factor, is

$$\begin{aligned}
 \int dx q(x) &= \frac{2Mn_q}{(2\pi)^2} \int dx \int_{|xM-\Omega/R|}^{\infty} d|\mathbf{k}| |\mathbf{k}| \bar{\tilde{\Psi}}_m(\mathbf{k}) \frac{\vec{\eta}}{2} \tilde{\Psi}_m(\mathbf{k}) \frac{|\phi_2(\mathbf{k})|^2}{|\phi_3(0)|^2} \\
 &= \frac{2n_q}{|\phi_3(0)|^2} \int \frac{d^3\mathbf{k}}{(2\pi)^3} \tilde{\Psi}_m^\dagger(\mathbf{k}) \frac{\vec{\eta}\vec{\eta}}{4} \tilde{\Psi}_m(\mathbf{k}) |\phi_2(\mathbf{k})|^2
 \end{aligned}$$

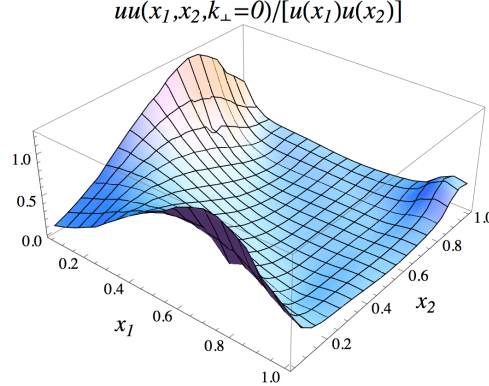


Figure 2.6: The correlation between the momentum fractions of two u quarks in the proton is shown by plotting the ratio of the double PDF $uu(x_1, x_2, \mathbf{k}_\perp = 0)$ to the product of two single PDFs $u(x_1)u(x_2)$.

$$\begin{aligned}
&= \frac{n_q}{|\phi_3(0)|^2} \int \frac{d^3 \mathbf{k}}{(2\pi)^3} \int d^3 \mathbf{x}_1 d^3 \mathbf{y}_1 e^{i\mathbf{k}\cdot\mathbf{x}_1} \Psi^\dagger(\mathbf{y}_1 - \mathbf{x}_1) \Psi(\mathbf{y}_1) \\
&\quad \times \int d^3 \mathbf{x}_2 e^{-i\mathbf{k}\cdot\mathbf{x}_2} \left[\int d\mathbf{y}_2 \Psi^\dagger(\mathbf{y}_2 - \mathbf{x}_2) \Psi(\mathbf{y}_2) \right]^2 \\
&= n_q,
\end{aligned} \tag{2.27}$$

and has the same normalization. However, the PY factor reduces the PDF at unphysical x . Specifically, 2% of the contribution to the integral in Eq. (2.27) is from the unphysical region, compared to 11% in Eq. (2.25).

For the dPDF, the normalization for the rigid bag follows from Eqs. (2.23) and (2.25)

$$\begin{aligned}
&\int dx_1 dx_2 d\mathbf{z}_\perp F_{q_1 q_2}(x_1, x_2, \mathbf{z}_\perp) \\
&= \frac{c_{q_1 q_2}}{n_{q_1} n_{q_2}} \int dx_1 dx_2 q_1(x_1) q_2(x_2) \\
&= c_{q_1 q_2},
\end{aligned} \tag{2.28}$$

where the coefficient $c_{q_1 q_2}$ is given in Eq. (2.24). The calculation including the PY factor

is similar to Eq. (2.27)

$$\begin{aligned}
& \int dx_1 dx_2 d^2 \mathbf{z}_\perp F_{qq}(x_1, x_2, \mathbf{z}_\perp) \\
&= 4c_{q_1 q_2} \int \frac{d^3 \mathbf{k}_1}{(2\pi)^3} \frac{d^3 \mathbf{k}_2}{(2\pi)^3} \tilde{\Psi}^\dagger(\mathbf{k}_1) \frac{\eta \bar{\eta}}{4} \tilde{\Psi}(\mathbf{k}_1) \\
&\quad \times \tilde{\Psi}^\dagger(\mathbf{k}_2) \frac{\eta \bar{\eta}}{4} \tilde{\Psi}(\mathbf{k}_2) \frac{|\phi_1(\mathbf{k}_1 + \mathbf{k}_2)|^2}{|\phi_3(0)|^2} \\
&= c_{q_1 q_2} [1 + \mathcal{O}(< 1\%)].
\end{aligned} \tag{2.29}$$

The small correction with respect to Eq. (2.28) arises because we can no longer replace $\eta \bar{\eta}/4 \rightarrow 1/2$. Specifically, Eq. (A.1) implies

$$\begin{aligned}
\tilde{\Psi}^\dagger(\mathbf{k}) \frac{\eta \bar{\eta}}{4} \tilde{\Psi}(\mathbf{k}) &= \frac{\pi R^3 \Omega^2}{2(\Omega^2 - \sin^2 \Omega)} (s_1^2 + 2s_1 s_2 \hat{\mathbf{k}}_z + s_2^2), \\
\tilde{\Psi}^\dagger(\mathbf{k}) \tilde{\Psi}(\mathbf{k}) &= \frac{\pi R^3 \Omega^2}{(\Omega^2 - \sin^2 \Omega)} (s_1^2 + s_2^2)
\end{aligned} \tag{2.30}$$

Since the momenta \mathbf{k}_{1z} and \mathbf{k}_{2z} become correlated through $\phi_1(\mathbf{k}_1 + \mathbf{k}_2)$, this implies that $\langle \mathbf{k}_{1z} \mathbf{k}_{2z} \rangle \neq \langle \mathbf{k}_{1z} \rangle \langle \mathbf{k}_{2z} \rangle = 0$.

2.3 Parton Correlations

We are now ready to investigate the size of the various diparton correlation effects using the bag model dPDFs. We start by studying the dependence of the dPDF $uu(x_1, x_2, \mathbf{k}_\perp)$ on x_1 and $|\mathbf{k}_\perp|$, keeping $x_2 = 0.4$ fixed for simplicity. As the left panel of Fig. 2.4 shows, the dPDF reduces significantly with increasing $|\mathbf{k}_\perp|$. In the right panel we test the ansatz in Eq. (2.2) that the dependence on x_i and \mathbf{k}_\perp is uncorrelated, by dividing by $uu(0.4, 0.4, \mathbf{k}_\perp)$. If the ansatz holds, the universal transverse function $G(\mathbf{k}_\perp)$ should drop out in this ratio, making the result independent of \mathbf{k}_\perp . As the plot shows, this seems to hold quite well. It only breaks down for the largest values of $|\mathbf{k}_\perp|$, where the dPDF is orders of magnitude smaller than at $|\mathbf{k}_\perp| = 0$. We also note that there is some leakage

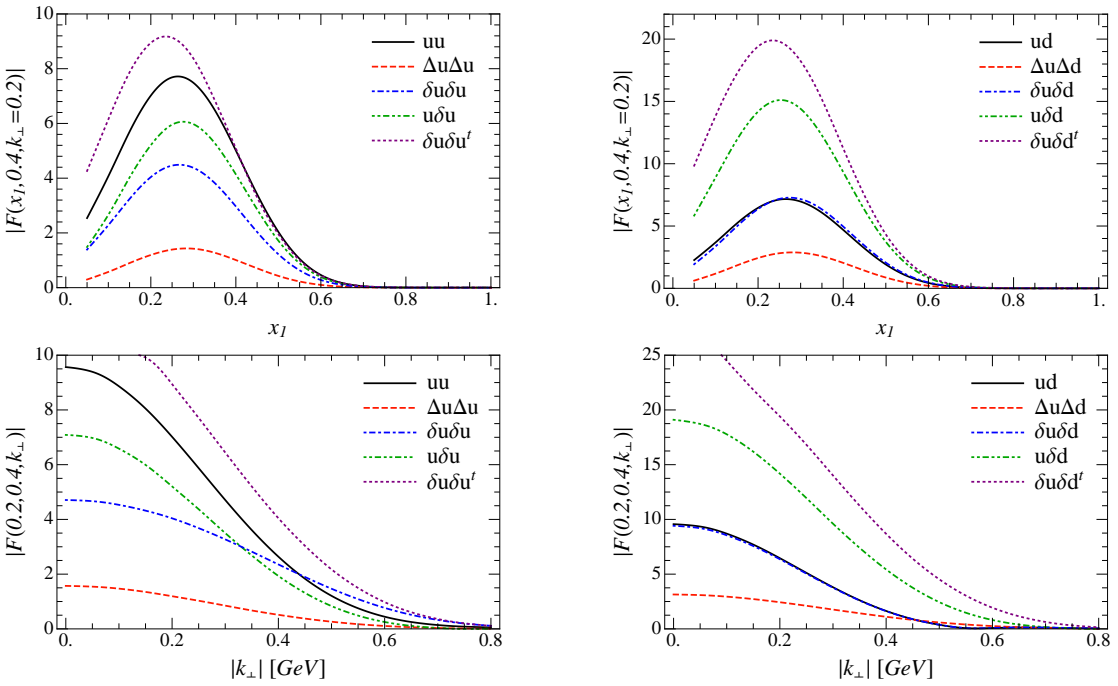


Figure 2.7: Comparison of the double PDF spin structures as functions of x_1 or $|k_\perp|$, keeping the other variables fixed. The left panels show the uu double PDFs, and the right panels show the ud double PDFs. The $u\delta u$, $\delta u\delta u$, $\delta u\delta u^t$, $\Delta u\Delta d$, $u\delta d$ and $\delta u\delta d^t$ distributions are negative, and we have changed their sign in these plots. Note that ud and $\delta u\delta d$ are almost indistinguishable.

into the unphysical region $x_1 + x_2 > 1$, as was the case for the single PDF in Fig. 2.3, though this effect is reasonably small.

Next we explore the x_1, x_2 dependence of dPDF $uu(x_1, x_2, \mathbf{k}_\perp)$ for $\mathbf{k}_\perp = \mathbf{0}$, which is shown in Fig. 2.5. As x_2 is increased, the peak of the x_1 distribution moves to smaller x_1 , responding to the reduced momentum available. The peak height reduces as well, though not for small x_2 since the bag model only describes the valence quarks. To test the factorization ansatz in Eq. (2.3) for $n = 0$, we divide by $u(x_2)$ in the right panel. Since the resulting distributions clearly still depend on x_2 , correlations between x_1 and x_2 are important. Inclusion of the factor of $(1 - x_1 - x_2)^n$ does not alter this conclusion. The correlations can also be seen in the three-dimensional plot of Fig. 2.6. We remind the reader that this conclusion depends on the treatment of the bag, since x_1 and x_2 would be uncorrelated if a rigid bag was assumed (see Sec. 2.2.4).

The relative size of the various spin structures in Sec. 2.2.3 are studied in Fig. 2.7. They are shown as a function of x_1 (top row) and $|\mathbf{k}_\perp|$ (bottom row), keeping all other variables fixed. All spin structures show a similar dependence on x_1 and \mathbf{k}_\perp , though there is a hierarchy between their sizes. Fig. 2.7 also illustrates the differences between the uu (left column) and ud (right column) dPDF. Unlike the single PDF, where the difference between u and d was simply an overall factor of $n_u/n_d = 2$, the dPDF has more flavor dependence. This arises through the spin dependence and the correlations in the spin-flavor wave function. As Fig. 2.7 shows, the difference between uu and ud is fairly small. However, the spin correlations are about twice as big for ud than for uu .

The shape of the $|\mathbf{k}_\perp|$ dependence is reasonably well described by a Gaussian,

$$G(\mathbf{k}_\perp) \approx \frac{1}{2\pi\sigma^2} e^{-\mathbf{k}_\perp^2/(2\sigma^2)}. \quad (2.31)$$

The width σ depends slightly on the spin structure:

	uu	$\Delta u \Delta u$	$\delta u \delta u$	$u \delta u$	$\delta u \delta u^t$
σ (GeV)	0.25	0.27	0.32	0.25	0.29

	ud	$\Delta u\Delta d$	$\delta u\delta d$	$u\delta d$	$\delta u\delta d^t$
σ (GeV)	0.22	0.27	0.22	0.25	0.26

Note that in the bag model $u\delta d = d\delta u$.

2.4 Conclusions

We have computed the dPDFs using a bag model for the proton. The bag model results should be treated as the dPDFs at a low scale, which can then be evolved to higher energy using the known QCD evolution equations [28, 31]. We find substantial diparton correlations in the proton in spin, flavor, and momentum fraction, which have traditionally been ignored in analyses of double parton scattering, but only a small correlation with the transverse momentum \mathbf{k}_\perp . The uu and ud dPDFs are not simply related to each other, or to the single PDFs u and d , because of the spin-flavor correlations in the proton quark model wave function in Eq. (2.7). The results in this chapter provide quantitative results for these diparton correlations, which will help in the experimental analysis of double parton scattering at the LHC.

This chapter is a reprint of material as it appears in “Double Parton Correlations in the Bag Model,” H.-M. Chang, A. V. Manohar and W. J. Waalewijn, Phys. Rev. D **87**, no. 3, 034009 (2013) [arXiv:1211.3132 [hep-ph]], of which I was a co-author.

Chapter 3

Calculating Track-Based Observables for the LHC

By using observables that only depend on charged particles (tracks), one can efficiently suppress pile-up contamination at the LHC. Such measurements are not infrared safe in perturbation theory, so any calculation of track-based observables must account for hadronization effects. We develop a formalism to perform these calculations in QCD, by matching partonic cross sections onto new non-perturbative objects called track functions which absorb infrared divergences. The track function $T_i(x)$ describes the energy fraction x of a hard parton i which is converted into charged hadrons. We give a field-theoretic definition of the track function and derive its renormalization group evolution, which is in excellent agreement with the PYTHIA parton shower. We then perform a next-to-leading order calculation of the total energy fraction of charged particles in $e^+e^- \rightarrow \text{hadrons}$. To demonstrate the implications of our framework for the LHC, we match the PYTHIA parton shower onto a set of track functions to describe the track mass distribution in Higgs plus one jet events. We also show how to reduce smearing due to hadronization fluctuations by measuring dimensionless track-based ratios.

3.1 Introduction

Jets are collimated sprays of particles that arise from the fragmentation of energetic quarks and gluons. Nearly every measurement at the Large Hadron Collider (LHC) involves jets in some way, either directly as probes of physics in and beyond the Standard Model, or indirectly as a source of backgrounds and systematic uncertainties. In order to predict jet-based observables using quantum chromodynamics (QCD), one typically performs infrared- and collinear-safe (IRC safe) jet measurements which involve only the kinematics of the jet constituents [49]. In particular, IRC safe jet measurements do not distinguish between charged and neutral particles, despite the fact that, for example, charged pions (π^\pm) are measured using both tracking and calorimetry whereas neutral pions (π^0) are measured using calorimetry alone.

In this chapter, we develop the theoretical formalism to calculate track-based observables, which depend on the kinematics of charged particles alone but not on their individual properties or multiplicities. The experimental motivation for track-based measurements is that tracking detectors offer better pointing and angular resolution than calorimetry. By only using tracks, one can substantially mitigate the effects of pileup (multiple collision events in a single bunch crossing) which is becoming more relevant as the LHC achieves higher luminosity (see e.g. [50, 51, 52, 53, 54] for alternative approaches). In addition, tracks can aid in jet substructure studies where the angular energy distribution in the jet discriminates between different jet types [55, 56]. While we focus on charged particles, this formalism applies to any (otherwise) IRC safe measurement performed only on a subset of particles.

3.2 Definition of Track Function

To describe track-based observables in QCD, we introduce the *track function* $T_i(x, \mu)$. A parton (quark or gluon) labelled by i with four-momentum p_i^μ hadronizes into charged particles with total four-momentum $\bar{p}_i^\mu \equiv x p_i^\mu + \mathcal{O}(\Lambda_{\text{QCD}})$. The distribution

in the energy fraction $0 \leq x \leq 1$ is the track function and is by definition normalized

$$\int_0^1 dx T_i(x, \mu) = 1. \quad (3.1)$$

The track function is similar to a fragmentation function (FF) or a parton distribution function (PDF) in that it is a fundamentally non-perturbative object that absorbs infrared (IR) divergences in partonic calculations. Like FFs and PDFs, the track function has a well-defined dependence on the renormalization group (RG) scale μ through a DGLAP-type evolution [6, 10, 11, 7, 8], though the specific evolution is more reminiscent of the jet charge distribution [57, 58]. For the observables we consider, each parton has its own independent track function. Hadronization correlations are captured by power corrections (beyond the scope of this chapter).

Consider the cross section for an IRC safe observable e measured using partons

$$\frac{d\sigma}{de} = \sum_N \int d\Pi_N \frac{d\sigma_N}{d\Pi_N} \delta[e - \hat{e}(\{p_i^\mu\})], \quad (3.2)$$

where we drop possible convolutions with PDFs to keep the notation simple. Here, Π_N denotes N -body phase space, $d\sigma_N/d\Pi_N$ is the corresponding partonic cross section, and $\hat{e}(\{p_i\})$ implements the measurement on the partonic four-momenta p_i^μ . Since e is an IRC safe observable, the KLN theorem [59, 60] guarantees a cancellation of final state IR divergences between real and virtual diagrams. The cross section for the same observable measured using only tracks is

$$\frac{d\sigma}{d\bar{e}} = \sum_N \int d\Pi_N \frac{d\bar{\sigma}_N}{d\Pi_N} \int \prod_{i=1}^N dx_i T_i(x_i) \delta[\bar{e} - \hat{e}(\{x_i p_i^\mu\})], \quad (3.3)$$

where $T_i(x_i)$ is the track function for parton i . This equation defines a matching onto track functions where $d\bar{\sigma}_N/d\Pi_N$ represents the short distance matching coefficient, which is calculable in perturbation theory. In the absence of track functions, $d\sigma/d\bar{e}$ would exhibit a mismatch between real and virtual diagrams in the form of uncompensated IR

$$\left| \text{Diagram} \right|^2 = \left| \text{Diagram} \right|^2 + \left| \text{Diagram} \right|^2$$

$$\sigma_3 = \bar{\sigma}_3 + \bar{\sigma}_2 \otimes T_q^{(1)}$$

Figure 3.1: Schematic relationship between the partonic matrix element σ_3 and the matching coefficient $\bar{\sigma}_3$ for $e^+e^- \rightarrow q\bar{q}g$. Here, black (blue) dots represent the tree-level ($\mathcal{O}(\alpha_s)$) track functions. Diagrams with emissions from the other quark leg are elided for simplicity. Note the trivial matching condition $\sigma_2 = \bar{\sigma}_2$.

divergences in the partonic computation. The track functions absorb these IR divergences, and the partonic cross section $\bar{\sigma}_N$ is correspondingly modified with respect to σ_N . We will show below for the example of $e^+e^- \rightarrow q\bar{q}g$ how the mismatch in the absence of $T_i(x_i)$ occurs. Fig. 3.1 shows schematically how we determine the IR-finite matching coefficient $\bar{\sigma}_3$ for this case, by using that Eq. (3.3) is valid both at the hadronic and partonic level. The fact that we consider factorizable (otherwise) IRC-safe observables modified to include only charged particles and that collinear divergences are known to be universal in QCD [61, 62, 63] guarantees a valid matching to all orders in the strong coupling constant α_s .

At leading order (LO) in α_s , the cross section depends on a single partonic multiplicity N and there are no IR divergences implying $\bar{\sigma}_N^{(0)} = \sigma_N^{(0)}$. The LO $T_i^{(0)}(x_i)$ is simply a finite distribution which can be obtained directly from the energy fraction of charged particles in a jet initiated by a parton i . Ideally, we would extract this information from data, but just for illustrative purposes, we can determine it from (tuned) Monte Carlo event generators. We stress that our formalism does not rely on the use of these programs nor on their built-in hadronization models. In Fig. 3.2, we show the track functions obtained from pure quark and gluon jet samples produced by PYTHIA 8.150 [1, 2] and clustered using the anti- k_T algorithm [64] in FASTJET 2.4.4 [65]. (To extract the track function at next-to-leading order (NLO) we use Eq. (3.11); the jet radius R is correlated with the RG scale μ .) As expected, the up- and down-quark track functions are very

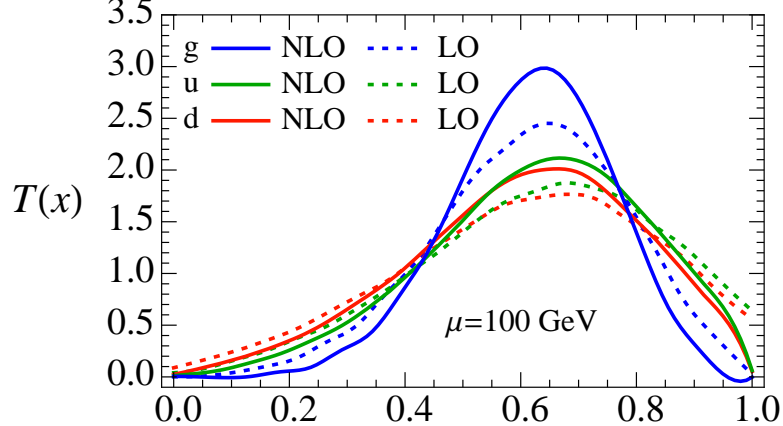


Figure 3.2: LO (dotted) and NLO (solid) track functions extracted in PYTHIA from the fraction of the jet energy carried by charged particles.

similar, with a peak at $x = 0.6$. This means that on average 60% of the energy of the initial quark is contained in charged hadrons, in agreement with a recent CMS study [66]. The small difference between up and down is due to strangeness, since $u\bar{s}$ mesons are charged whereas $d\bar{s}$ mesons are neutral. Because gluons have a larger color factor than quarks, they yield a higher track multiplicity, and the corresponding track functions are narrower, as expected from the central limit theorem.

Formally, the (bare) track function is defined in QCD in a fashion analogous to the unpolarized FF (cf. [67, 68]). Expressed in terms of light-cone components,

$$T_q(x) = \int dy^+ d^2 y_\perp e^{ik^- y^+/2} \frac{1}{2N_c} \sum_{C,N} \delta\left(x - \frac{p_C^-}{k^-}\right) \times \text{tr} \left[\frac{\gamma^-}{2} \langle 0 | \psi(y^+, 0, y_\perp) | CN \rangle \langle CN | \bar{\psi}(0) | 0 \rangle \right], \quad (3.4)$$

where ψ is the quark field, C (N) denote charged (neutral) hadrons, and p_C^- is the large momentum component of all charged particles. Whereas the FF describes the energy fraction carried by an individual hadron, the track function describes the energy fraction carried by all charged particles. As for the FF, gauge invariance requires the addition of eikonal Wilson lines. The gluon track function is defined analogously [69].

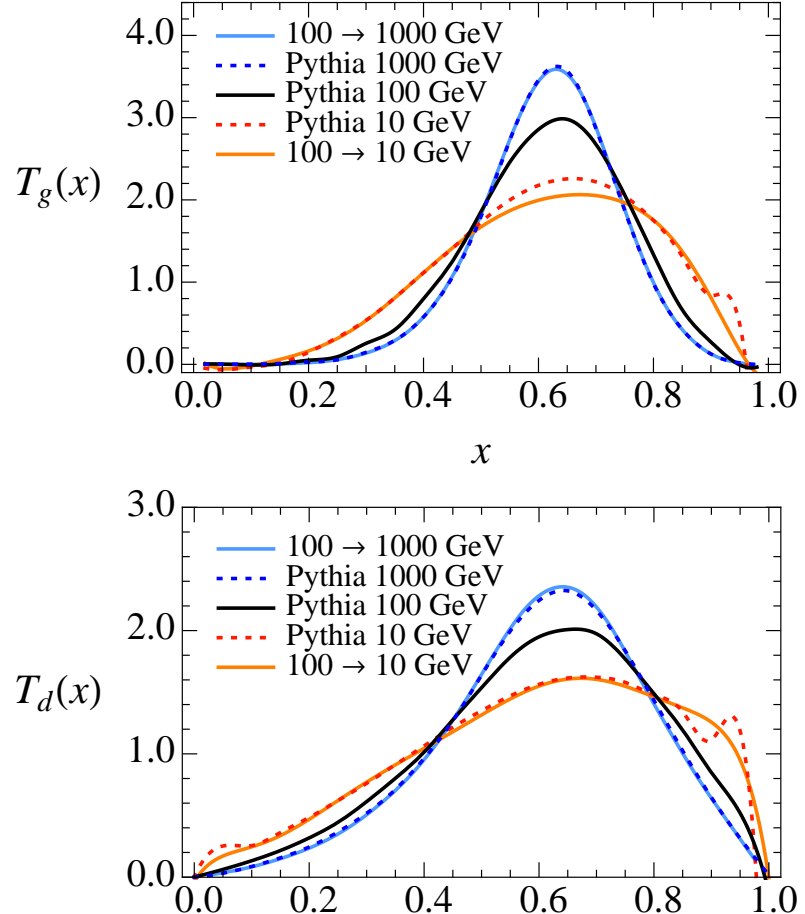


Figure 3.3: The evolution of the NLO gluon (top) and d -quark (bottom) track functions compared to PYTHIA. Starting from $\mu = 100 \text{ GeV}$ (shown in Fig. 3.2), we evolve using Eq. (3.6) down to $\mu = 10 \text{ GeV}$ and up to $\mu = 1000 \text{ GeV}$. The bumps in the PYTHIA distributions near $x = 0, 1$ at $Q = 10 \text{ GeV}$ correspond to genuine non-perturbative effects at Λ_{QCD} .

3.3 NLO Track Function

Treating the intermediate states in Eq. (3.4) partonically, we obtain the bare track functions $T_{i,\text{bare}}^{(1)}$ at NLO in pure dimensional regularization with $d = 4 - 2\epsilon$,

$$\begin{aligned} T_{i,\text{bare}}^{(1)}(x) &= \frac{1}{2} \sum_{j,k} \int dz \left[\frac{\alpha_s(\mu)}{2\pi} \left(\frac{1}{\epsilon_{\text{UV}}} - \frac{1}{\epsilon_{\text{IR}}} \right) P_{i \rightarrow jk}(z) \right] \\ &\quad \times \int dx_1 dx_2 T_j^{(0)}(x_1, \mu) T_k^{(0)}(x_2, \mu) \\ &\quad \times \delta[x - zx_1 - (1-z)x_2], \end{aligned} \quad (3.5)$$

which arise from collinear splittings, controlled by the timelike Altarelli-Parisi splitting functions $P_{i \rightarrow jk}(x)$ [7]. In contrast with the analogous partonic FF calculation, track functions involve contributions from both branches of the splitting. Renormalizing the ultraviolet divergences in Eq. (3.5) in $\overline{\text{MS}}$ leads to the evolution equation for the track function

$$\begin{aligned} \mu \frac{d}{d\mu} T_i(x, \mu) &= \frac{1}{2} \sum_{j,k} \int dz dx_1 dx_2 \frac{\alpha_s(\mu)}{\pi} P_{i \rightarrow jk}(z) \\ &\quad \times T_j(x_1, \mu) T_k(x_2, \mu) \delta[x - zx_1 - (1-z)x_2]. \end{aligned} \quad (3.6)$$

Like for a PDF, the track function can be extracted at one scale and RG evolved to another scale, and the evolution preserves the normalization in Eq. (3.1). Unlike a PDF, Eq. (3.6) involves a convolution of two track functions at NLO (and more convolutions at higher orders corresponding to multiple branchings), so it is numerically more involved to perform the μ -evolution. At leading logarithmic (LL) order, the RG evolution in Eq. (3.6) is equivalent to a parton shower, and Fig. 3.3 demonstrates excellent agreement between our numerical evolution and the parton shower in PYTHIA.

For a calculation at NLO, both the partonic cross section and the track functions have IR divergences which cancel in Eq. (3.3). To demonstrate this in a simple example, consider the process $e^+e^- \rightarrow \text{hadrons}$ at a center-of-mass energy Q where one measures

the total energy fraction w of charged particles. At NLO the partonic process is $e^+e^- \rightarrow q\bar{q}g$, whose kinematics are described by the energy fractions y_1 and y_2 of the quark and anti-quark. Applying Eq. (3.3) we find

$$\begin{aligned} \frac{d\sigma}{dw} &= \int dy_1 dy_2 \frac{d\bar{\sigma}}{dy_1 dy_2} \int dx_1 dx_2 dx_3 T_q(x_1) T_q(x_2) T_g(x_3) \\ &\quad \times \delta(w - [y_1 x_1 + y_2 x_2 + (2 - y_1 - y_2)x_3]/2), \end{aligned} \quad (3.7)$$

since $T_q = T_{\bar{q}}$. The matching coefficient $d\bar{\sigma}$ is extracted by evaluating this equation at the partonic level (see Fig. 3.1). We then use it in Eq. (3.7) together with non-perturbative hadronic track functions to obtain the physical cross section $d\sigma/dw$. At the LO partonic level

$$\frac{d\sigma^{(0)}}{dy_1 dy_2} = \sigma^{(0)} \delta(1 - y_1) \delta(1 - y_2), \quad (3.8)$$

where $\sigma^{(0)}$ is the total Born cross section. At NLO, the cross section can be expressed using plus-functions as

$$\begin{aligned} \frac{d\sigma^{(1)}}{dy_1 dy_2} &= \sigma^{(0)} \frac{\alpha_s(\mu) C_F}{2\pi} \left\{ \left(\frac{\pi^2}{2} - 4 \right) \delta(1 - y_1) \delta(1 - y_2) + \frac{\theta(y_1 + y_2 - 1)(y_1^2 + y_2^2)}{2(1 - y_1)_+(1 - y_2)_+} \right. \\ &\quad + \delta(1 - y_1) \left[- \frac{1}{\epsilon_{\text{IR}}} \frac{P_{q \rightarrow qg}(y_2)}{C_F} + (1 + y_2^2) \left[\frac{\ln(1 - y_2)}{1 - y_2} \right]_+ \right. \\ &\quad \left. \left. + \frac{P_{q \rightarrow qg}(y_2)}{C_F} \ln \frac{y_2 Q^2}{\mu^2} + 1 - y_2 \right] + (y_1 \leftrightarrow y_2) \right\}, \end{aligned} \quad (3.9)$$

where $C_F = 4/3$ and both real and virtual contributions are included. The $1/\epsilon_{\text{IR}}$ -divergences in $\sigma^{(1)}$ are cancelled by the ones in $T^{(1)}$ from Eq. (3.5), and the finite remainder defines $\bar{\sigma}^{(1)}$ in $\overline{\text{MS}}$. (For different IR regulators, the track function may also contribute finite terms to the matching.) By performing this kind of matching calculation, one can determine $\bar{\sigma}_N$ for any process to any order in α_s . For the case of Eq. (3.9) which involves a single scale Q , we choose $\mu \simeq Q$ to minimize the logarithms in $\bar{\sigma}$. In Fig. 3.4 we show the LO and NLO distributions for the energy fraction w , using the track

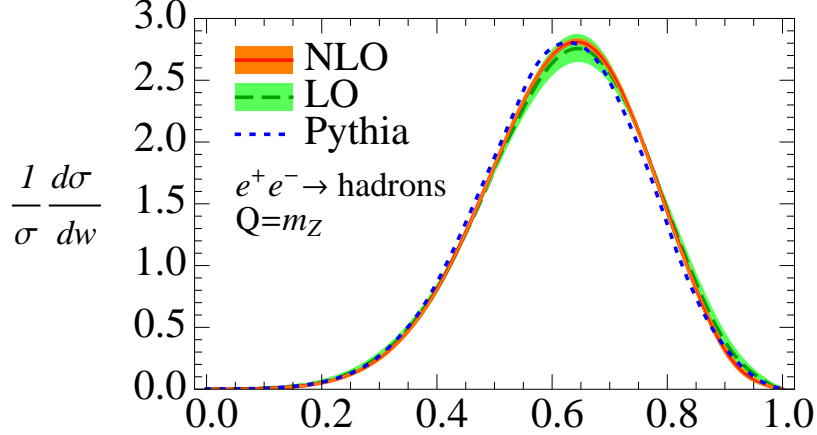


Figure 3.4: Normalized distribution of the energy fraction w of charged particles in e^+e^- at $Q = 91$ GeV, calculated at LO (green) and NLO (orange), compared with PYTHIA (blue). The uncertainty bands are obtained by varying μ between $Q/2$ and $2Q$, and do not include track function uncertainties.

functions extracted from PYTHIA by means of Eq. (3.11). There is good convergence from LO to NLO and our fixed-order calculation agrees well with PYTHIA.

Ultimately, we are interested in applying the track function formalism to jet-based measurements at the LHC, which typically involve multiple scales. For narrow well-separated jets, though, the contributions from soft radiation are power-suppressed, so the energy fraction x of the charged particles within a single jet depends on the jet scale

$$\mu_J \simeq p_T R, \quad (3.10)$$

where p_T is the transverse momentum of the jet and R denotes its azimuthal-rapidity size as defined by a jet algorithm (anti- k_T in this chapter). Indeed, by varying R (and trying different jet algorithms) while keeping $\mu_J = p_T R$ fixed, we find nearly identical x distributions in PYTHIA. At LO, the normalized distribution in x defines $T_i^{(0)}(x)$ itself, shown in Fig. 3.2. At NLO, the distribution of the energy fraction x within a jet initiated by parton i has the same form as for the jet charge distribution [58]

$$\frac{1}{\sigma_i} \frac{d\sigma_i}{dx} = \frac{1}{2} \sum_{j,k} \int dx_1 dx_2 dz \frac{\mathcal{J}_{ij}(p_T R, z, \mu_J)}{2(2\pi)^3 J_i(p_T R, \mu_J)} \quad (3.11)$$

$$\times T_j(x_1, \mu_J) T_k(x_2, \mu_J) \delta[x - zx_1 - (1 - z)x_2].$$

The jet functions $J_i(p_T R, \mu)$ [70] arise from the $1/\sigma_i$ normalization factor and describe jet production without any additional measurement. The matching coefficients are \mathcal{J}_{ij} [71, 58]. At NLO there is at most a $1 \rightarrow 2$ splitting which completely fixes the kinematics, so the same \mathcal{J}_{ij} appear in the jet charge [58] and in fragmentation inside an identified jet [72, 73]. The coefficients will not be the same at higher orders. We can invert Eq. (3.11) to determine the NLO track functions in Fig. 3.2.

3.4 Application to Higgs Plus One Jet

As a track-based measurement relevant for the LHC, consider the track-only jet mass spectrum in pp to Higgs plus one jet. This example is more complicated than the e^+e^- example above since it involves several scales: the hard scale set by the transverse momentum of the jet p_T^J , the jet mass scale m_J , and the scale associated with soft radiation m_J^2/p_T^J . In a resummed jet mass calculation, one would need to treat each emission in the exponentiated soft function as hadronizing independently, i.e. convolved with its own track function [69]. At LL order, however, we can use the fact that the parton shower already describes the numerous parton emissions that build up the jet mass distribution. Thus, a correct and instructive use of our formalism at LL is to run the perturbative PYTHIA parton shower down to a low scale $\mu \simeq \Lambda_{\text{QCD}}$ and match each final state parton onto a track function (also evolved to $\mu \simeq \Lambda_{\text{QCD}}$).

In Fig. 3.5, we show the track mass \bar{m}_J spectrum using the E-scheme [74] for the anti- k_T jet algorithm with $R = 1.0$. We impose realistic cuts on the jet rapidity η_J and p_T^J at the calorimeter level (using all the particles), to select the same events for both curves. There is excellent agreement between the track function and the Lund hadronization model [75] in PYTHIA, which is a non-trivial check considering that the track functions were originally extracted from PYTHIA using jet energies (and not jet mass) at $\mu = 100$ GeV. Since the track function does not include correlations between the hadronization

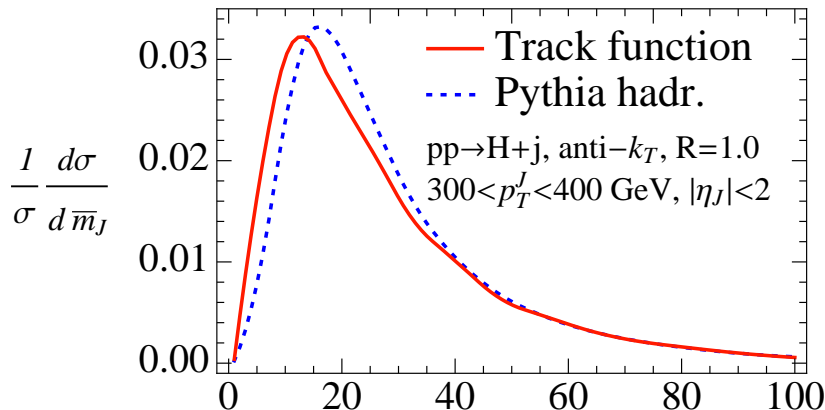


Figure 3.5: Track mass distribution in $pp \rightarrow H + \text{jet}$ obtained from the PYTHIA parton shower matched onto either track functions or the Lund string model.

of different partons, the agreement in Fig. 3.5 shows that independent fragmentation is an excellent approximation for these observables. The small difference between the two distributions in the peak region is due to nonperturbative power corrections, which to first approximation can be described by a shift in m_J^2 (see e.g. [76, 74, 77, 78]).

3.5 Conclusions

Despite the advantages of using track-based observables for pile-up suppression, it should be noted that the track functions have a rather large width (see Fig. 3.2). Fluctuations in the charged energy fraction produce an effective energy smearing for a track-based measurement relative to a calorimetric one. To partially address this issue, one can focus on observables for which the track function would only have a modest effect, such as for dimensionless ratios of observables. A particularly useful example are N -subjettiness ratios [79], which are relevant for jet substructure studies. Though a calculation of such ratios is beyond the scope of this chapter, we plot in Fig. 3.6 the ratio of the jet mass to jet p_T in PYTHIA, measured using either tracks alone or all particles (calorimeter). As expected, the smearing effect is reduced since hadronization fluctuations are correlated between the numerator and denominator.

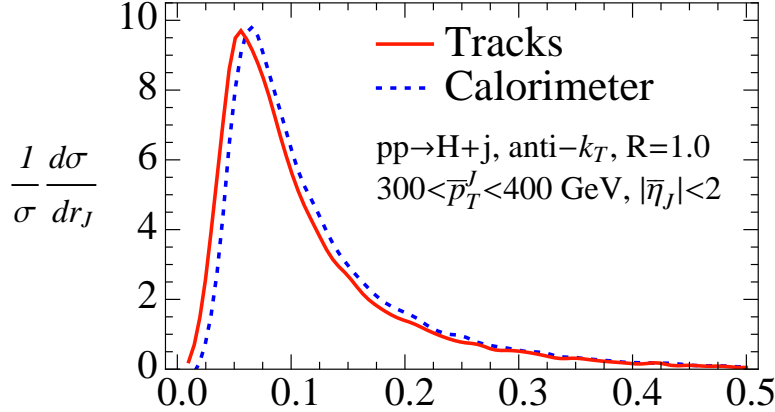


Figure 3.6: Comparison between track and calorimeter measurements of ratio of jet mass and jet p_T . Here the cuts are on \bar{p}_T^J and $\bar{\eta}_J$ from the tracks in the jet.

Given the potential experimental benefits from track-only measurements at high luminosities, we expect that track functions will offer an important theoretical handle for future precision jet studies at the LHC. Beyond the tests of our formalism against PYTHIA performed here, we stress that it is possible to systematically improve the accuracy of track-based predictions. At fixed order in α_s , one can calculate higher-order corrections for the (process-dependent) matching onto track functions. More ambitiously, one could match track functions onto automated NLO calculations, perhaps using a more convenient IR regulator (such as dipole subtraction [80]) rather than the $\overline{\text{MS}}$ scheme used here. To improve the accuracy of resummation, one needs to determine higher-order RG evolution of the track functions, and precision track-based studies would also require power corrections. Ultimately, one would want to follow the example of PDFs and extract track functions for the LHC from global fits to data.

This chapter is a reprint of material as it appears in “Calculating Track-Based Observables for the LHC,” H.-M. Chang, M. Procura, J. Thaler and W. J. Waalewijn, Phys. Rev. Lett. **111**, 102002 (2013) [arXiv:1303.6637 [hep-ph]], of which I was a co-author.

Chapter 4

Calculating Track Thrust with Track Functions

In e^+e^- event shapes studies at LEP, two different measurements were sometimes performed: a “calorimetric” measurement using both charged and neutral particles, and a “track-based” measurement using just charged particles. Whereas calorimetric measurements are infrared and collinear safe and therefore calculable in perturbative QCD, track-based measurements necessarily depend on non-perturbative hadronization effects. On the other hand, track-based measurements typically have smaller experimental uncertainties. In this chapter, we present the first calculation of the event shape *track thrust* and compare to measurements performed at ALEPH and DELPHI. This calculation is made possible through the recently developed formalism of track functions, which are non-perturbative objects describing how energetic partons fragment into charged hadrons. By incorporating track functions into soft-collinear effective theory, we calculate the distribution for track thrust with next-to-leading logarithmic resummation. Due to a partial cancellation between non-perturbative parameters, the distributions for calorimeter thrust and track thrust are remarkably similar, a feature also seen in LEP data.

4.1 Introduction

Detailed investigations of hadronic final states are crucial for understanding the dynamics of high-energy particle collisions. Charged particles play a particularly important role in these investigations. Whereas neutral particles can only be measured using calorimetry, charged particles can also be measured using tracking detectors, which allows for excellent momentum resolution and vertex identification. At colliders like LEP, tracks were used to perform precision tests of quantum chromodynamics (QCD) through measurements of e^+e^- event shapes and N -jet production rates [81, 82] (see Refs. [83, 84, 85, 86, 87] for reviews). These LEP studies also tested hadronization models through measurements of charged hadron inclusive distributions. Presently at the LHC, tracking information is used to improve jet measurements, to understand jet substructure, and to mitigate the effects of multiple “pileup” collisions per single bunch crossing.

Despite the experimental advantages offered by tracks, most experimental and theoretical studies are aimed at infrared and collinear (IRC) safe observables, which include contributions from both neutral and charged particles. In contrast, there are comparatively few theoretical tools available to understand and predict track-based observables. While fragmentation functions (FFs) are useful for understanding the distribution of single charged particles, more general observables require non-perturbative information about charged particle correlations. For example, Refs. [57, 58] showed how new non-perturbative functions are needed to calculate the energy-weighted charge of a jet. Recently in Ref. [3], we introduced the formalism of *track functions*, which enables QCD calculations to be performed on a broad class of track-based observables where (otherwise) IRC-safe observables are modified to include only charged particles.

In this chapter, we show how to use track functions to calculate track-based e^+e^- event shapes in perturbative QCD. The track function $T_i(x, \mu)$ is a non-perturbative object which describes how an energetic parton i fragments to a collection of tracks carrying a fraction x of the original parton energy [3]. Like the FF and the jet charge distribution,

the track function has a well-defined renormalization group (RG) evolution in μ , such that one can measure $T_i(x, \mu)$ at one scale μ and use QCD perturbation theory to make predictions at another scale μ' . We will focus on the *track thrust* event shape and compare our calculations to LEP measurements made by the ALEPH [81] and DELPHI [82] collaborations.

Our previous work in Ref. [3] explained how to interface track functions with fixed-order calculations up to next-to-leading order (NLO). To get reliable predictions for track thrust, we need to include the effects of logarithmic resummation. With the help of soft-collinear effective theory (SCET) [88, 89, 90, 91], we obtain results at next-to-leading logarithmic accuracy (NLL) including $\mathcal{O}(\alpha_s)$ fixed-order matching contributions, i.e. up to NLL' order. This turns out to be sufficiently accurate to understand both the qualitative and quantitative behavior of the track thrust distribution.

We will show that ordinary (i.e. calorimeter) thrust and track thrust are remarkably similar, with the leading differences encoded in a small number of non-perturbative parameters. Since an extraction of track functions from data has not yet been performed, we estimate these non-perturbative parameters using Monte Carlo event generators that have been tuned to LEP data (PYTHIA 8 [1, 2] in this study). We find cancellations between the non-perturbative parameters, such that the predicted distributions for calorimeter thrust and track thrust are nearly identical, a feature also seen in LEP data. This behavior could have been anticipated based on the observation in Ref. [3] that hadronization effects are strongly correlated between the numerator and denominator of dimensionless track-based ratios. We can now put this qualitative observation on a firmer quantitative footing.

An interesting theoretical feature of our calculation is that hadronization effects enter directly into the track thrust resummation. In particular, non-perturbative track parameters appear in the anomalous dimensions of the (track-based) jet and soft functions, two important objects in the factorization theorem for the track thrust distribution. As a nice consistency check of our formalism, we find that the hard, jet, and soft anomalous dimensions still cancel, despite the appearance of these parameters. We also show how to incorporate the leading non-perturbative power correction in the track thrust distribution.

This chapter is structured as follows. Sec. 4.2 contains a summary of our results and the most significant plots, including a comparison to LEP data. The underlying technical details are discussed in the rest of the chapter. We review our track function formalism in Sec. 4.3 and calculate track thrust at $\mathcal{O}(\alpha_s)$ in Sec. 4.4. In Sec. 4.5 we present the factorization theorem for track thrust as well as the ingredients needed for a resummation up to NLL' order in SCET, with details on the RG evolution given in the appendices. A simple expression for track thrust at NLL order is derived in Sec. 4.6, which allows us to better understand the similarity between calorimeter and track thrust. Our final numerical results are presented in Sec. 5.2. We conclude in Sec. 4.8 with a discussion of possible generalizations of our results to other track-based observables.

4.2 Summary of Results

To begin, we define the two main event shapes used in our study: calorimeter thrust τ and track thrust $\bar{\tau}$. The classic event shape thrust [92] is defined as

$$T = \max_{\hat{t}} \frac{\sum_i |\hat{t} \cdot \vec{p}_i|}{\sum_i |\vec{p}_i|}, \quad (4.1)$$

where the sum runs over all final-state hadrons with momenta \vec{p}_i , and the unit vector \hat{t} defines the thrust axis. It is more convenient to work with

$$\tau \equiv 1 - T = \min_{\hat{t}} \frac{\sum_i (|\vec{p}_i| - |\hat{t} \cdot \vec{p}_i|)}{\sum_i |\vec{p}_i|}, \quad (4.2)$$

which we will refer to as “thrust” from now on. Since this is measured using all final-state hadrons (charged plus neutral), we call τ *calorimeter thrust*. *Track thrust* $\bar{\tau}$ is defined analogously to Eq. (4.2), except that the sum over i is restricted to charged particles in both the numerator and the denominator. In this chapter, a bar will always indicate a track-based quantity.

For the later discussion of the factorization theorem for track thrust in Sec. 4.5, it

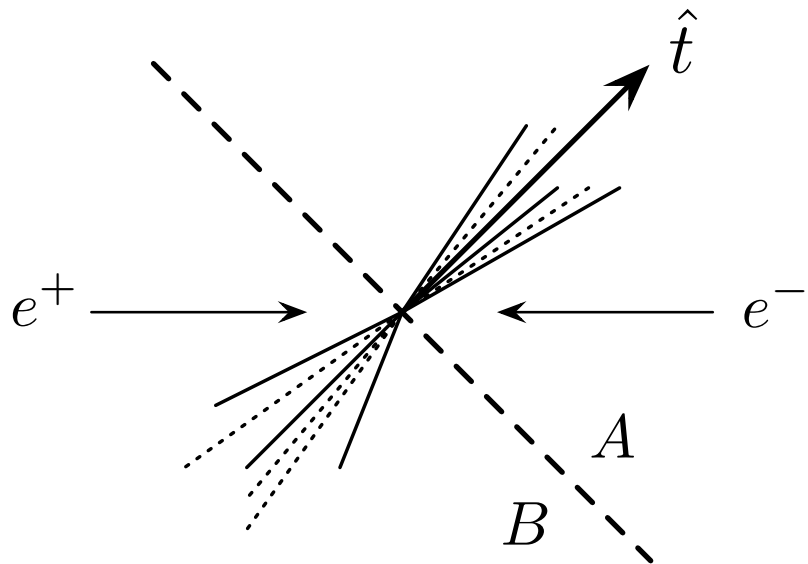


Figure 4.1: Illustration of the track thrust measurement in an e^+e^- event with jets initiated by a $q\bar{q}$ pair. Solid lines indicate charged particles and dashed lines indicate neutral particles. For track thrust, the thrust axis \hat{t} is determined by the charged particles alone. The event is divided into hemispheres A and B by a plane perpendicular to the thrust axis.

will be convenient to rewrite thrust in terms of contributions from hemispheres A and B , separated by a plane perpendicular to the thrust axis. The relevant kinematics are illustrated in Fig. 4.1. Fixing two light-cone vectors n^μ and \bar{n}^μ such that $n \cdot \bar{n} = 2$, the light-cone components of any four-vector w^μ are given by $w^+ = n \cdot w$, $w^- = \bar{n} \cdot w$, and w_\perp^μ , such that

$$w^\mu = w^+ \frac{\bar{n}^\mu}{2} + w^- \frac{n^\mu}{2} + w_\perp^\mu. \quad (4.3)$$

Choosing $n^\mu = (1, 0, 0, 1)$ and $\bar{n}^\mu = (1, 0, 0, -1)$ with the 3-axis aligned along \hat{t} , we can rewrite Eq. (4.2) for tracks as

$$\bar{\tau} = \frac{2(\bar{k}_A^+ + \bar{k}_B^-)}{(x_A + x_B)Q}. \quad (4.4)$$

Here, Q is the e^+e^- center-of-mass energy, $x_{A,B}$ are the energy fractions of charged particles in the respective hemispheres, and $\bar{k}_A^+ = \bar{k}_A^0 - \bar{k}_A^3$ and $\bar{k}_B^- = \bar{k}_B^0 + \bar{k}_B^3$ are the small light-cone momentum components of all the charged particles in hemisphere A and B , respectively. In this chapter, we ignore the subtleties of hadron masses and measurement schemes, which will affect power corrections (see Refs. [74, 78]).

At LEP, differential cross sections for calorimeter thrust τ and track thrust $\bar{\tau}$ were measured at both ALEPH [81] and DELPHI [82] on the Z pole ($Q = 91$ GeV). (To our knowledge, these are the only two experiments with public data on track thrust.) In both experiments, measurements were unfolded to the hadron level (including both charged and neutral hadrons for τ , and only charged hadrons for $\bar{\tau}$). The ALEPH and DELPHI normalized distributions are shown in Fig. 4.2, where we note a remarkable similarity between the calorimetric and track-based measurements. Indeed, for all bins outside of the peak region, the distributions are compatible within error bars, and a key goal of this chapter is to gain an analytic understanding for why the τ and $\bar{\tau}$ distributions are so similar. Note also that the experimental uncertainty is significantly smaller for the thrust measurements made using tracks.

In Fig. 4.3, we show the main result of the chapter: the resummed NLL' distri-

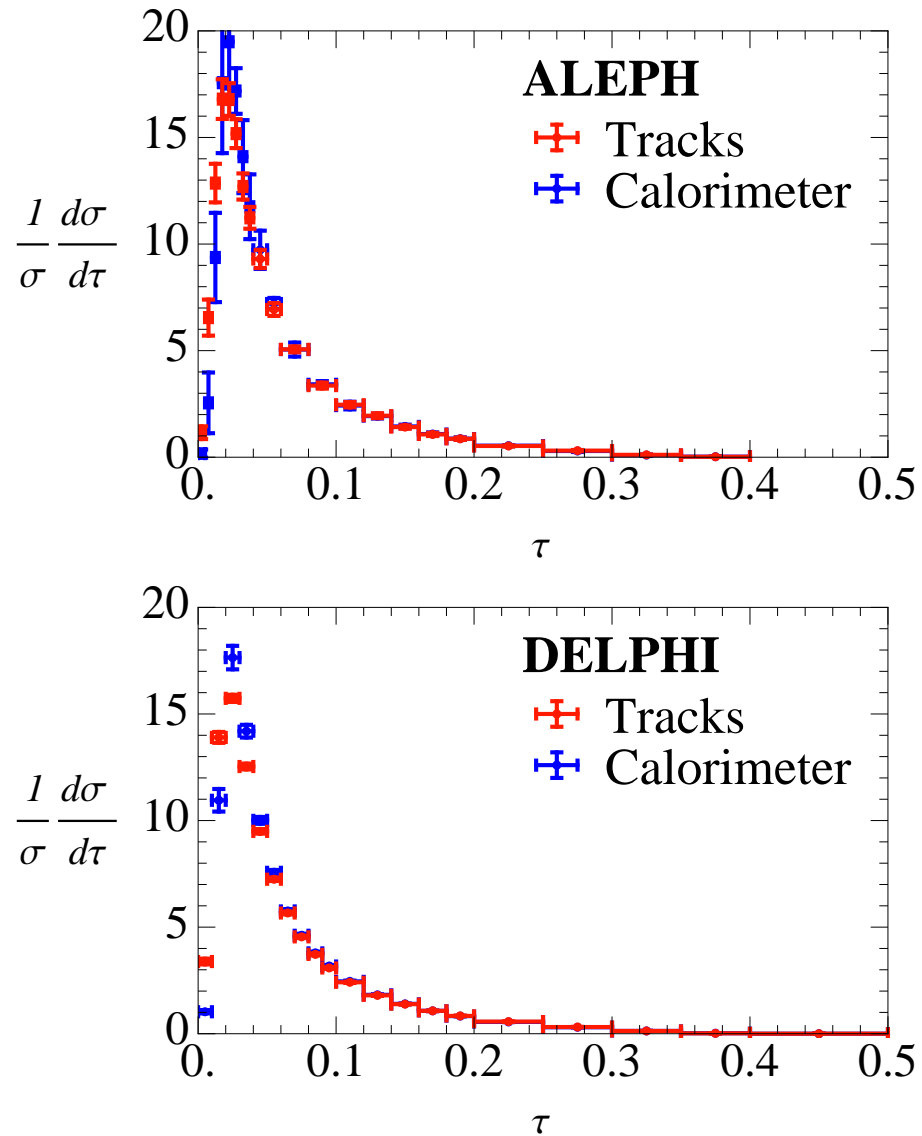


Figure 4.2: ALEPH (top) and DELPHI (bottom) measurements of calorimeter and track thrust. Error bars correspond to the statistical and systematic uncertainties added in quadrature. The experimental uncertainties associated with the track-based measurements are noticeably smaller.

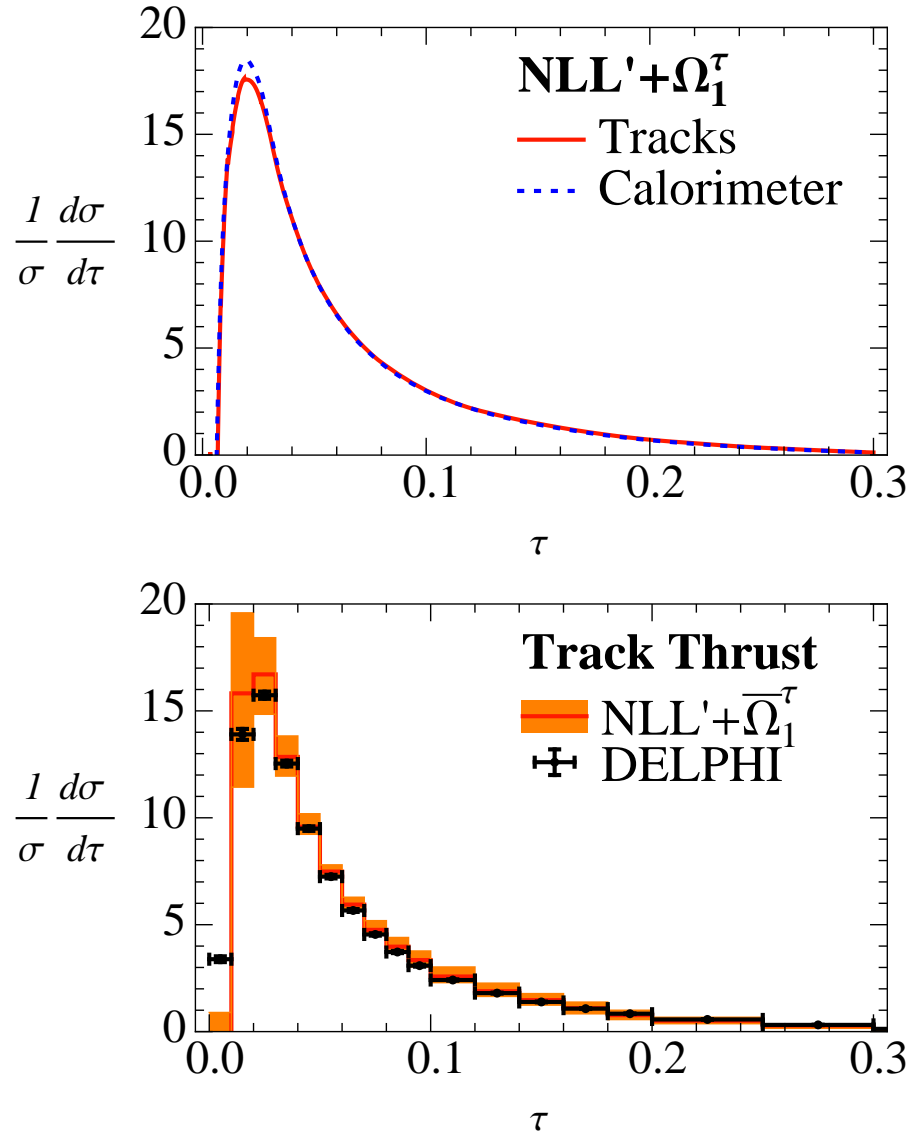


Figure 4.3: Top: NLL' distributions for calorimeter and track thrust including the leading non-perturbative correction Ω_1^τ . Next-to-leading logarithmic resummation is included together with $\mathcal{O}(\alpha_s)$ fixed-order matching contributions. The NLL' calculation exhibits the same qualitative similarity between calorimeter and track thrust as seen in LEP data. Bottom: comparing our analytic results to the DELPHI measurement. There is good quantitative agreement in the tail region where our NLL' calculation is most accurate. The theoretical uncertainties are from scale variation alone, and do not include the (correlated) uncertainties in α_s or Ω_1^τ , nor uncertainties in our track function extraction.

butions for calorimeter and track thrust. The latter was obtained using track functions extracted from PYTHIA 8, which itself was tuned to LEP data. The effects of the leading non-perturbative power correction are included through the parameters Ω_1^τ and $\bar{\Omega}_1^\tau$, which are different for calorimeter and track thrust. Interestingly, the NLL' distributions exhibit the qualitative similarity seen in data between calorimeter thrust and track thrust. We also see excellent quantitative agreement between our result and DELPHI measurements in the peak and tail regions. To the left of the peak there are deviations due to important non-perturbative corrections and in the far-tail region our calculation is missing (known) higher-order perturbative effects.

We now briefly discuss why the τ and $\bar{\tau}$ distributions are so similar, referring the reader to Sec. 4.6 for further details. In Eq. (4.4), the numerator is dominated by soft gluon emissions which broaden the hemisphere jets, whereas the denominator is mainly affected by fragmentation of the energetic quark and antiquark emerging from the underlying scattering process. These effects are thus controlled by different track functions (gluon vs. quark) but nearly cancel each other out due to the specific form of the (PYTHIA-based) track functions.

This cancellation is best understood by studying the resummed form of cumulative distributions

$$\Sigma(\tau^c) \equiv \int_0^{\tau^c} d\tau \frac{d\sigma}{d\tau}, \quad \bar{\Sigma}(\bar{\tau}^c) \equiv \int_0^{\bar{\tau}^c} d\bar{\tau} \frac{d\sigma}{d\bar{\tau}}. \quad (4.5)$$

As we show in Sec. 4.6, at NLL the difference between the cumulative distributions (for $\tau^c < 1/3$) is almost entirely captured by

$$\bar{\Sigma}(\bar{\tau}^c) \simeq \Sigma(\bar{\tau}^c) \times (3\bar{\tau}^c)^\Delta, \quad (4.6)$$

where the exponent Δ redistributes the cross section between the peak and tail regions. In terms of the strong coupling constant α_s and the quark color-factor $C_F = 4/3$, the explicit form of Δ is

$$\Delta = \frac{2\alpha_s C_F}{\pi} (g_1^L - q^L), \quad (4.7)$$

which depends on just two non-perturbative parameters: a logarithmic moment of a single gluon track function g_1^L and a logarithmic moment of two quark track functions q^L . The similarity between the τ and $\bar{\tau}$ distributions can thus be traced to a cancellation between g_1^L and q^L such that $|\Delta| \simeq 0.004$ (see Eq. (4.62)).

There are additional effects at NLL' from the fixed-order matching which yield further (small) differences between τ and $\bar{\tau}$ which are compatible with the ALEPH and DELPHI measurements. The non-perturbative power corrections Ω_1^τ and $\bar{\Omega}_1^\tau$ lead to a respective shift of the τ and $\bar{\tau}$ distributions by a very similar amount, but increase the difference in the peak region. Overall, though, the similarity between calorimeter and track thrust is well-described by the NLL distribution, and we expect similar cancellations to occur for a variety of (dimensionless) track-based observables.

4.3 Review of Track Function Formalism

A rigorous QCD description of track-based observables involves *track functions* $T_i(x, \mu)$ [3] as key ingredients. A parton (quark or gluon) with flavor index i and four-momentum p_i^μ hadronizes into charged particles (tracks) with total four-momentum $\bar{p}_i^\mu \equiv xp_i^\mu + \mathcal{O}(\Lambda_{\text{QCD}})$. The track function is the distribution in the energy fraction x of all tracks (irrespective of their multiplicity or individual properties), and it is normalized as

$$\int_0^1 dx T_i(x, \mu) = 1. \quad (4.8)$$

We will often refer to x as the track fraction.

In the context of factorization theorems, track functions can be used for track-based observables where partons in the underlying process are well-separated, i.e. where their typical pairwise invariant masses are larger than Λ_{QCD} . In this limit, each parton has its own independent track function, with correlations captured by power corrections (to be discussed more in Sec. 4.5.3). The track functions then encode process-independent

non-perturbative information about the hadronization. Like a FF or a parton distribution function (PDF), $T_i(x, \mu)$ absorbs infrared (IR) divergences in partonic calculations. It has a well-defined dependence on the RG scale μ through an evolution equation which is closely reminiscent of the jet charge distribution [58].

QCD calculations of track-based observables require the determination of matching contributions from partonic cross sections. First recall that the cross section for an IRC safe observable e measured using partons has the form

$$\frac{d\sigma}{de} = \sum_N \int d\Pi_N \frac{d\sigma_N}{d\Pi_N} \delta[e - \hat{e}(\{p_i^\mu\})], \quad (4.9)$$

where we drop possible convolutions with PDFs to keep the notation simple. Here, Π_N denotes the N -body phase space, $d\sigma_N/d\Pi_N$ is the corresponding partonic cross section, and $\hat{e}(\{p_i\})$ implements the measurement on the partonic four-momenta p_i^μ . Since e is IRC safe, a cancellation of final state IR divergences between real and virtual diagrams is guaranteed by the KLN theorem [59, 60].

For the same observable measured using only tracks, we can write the cross section in the form

$$\frac{d\sigma}{d\bar{e}} = \sum_N \int d\Pi_N \frac{d\bar{\sigma}_N}{d\Pi_N} \int \prod_{i=1}^N dx_i T_i(x_i) \delta[\bar{e} - \hat{e}(\{x_i p_i^\mu\})]. \quad (4.10)$$

Here, the partonic cross section $\bar{\sigma}_N$ should be thought of as a finite matching coefficient where the IR divergences in σ_N have been removed using some scheme. These IR (collinear) divergences are absorbed by the track function $T_i(x_i)$ (which is similarly scheme-dependent). The universality of collinear divergences in QCD [61, 62, 63] guarantees the feasibility of this matching to all orders in α_s . In Ref. [3] we explicitly showed the cancellation of IR-divergent terms in the partonic cross section $e^+e^- \rightarrow q\bar{q}g$, which enters the NLO distribution for the energy fraction of charged particles in e^+e^- collisions.

The (bare) track function is defined in QCD in a fashion analogous to the unpo-

larized FF (cf. [67, 68]). Expressed in terms of light-cone components (see Eq. (4.3)), the quark track function is

$$T_q(x) = \int dy^+ d^2 y_\perp e^{ik^- y^+/2} \frac{1}{2N_c} \sum_{C,N} \delta\left(x - \frac{p_C^-}{k^-}\right) \times \text{tr} \left[\frac{\vec{\eta}}{2} \langle 0 | \psi(y^+, 0, y_\perp) | CN \rangle \langle CN | \bar{\psi}(0) | 0 \rangle \right], \quad (4.11)$$

where ψ is the quark field, C (N) denote charged (neutral) hadrons, and p_C^- is the large momentum component of all charged particles. As for the FF, gauge invariance requires the addition of eikonal Wilson lines. The factor $1/(2N_c)$ in Eq. (4.11) comes from averaging over the color and spin of the hadronizing quark. The gluon track function is defined analogously. In d space-time dimensions,

$$T_g(x) = -\frac{1}{(d-2)(N_c^2-1)k^-} \times \int dy^+ d^2 y_\perp e^{ik^- y^+/2} \sum_{C,N} \delta\left(x - \frac{p_C^-}{k^-}\right) \times \bar{n}^\mu \bar{n}^\nu \langle 0 | G_{\mu\lambda}^a(y^+, 0, y_\perp) | CN \rangle \langle CN | G_\nu^{\lambda,a}(0) | 0 \rangle, \quad (4.12)$$

where $G_{\mu\nu} = \sum_a G_{\mu\nu}^a T^a$ is the QCD field-strength tensor and an average over colors and the $(d-2)$ polarizations of the gluon is performed.

For the sake of completeness, we also give SCET expressions for the quark and gluon track functions, given in a form which is invariant under non-singular gauge transformations. In terms of the SCET n -collinear quark $\chi_n(y)$ and gluon $B_{n\perp}^\mu(y)$ fields, we obtain

$$T_q(x) = 2(2\pi)^3 \frac{1}{2N_c} \sum_{C,N} \delta\left(x - \frac{p_C^-}{k^-}\right) \times \text{tr} \left[\frac{\vec{\eta}}{2} \langle 0 | [\delta(k^- - \bar{\mathcal{P}}) \delta^2(\mathcal{P}_\perp) \chi_n(0)] | CN \rangle \times \langle CN | \bar{\chi}_n(0) | 0 \rangle \right], \quad (4.13)$$

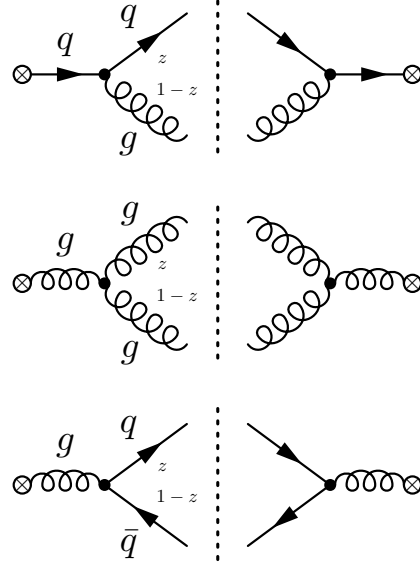


Figure 4.4: Perturbative QCD calculation of the quark (top) and gluon (middle and bottom) track functions at NLO from Eqs. (4.11) and (4.12) with partonic intermediate states. The NLO track function gets contributions from both branches of the collinear splitting. We do not display virtual diagrams, which vanish in pure dimensional regularization, or diagrams corresponding to Wilson line emissions.

and

$$\begin{aligned}
 T_g(x) = & -2(2\pi)^3 \frac{k^-}{(d-2)(N_c^2-1)} \sum_{C,N} \delta\left(x - \frac{p_C^-}{k^-}\right) \\
 & \times \langle 0 | [\delta(k^- - \bar{\mathcal{P}}) \delta^2(\mathcal{P}_\perp) \mathcal{B}_{n\perp}^{\mu,a}(0)] | CN \rangle \\
 & \times \langle CN | \mathcal{B}_{n\perp,\mu}^a(0) | 0 \rangle,
 \end{aligned} \tag{4.14}$$

where the momentum operators $\bar{\mathcal{P}} = \bar{n}\mathcal{P}$ (\mathcal{P}_\perp^μ) return the sum of the minus (perpendicular) *label* momentum components of all collinear fields on which they act. For the definition of the SCET fields, we refer the reader to e.g. Ref. [73].

Although the track function is a non-perturbative object, some of its properties can be calculated in perturbation theory. In particular, the RG evolution of the track function follows from its ultraviolet (UV) divergences, as we show below. A partonic calculation of the track function is also necessary for extracting the matching coefficient

$\bar{\sigma}_N$ in Eq. (4.10), by using that this equation holds at both the hadronic and partonic level.

At NLO, we can relate the bare track function $T_{i,\text{bare}}^{(1)}(x)$ to the tree-level track functions $T_j^{(0)}(x_1)$ and $T_k^{(0)}(x_2)$ via a collinear splitting $i \rightarrow jk$. As indicated in Fig. 4.4, this splitting is controlled by the timelike Altarelli-Parisi splitting functions $P_{i \rightarrow jk}(x)$ [7]. In pure dimensional regularization with $d = 4 - 2\epsilon$,

$$\begin{aligned} T_{i,\text{bare}}^{(1)}(x) &= \frac{1}{2} \sum_{j,k} \int_0^1 dz \left[\frac{\alpha_s(\mu)}{2\pi} \left(\frac{1}{\epsilon_{\text{UV}}} - \frac{1}{\epsilon_{\text{IR}}} \right) P_{i \rightarrow jk}(z) \right] \\ &\quad \times \int dx_1 dx_2 T_j^{(0)}(x_1) T_k^{(0)}(x_2) \\ &\quad \times \delta[x - zx_1 - (1-z)x_2]. \end{aligned} \quad (4.15)$$

If $j = k$, the factor $1/2$ is needed for identical particles, whereas if $j \neq k$ this factor gets cancelled by permutations of the two indices. In contrast to the FF or PDF, the NLO track function gets contributions from both branches of the splitting.

Renormalizing the UV divergences in the $\overline{\text{MS}}$ -scheme leads to the following evolution equation for the track function,

$$\begin{aligned} \mu \frac{d}{d\mu} T_i(x, \mu) &= \frac{1}{2} \sum_{j,k} \int_0^1 dz dx_1 dx_2 \frac{\alpha_s(\mu)}{\pi} P_{i \rightarrow jk}(z) \\ &\quad \times T_j(x_1, \mu) T_k(x_2, \mu) \\ &\quad \times \delta[x - zx_1 - (1-z)x_2]. \end{aligned} \quad (4.16)$$

By solving this, $T_i(x, \mu)$ can be extracted at one scale and RG evolved to another scale, and the evolution preserves the normalization in Eq. (4.8). We note that the number of convolutions in the track function RG equation (RGE) grows accordingly to the perturbative order due to multiple branchings, so it becomes numerically more involved to solve this RGE at higher orders. At leading logarithmic (LL) accuracy, the RG evolution in Eq. (4.16) is equivalent to a parton shower [58], and is in excellent agreement with the parton shower evolution in PYTHIA [3].

Throughout this chapter, we determine the track functions used in our analytic

formulae using the method of Ref. [3]. That is, we generate pure quark and gluon jet samples with PYTHIA 8.150 [1, 2], measure the normalized distribution for the track fraction x within those jets, and extract the track functions by numerically inverting the analytic expression for the same quantity at either LO or NLO. In all of the plots shown here, we use NLO track functions. We emphasize that the use of PYTHIA is not fundamental, and one could imagine extracting the same information from e^+e^- data. That said, since PYTHIA is tuned to LEP data, we expect these track functions to be realistic, but we have not attempted to assign uncertainties to the track functions.

One important point is the choice of α_s . Since we are working at NLL' order in the $\overline{\text{MS}}$ scheme, it would be natural to take the value from Ref. [93] of $\alpha_s(M_Z) = 0.1203 \pm 0.0079$. However, we have extracted the track functions from PYTHIA 8 whose default value is $\alpha_s(M_Z) = 0.1383$ for the final state parton shower, leading to a formal mismatch between our perturbative and non-perturbative objects. Given the large uncertainties at NLL', we will make an (imperfect) compromise, and extract the NLO track functions from PYTHIA using PYTHIA's value of α_s , but then use

$$\alpha_s(M_Z) = 0.125, \quad (4.17)$$

for all subsequent calculations. This choice, along with the leading power correction in Sec. 4.5.3, gives a good description of the LEP calorimeter thrust data. As emphasized in Ref. [93], there are strong correlations between the value of α_s and the leading power correction Ω_1^τ , so there are many different choices which would give comparable results; for example the PYTHIA value $\alpha_s(M_Z) = 0.1383$ matches the LEP calorimeter thrust distributions quite well with $\Omega_1^\tau = 0$. A proper treatment of the correlations between these parameters is beyond the scope of this chapter, so we will not show the uncertainties associated with $\alpha_s(M_Z)$ or Ω_1^τ .

4.4 Fixed Order Analysis of Track Thrust

The leading non-trivial process for thrust at the partonic level is $e^+e^- \rightarrow q\bar{q}g$, which appears at $\mathcal{O}(\alpha_s)$ in a fixed-order expansion. Given an e^+e^- collision at a center-of-mass energy Q , the kinematics of this process are determined by the partonic energy fractions $y_i = 2E_i/Q$ carried by the quark and antiquark, with the gluon energy fraction given by $y_3 = 2 - y_1 - y_2$. From this information, one can readily find the three-momenta of the partons \vec{p}_1 , \vec{p}_2 , and \vec{p}_3 and determine calorimeter thrust from Eq. (4.2). For three partons, finding the thrust axis is straightforward, and thrust takes a reasonably simple form

$$\tau = 1 - \frac{\max_{i=1,2,3} |\vec{p}_{\text{CM}} - 2\vec{p}_i|}{\sum_i |\vec{p}_i|}, \quad (4.18)$$

where we have defined

$$\vec{p}_{\text{CM}} \equiv \vec{p}_1 + \vec{p}_2 + \vec{p}_3. \quad (4.19)$$

To obtain the charged track three-momenta, one simply rescales the parton momenta by the track fraction x_i ,

$$\vec{p}_i = x_i \vec{p}_i. \quad (4.20)$$

Track thrust can then be calculated from Eq. (4.18) with all \vec{p} replaced by \vec{p} . Note that in the e^+e^- rest frame, $|\vec{p}_{\text{CM}}| = 0$, but $|\vec{p}_{\text{CM}}|$ is typically non-zero.

The calculation of the track thrust distribution at $\mathcal{O}(\alpha_s)$ is very similar to the one performed in Ref. [3] for the total charged particle energy fraction. Weighting each parton by the corresponding track function, we find

$$\begin{aligned} \frac{d\sigma}{d\bar{\tau}} = & \int_0^1 dy_1 dy_2 \frac{d\bar{\sigma}(\mu)}{dy_1 dy_2} \int_0^1 dx_1 dx_2 dx_3 T_q(x_1, \mu) T_q(x_2, \mu) \\ & \times T_g(x_3, \mu) \delta[\bar{\tau} - \bar{\tau}(y_1, y_2, x_1, x_2, x_3)]. \end{aligned} \quad (4.21)$$

where the measurement function $\bar{\tau}(y_1, y_2, x_1, x_2, x_3)$ implements Eq. (4.18). Note that $T_q = T_{\bar{q}}$, by charge conjugation. The relevant doubly differential partonic cross section is given in Ref. [3] in the $\overline{\text{MS}}$ scheme. Ignoring the singularities at $y_1 = 1$ and $y_2 = 1$

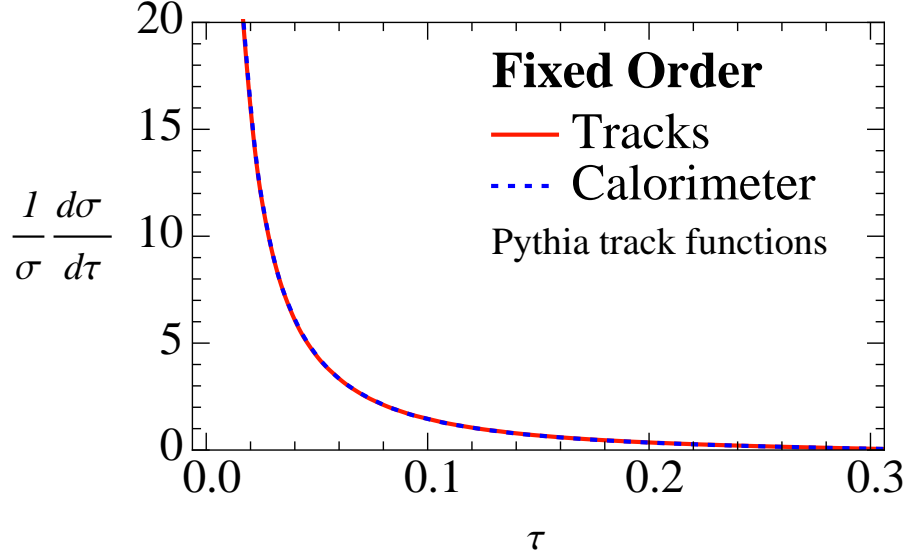


Figure 4.5: Distributions for calorimeter and track thrust from Eq. (4.21) at $\mathcal{O}(\alpha_s)$. The NLO track functions are extracted from PYTHIA 8.150 [1, 2] using the procedure in Ref. [3].

(which only contribute to a delta function at $\bar{\tau} = 0$),

$$\frac{d\bar{\sigma}(\mu)}{dy_1 dy_2} = \sigma_0 \frac{\alpha_s(\mu) C_F}{2\pi} \frac{\theta(y_1 + y_2 - 1)(y_1^2 + y_2^2)}{(1 - y_1)(1 - y_2)} + \dots \quad (4.22)$$

Here, σ_0 is the total Born cross section

$$\begin{aligned} \sigma_0 &= \frac{4\pi\alpha^2 N_c}{3Q^2} \\ &\times \left(Q_q^2 + \frac{(v_q^2 + a_q^2)(v_\ell^2 + a_\ell^2) - 2Q_q v_q v_\ell (1 - M_Z^2/Q^2)}{(1 - M_Z^2/Q^2)^2 + M_Z^2 \Gamma_Z^2/Q^4} \right), \end{aligned} \quad (4.23)$$

which depends on the (anti)quark flavor through its electric charge Q_q and vector and axial couplings v_q and a_q to the intermediate vector boson.

In Fig. 4.5 we compare the calorimeter versus track thrust distributions at $\mathcal{O}(\alpha_s)$, and find that they are remarkably similar. One might wonder if this small difference is a fundamental feature of Eq. (4.21) or simply an accident of the specific forms of our (PYTHIA-based) track functions. We can test this by calculating track thrust using the

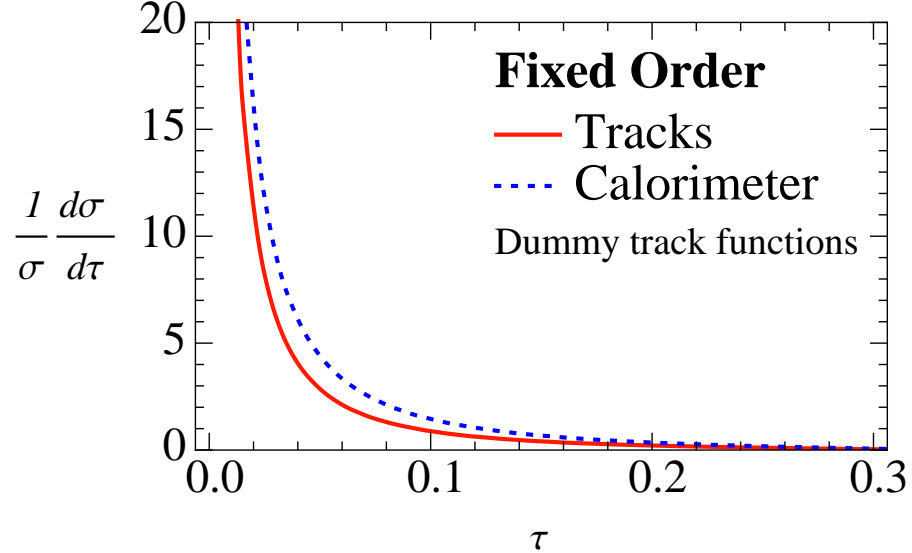


Figure 4.6: Distributions for calorimeter and track thrust using dummy track functions. Comparing to Fig. 4.5, we conclude that the similarity between τ and $\bar{\tau}$ is due to the specific form of the track function.

following *dummy* track functions

$$\begin{aligned} T_q(x, \mu = M_Z) &= 30 x^4(1 - x), \\ T_g(x, \mu = M_Z) &= 252 x^2(1 - x)^6. \end{aligned} \quad (4.24)$$

Indeed, the difference in Fig. 4.6 between track and calorimeter thrust is now large. Thus, the similarity between the τ and $\bar{\tau}$ distributions has to do with the specific properties of the track function. We will be able to achieve a better analytic understanding of why the effect of switching from calorimeter to tracks is so small in Sec. 4.6.

4.5 Factorization and Resummation of Track Thrust

The thrust distribution can be divided into three regions: the peak region ($\tau \simeq 2\Lambda_{\text{QCD}}/Q$), the tail region ($2\Lambda_{\text{QCD}}/Q \ll \tau < 1/3$), and the far-tail region ($1/3 \lesssim \tau \leq 1/2$). For $\tau \simeq 0$, events are described by two narrow back-to-back jets, each carrying about half of the center-of-mass energy. For τ close to the kinematic endpoint $1/2$, the

event is characterized by an isotropic multi-particle final state. At $\mathcal{O}(\alpha_s)$ from Sec. 4.4, the kinematic endpoint is $1/3$ corresponding to three maximally separated jets. We therefore do not obtain a reliable description of the far-tail region.

In this chapter, we are interested in properly describing the tail region of the thrust distribution, which dominantly consists of broader dijets and 3-jet events. In this region, the dynamics is governed by three well-separated scales: the *hard scale* ($\mu_H \simeq Q$) which is set by the e^+e^- center-of-mass energy Q , the *jet scale* ($\mu_J \simeq Q\sqrt{\tau}$) which is set by the momentum of the particles transverse to thrust axis, and the *soft scale* ($\mu_S \simeq Q\tau$) which is set by the typical energy of soft radiation between the hard jets. When $\tau \ll 1$, there will be large hierarchies between these scales, so we will need to resum double logarithms of the form $\alpha_s^n \ln^m \tau$ ($m \leq 2n$). Because we focus on the region where $\mu_S \simeq \tau Q \gg \Lambda_{\text{QCD}}$, the contribution from soft radiation is accurately described by perturbation theory, with non-perturbative effects captured by a series of power correction parameters. We will only use the leading power correction $\bar{\Omega}_1^\tau$ in our analysis, though if we were interested in describing the peak region correctly we would have to include a full non-perturbative shape function, see Sec. 4.5.3.

The leading-power factorization theorem for calorimeter thrust is well known [94, 95, 96, 97]:

$$\begin{aligned} \frac{d\sigma}{d\tau} = & \sigma_0 H(Q^2, \mu) \int_0^\infty dk ds_A ds_B S(k, \mu) J(s_A, \mu) J(s_B, \mu) \\ & \times \delta\left[\tau - \frac{1}{Q}\left(\frac{s_A}{Q} + \frac{s_B}{Q} + k\right)\right]. \end{aligned} \quad (4.25)$$

Here, σ_0 is the Born cross section from Eq. (4.23), H , J , and S are respectively the hard, jet, and soft functions, $s_{A,B}$ are the invariant mass-squareds of collinear radiation in hemispheres A and B , and k is the contribution to thrust from soft radiation.

The goal of this section is to translate Eq. (4.25) into a factorization theorem for track thrust. This procedure is made straightforward by applying the matching procedure

defined in Eq. (4.10) to the objects S and J . The final answer is:

$$\begin{aligned} \frac{d\sigma}{d\bar{\tau}} = & \sigma_0 H(Q^2, \mu) \int_0^\infty d\bar{k} d\bar{s}_A d\bar{s}_B \int_0^1 dx_A dx_B \\ & \times \bar{S}(\bar{k}, \mu) \bar{J}(\bar{s}_A, x_A, \mu) \bar{J}(\bar{s}_B, x_B, \mu) \\ & \times \delta\left[\bar{\tau} - \frac{2}{(x_A + x_B)Q} \left(\frac{\bar{s}_A}{Q} + \frac{\bar{s}_B}{Q} + \bar{k}\right)\right]. \end{aligned} \quad (4.26)$$

We now explain each of the ingredients in this formula, with details to appear in the subsequent subsections.

The delta function in Eq. (4.26) comes from the form of $\bar{\tau}$ given in Eq. (4.4). Dividing phase space into hemispheres A and B defined by the thrust axis, track thrust depends on the track fractions x_i , the rescaled track invariant mass-squared of collinear radiation $\bar{s}_i = s_i^{\text{tracks}}/x_i$, and the track soft contribution \bar{k} . The reason we are using the rescaled \bar{s}_i (and not s_i^{tracks} directly) is that $\bar{s}_A = Q\bar{k}_A^+$ and $\bar{s}_B = Q\bar{k}_B^-$ directly enter the definition of track thrust.

The hard function $H(Q^2, \mu)$ is the same as for calorimeter thrust and encodes virtual effects arising from the production of the $q\bar{q}$ pair at the hard scale. We give the form of H in Sec. 4.5.1.

The track thrust soft function $\bar{S}(\bar{k}, \mu)$, where $\bar{k} = \bar{k}_A^+ + \bar{k}_B^-$, describes the contribution to track thrust due to soft parton emissions which then hadronize into tracks. At NLO, soft radiation consists of only a single gluon emission so we can simply rescale

$$\bar{k} = xk, \quad (4.27)$$

where x is the track fraction of the gluon. This leads to a straightforward relationship between the ordinary thrust soft function and the track-based version, as discussed in Sec. 4.5.2. At higher orders, the expression for \bar{k} will become more complicated. The track-based soft function also incorporates information about non-perturbative physics through power corrections, and we discuss the leading power correction $\bar{\Omega}_1^\tau$ in Sec. 4.5.3.

The track-based jet function $\bar{J}(\bar{s}, x, \mu)$ encodes the (real and virtual) collinear

radiation in each hemisphere. At NLO, a hemisphere jet consists of just two partons, so

$$\bar{s}_i = \frac{x_1 x_2}{x_i} s_i, \quad (4.28)$$

where x_1 and x_2 are the track fractions of the two partons, x_i is the track fraction of the hemisphere ($i = A, B$), and s_i is the (calorimeter) invariant mass of the hemisphere. Unlike the calorimetric version, \bar{J} depends not only on the rescaled track invariant mass \bar{s} (given by Eq. (4.28) at NLO), but also on the track fraction x . For this reason, the track-based jet function is considerably more complicated than the usual jet function, and requires a more complicated matching calculation, as described in Sec. 4.5.4.

In order to resum logarithms, we not only need the forms of the H , \bar{J} , and \bar{S} , but also their anomalous dimensions. At LL order, this means incorporating the one-loop cusp anomalous dimension to resum the Sudakov double logs. In this chapter, we incorporate NLL resummation, which includes the two-loop cusp and the one-loop non-cusp anomalous dimension terms. Correspondingly, the running of α_s is consistently implemented at two loops, using the Z pole value for α_s in Eq. (4.17). Track thrust resummation is very similar to the calorimetric case, as discussed in Sec. 4.6 and the appendices. The main difference is that the anomalous dimensions of \bar{J} and \bar{S} now depend on non-perturbative parameters.

In addition to the ingredients above, we will incorporate fixed-order non-singular corrections described in Sec. 4.5.6. Following the primed counting scheme of Ref. [93], fixed-order matching contributions are included at one order higher in the expansion in α_s compared to the usual (non-primed) counting. Here we work to NLL' order which incorporates all of the the $\mathcal{O}(\alpha_s)$ terms contained in Eq. (4.21).

4.5.1 Hard Function

$$H(Q^2, \mu) = 1 + \frac{\alpha_s(\mu) C_F}{2\pi} \left[-\ln^2\left(\frac{Q^2}{\mu^2}\right) + 3 \ln\left(\frac{Q^2}{\mu^2}\right) - 8 + \frac{7\pi^2}{6} \right]. \quad (4.29)$$

The anomalous dimension of this object is

$$\begin{aligned} \mu \frac{d}{d\mu} H(Q^2, \mu) &= \gamma_H(Q^2, \mu) H(Q^2, \mu), \\ \gamma_H(Q^2, \mu) &= 2\Gamma_{\text{cusp}}[\alpha_s(\mu)] \ln \frac{Q^2}{\mu^2} + \gamma_H[\alpha_s(\mu)], \\ \gamma_H[\alpha_s] &= -\frac{3\alpha_s C_F}{\pi}. \end{aligned} \quad (4.30)$$

The cusp anomalous dimension Γ_{cusp} is given in Eqs. (C.6) and (C.7). We will use the non-cusp γ_H to perform a consistency check on our factorization theorem in Eq. (4.51).

4.5.2 Soft Function

At NLO, there is only one soft gluon emission, so in order to obtain the soft function, we can simply convolve the NLO thrust soft function with the gluon track function,

$$\bar{S}(\bar{k}, \mu) = \int_0^\infty dk S(k, \mu) \int_0^1 dx T_g(x, \mu) \delta(\bar{k} - xk), \quad (4.31)$$

where we have used the relationship between the kinematics in Eq. (4.27). This is the simplest possible version of the matching equation in Eq. (4.10).

The ordinary thrust soft function S is defined through the vacuum matrix element of eikonal Wilson lines and its one-loop perturbative expression for calorimeter thrust can be obtained from Refs. [97, 98],

$$S(k, \mu) = \delta(k) + \frac{\alpha_s(\mu) C_F}{2\pi} \left[-\frac{8}{\mu} \mathcal{L}_1\left(\frac{k}{\mu}\right) + \frac{\pi^2}{6} \delta(k) \right], \quad (4.32)$$

where the plus distributions \mathcal{L}_n are defined in Appendix E.

Using Eq. (4.31), the corresponding track-based version \bar{S} is given by

$$\begin{aligned}\bar{S}(\bar{k}, \mu) &= \int_0^1 \frac{dx}{x} T_g(x, \mu) \left(\delta(\bar{k}/x) + \frac{\alpha_s C_F}{2\pi} \left[-\frac{8}{\mu} \mathcal{L}_1 \left(\frac{\bar{k}}{x\mu} \right) + \frac{\pi^2}{6} \delta(\bar{k}/x) \right] \right) \\ &= \delta(\bar{k}) + \frac{\alpha_s C_F}{2\pi} \left[-\frac{8}{\mu} \mathcal{L}_1 \left(\frac{\bar{k}}{\mu} \right) + \frac{8g_1^L}{\mu} \mathcal{L}_0 \left(\frac{\bar{k}}{\mu} \right) + \left(\frac{\pi^2}{6} - 4g_2^L \right) \delta(\bar{k}) \right].\end{aligned}\quad (4.33)$$

While one naively might think that \bar{S} would depend on the entire track function, from the rescaling properties of the plus distributions in Eq. (E.4), we see that only two logarithmic moments of the gluon track function appear in the soft function, namely g_1^L and g_2^L , defined as

$$g_n^L(\mu) \equiv \int_0^1 dx T_g(x, \mu) \ln^n x. \quad (4.34)$$

From Eq. (4.33), we can derive the anomalous dimension of the track soft function

$$\begin{aligned}\mu \frac{d}{d\mu} \bar{S}(\bar{k}, \mu) &= \int_0^{\bar{k}} d\bar{k}' \gamma_{\bar{S}}(\bar{k} - \bar{k}', \mu) \bar{S}(\bar{k}', \mu), \\ \gamma_{\bar{S}}(\bar{k}, \mu) &= 4\Gamma_{\text{cusp}}[\alpha_s(\mu)] \frac{1}{\mu} \mathcal{L}_0 \left(\frac{\bar{k}}{\mu} \right) + \gamma_{\bar{S}}[\alpha_s(\mu)] \delta(k), \\ \gamma_{\bar{S}}[\alpha_s] &= -\frac{4\alpha_s C_F}{\pi} g_1^L.\end{aligned}\quad (4.35)$$

Interestingly, the non-cusp anomalous dimension depends on the logarithmic moment g_1^L of the gluon track function. This arises because the RG evolution sums multiple emissions, and thus the effect of the hadronization of these emissions must be exponentiated. Note that g_1^L depends (weakly) on the renormalization scale μ , but this effect is beyond the order that we are working.

4.5.3 Leading Power Correction

In the tail region of the thrust distribution, non-perturbative physics is captured via power corrections. As we will now review, the leading power correction simply acts as a shift of the soft function in Eq. (4.33) by an amount proportional to Λ_{QCD} [99, 100,

[101, 102]. The amount of the shift is different for calorimeter and track thrust, but the essential formalism is the same in both cases.

Given a hadronic final state with charged hadrons C and neutral hadrons N , we define a calorimeter measurement operator

$$\hat{k} |CN\rangle = \sum_{i \in C, N} (|\vec{p}_i| - |\hat{t} \cdot \vec{p}_i|) |CN\rangle, \quad (4.36)$$

where the sum runs over all hadrons in C and N , \hat{t} is the thrust axis, and \vec{p}_i is the three-momentum for hadron i . This operator measures the numerator of Eq. (4.2). The track measurement operator is almost the same, but the sum only runs over the charged hadrons C .

The soft function S describes the cross section to produce a measurement k in the presence of back-to-back eikonal quarks. Formally, it is defined as

$$S(k, \mu) = \frac{1}{N_c} \langle 0 | \text{tr} \bar{Y}_{\bar{n}}^T Y_n \delta(k - \hat{k}) Y_n^\dagger \bar{Y}_{\bar{n}}^* | 0 \rangle, \quad (4.37)$$

where $Y_n^\dagger(0) = P \exp(ig \int_0^\infty ds n \cdot A(ns))$ is a (ultra)soft Wilson line in the fundamental representation, $\bar{Y}_{\bar{n}}^\dagger$ is the analogue in the $\bar{3}$ representation, and the trace is taken over color indices.

For an additive observable like thrust, the soft function factorizes into a partonic perturbative part S^{part} (calculated already in Eq. (4.32)) and a non-perturbative part S^{NP} (also called the shape function [95, 103, 104, 105])

$$S(k) = \int_0^\infty d\ell S^{\text{part}}(k - \ell) S^{\text{NP}}(\ell). \quad (4.38)$$

In the tail region where $k \simeq Q\tau \gg \Lambda_{\text{QCD}}$, we can perform an operator product expansion (OPE) on $S^{\text{NP}}(\ell)$

$$S^{\text{NP}}(\ell) = \delta(\ell) - \delta'(\ell)\Omega_1^\tau + \dots, \quad (4.39)$$

where the leading power correction for thrust $\Omega_1^\tau \simeq \Lambda_{\text{QCD}}$ is defined via the non-

perturbative matrix element

$$\Omega_1^\tau = \frac{1}{N_c} \left\langle 0 \left| \text{tr} \bar{Y}_{\bar{n}}^T(0) Y_n(0) \hat{k} Y_n^\dagger(0) \bar{Y}_{\bar{n}}^*(0) \right| 0 \right\rangle. \quad (4.40)$$

The full soft function in Eq. (4.38) can then be approximated as a shift

$$S(k) \simeq S^{\text{part}}(k - \Omega_1^\tau) + \mathcal{O}\left(\frac{\alpha_s \Lambda_{\text{QCD}}}{k^2}\right) + \mathcal{O}\left(\frac{\Lambda_{\text{QCD}}^2}{k^3}\right). \quad (4.41)$$

This in turn leads to an overall shift in the thrust distribution, whose effect is most prominent at small τ .

The formalism above applies equally well to calorimeter thrust and track thrust. Focussing on calorimeter thrust, the value of Ω_1^τ must be extracted from data, since it is a fundamentally non-perturbative parameter. Typically, one expresses Ω_1^τ in terms of the universal power correction Ω_1 [102, 106, 77]

$$\Omega_1^\tau \equiv 2\Omega_1, \quad (4.42)$$

though strictly speaking, Ω_1 is only universal for measurements in the same universality class (see Ref. [78]). Putting aside that subtlety, the analysis in Ref. [93] extracted a value of $\Omega_1 = 0.264 \pm 0.213$ GeV in the $\overline{\text{MS}}$ scheme at NLL' from fits to (calorimeter) thrust data. We will therefore take a value of

$$\Omega_1^\tau = 0.5 \text{ GeV} \quad (4.43)$$

for our analysis of calorimeter thrust. As mentioned near Eq. (4.17), there are strong correlations between α_s and Ω_1^τ , and this choice gives a reasonable (but not perfect) description of LEP data.

For track thrust, we estimate that the parameter $\bar{\Omega}_1^\tau$ entering the analogous OPE for $\bar{S}^{\text{NP}}(\bar{k})$ is given by

$$\bar{\Omega}_1^\tau \simeq \langle x \rangle \Omega_1^\tau = 0.3 \text{ GeV}, \quad (4.44)$$

where we have taken the average track fraction $\langle x \rangle$ to be 0.6 [3]. This approximation is only justified if the matrix element defining $\bar{\Omega}_1^\tau$ is dominated by a single gluon emission and if the gluon track function has a narrow width. More generally, $\bar{\Omega}_1^\tau$ will encode hadronization correlations.

We emphasize that we have applied this non-perturbative shift $\bar{\Omega}_1^\tau$ to the track-based soft function directly,

$$\bar{S}(\bar{k}, \mu) \simeq \bar{S}^{\text{part}}(\bar{k} - \bar{\Omega}_1^\tau, \mu). \quad (4.45)$$

Note that a shift in the track soft function $\bar{S}(\bar{k})$ does not amount to an overall shift of the whole track thrust distribution due to the more complicated convolution structure in Eq. (4.26). Looking at Eq. (4.31), we could have tried to apply the usual shift Ω_1^τ to S instead, but this would have ignored the important fact that the track function T_g itself has non-perturbative power corrections. The power correction $\bar{\Omega}_1^\tau$ includes both of these effects. For the subleading power corrections (beyond the scope of this chapter), it may or may not be preferable to separately treat the non-perturbative corrections to S and T_g .

4.5.4 Jet Function

For the collinear radiation, described by the jet function, we need both the dependence on the energy fraction x of the collinear tracks as well as their contribution to the rescaled hemisphere track invariant mass-squared \bar{s} . The NLO jet function consists of one perturbative $q \rightarrow qg$ splitting whose branches hadronize independently. To carry out the matching in Eq. (4.10), we can use the matching coefficient $\mathcal{J}_{qg}(s, z, \mu)$ given in Refs. [107, 73], since the cancellation of IR divergences proceeds in an identical manner. Here, s is the qg invariant mass and z is the momentum fraction of the final quark. Inserting this matching coefficient into Eq. (4.10), the matching calculation yields

$$\begin{aligned} \bar{J}(\bar{s}, x, \mu) &= \int_0^\infty ds \int_0^1 dz \frac{\mathcal{J}_{qq}(s, z, \mu)}{2(2\pi)^3} \\ &\times \int_0^1 dx_1 dx_2 T_q(x_1, \mu) T_g(x_2, \mu) \\ &\times \delta[x - zx_1 - (1-z)x_2] \delta\left(\bar{s} - \frac{x_1 x_2}{x}\right), \end{aligned} \quad (4.46)$$

where we have used the kinematics in Eq. (4.28). The same coefficients $\mathcal{J}_{ij}(s, z, \mu)$ also appeared in the description of the fragmentation of a hadron inside a jet [72, 73], as they describe the perturbative splittings building up the jet radiation.

The expression for the matching coefficient is [107, 73]

$$\begin{aligned} \frac{\mathcal{J}_{qq}(s, z, \mu)}{2(2\pi)^3} &= \delta(s) \delta(1-z) \\ &+ \frac{\alpha_s(\mu) C_F}{2\pi} \left\{ \frac{2}{\mu^2} \mathcal{L}_1\left(\frac{s}{\mu^2}\right) \delta(1-z) + \frac{1}{\mu^2} \mathcal{L}_0\left(\frac{s}{\mu^2}\right) (1+z^2) \mathcal{L}_0(1-z) \right. \\ &\left. + \delta(s) \left[(1+z^2) \mathcal{L}_1(1-z) + \frac{1+z^2}{1-z} \ln z + 1-z - \frac{\pi^2}{6} \delta(1-z) \right] \right\}, \end{aligned} \quad (4.47)$$

so evaluating Eq. (4.46), we obtain

$$\begin{aligned} \bar{J}(\bar{s}, x, \mu) &= \left(\delta(\bar{s}) + \frac{\alpha_s C_F}{2\pi} \left[\frac{2}{\mu^2} \mathcal{L}_1\left(\frac{\bar{s}}{\mu^2}\right) - \frac{2g_1^L}{\mu^2} \mathcal{L}_0\left(\frac{\bar{s}}{\mu^2}\right) + \delta(\bar{s}) \left(g_2^L - \frac{\pi^2}{6} \right) \right] \right) T_q(x) \\ &+ \frac{\alpha_s C_F}{2\pi} \int_0^1 dx_2 \int_0^1 \frac{dz}{z} \left\{ \frac{1}{\mu^2} \mathcal{L}_0\left(\frac{\bar{s}}{\mu^2}\right) (1+z^2) \mathcal{L}_0(1-z) \right. \\ &+ \delta(\bar{s}) \left[(1+z^2) \mathcal{L}_1(1-z) + \ln \left(\frac{xz^2}{[x-(1-z)x_2]x_2} \right) (1+z^2) \mathcal{L}_0(1-z) \right. \\ &\left. \left. + 1-z \right] \right\} T_q\left(\frac{x - (1-z)x_2}{z}\right) T_g(x_2). \end{aligned} \quad (4.48)$$

Here we use that the track function vanishes outside the range $x \in [0, 1]$ to avoid writing explicit Heaviside functions. Unlike the soft function, the jet function depends on the full functional form of the quark and gluon track functions, and not just the logarithmic

moments. To perform these integrals numerically, we used the CUBA package [48].

The corresponding anomalous dimension is given by

$$\begin{aligned} \mu \frac{d}{d\mu} \bar{J}(\bar{s}, x, \mu) &= \int_0^{\bar{s}} d\bar{s}' \gamma_{\bar{J}}(\bar{s} - \bar{s}', \mu) \bar{J}(\bar{s}', x, \mu), \\ \gamma_{\bar{J}}(\bar{s}, \mu) &= -2\Gamma_{\text{cusp}}[\alpha_s(\mu)] \frac{1}{\mu^2} \mathcal{L}_0\left(\frac{\bar{s}}{\mu^2}\right) \\ &\quad + \gamma_{\bar{J}}[\alpha_s(\mu)] \delta(\bar{s}), \\ \gamma_{\bar{J}}[\alpha_s] &= \frac{\alpha_s C_F}{\pi} \left(2g_1^L + \frac{3}{2}\right). \end{aligned} \quad (4.49)$$

Note that the evolution only affects \bar{s} and not x . As for the soft function, the logarithmic moment of the gluon track function g_1^L contributes to the non-cusp anomalous dimension.

4.5.5 Resummation

In the effective field theory approach we follow here, the resummation of large double logarithms $\alpha_s^n \ln^m \tau$ ($m \leq 2n$) is achieved by evaluating the hard, jet, and soft functions at their natural scales μ_H , μ_J , and μ_S where they contain no large logarithms, and running them to a common scale μ using their respective RG equations.

These RG evolution kernels were implicit in the cross section in Eq. (4.26) and are given in Appendix C. Explicitly including them,

$$\begin{aligned} \frac{d\sigma}{d\bar{\tau}} &= \sigma_0 H(Q^2, \mu_H) U_H(Q^2, \mu_H, \mu) \\ &\quad \times \int d\bar{s}_A d\bar{s}'_A \bar{J}(\bar{s}_A - \bar{s}'_A, \mu_J) U_{\bar{J}}(\bar{s}'_A, \mu_J, \mu) \\ &\quad \times \int d\bar{s}_B d\bar{s}'_B \bar{J}(\bar{s}_B - \bar{s}'_B, \mu_J) U_{\bar{J}}(\bar{s}'_B, \mu_J, \mu) \\ &\quad \times \int d\bar{k} d\bar{k}' \bar{S}(\bar{k} - \bar{k}', \mu_S) U_{\bar{S}}(\bar{k}', \mu_S, \mu) \\ &\quad \times \delta\left[\bar{\tau} - \frac{2}{(x_A + x_B)Q} \left(\frac{\bar{s}_A}{Q} + \frac{\bar{s}_B}{Q} + \bar{k}\right)\right]. \end{aligned} \quad (4.50)$$

Consistency of the factorization theorem requires that the cross section is μ -independent at the order that we are working, implying a cancellation between the

anomalous dimensions. For the cusp anomalous dimension, this cancellation is the same as for calorimeter thrust. For the non-cusp pieces from Eqs. (4.30), (4.35), and (4.49), there are additional terms involving g_1^L in $\gamma_{\bar{S}}$ and $\gamma_{\bar{J}}$, but they cancel in the sum

$$\gamma_H^{\text{non-cusp}} + 2\gamma_{\bar{J}}^{\text{non-cusp}} + \gamma_{\bar{S}}^{\text{non-cusp}} = 0, \quad (4.51)$$

to fulfill consistency requirements.

An important question is the choice of scales μ_H , μ_J , and μ_S to use in this formula. While our focus is on the tail region of the thrust distribution, where $\mu_H \simeq Q$, $\mu_J \simeq \sqrt{\tau}Q$ and $\mu_S \simeq \tau Q$, we do want our formulas to be accurate for all values of τ . Since there are three distinct kinematic regions characterizing the thrust distribution, the resummation of the logarithms of τ must be handled in different ways. A smooth transition between the three regions is achieved through profile functions [105, 93] as described in Appendix D. Our choice of the profile parameters is such that resummation is turned off at $\bar{\tau} \simeq 1/3$, which is the $\mathcal{O}(\alpha_s)$ endpoint from Sec. 4.4. (This is in contrast to the higher-order calculation in Ref. [93, 108] where the resummation is only turned off at the true endpoint $\tau \simeq 1/2$.)

For the plots in Sec. 5.2, we calculate the cumulative version of Eq. (4.50)

$$\bar{\Sigma}(\bar{\tau}^c) \equiv \int_0^{\bar{\tau}^c} d\bar{\tau} \frac{d\sigma}{d\bar{\tau}} \quad (4.52)$$

at NLL' using the scales μ_H , μ_J , and μ_S set by the value of $\bar{\tau}^c$. We then take the numerical derivative of $\bar{\Sigma}(\bar{\tau}^c)$ to find the track thrust distribution (see Ref. [93] for a discussion of alternative choices). This derivative picks up both the explicit $\bar{\tau}$ -dependence as well as the implicit $\bar{\tau}$ -dependence of our scale choice for μ_H , μ_J , and μ_S . The differential version in Eq. (4.50) misses the latter contribution, though it is a small effect.

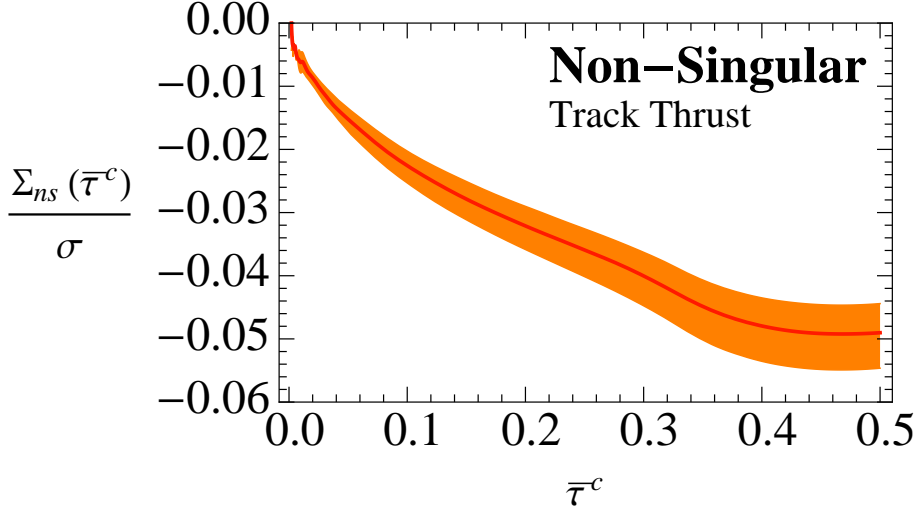


Figure 4.7: Non-singular contribution to the normalized cumulative thrust distribution at $\mathcal{O}(\alpha_s)$. The central value corresponds to $\mu = M_Z$, with the uncertainty bands from varying $\mu \in [M_Z/2, 2M_Z]$.

4.5.6 Non-Singular Contribution

The factorization theorem in Eqs. (4.26) and (4.50) includes all the terms in the track thrust distribution that are singular in τ as $\tau \rightarrow 0$. There is an additional non-singular contribution of $\mathcal{O}(\tau)$, which is thus important in the endpoint region. This contribution needs to be included to have our distribution formally accurate to $\mathcal{O}(\alpha_s)$ and is the last step in attaining NLL' accuracy.

We can extract the non-singular corrections by subtracting the singular terms (obtained from setting $\mu_H = \mu_J = \mu_S = \mu$ in Eq. (4.26)) from the fixed-order $\mathcal{O}(\alpha_s)$ cross section in Eq. (4.21). At the level of the cumulative cross section in Eq. (4.52)

$$\bar{\Sigma}_{ns}(\bar{\tau}^c) = \bar{\Sigma}_{FO}(\bar{\tau}^c) - \bar{\Sigma}_{sing}(\bar{\tau}^c). \quad (4.53)$$

Our extraction of $\bar{\Sigma}_{ns}(\bar{\tau}^c)$ is shown in Fig. 4.7. The fact that $\bar{\Sigma}_{ns}(\bar{\tau}^c = 0) = 0$ provides another consistency check of our formalism, showing that our factorization formula successfully reproduces the singular part of the $\mathcal{O}(\alpha_s)$ cross section. We use $\mu = M_Z$ as the central value for extracting $\bar{\Sigma}_{ns}(\bar{\tau}^c)$, and estimate perturbative uncertainties by

varying μ between $M_Z/2$ and $2M_Z$.

4.6 Simplifications at NLL

In both the LEP data in Fig. 4.2 and the fixed-order calculation in Fig. 4.5, we saw a remarkable similarity between the calorimeter and track thrust distributions. We will now try to understand this from our resummed calculation by looking at the leading effect of switching to tracks.

The first non-trivial order in the resummed distribution is NLL. This consists of evaluating Eq. (4.50) with only the leading order hard, jet, and soft functions, but including the subleading evolution kernels. Using the solutions to the RG equations in Appendix C, the NLL cumulative distribution is

$$\bar{\Sigma}(\bar{\tau}^c) = \sigma_0 e^{K_H} \left(\frac{Q^2}{\mu_H^2} \right)^{\eta_H} \frac{e^{K_{\bar{S}} - \gamma_E \eta_{\bar{S}}}}{\Gamma(1 + \eta_{\bar{S}})} \left(\frac{Q \bar{\tau}^c}{\mu_S} \right)^{\eta_{\bar{S}}} \times \int dx_A dx_B T_q(x_A, \mu_J) T_q(x_B, \mu_J) \left(\frac{x_A + x_B}{2} \right)^{\eta_{\bar{S}}}, \quad (4.54)$$

where γ_E is Euler's constant, and we have chosen to evolve the hard and soft scales to the jet scale μ_J . The functions $K_H(\mu_H, \mu_J)$, $\eta_H(\mu_H, \mu_J)$, $K_{\bar{S}}(\mu_S, \mu_J)$ and $\eta_{\bar{S}}(\mu_S, \mu_J)$ are given in Appendix C and depend on our choice for μ_H , μ_J , and μ_S , which we discuss below. Note that this expression contains an explicit dependence on the quark track functions T_q since they appear in the tree-level jet functions. Eq. (4.54) contains only the information needed at NLL accuracy, and therefore does not include the leading hadronization power correction or non-singular contributions.

There are various steps we can take to simplify the expression in Eq. (4.54). We first consider the scales μ_H , μ_J , and μ_S . In Sec. 4.5.5, we advocated the use of the profile functions in Appendix D to achieve a smooth transition between the different regions of the thrust distribution. Here, we simplify our choice of natural scales to obtain a more

illuminating analytic formula:

$$\mu_H = Q, \quad \mu_J = \sqrt{3\bar{\tau}^c}Q, \quad \mu_S = 3\bar{\tau}^cQ. \quad (4.55)$$

This choice has still the effect of turning off the resummation at $\bar{\tau}^c = 1/3$.

Second, we can simplify the dependence on the two quark track functions. Defining

$$q^L(\mu) \equiv \int dx_A dx_B T_q(x_A, \mu) T_q(x_B, \mu) \ln\left(\frac{x_A + x_B}{2}\right), \quad (4.56)$$

it is helpful to use the approximation

$$\int dx_A dx_B T_q(x_A) T_q(x_B) \left(\frac{x_A + x_B}{2}\right)^{\eta_{\bar{S}}} \approx \exp(q^L \eta_{\bar{S}}). \quad (4.57)$$

This is formally justified only for $\eta_{\bar{S}} \ll 1$, but for the (PYTHIA-based) track functions, the error is only a few percent even for $\eta_{\bar{S}} = 1$. By contrast, using a linear (as opposed to exponential) approximation in Eq. (4.57) would yield a $\simeq 20\%$ error at $\eta_{\bar{S}} = 1$.

Finally, because the only difference between the NLL evolution kernels for calorimeter thrust and track thrust appears in the non-cusp anomalous dimensions, we can write the track thrust cumulative $\bar{\Sigma}$ in terms of the calorimeter thrust cumulative Σ as

$$\bar{\Sigma}(\bar{\tau}^c) = \Sigma(\bar{\tau}^c) \exp(K_{\bar{S}} - K_S) \exp(q^L \eta_{\bar{S}}). \quad (4.58)$$

From Eq. (C.5), we find that the difference between $K_{\bar{S}}$ and K_S is

$$\begin{aligned} K_{\bar{S}}(\mu_S, \mu_J) - K_S(\mu_S, \mu_J) &= \frac{8C_F g_1^L}{\beta_0} \ln \frac{\alpha_s(\mu_J)}{\alpha_s(\mu_S)} \\ &\approx \frac{4\alpha_s C_F}{\pi} g_1^L \ln \frac{\mu_S}{\mu_J} \\ &= \frac{2\alpha_s C_F}{\pi} g_1^L \ln(3\bar{\tau}^c). \end{aligned} \quad (4.59)$$

Here we used the running of α_s to obtain the second line, and inserted the natural scales from Eq. (4.55) in the last step. (Since we only kept the leading term in α_s , different

choices for the scale of α_s correspond to effects beyond the order we are working.) Similarly, we find that $\eta_{\bar{S}}$ is given by

$$\begin{aligned}\eta_{\bar{S}}(\mu_S, \mu_J) &= -\frac{8C_F}{\beta_0} \ln \frac{\alpha_s(\mu_J)}{\alpha_s(\mu_S)} \\ &\approx -\frac{2\alpha_s C_F}{\pi} \ln(3\bar{\tau}^c).\end{aligned}\quad (4.60)$$

This leads to

$$\bar{\Sigma}(\bar{\tau}^c) \approx \Sigma(\bar{\tau}^c) \exp \left[\frac{2\alpha_s C_F}{\pi} (g_1^L - q^L) \ln(3\bar{\tau}^c) \right], \quad (4.61)$$

as anticipated in Eq. (4.6).

Based on Eq. (4.61), we now have a better understanding of why track thrust and calorimeter thrust are so similar. At NLL order, the difference between the cumulative distributions for track and calorimeter thrust is basically given by an exponential factor. However, this factor depends on g_1^L and q^L , which happen to be nearly equal for the track functions extracted from PYTHIA. For concreteness, we evaluate g_1^L and q^L at the scale $\mu \simeq 20$ GeV, though any choice of scale between μ_S and μ_J is acceptable at this order. We find

$$g_1^L \simeq -0.52, \quad q^L \in [-0.49, -0.54], \quad (4.62)$$

where the range corresponds to the variation between different quark flavors. This leads to a cancellation in Eq. (4.61), which is responsible for the similarity between the calorimeter and track thrust distributions. These parameters have only a mild μ -dependence, and the partial cancellation between g_1^L and q^L persists over a wide range of scales.

4.7 Numerical Results

With all of the ingredients for the track thrust distribution in place, we now show numerical results as we increase the accuracy of our calculation. In all cases, we show normalized cross sections $(1/\sigma)(d\sigma/d\tau)$, and use our (PYTHIA-based) NLO track

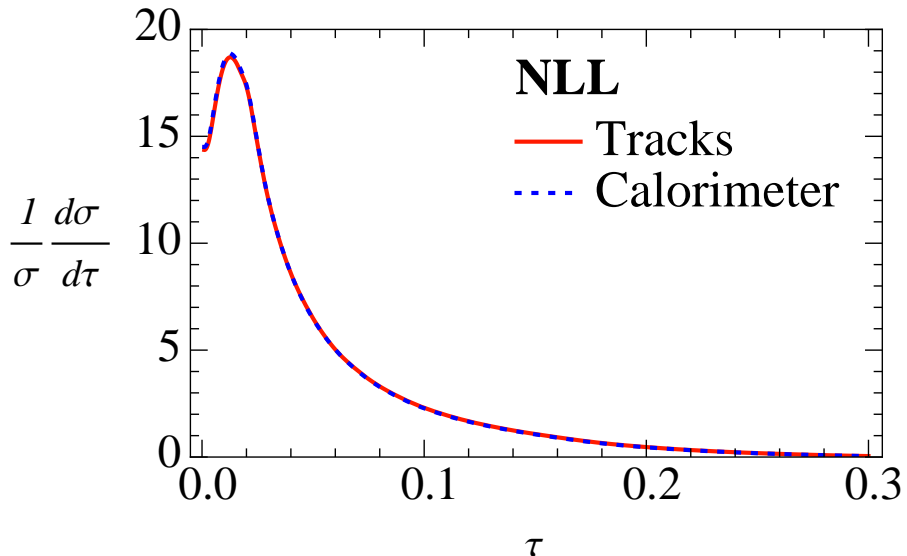


Figure 4.8: Track thrust and calorimeter thrust at NLL. As explained in Sec. 4.6, these distributions are remarkably similar.

functions as input.

In Fig. 4.8, we show the NLL result from Eq. (4.54) for calorimeter and track thrust. Here we use the central values for the canonical running scales described in Appendix D. As argued in Sec. 4.6, the difference between calorimeter and track thrust is very small at NLL order, and is in fact barely visible on this plot.

To achieve NLL' accuracy, we have to take into account higher-order terms in H , \bar{J} , and \bar{S} in Eq. (4.50), as well as the non-singular terms from Sec. 4.5.6. The result of going from NLL to NLL' is shown in Fig. 4.9, which compares the track thrust distributions in the peak and tail regions. The inclusion of the one-loop corrections to the hard, jet, and soft functions at NLL' reduces the purely perturbative uncertainty bands coming from scale variations. Note that this uncertainty estimate does not include the uncertainty associated with the value of $\alpha_s(M_Z)$ or with the input track functions.

The effect of the non-singular terms on the tail and far-tail regions are highlighted in Fig. 4.10. The inclusion of these terms guarantees that the cross section merges with the $\mathcal{O}(\alpha_s)$ fixed-order result in the region where the resummation is no longer important. It also ensures that the cross section vanishes beyond the $\mathcal{O}(\alpha_s)$ kinematic endpoint

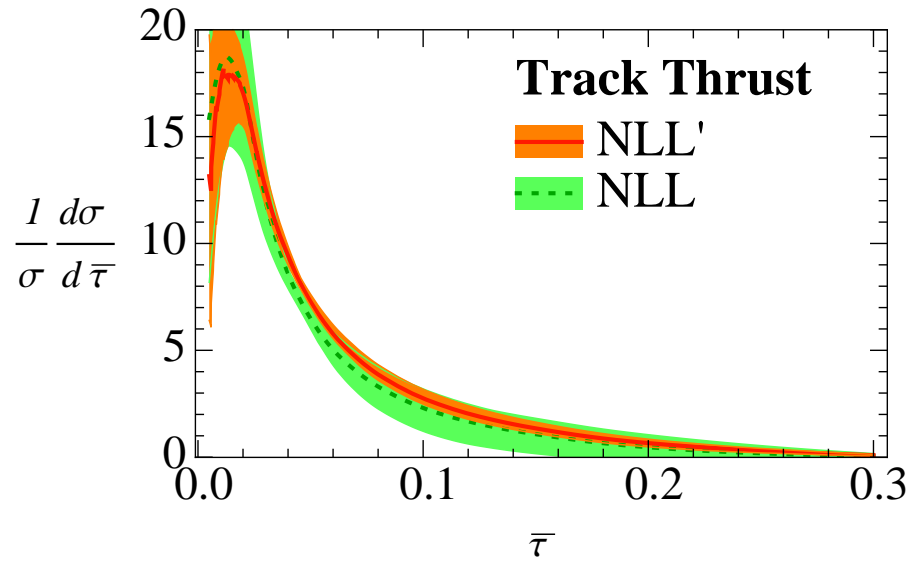


Figure 4.9: Track thrust distribution going from NLL to NLL'. The bands encode perturbative uncertainties from RG scale variations, but not uncertainties in α_s or the track functions themselves.

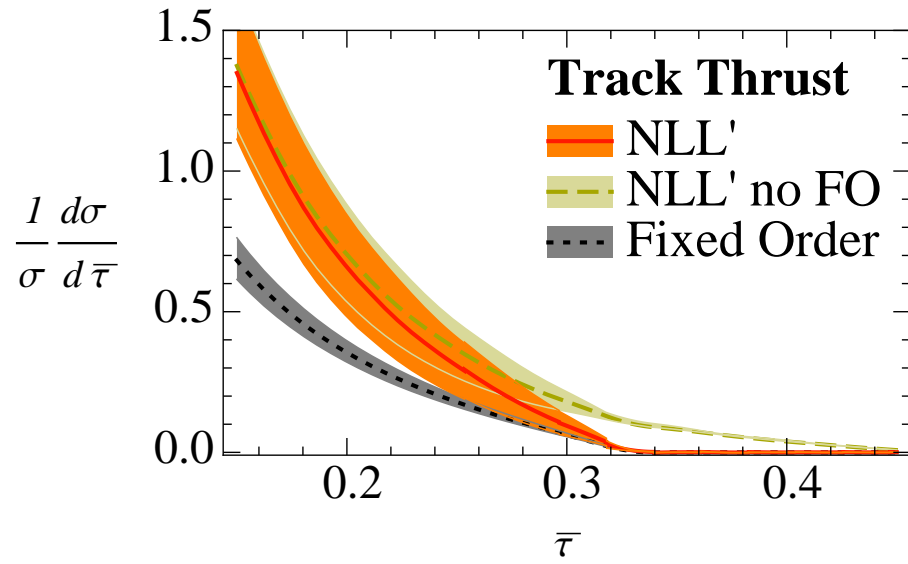


Figure 4.10: Track thrust distribution in the tail and far-tail regions, illustrating the effect of including the non-singular contribution at NLL' order. The full NLL' distribution interpolates between the resummed and fixed-order results.

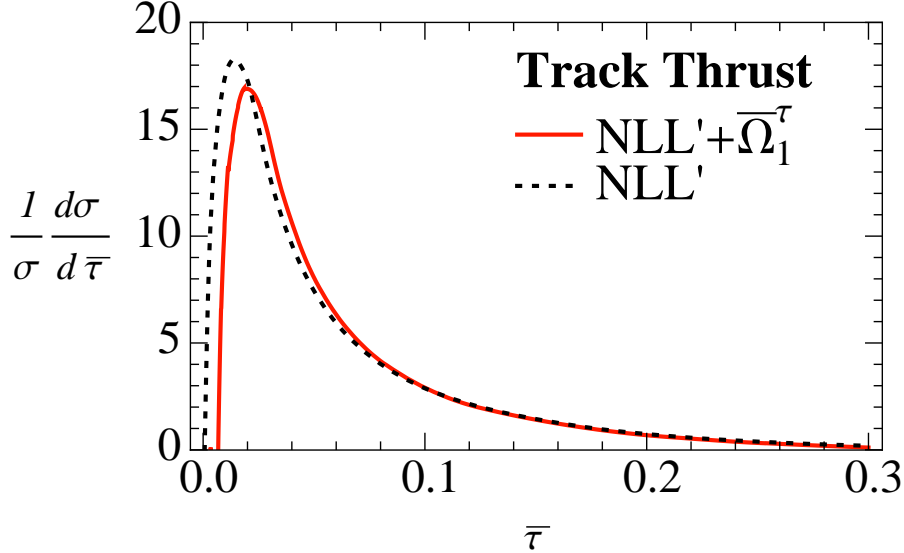


Figure 4.11: Track thrust at NLL' adding the leading power correction.

$\tau = 1/3$. (For this to happen, it is crucial that the profile functions in Appendix D turn off the resummation at the endpoint.) As desired, the full NLL' distribution interpolates between the NLL' result (without non-singular terms) at small τ and the fixed-order result at large τ .

In Fig. 4.11, we augment the NLL' results with the leading power correction $\bar{\Omega}_1^\tau$. For track thrust, the dominant effect of $\bar{\Omega}_1^\tau$ is a shift, though there are important effects in the peak region which do not amount to a shift. (For the calorimeter thrust distribution, the only effect of Ω_1^τ is to shift the distribution.) Note, however, that the peak region is also sensitive to higher-order power corrections which we have not included. The comparison between calorimeter and track thrust with the leading power correction is shown in Fig. 4.3.

In Fig. 4.12 we superimpose our theoretical predictions for the calorimeter and track thrust distributions with experimental data from the DELPHI collaboration. At NLL' order with the leading power correction $\bar{\Omega}_1^\tau$, the agreement is quite good, though we emphasize that we chose values of α_s and $\bar{\Omega}_1^\tau$ to ensure reasonable agreement with the calorimeter thrust data. We show the effect of scale uncertainties in Fig. 4.3, which are in general larger than the experimental uncertainties, motivating future studies of track

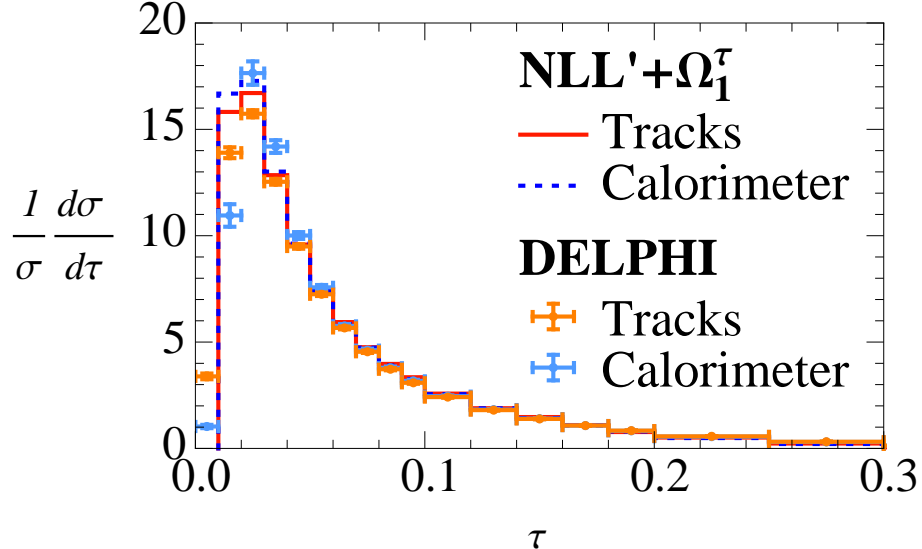


Figure 4.12: Comparison of analytical predictions with DELPHI data for both track and calorimeter thrust distributions. There is good qualitative and quantitative agreement in the tail region, though as shown in Fig. 4.3, the theoretical uncertainties at NLL' are larger than the experimental ones.

thrust with higher orders of resummation and more accurate fixed-order corrections.

As a final cross check of our analysis, we show the calorimeter and track thrust distributions from PYTHIA in Fig. 4.13. Since PYTHIA has been tuned to LEP data, it agrees well with the DELPHI measurements. There is good agreement between PYTHIA and our NLL' result in the tail region, but there are differences in the peak region due to the fact that PYTHIA includes an estimate of the full non-perturbative corrections, whereas we only include the leading power correction. Future track thrust calculations could use a full non-perturbative shape function for better modeling of the $\bar{\tau} \simeq 0$ region.

4.8 Discussion

In this chapter, we have presented the first calculation of track thrust in perturbative QCD. Our result is accurate to $\mathcal{O}(\alpha_s)$ in a fixed-order expansion while also including NLL resummation, i.e. NLL' order. By incorporating both track functions and the leading power correction, we have accounted for the dominant non-perturbative effects that

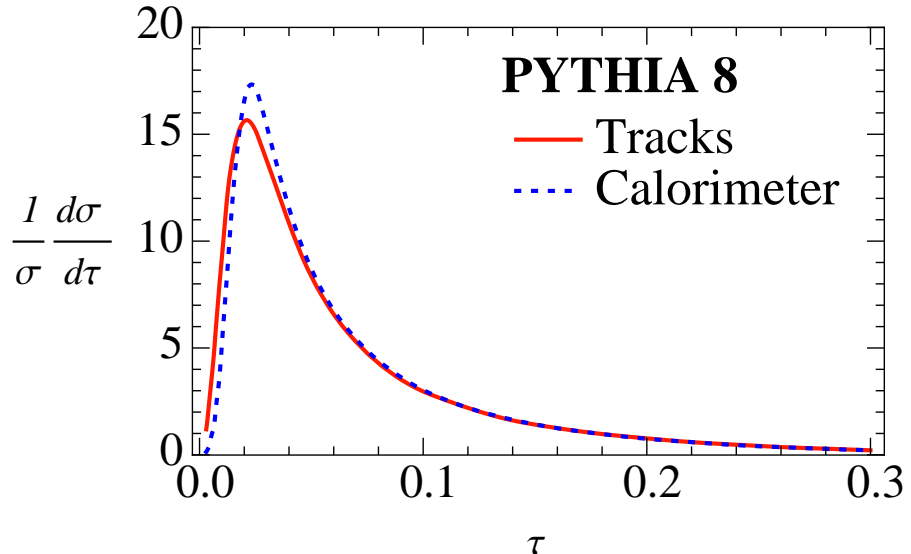


Figure 4.13: Calorimeter and track thrust distributions obtained from PYTHIA 8. Apart from deviations in the peak region due to higher-order non-perturbative corrections, these agree well with our NLL' calculation after the leading power correction is included (compare to Fig. 4.3).

determine the track thrust distribution. Our result is in good agreement with track thrust measurements performed at ALEPH and DELPHI.

One feature seen in the data is a remarkable similarity between the calorimeter thrust and track thrust distributions. At NLL, we traced this feature to a partial cancellation between two non-perturbative parameters—one associated with the gluon track function g_1^L , and one associated with pairs of quark track functions q^L . We conjecture that a similar cancellation should be present in most (if not all) dimensionless track-based observables. This should be relatively straightforward to prove for e^+e^- dijet event shapes with a thrust-like factorization theorem, but is likely to persist for more general track-based observables, including jet shapes relevant for the LHC such as N -subjettiness ratios [79, 109] or energy correlation functions ratios [110]. It is worth further study to understand whether this partial cancellation is just an accident or reflects some deeper property of track functions. Crucially, we have seen that neither higher-order terms at NLL' nor the leading power correction qualitatively spoil the similarity.

The track functions were originally designed to describe the energy fraction of a

parton carried by tracks (i.e. the large component of the light-cone momentum). Track thrust essentially measures the small component of the light-cone momentum carried by tracks, so it is perhaps surprising that the same track functions can be used in this context. The reason this works is that the track thrust distribution can be thought of as arising from multiple gluon emissions, each of which carries its own track function. Just as multiple emissions can be exponentiated in the case of calorimeter thrust, multiple emissions with track functions can also be exponentiated. In our calculation, this shows up in the fact that the anomalous dimension of the soft and jet functions depend on the logarithmic moment of the gluon track function g_1^L . We are confident that similar techniques could be applied to any track-based observable, as long as the calorimetric version of that observable has a valid factorization theorem. This motivates future experimental and theoretical studies of track-based observables.

This chapter is a reprint of material as it appears in “Calculating Track Thrust with Track Functions,” H.-M. Chang, M. Procura, J. Thaler and W. J. Waalewijn, Phys. Rev. D **88**, 034030 (2013) [arXiv:1306.6630 [hep-ph]], of which I was a co-author.

Chapter 5

Renormalization Group Evolution of Dimension-Six Baryon Number Violating Operators

We calculate the one-loop anomalous dimension matrix for the dimension-six baryon number violating operators of the Standard Model effective field theory, including right-handed neutrino fields. We discuss the flavor structure of the renormalization group evolution in the contexts of minimal flavor violation and unification.

5.1 Introduction

The baryon asymmetry of the universe hints at baryon number violating (BNV) interactions beyond the Standard Model (SM) of particle physics. Baryon number is an accidental symmetry of the SM violated by quantum effects [111], and there is no fundamental reason why it cannot be violated in extensions of the SM. Indeed, well-motivated theories like grand unified theories [112, 113, 114] violate baryon number at tree level through the exchange of very massive gauge bosons.

There has been no direct experimental observation of baryon number violation

to date. The large lower bound for the lifetime of the proton [115, 116] requires that the scale of baryon number violation M_B be much greater than accessible energy scales, and, in particular, much greater than the SM electroweak scale M_Z . The decay of baryons (such as the proton) can then be computed using an Effective Field Theory (EFT) formalism. In the model-independent treatment of EFT, the SM Lagrangian is extended by higher dimensional non-renormalizable operators ($d \geq 5$) suppressed by inverse powers of the new physics scale.

The leading order BNV operators arise at dimension $d = 6$. The most general dimension-six Lagrangian can be cast in 63 independent operators [117, 118, 119, 120, 121]. Out of these 63 operators, 59 operators preserve baryon number, and the complete set of one-loop renormalization group equations for these 59 operators was recently computed in Refs. [12, 13, 14, 122]. In the present work, we focus on the four BNV operators [119, 120, 121], and we extend the one-loop renormalization group evolution (RGE) analysis to these remaining dimension-six operators.

The four BNV operators can be written¹ as [121]

$$\begin{aligned} Q_{prst}^{duq\ell} &= \epsilon_{\alpha\beta\gamma}\epsilon_{ij}(d_p^\alpha Cu_r^\beta)(q_s^{i\gamma} C\ell_t^j), \\ Q_{prst}^{qque} &= \epsilon_{\alpha\beta\gamma}\epsilon_{ij}(q_p^{i\alpha} Cq_r^{j\beta})(u_s^\gamma Ce_t), \\ Q_{prst}^{qqql} &= \epsilon_{\alpha\beta\gamma}\epsilon_{il}\epsilon_{jk}(q_p^{i\alpha} Cq_r^{j\beta})(q_s^{k\gamma} C\ell_t^l), \\ Q_{prst}^{due} &= \epsilon_{\alpha\beta\gamma}(d_p^\alpha Cu_r^\beta)(u_s^\gamma Ce_t), \end{aligned} \tag{5.1}$$

where C is the Dirac matrix of charge conjugation, q and ℓ are the quark and lepton left-handed doublets, and we use u , d and e for up-type, down-type, and charged lepton right-handed fermions. Greek letters denote $SU(3)_c$ color indices and Roman letters from i to l refer to $SU(2)_L$ indices. Roman letters towards the end of the alphabet $p-w$ refer to flavor (generation) indices and take on values from $1, \dots, n_g = 3$.

In this work, we also will accommodate neutrino masses for the light neutrinos by including singlet fermions N (right-handed neutrinos) under the SM gauge group. Includ-

¹The connection with the basis of Ref. [119] is given in Appendix F.

ing singlet N fields, two additional dimension-six BNV operators can be constructed:

$$\begin{aligned} Q_{prst}^{qqdN} &= \epsilon_{\alpha\beta\gamma}\epsilon_{ij}(q_p^{i\alpha}Cq_r^{j\beta})(d_s^\gamma CN_t), \\ Q_{prst}^{uddN} &= \epsilon_{\alpha\beta\gamma}(u_p^\alpha Cd_r^\beta)(d_s^\gamma CN_t). \end{aligned} \quad (5.2)$$

The singlet neutrinos N , in contrast to the SM fermions, are allowed a Majorana mass M_N by the SM gauge symmetry. M_N can range from a very high scale as in the standard type-I seesaw model [123, 124, 125, 126] to the Dirac neutrino limit for which it vanishes — see Ref. [127] for a general parametrization in terms of light masses and mixing angles. Even in the case of a very high Majorana mass scale M_N , naïve estimates of proton decay and light neutrino masses imply that $M_N < M_B$. This hierarchy of scales implies that an EFT with the operators in Eq. (5.2) holds in the energy regime $M_N < \mu < M_B$. Below the scale M_N , one integrates out the N fields, matching onto the EFT containing only the four operators of Eq. (5.1), and drops the terms of Eq. (5.2) in the renormalization group equations.

We will use the conventions of Ref. [12], generalized to include singlet fermions N at energies above M_N . Specifically, for $\mu > M_N$, the $\mathcal{L}_{d \leq 4}$ SM Lagrangian includes a Majorana mass term M_N for the N fermions as well as Yukawa couplings Y_N for the N and ℓ fermions to the electroweak Higgs doublet H . For $\mu < M_N$, the N fields are integrated out of the EFT, and $\mathcal{L}_{d \leq 4}$ reduces to the conventional SM Lagrangian.

Baryon number is an (anomalous) symmetry that is preserved by the one-loop renormalization group equations, so the dimension-six BNV operators only mix among themselves. The gauge contribution to the anomalous dimensions of Eq. (5.1) was computed in Ref. [121], and we agree with those results. In addition, we compute the anomalous dimensions of Eq. (5.2), and the Yukawa terms. We also classify the operators in terms of representations of the permutation group, which diagonalizes the gauge contributions to the anomalous dimension matrix.

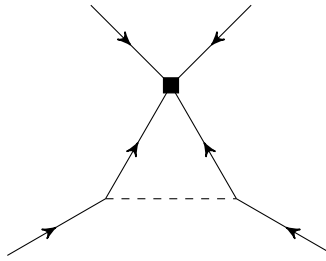


Figure 5.1: The one-loop Yukawa renormalization graph.

5.2 Results

The one-loop anomalous dimension matrix of the BNV operators decomposes into a sum of gauge and Yukawa terms. The gauge anomalous dimension matrix of the operators in Eq. (5.1) was computed in Ref. [121]. The gauge terms for Eq. (5.2) have not been computed previously. The Yukawa terms are generated by the diagram in Fig. 5.1, where all the fermion lines are incoming, because of the chiral structure of the BNV operators. The gauge coupling dependence is obtained from an analogous diagram with the scalar replaced by a gauge boson.

The calculation is done using dimensional regularization in $d = 4 - 2\epsilon$ dimensions in a general ξ gauge. Cancellation of the gauge parameter ξ provides a check on the calculation. The sum of the hypercharges y_i of the four fermions for each operator is constrained to be equal to zero for the ξ -dependence to cancel. Furthermore, the number of colors $N_c = 3$ for the operator to be $SU(3)$ gauge invariant. The RGE for the operator coefficients $\mathcal{L} = \sum_i C^i Q^i$ are ($\dot{C} \equiv 16\pi^2 \mu dC/d\mu$):

$$\begin{aligned}
\dot{C}_{prst}^{duq\ell} = & -C_{prst}^{duq\ell} \left[4g_3^2 + \frac{9}{2}g_2^2 - 6(y_d y_u + y_q y_l) g_1^2 \right] - C_{vrwt}^{duq\ell} (Y_d)_{vs} (Y_d^\dagger)_{wp} \\
& - C_{pvwt}^{duq\ell} (Y_u)_{vs} (Y_u^\dagger)_{wr} + \left\{ 2C_{prwv}^{duue} + C_{pwrv}^{duue} \right\} (Y_e)_{vt} (Y_u)_{ws} \\
& - 2C_{swpv}^{qgdN} (Y_N)_{vt} (Y_u^\dagger)_{wr} + \left\{ 2C_{rpwv}^{uddN} + C_{rwpv}^{uddN} \right\} (Y_N)_{vt} (Y_d)_{ws} \\
& + \left\{ 2C_{vwst}^{qq\ell} + 2C_{wvst}^{qq\ell} - C_{vsht}^{qq\ell} - C_{wsht}^{qq\ell} + 2C_{svht}^{qq\ell} + 2C_{swht}^{qq\ell} \right\} (Y_d^\dagger)_{vp} (Y_u^\dagger)_{wr} \\
& + 2C_{wsrv}^{qque} (Y_d^\dagger)_{wp} (Y_e)_{vt} + C_{vrst}^{duq\ell} (Y_d Y_d^\dagger)_{vp} + C_{pvst}^{duq\ell} (Y_u Y_u^\dagger)_{vr} \\
& + \frac{1}{2} C_{prvt}^{duq\ell} (Y_u^\dagger Y_u + Y_d^\dagger Y_d)_{vs} + \frac{1}{2} C_{prsv}^{duq\ell} (Y_N^\dagger Y_N + Y_e^\dagger Y_e)_{vt}
\end{aligned} \tag{5.3}$$

$$\begin{aligned}
\dot{C}_{prst}^{qque} = & -C_{prst}^{qque} \left[4g_3^2 + \frac{9}{2}g_2^2 - 6(y_q^2 + y_u y_e) g_1^2 \right] - C_{pvwt}^{qque} (Y_u)_{vr} (Y_u^\dagger)_{ws} \\
& - C_{rwvt}^{qque} (Y_u)_{vp} (Y_u^\dagger)_{ws} + \frac{1}{2} C_{vspw}^{duq\ell} (Y_e^\dagger)_{wt} (Y_d)_{vr} + \frac{1}{2} C_{vsrw}^{duq\ell} (Y_e^\dagger)_{wt} (Y_d)_{vp} \\
& - \frac{1}{2} \left\{ 2C_{vwst}^{duue} + C_{vsht}^{duue} \right\} [(Y_d)_{vp} (Y_u)_{wr} + (Y_d)_{vr} (Y_u)_{wp}] \\
& + \frac{1}{2} \left\{ -2C_{prwv}^{qq\ell} - 2C_{rpwv}^{qq\ell} + C_{pwrv}^{qq\ell} + C_{rwpv}^{qq\ell} - 2C_{wprv}^{qq\ell} - 2C_{wrpv}^{qq\ell} \right\} (Y_u^\dagger)_{ws} (Y_e^\dagger)_{vt} \\
& + \frac{1}{2} C_{vrst}^{qque} (Y_u^\dagger Y_u + Y_d^\dagger Y_d)_{vp} + \frac{1}{2} C_{pvst}^{qque} (Y_u^\dagger Y_u + Y_d^\dagger Y_d)_{vr} + C_{prvt}^{qque} (Y_u Y_u^\dagger)_{vs} \\
& + C_{prsv}^{qque} (Y_e Y_e^\dagger)_{vt}
\end{aligned} \tag{5.4}$$

$$\begin{aligned}
\dot{C}_{prst}^{qqdN} = & -C_{prst}^{qqdN} \left[4g_3^2 + \frac{9}{2}g_2^2 - 6y_q^2 g_1^2 \right] - C_{vrwt}^{qqdN}(Y_d^\dagger)_{vs}(Y_d)_{wp} - C_{vpwt}^{qqdN}(Y_d^\dagger)_{vs}(Y_d)_{wr} \\
& - \frac{1}{2}C_{swrv}^{duq\ell}(Y_N^\dagger)_{vt}(Y_u)_{wp} - \frac{1}{2}C_{swpv}^{duq\ell}(Y_N^\dagger)_{vt}(Y_u)_{wr} \\
& + \frac{1}{2} \left\{ 2C_{vwst}^{uddN} + C_{vswt}^{uddN} \right\} [(Y_u)_{vp}(Y_d)_{wr} + (Y_u)_{vr}(Y_d)_{wp}] \\
& + \frac{1}{2} \left\{ 2C_{prwv}^{qqq\ell} + 2C_{rpwv}^{qqq\ell} - C_{pwrv}^{qqq\ell} - C_{rwpv}^{qqq\ell} + 2C_{wprv}^{qqq\ell} + 2C_{wrpv}^{qqq\ell} \right\} (Y_d^\dagger)_{ws}(Y_N^\dagger)_{vt} \\
& + \frac{1}{2}C_{vrst}^{qqdN}(Y_u^\dagger Y_u + Y_d^\dagger Y_d)_{vp} + \frac{1}{2}C_{pvst}^{qqdN}(Y_u^\dagger Y_u + Y_d^\dagger Y_d)_{vr} + C_{prvt}^{qqdN}(Y_d Y_d^\dagger)_{vs} \\
& + C_{prsv}^{qqdN}(Y_N Y_N^\dagger)_{vt}
\end{aligned} \tag{5.5}$$

$$\begin{aligned}
\dot{C}_{prst}^{qqq\ell} = & -C_{prst}^{qqq\ell} \left[4g_3^2 + 3g_2^2 - 6(y_q^2 + y_q y_l) g_1^2 \right] - 4 \left\{ C_{rpst}^{qqq\ell} + C_{srpt}^{qqq\ell} + C_{psrt}^{qqq\ell} \right\} g_2^2 \\
& - 4C_{prwv}^{qque}(Y_e)_{vt}(Y_u)_{ws} + 4C_{prwv}^{qqdN}(Y_N)_{vt}(Y_d)_{ws} \\
& + 2C_{vwst}^{duq\ell} [(Y_d)_{vp}(Y_u)_{wr} + (Y_d)_{vr}(Y_u)_{wp}] + \frac{1}{2}C_{vrst}^{qqq\ell}(Y_u^\dagger Y_u + Y_d^\dagger Y_d)_{vp} \\
& + \frac{1}{2}C_{pvst}^{qqq\ell}(Y_u^\dagger Y_u + Y_d^\dagger Y_d)_{vr} + \frac{1}{2}C_{prvt}^{qqq\ell}(Y_u^\dagger Y_u + Y_d^\dagger Y_d)_{vs} \\
& + \frac{1}{2}C_{prsv}^{qqq\ell}(Y_N^\dagger Y_N + Y_e^\dagger Y_e)_{vt}
\end{aligned} \tag{5.6}$$

$$\begin{aligned}
\dot{C}_{prst}^{duue} = & -C_{prst}^{duue} \left[4g_3^2 - 2 \left(2y_d y_u + 2y_e y_u + y_u^2 + y_e y_d \right) g_1^2 \right] \\
& + 4C_{psrt}^{duue} \left((y_d + y_e) y_u - y_u^2 - y_e y_d \right) g_1^2 + 4C_{prwv}^{duq\ell}(Y_u^\dagger)_{ws}(Y_e^\dagger)_{vt} \\
& - 8C_{vwst}^{qque}(Y_d^\dagger)_{vp}(Y_u^\dagger)_{wr} + C_{vrst}^{duue}(Y_d Y_d^\dagger)_{vp} + C_{pvst}^{duue}(Y_u Y_u^\dagger)_{vr} \\
& + C_{prvt}^{duue}(Y_u Y_u^\dagger)_{vs} + C_{prsv}^{duue}(Y_e Y_e^\dagger)_{vt}
\end{aligned} \tag{5.7}$$

$$\begin{aligned}
\dot{C}_{prst}^{uddN} = & -C_{prst}^{uddN} \left[4g_3^2 - 2 \left(2y_u y_d + y_d^2 \right) g_1^2 \right] + 4C_{psrt}^{uddN} \left(y_u y_d - y_d^2 \right) g_1^2 \\
& + 4C_{rpwv}^{duq\ell}(Y_d^\dagger)_{ws}(Y_N^\dagger)_{vt} + 8C_{vwst}^{qqdN}(Y_u^\dagger)_{vp}(Y_d^\dagger)_{wr} + C_{vrst}^{uddN}(Y_u Y_u^\dagger)_{vp} \\
& + C_{pvst}^{uddN}(Y_d Y_d^\dagger)_{vr} + C_{prvt}^{uddN}(Y_d Y_d^\dagger)_{vs} + C_{prsv}^{uddN}(Y_N Y_N^\dagger)_{vt}
\end{aligned} \tag{5.8}$$

A non-trivial check on these equations is provided by the custodial symmetry

limit ($Y_{u(N)} \rightarrow Y_{d(e)}$, $g_1 \rightarrow 0$). In order to respect the custodial symmetry, the BNV operator coefficients have to satisfy certain relations given in appendix A, and the RGE flow should preserve these relations. Remarkably, the construction of custodial invariant operators is compatible with $U(1)_Y$ invariance.

The structure of the anomalous dimensions can be clarified by studying the symmetry properties of the BNV operators. The operators Q^{qque} and Q^{qqdN} are symmetric in the two q indices [121],

$$Q_{prst}^{qque} = Q_{rpst}^{qque}, \quad Q_{prst}^{qqdN} = Q_{rpst}^{qqdN}. \quad (5.9)$$

The operator $Q^{qqq\ell}$ satisfies the relation [121],

$$Q_{prst}^{qqq\ell} + Q_{rpst}^{qqq\ell} = Q_{spst}^{qqq\ell} + Q_{srpt}^{qqq\ell}. \quad (5.10)$$

$Q^{qqq\ell}$ has three q indices, and so transforms like $\square \otimes \square \otimes \square$, which gives one completely symmetric, one completely antisymmetric, and two mixed symmetry tensors. Eq. (5.10) implies that one of the mixed symmetry tensors vanishes. The allowed representations of the BNV operators are shown in Table 5.1.

The coefficients C_{prst}^{due} and C_{prst}^{uddN} can be decomposed into the symmetric and antisymmetric combinations,

$$\begin{aligned} C_{prst}^{due(\pm)} &= \frac{1}{2} [C_{prst}^{due} \pm C_{psrt}^{due}], \\ C_{prst}^{uddN(\pm)} &= \frac{1}{2} [C_{prst}^{uddN} \pm C_{psrt}^{uddN}]. \end{aligned} \quad (5.11)$$

The coefficient $C_{prst}^{qqq\ell}$ can be decomposed into terms with definite symmetry under permutations,

$$C_{prst}^{qqq\ell} = S_{prst}^{qqq\ell} + A_{prst}^{qqq\ell} + M_{prst}^{qqq\ell} + N_{prst}^{qqq\ell}, \quad (5.12)$$

where $S_{prst}^{qqq\ell}$ is totally symmetric in (p, r, s) , $A_{prst}^{qqq\ell}$ is totally antisymmetric in (p, r, s) , and

Table 5.1: Flavor representations of the BNV operators, and their dimensions. There are 273 operators in Eq. (5.1) and 135 in Eq. (5.2), for a total of 408 $\Delta B = 1$ operators with complex coefficients. One coefficient can be made real by a phase rotation of fields proportional to baryon number.

	dim	$SU(n_g)_q$	$SU(n_g)_u$	$SU(n_g)_d$	$SU(n_g)_l$	$SU(n_g)_e$	$SU(n_g)_N$
$Q_{prst}^{duq\ell}$	n_g^4	\square	\square	\square	\square	1	1
Q_{prst}^{gque}	$\frac{1}{2}n_g^3(n_g + 1)$	$\square\square$	\square	1	1	\square	1
Q_{prst}^{gqaN}	$\frac{1}{2}n_g^3(n_g + 1)$	$\square\square$	1	\square	1	1	\square
	$\frac{1}{6}n_g^2(n_g + 1)(n_g + 2)$	$\square\square\square$	1	1	\square	1	1
	$\frac{1}{3}n_g^2(n_g^2 - 1)$	$\square\square$	1	1	\square	1	1
$Q_{prst}^{qqq\ell}$	$\frac{1}{6}n_g^2(n_g - 1)(n_g - 2)$	$\square\square\square$	1	1	\square	1	1
	$\frac{1}{2}n_g^3(n_g + 1)$	1	$\square\square$	\square	1	\square	1
Q_{prst}^{duqe}	$\frac{1}{2}n_g^3(n_g - 1)$	1	$\square\square$	\square	1	\square	1
	$\frac{1}{2}n_g^3(n_g + 1)$	1	\square	$\square\square$	1	1	\square
Q_{prst}^{udqN}	$\frac{1}{2}n_g^3(n_g - 1)$	1	\square	$\square\square$	1	1	\square

$M_{prst}^{qqq\ell}$ and $N_{prst}^{qqq\ell}$ have mixed symmetry.

A convenient choice of basis is

$$\begin{aligned} S_{prst}^{qqq\ell} &= \frac{1}{6} [C_{prst}^{qqq\ell} + C_{sprt}^{qqq\ell} + C_{rspt}^{qqq\ell} + C_{psrt}^{qqq\ell} + C_{srpt}^{qqq\ell} + C_{rpst}^{qqq\ell}] , \\ A_{prst}^{qqq\ell} &= \frac{1}{6} [C_{prst}^{qqq\ell} + C_{sprt}^{qqq\ell} + C_{rspt}^{qqq\ell} - C_{psrt}^{qqq\ell} - C_{srpt}^{qqq\ell} - C_{rpst}^{qqq\ell}] , \\ M_{prst}^{qqq\ell} &= \frac{1}{3} [C_{prst}^{qqq\ell} - C_{rspt}^{qqq\ell} - C_{rpst}^{qqq\ell} + C_{srpt}^{qqq\ell}] , \\ N_{prst}^{qqq\ell} &= \frac{1}{3} [C_{prst}^{qqq\ell} - C_{sprt}^{qqq\ell} + C_{rpst}^{qqq\ell} - C_{srpt}^{qqq\ell}] . \end{aligned} \quad (5.13)$$

The coefficient $M_{prst}^{qqq\ell}$ is obtained by first anti-symmetrizing $C_{prst}^{qqq\ell}$ in (p, r) , and then symmetrizing in (p, s) . Likewise, $N_{prst}^{qqq\ell}$ is obtained by first anti-symmetrizing in (p, s) , and then symmetrizing in (p, r) . Eq. (5.10) implies that $N_{prst}^{qqq\ell}$ vanishes.

The gauge contributions to the anomalous dimensions respect the flavor symmetry of the operators. With the decomposition Eq. (5.13), the gauge contribution to the anomalous dimension matrix diagonalizes,

$$\begin{aligned} \dot{C}_{prst}^{duue(\pm)} &= - \left[4g_3^2 + \left(2 \pm \frac{20}{3} \right) g_1^2 \right] C_{prst}^{duue(\pm)} + \dots \\ \dot{C}_{prst}^{uddN(\pm)} &= - \left[4g_3^2 + \left(\frac{2}{3} \pm \frac{4}{3} \right) g_1^2 \right] C_{prst}^{uddN(\pm)} + \dots \\ \dot{S}_{prst}^{qqq\ell} &= - \left[4g_3^2 + 15g_2^2 + \frac{1}{3}g_1^2 \right] S_{prst}^{qqq\ell} + \dots \\ \dot{A}_{prst}^{qqq\ell} &= - \left[4g_3^2 - 9g_2^2 + \frac{1}{3}g_1^2 \right] A_{prst}^{qqq\ell} + \dots \\ \dot{M}_{prst}^{qqq\ell} &= - \left[4g_3^2 + 3g_2^2 + \frac{1}{3}g_1^2 \right] M_{prst}^{qqq\ell} + \dots . \end{aligned} \quad (5.14)$$

The “ \dots ” refers to the Yukawa contributions, which can mix different permutation representations.

5.3 Discussion

The renormalization group equations presented here have an involved flavor structure; to better understand the generic features, we turn now to certain simplifying hypotheses and models that produce a simple subclass of BNV operators.

5.3.1 *Minimal Flavor Violation*

The SM has an $SU(3)^5$ flavor symmetry for the q, u, d, l , and e fields, broken only by the Higgs Yukawa interactions. The symmetry is preserved if we promote the Yukawa coupling matrices to spurions that transform appropriately under the flavor group. Minimal flavor violation (MFV) [128, 129] is the hypothesis that any new physics beyond the SM preserves this symmetry, so the Yukawa coupling matrices are the only spurions.

Dimension-six BNV operators do not satisfy naïve minimal flavor violation because of triality. The argument proceeds as follows: under every $SU(3)_i$ flavor transformation, each BNV operator transforms as a representation of $SU(3)_i$ with n_i upper indices and m_i lower indices. All BNV operators satisfy $\sum_{i=1}^5 (n_i - m_i) \equiv 1 \pmod{3}$. No combination of Yukawa matrices (or other invariant tensors) can change this into a singlet, as they all have $(n - m) \equiv 0 \pmod{3}$.

In extensions of the MFV hypothesis to account for massive neutrinos [130, 131, 132], a Majorana mass term introduces a spurion with $(n - m) \equiv 2 \pmod{3}$. This in turn allows for the implementation of MFV, as pointed out in Ref. [133]. Note also that if the Yukawa spurions are built out of objects with simpler flavor-transformation properties [134], a variant of minimal flavor violation is possible without Lepton number violation.

Finally, there is the possibility that the fermion fields do not each separately have an $SU(3)$ flavor symmetry, but that some transform simultaneously [135]. The latter is an attractive option that is realized in Grand Unified Theories (GUTs), and we explore this possibility in the next subsection.

5.3.2 Grand Unified Theories

The Georgi-Glashow $SU(5)$ theory [112] places u^c , q , and e^c in a **10** representation of $SU(5)$, and d^c and l in a $\bar{\textbf{5}}$. In the context of the type-I seesaw, N is a **1**. The flavor group in this case cannot be that of putative MFV since the fields in each $SU(5)$ representation must transform simultaneously. The flavor symmetry is instead $SU(3)^3 = SU(3)_{\textbf{10}} \otimes SU(3)_{\bar{\textbf{5}}} \otimes SU(3)_{\textbf{1}}$, where each $SU(3)$ stands for transformations in flavor space of the corresponding $SU(5)$ representation [135]. The fermions and spurions then fall into the representations

$$\begin{aligned} u^c, q, e^c &\sim (\mathbf{3}, \mathbf{1}, \mathbf{1}), & Y_u &\sim (\bar{\mathbf{6}}, \mathbf{1}, \mathbf{1}), \\ d^c, l &\sim (\mathbf{1}, \mathbf{3}, \mathbf{1}), & Y_d, Y_e^T &\sim (\bar{\mathbf{3}}, \bar{\mathbf{3}}, \mathbf{1}), \\ N^c &\sim (\mathbf{1}, \mathbf{1}, \mathbf{3}), & Y_N &\sim (\mathbf{1}, \bar{\mathbf{3}}, \bar{\mathbf{3}}), \\ && M_N &\sim (\mathbf{1}, \mathbf{1}, \mathbf{6}), \end{aligned} \tag{5.15}$$

where the right-handed neutrino Majorana mass M_N also needs to be promoted to a spurion. Note that the triality argument given previously does not apply to the Yukawa matrices in this scenario. With the $SU(5)$ GUT in mind, we will relabel the Yukawas $Y_u \rightarrow Y_{10}$, $(Y_d, Y_e^T) \rightarrow Y_5$, and $Y_N \rightarrow Y_1$.

The operators transform as

$$\begin{aligned} Q^{duq\ell} &\sim (\mathbf{3} \otimes \bar{\mathbf{3}}, \mathbf{3} \otimes \bar{\mathbf{3}}, \mathbf{1}), \\ Q^{qqq\ell} &\sim (\mathbf{3} \otimes \mathbf{3} \otimes \mathbf{3}, \mathbf{3}, \mathbf{1}), \\ Q^{uddN} &\sim (\bar{\mathbf{3}}, \bar{\mathbf{3}} \otimes \bar{\mathbf{3}}, \bar{\mathbf{3}}), \\ Q^{duee} &\sim (\bar{\mathbf{3}} \otimes \bar{\mathbf{3}} \otimes \bar{\mathbf{3}}, \bar{\mathbf{3}}, \mathbf{1}), \\ Q^{qqdN} &\sim (\mathbf{3} \otimes \mathbf{3}, \bar{\mathbf{3}}, \bar{\mathbf{3}}), \\ Q^{quee} &\sim (\mathbf{3} \otimes \bar{\mathbf{3}} \otimes \mathbf{3} \otimes \bar{\mathbf{3}}, \mathbf{1}, \mathbf{1}), \end{aligned} \tag{5.16}$$

which now can be combined with Yukawa couplings to build up invariant terms in the

Lagrangian. Explicitly, the coefficients of the operators in terms of Yukawa matrices up to second order are

$$\begin{aligned}
C^{duq\ell} &\sim 1 \oplus Y_{10}^\dagger Y_{10} \oplus Y_5^\dagger Y_5, \\
C^{qqq\ell} &\sim Y_{10} \otimes Y_5, \\
C^{uddN} &\sim Y_5^\dagger \otimes Y_1^\dagger, \\
C^{due} &\sim Y_{10}^\dagger \otimes Y_5^\dagger, \\
C^{qdN} &\sim Y_{10} \otimes Y_1^\dagger, \\
C^{que} &\sim 1 \oplus Y_{10} Y_{10}^\dagger \oplus Y_{10} \otimes Y_{10}^\dagger.
\end{aligned} \tag{5.17}$$

Notice that only $C^{duq\ell}$ and C^{que} can be constructed out of flavor singlets. These are the only two operators that can be generated by integrating out heavy gauge bosons in the context of $SU(5)$ or, in general, by flavor-blind $SU(5)$ invariant dynamics. In addition, these are the only two coefficients that remain in the limit $Y_5, Y_1 \rightarrow 0$ ($Y_d, Y_e, Y_N \rightarrow 0$).

To close this section, let us comment on the implications for supersymmetric GUTs in our framework. BNV dimension-five operators are produced by integrating out GUT particles in supersymmetric theories in the absence of selection rules like R -parity [136, 137, 138]. Below the supersymmetry breaking scale, these will translate into the operators $Q^{qqq\ell}$, Q^{due} and Q^{uddN} in terms of the SM EFT Lagrangian, being only suppressed by one power of the BNV scale: $1/(M_B M_{\text{SUSY}})$. A feature of this scenario is that, as a result of the supersymmetric origin of the operators, all diagonal entries in flavor vanish [137], so that proton decay would require a strange particle. The renormalization group equations presented here only apply in the regime $\mu < M_{\text{SUSY}}$ since they depend on the spectrum of the theory, and we have assumed only dynamical SM particles. See Ref. [139] for a RGE study of BNV effects in the context of supersymmetry.

5.3.3 Magnitude of Effects

In this subsection, we simplify the RGE to estimate the magnitude of running a BNV operator coefficient from the GUT scale to the electroweak scale. Working in the context of a MFV GUT discussed in Sec. 5.3.2, we set $Y_d = Y_e = Y_N = 0$, assuming top-Yukawa dominance. In that limit, the only two non-vanishing operators are $Q_{prst}^{duq\ell}$ and Q_{prst}^{que} , whose RGE equations decouple. The coefficients of these two operators are given by appropriate combinations of Y_{10} which transforms as the symmetric representation, $\bar{6}$.

As an example, we focus on $Q_{prst}^{duq\ell}$, whose coefficient takes on a simple form:

$$C_{prst}^{duq\ell} = C_{rs}^{duq\ell} \delta_{pt}, \quad \text{where } C_{rs}^{duq\ell} = f(Y_{10}^\dagger Y_{10})_{rs}, \quad (5.18)$$

and $f(0)_{rs} \propto \delta_{rs}$. The RGE of this coefficient becomes

$$\dot{C}_{rs}^{duq\ell} \rightarrow \left[\frac{1}{2} Y_{10}^\dagger Y_{10} - 4g_3^2 - \frac{9}{2} g_2^2 - \frac{11}{6} g_1^2 \right]_{rw} C_{ws}^{duq\ell}. \quad (5.19)$$

We can now choose the basis $Y_{10} = Y_u = \text{diag}(0, 0, y_t)$, where y_t is the top-quark Yukawa coupling and lighter up-type quark masses are neglected. With this simplification, $C_{rs}^{duq\ell}$ is a diagonal matrix. Setting $M_{GUT} \approx 10^{15} \text{ GeV}$, the $C^{duq\ell}$ coefficients at the electroweak and GUT scales are related by

$$\begin{aligned} C_{33}^{duq\ell}(M_Z) &\approx (2.26)(0.96) C_{33}^{duq\ell}(M_{GUT}), \\ C_{22(11)}^{duq\ell}(M_Z) &\approx (2.26) C_{22(11)}^{duq\ell}(M_{GUT}). \end{aligned} \quad (5.20)$$

The first factor in parentheses comes from the gauge contribution alone, is dominated by the QCD coupling, and is common to all flavor coefficients. The second factor is the extra correction from including the Yukawa contribution, with only the top entry sizeable. Whereas the gauge contribution to the RGE enhances the $C_{rs}^{duq\ell}$ coefficient at lower energy scales, the Yukawa contribution gives a small suppression.

The Yukawa-induced running will in general be negligible for the lightest genera-

tion coefficients and processes like proton or neutron decay are unaffected. The Yukawa running gives a small correction for heavier generations. Note that the relatively small correction from Yukawa running compared to gauge-induced running stems from the different numerical coefficients of the anomalous dimension, since $g_3 \sim y_t$. For example, in Eq. (5.19), the color and $SU(2)_L$ gauge contributions have *each* a pre-factor ~ 8 times that of the Yukawas. These numerical factors cannot be estimated and require the explicit computation presented here.

The Yukawa running studied in this section have the most impact in heavy flavor BNV transitions, which are searched for experimentally [140, 141]. In this regard, the fact that W boson exchange below the electroweak symmetry-breaking scale produces flavor mixing is relevant. In particular, at two-loop order, proton or neutron decay is sensitive to BNV operators with arbitrary flavor. Even though a two-loop effect, this places a strong bound on heavy flavor BNV. Discussions of heavy BNV transitions taking into account these effects can be found in Refs. [142, 143, 144].

5.4 Conclusions

In this chapter, we have included the Yukawa contribution to the anomalous dimension matrix of baryon number violating operators and have thus completed the one-loop renormalization group evolution. Together with the computation of Refs. [12, 13, 14], this completes the anomalous dimension matrix for the totality of dimension-six operators of the SM. We included right-handed neutrinos and therefore two new BNV operators, and classified all the operators under flavor symmetry. None of the operators satisfies $SU(3)^5$ minimal flavor violation, but it is possible to impose a weaker grand unified theory variant of MFV. The Yukawa coupling corrections only give small corrections to the operator evolution.

This chapter is a reprint of material as it appears in “Renormalization group evolution of dimension-six baryon number violating operators,” R. Alonso, H.-M. Chang, E. E. Jenkins, A. V. Manohar and B. Shotwell, Phys. Lett. B **734**, 302 (2014) [arXiv:1405.0486

[hep-ph]], of which I was a co-author.

Chapter 6

Non-Standard Semileptonic Hyperon Decays

We investigate the discovery potential of semileptonic hyperon decays in terms of searches of new physics at teraelectronvolt scales. These decays are controlled by a small $SU(3)$ -flavor breaking parameter that allows for systematic expansions and accurate predictions in terms of a reduced dependence on hadronic form factors. We find that muonic modes are very sensitive to non-standard scalar and tensor contributions and demonstrate that these could provide a powerful synergy with direct searches of new physics at the LHC.

6.1 Introduction

The meson and baryon semileptonic decays have played a crucial role in the discovery of the $V - A$ structure [145] and quark-flavor mixing [146] of the (charged current) electroweak interactions in the Standard Model (SM). From a modern perspective, high-precision measurements of these decays provide a benchmark to test the SM and complement the direct searches of new physics (NP) at teraelectronvolt (TeV) energies.

For example, the accurate determination of the elements V_{ud} and V_{us} of the

Cabibbo-Kobayashi-Maskawa (CKM) matrix can be used to test its unitarity, constraining NP with characteristic scales as high as $\Lambda \sim 10$ TeV [147]. Furthermore, one can test the $V - A$ structure of the charged currents in $d \rightarrow u$ transitions using neutron and nuclear β decays [148, 149, 147, 150, 151, 152, 153] and pion decays [154, 155]. Current limits for the associated NP scale are also at the TeV level, and important improvements are expected from future experiments [156]. Searches of non-standard $d \rightarrow u$ transitions can also be done using LHC data, through e.g. the collision of d and u partons in the $pp \rightarrow e^\pm + MET + X$ channel (where MET stands for missing transverse energy) [156]. This leads to an interesting synergy between low- and high-energy NP searches in these flavor-changing processes.

A similar comprehensive analysis of exotic effects in $s \rightarrow u$ transitions has not been done yet. The (semi)leptonic kaon decays are optimal laboratories for this study due to the intense program of high-precision measurements and accurate calculations of the relevant form factors that has been carried out over the last decades [157]. Indeed, bounds on right-handed [158, 159] or scalar and tensor [160] NP interactions at the $10^{-2} - 10^{-3}$ level (relative to the SM) can be obtained [161, 162]. Generally speaking, (pseudo)scalar and tensor operators modify the spectrum of the decay and a detailed knowledge of the q^2 dependence of the form factors becomes necessary [163].

In this chapter we investigate the physics potential of the semileptonic hyperon decays (SHD) to search for NP. Although the description of these modes may seem involved due to the presence of six nonperturbative matrix elements or form factors, they present interesting features [164, 165, 166, 167]: (i) In the isospin limit, there are a total of 8 different channels, each having a differential decay rate with a rich angular distribution that could involve the polarizations of the baryons. (ii) The same form factors in different channels can be connected to each other and with other observables (e.g. electromagnetic form factors) in a model-independent fashion using the approximate $SU(3)$ -flavor symmetry of QCD. (iii) The maximal momentum transfer is small compared to the baryon masses and it is parametrically controlled by the breaking of this symmetry. Therefore, a simultaneous $SU(3)$ -breaking and “recoil” expansion can be

performed that simplifies, systematically, the dependence of the decay rate on the form factors.

On the experimental side there is much room for improvement. Except for the measurements performed by the KTeV and NA-48 Collaborations in the $\Xi^0 \rightarrow \Sigma^+$ channel [168, 169, 170, 171, 172], most of the SHD data is more than 30 years old [173]. On the other hand, (polarized) hyperons could be produced abundantly in the NA62 experiment at CERN or in any other hadron collider like the future $p\bar{p}$ facility PANDA [174] at FAIR/GSI or J-PARC [175].

In the following, we investigate the physics reach of the SHD with a discussion based on the sensitivity of the total decay rates to non-standard scalar and tensor interactions. We show that the bounds from SHD are competitive with those derived from the LHC data on the $pp \rightarrow e^\pm + MET + X$ channel and leave the interplay with kaon decays for future work (see [158, 159, 160, 161] for the current status).

6.2 The SM Effective Field Theory

In the SM, and at energies much lower than the electroweak symmetry breaking scale, $v = (\sqrt{2}G_F)^{-1/2} \simeq 246$ GeV, all charged-current weak processes involving up and strange quarks are described by the Fermi $(V - A) \times (V - A)$ four-fermion interaction. Beyond the SM, the most general effective Lagrangian is [147]:

$$\begin{aligned} \mathcal{L}_{\text{eff}} = & -\frac{G_F V_{us}}{\sqrt{2}} \left(1 + \epsilon_L + \epsilon_R \right) \times \\ & \sum_{\ell=e,\mu} \left[\bar{\ell} \gamma_\mu (1 - \gamma_5) \nu_\ell \cdot \bar{u} \left[\gamma^\mu - (1 - 2\epsilon_R) \gamma^\mu \gamma_5 \right] s \right. \\ & + \bar{\ell} (1 - \gamma_5) \nu_\ell \cdot \bar{u} \left[\epsilon_S - \epsilon_P \gamma_5 \right] s \\ & \left. + \epsilon_T \bar{\ell} \sigma_{\mu\nu} (1 - \gamma_5) \nu_\ell \cdot \bar{u} \sigma^{\mu\nu} (1 - \gamma_5) s \right] + \text{h.c.}, \end{aligned} \quad (6.1)$$

neglecting $\mathcal{O}(\epsilon^2)$ terms and derivative interactions, and where we use $\sigma^{\mu\nu} = [\gamma^\mu, \gamma^\nu]/2$. This Lagrangian has been constructed using only the SM fields relevant at low scales, $\mu \sim 1$ GeV, and demanding the operators to be color and electromagnetic singlets. Furthermore, we have restricted our attention to non-standard interactions that conserve lepton flavor and are lepton universal. Finally, we assume that the Wilson coefficients (WC) ϵ_i are real, since we focus on CP -even observables.

In light of the null results in direct searches of NP at colliders, we assume that its typical scale, Λ , is much larger than v . In such case, NP can be parameterized using an effective (non-renormalizable) Lagrangian, $\mathcal{L}_{\text{eff}} = \mathcal{L}_{\text{SM}} + (1/\Lambda^2) \sum_i \alpha_i \mathcal{O}_i^{(6)} + \dots$, where the $\mathcal{O}_i^{(6)}$ are now operators built with *all* the SM fields and subject to the structures of its full (unbroken) gauge symmetry group [117]. The WC ϵ_i in eq. (6.1) are generated by the high-energy WC α_i , which in turn can be obtained by matching to a particular NP model at $\mu = \Lambda$, and by running down to $\mu \sim 1$ GeV using the renormalization group equations, with the heavier fermions and weak bosons integrated out in the process [118, 12, 13, 14, 176].

This framework, usually referred to as the SM effective field theory (SMEFT), allows for a bottom-up investigation of NP, describing the implications of collider searches for low-energy experiments and vice versa. Needless to say, this interplay would become crucial in shaping the NP if a discrepancy with the SM is to be found. Examples of top-down applications, with correlated effects at high- and low-energies, can be found in scenarios with lepto-quarks [177] or extra scalar fields [163, 150].

6.3 Semileptonic Hyperon Decays

Neglecting electromagnetic corrections, the amplitude for a particular SHD $B_1(p_1) \rightarrow B_2(p_2)\ell^-(p_\ell)\bar{\nu}_\ell(p_\nu)$ factorizes into the leptonic and baryonic matrix elements. For the (axial)vector hadronic currents we have the parametrization in terms of the

standard form factors [166, 178]:

$$\begin{aligned} & \langle B_2(p_2) | \bar{u} \gamma_\mu s | B_1(p_1) \rangle \\ &= \bar{u}_2(p_2) \left[f_1(q^2) \gamma_\mu + \frac{f_2(q^2)}{M_1} \sigma_{\mu\nu} q^\nu + \frac{f_3(q^2)}{M_1} q_\mu \right] u_1(p_1), \end{aligned} \quad (6.2)$$

$$\begin{aligned} & \langle B_2(p_2) | \bar{u} \gamma_\mu \gamma_5 s | B_1(p_1) \rangle \\ &= \bar{u}_2(p_2) \left[g_1(q^2) \gamma_\mu + \frac{g_2(q^2)}{M_1} \sigma_{\mu\nu} q^\nu + \frac{g_3(q^2)}{M_1} q_\mu \right] \gamma_5 u_1(p_1), \end{aligned} \quad (6.3)$$

whereas the non-standard (pseudo)scalar and tensor interactions introduce new form factors [178]:

$$\langle B_2(p_2) | \bar{u} s | B_1(p_1) \rangle = f_S(q^2) \bar{u}_2(p_2) u_1(p_1), \quad (6.4)$$

$$\langle B_2(p_2) | \bar{u} \gamma_5 s | B_1(p_1) \rangle = g_P(q^2) \bar{u}_2(p_2) \gamma_5 u_1(p_1), \quad (6.5)$$

$$\langle B_2(p_2) | \bar{u} \sigma_{\mu\nu} s | B_1(p_1) \rangle \simeq f_T(q^2) \bar{u}_2(p_2) \sigma_{\mu\nu} u_1(p_1). \quad (6.6)$$

In eqs. (6.2)-(6.6), $u_{1,2}$ are the parent and daughter baryon spinor amplitudes, $M_{1,2}$ their respective masses, $q = p_1 - p_2$ is the momentum transfer, with $m_\ell^2 \leq q^2 \leq (M_1 - M_2)^2$. Furthermore, in Eq. (6.6) we have neglected other contributions to the matrix element of the tensor current since they are kinematically suppressed $\sim \mathcal{O}(q/M_1)$ [178].

A crucial aspect in the study of the SHD is the approximate $SU(3)$ -flavor symmetry of QCD. It controls the phase space of the decay and allows for a systematic expansion of the observables in the *generic* symmetry breaking parameter, $\delta = (M_1 - M_2)/M_1$ [165]. Relations among form factors are obtained in the exact symmetric limit using standard group theory (see e.g. Ref. [179]) and $\mathcal{O}(\delta)$ corrections can be calculated using model independent methods [180, 181, 182, 183, 184, 185, 186, 187]. In addition, the form factors can be expanded around $q^2 = 0$ in powers of $q^2/M_X^2 \sim \delta^2$, where $M_X \sim 1$ GeV is a hadronic scale related to the mass of the resonances coupling to the currents [188, 189].

Let us illustrate this with the total decay rate for the electronic mode in the SM

which, expanded up to next-to-leading order (NLO) in δ and neglecting m_e , is [165]:

$$\begin{aligned}\Gamma_{e,\text{SM}} \simeq & \frac{G_F^2 |V_{us} f_1(0)|^2 \Delta^5}{60 \pi^3} \left[\left(1 - \frac{3}{2}\delta\right) \right. \\ & \left. + 3 \left(1 - \frac{3}{2}\delta\right) \frac{g_1(0)^2}{f_1(0)^2} - 4\delta \frac{g_2(0)}{f_1(0)} \frac{g_1(0)}{f_1(0)} \right],\end{aligned}\quad (6.7)$$

with $\Delta = M_1 - M_2$. This expression contains a minimal dependence on the form factors. No information on their q^2 dependence is required and, moreover, the last term can be neglected because the weak-electric charge, $g_2(0)$, is itself $\mathcal{O}(\delta)$ [178]. Thus, besides G_F and V_{us} , and up to a theoretical accuracy of $\mathcal{O}(\delta^2) \sim 1 - 5\%$, the total decay rate of the electronic mode in the SM only depends on hyperon vector and axial charges, $f_1(0)$ and $g_1(0)$. Eq. (6.7) makes manifest that $f_1(0)$ is essential for extracting V_{us} from the rates, while the ratio $g_1(0)/f_1(0)$ can be obtained measuring the angular distribution of the final lepton [165, 166]. Neglected electromagnetic corrections are of a few percent [165, 190], well within the accuracy achieved at NLO in the $SU(3)$ expansion.

Beyond the SM, we generally have two types of effects. On one hand, (axial)vector modifications to the SM, described by the WC $\epsilon_{L,R}$, can be arranged (cf. Eq. 6.1) into a change of the normalization of the rate according to the replacement $V_{us} \rightarrow \tilde{V}_{us} = (1 + \epsilon_L + \epsilon_R)V_{us}$, and of the axial coupling to the leptonic current by the factor $(1 - 2\epsilon_R)$. The former combination involves a modification of V_{us} which has been tightly constrained by testing CKM unitarity [147]. The latter could be determined in SHD from the measured $g_1(0) \rightarrow \tilde{g}_1(0) = (1 - 2\epsilon_R)g_1(0)$ only if $g_1(0)$ was known accurately from QCD (for recent progress in the lattice see Refs. [191, 192]).

On the other hand, the WC $\epsilon_{S,P,T}$ introduce new structures in the energy and angular distributions. Restricting ourselves to $\mathcal{O}(v^2/\Lambda^2)$ (or linear in the WC), they appear from the interference of the NP terms with the SM and the contributions of the (pseudo)scalar and tensor operators are suppressed by $m_\ell/\sqrt{q^2}$. Therefore, while the electronic channels can be analyzed specifically to measure and study the normalization of the rates $|\tilde{V}_{us} f_1(0)|$ and the relevant form factors, the muonic modes could use the

Table 6.1: Comparison between the predictions of $R^{\mu e}$ in the SM at NLO and experimental measurements for different SHD.

	$\Lambda \rightarrow p$	$\Sigma^- \rightarrow n$	$\Xi^0 \rightarrow \Sigma^+$	$\Xi^- \rightarrow \Lambda$
Expt.	0.189(41)	0.442(39)	0.0092(14)	0.6(5)
SM-NLO	0.153(8)	0.444(22)	0.0084(4)	0.275(14)

information thus obtained to constrain the (pseudo)scalar and tensor operators. Besides that, it is important to note that the pseudoscalar quark bilinear receives a kinematical $\mathcal{O}(q/M_1)$ suppression that largely neutralizes the sensitivity of SHD to ϵ_P (see however Ref. [153]). For this reason, we center our discussion below on the study of ϵ_S and ϵ_T .

We expand the contributions in the SM up to $\mathcal{O}(\delta)$, but we keep only the leading terms in the NP terms. This implies a relative $\mathcal{O}(\delta^2)$ error in the SM predictions, which we fix to a 5% in all channels for definiteness, and an uncertainty $\mathcal{O}(\delta) \sim 10 - 20\%$ in the sensitivity to NP that will not affect the conclusions of our analysis.

6.4 Bounds on Scalar and Tensor Operators

Let us now introduce the ratio:

$$R^{\mu e} = \frac{\Gamma(B_1 \rightarrow B_2 \mu^- \bar{\nu}_\mu)}{\Gamma(B_1 \rightarrow B_2 e^- \bar{\nu}_e)}. \quad (6.8)$$

This observable is not only sensitive to lepton-universality violation but also linearly sensitive to ϵ_S and ϵ_T . In addition, one expects the dependence on the form factors in the SM to simplify in the ratio. In fact, working at NLO we obtain:

$$\begin{aligned} R_{\text{SM}}^{\mu e} &= \sqrt{1 - \frac{m_\mu^2}{\Delta^2}} \left(1 - \frac{9}{2} \frac{m_\mu^2}{\Delta^2} - 4 \frac{m_\mu^4}{\Delta^4} \right) \\ &\quad + \frac{15}{2} \frac{m_\mu^4}{\Delta^4} \operatorname{arctanh} \left(\sqrt{1 - \frac{m_\mu^2}{\Delta^2}} \right). \end{aligned} \quad (6.9)$$

This is a remarkable result: up to a relative theoretical accuracy of $\mathcal{O}(\delta^2)$, $R^{\mu e}$ in the SM does not depend on any form factor. In Table 6.1 we compare the experimental ratios to the results predicted in the SM. As discussed above, the main reason for the large experimental errors is that most of the data in the muonic channel is very old and scarce. At this level of precision, which generously covers the theoretical accuracy attained by Eq. (6.9), we observe that the experimental data on $R^{\mu e}$ agrees with the SM.

One can now use this consistency of the data with the SM to set bounds on the WC of the scalar and tensor operators, which generate the following non-standard contribution:

$$R_{\text{NP}}^{\mu e} \simeq \frac{\left(\epsilon_S \frac{f_S(0)}{f_1(0)} + 12 \epsilon_T \frac{g_1(0)}{f_1(0)} \frac{f_T(0)}{f_1(0)} \right)}{\left(1 - \frac{3}{2} \delta \right) \left(1 + 3 \frac{g_1(0)^2}{f_1(0)^2} \right)} \Pi(\Delta, m_\mu), \quad (6.10)$$

where $\Pi(\Delta, m_\mu)$ is a phase-space integral:

$$\begin{aligned} \Pi(\Delta, m_\mu) = & \frac{5}{2} \frac{m_\mu}{\Delta} \left[\left(2 + 13 \frac{m_\mu^2}{\Delta^2} \right) \sqrt{1 - \frac{m_\mu^2}{\Delta^2}} \right. \\ & \left. - 3 \left(4 \frac{m_\mu^2}{\Delta^2} + \frac{m_\mu^4}{\Delta^4} \right) \operatorname{arctanh} \left(\sqrt{1 - \frac{m_\mu^2}{\Delta^2}} \right) \right]. \end{aligned} \quad (6.11)$$

It is particularly convenient to express the dependence on the WC in “units” of the SM ratio:

$$\frac{R^{\mu e}}{R_{\text{SM}}^{\mu e}} = 1 + r_S \epsilon_S + r_T \epsilon_T, \quad (6.12)$$

where $r_{S,T}$ are dimensionless numbers encapsulating the net sensitivity to the WC.

The values of the form factors that we use to calculate $r_{S,T}$ are given in Tab. 6.2. The ratio $g_1(0)/f_1(0)$ is measured from the angular distribution of the electronic channels [173]. The scalar form factor can be obtained, up to electromagnetic corrections, using the conservation of vector current in QCD, $f_S(0)/f_1(0) = \Delta/(m_s - m_u)$ [153]. For the tensor form factors we need to use model calculations [193], whose errors are

Table 6.2: SHD data for $g_1(0)/f_1(0)$ and theoretical determinations of $f_{S,T}(0)/f_1(0)$ at $\mu = 2 \text{ GeV}$ used in this work. The corresponding $r_{S,T}$ are shown in the last two lines.

	$\Lambda \rightarrow p$	$\Sigma^- \rightarrow n$	$\Xi^0 \rightarrow \Sigma^+$	$\Xi^- \rightarrow \Lambda$
$g_1(0)/f_1(0)$	0.718(15)	-0.340(17)	1.210(50)	0.250(50)
$f_S(0)/f_1(0)$	1.90(10)	2.80(14)	1.36(7)	2.25(11)
$f_T(0)/f_1(0)$	0.72	-0.28	1.22	0.22
r_S	1.60	4.1	0.56	3.7
r_T	5.2	1.7	7.2	1.1

difficult to quantify. Nevertheless, it is interesting to note that the tensor form factor for the neutron β -decay is predicted to be 1.22, which is in the ballpark of the values obtained in the lattice [150, 194, 195, 192, 196]. This situation should be easily improved by future lattice calculations of the hyperon decay tensor charges.

The sensitivities to $\epsilon_{S,T}$ exhibited by the SHD (last two lines of Tab. 6.2) are strongly channel-dependent. In Fig. 6.1, we show 90% confidence level contours in the (ϵ_S, ϵ_T) plane using a χ^2 that includes the experimental measurements of $R^{\mu e}$ and where we propagate the experimental and theoretical uncertainties of the SM predictions in quadratures. For $r_{S,T}$ we use the values in Tab. 6.2. As we can see, even though the experimental data on $R^{\mu e}$ is not precise, the strong sensitivity of SHD to NP leads to stringent bounds in $\epsilon_{S,T}$; namely:

$$\epsilon_S = 0.003(40), \quad \epsilon_T = 0.017(34) , \quad (6.13)$$

at 90% C.L. Accounting for the running of $\epsilon_{S,T}$ on the renormalization scale μ [197], and assuming natural values for the WC at $\mu = \Lambda$, these bounds translate into $\Lambda \sim v (V_{us} \epsilon_{S,T})^{-1/2} \sim 2 - 4 \text{ TeV}$ [156].

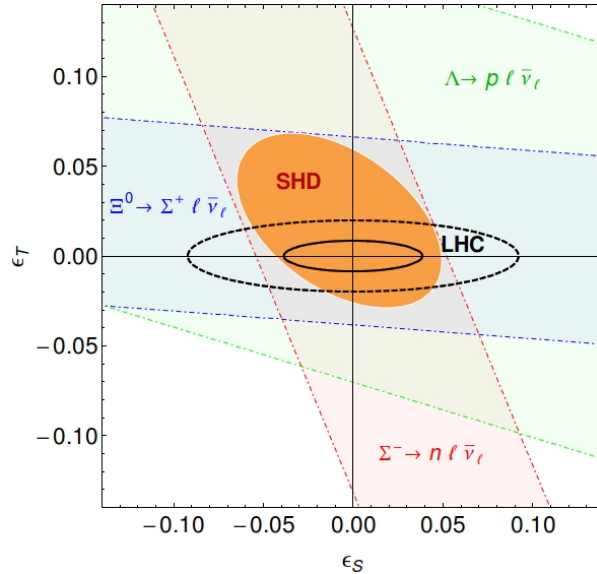


Figure 6.1: 90% CL constraints on $\epsilon_{S,T}$ at $\mu = 2$ GeV from the measurements of $R^{\mu e}$ in different channels (dot-dashed lines) and combined (filled ellipse). LHC bounds obtained from CMS data at $\sqrt{s} = 8$ TeV (7 TeV) are represented by the black solid (dashed) ellipse.

6.5 Limits from LHC Data

As discussed above, the SMEFT allows to interpret model-independently high- and low-energies searches of NP. In particular the cross-section $\sigma(pp \rightarrow e + \text{MET} + X)$ with transverse mass higher than \bar{m}_T is modified by non-standard $\bar{u}s \rightarrow e\bar{\nu}$ partonic interactions as follows:

$$\sigma(m_T > \bar{m}_T) = \sigma_W + \sigma_S |\epsilon_S|^2 + \sigma_T |\epsilon_T|^2 , \quad (6.14)$$

where $\sigma_W(\bar{m}_T)$ represents the SM contribution and $\sigma_{S,T}(\bar{m}_T)$ are new functions, whose explicit form can be found in Ref. [156] (up to trivial flavor indexes changes). Thus, comparing the observed events above \bar{m}_T with the SM expectation we can set bounds on $\epsilon_{S,T}$. In particular, one (three) event is found with a transverse mass above $\bar{m}_T = 1.5$ TeV (1.2 TeV) in the 20 fb^{-1} (5 fb^{-1}) dataset recorded at $\sqrt{s} = 8$ TeV (7 TeV) by the CMS collaboration [198, 199], in good agreement with the SM background of 2.02 ± 0.26

(2.8 ± 1.0) events. Using Eq. (6.14) this agreement translates in the 90% C.L. limits on $\epsilon_{S,T}$ shown in Fig. 6.1. We use the MSTW2008 PDF sets evaluated at $Q^2 = 1 \text{ TeV}^2$ [200] to calculate $\sigma_{S,T}$. Further details can be found in Ref. [156].

Fig. 6.1 illustrates the interesting competition that future SHD measurements could have with LHC searches of NP affecting $s \rightarrow u$ transitions. It is important to note that the dependence of the cross section (6.14) on the WC is quadratic, whereas in SHD it is linear. Besides reducing the sensitivity of the future collider searches of NP in this channel, one might also need to consider possible cancellations with linear effects from dimension-8 operators in the SMEFT.

6.6 Conclusions and Outlook

In summary, the most important features of SHD in relation to searches of NP at TeV scales are: (i) The SHD are controlled by a small $SU(3)$ -breaking parameter, allowing for systematic expansions that lead to accurate expressions in terms of a reduced dependence on form factors, cf. Eq. (6.9). (ii) The interference of the (pseudo)scalar and tensor NP operators with the SM in the rate is chirally suppressed. Therefore, electronic modes are well suited to measure normalization factors $|\tilde{V}_{us} f_1(0)|$, NP-modified $\tilde{g}_1(0)$ and other form factors. (iii) The muonic modes, on the other hand, show a strong linear sensitivity to scalar and tensor contributions that depend on the different combinations of form factors in each channel. This allows to constrain them using SHD alone, with a precision that is competitive with the LHC data, cf. Fig. 6.1 and Eq. (6.13).

Our hope is that the present study triggers a program of high-precision measurements of different observables in the SHD. Hyperons can be produced in great numbers in current [175] and future facilities [174]. One may also wonder if better measurements could be extracted from the analysis of the data collected in past experiments like HyperCP [201], KTeV and NA48. Any development on the experimental side will directly improve the bounds on NP obtained in this work with an observable as simple as $R^{\mu e}$, and using data with $\sim 10 - 20\%$ relative errors.

Future improvements on the experimental precision will need to be accompanied by similar efforts on the theory side. In particular, the inclusion of $\mathcal{O}(\delta^2)$ terms in the SM predictions would improve the accuracy to $\sim 0.1\% - 1\%$. Besides that, further nonperturbative calculations of the tensor form factors would improve the assessment of the sensitivity to ϵ_T . Finally, it will be important to perform this comprehensive analysis of the SHD in complementarity with the kaon decays. Work along these lines is in progress.

This chapter is a reprint of material as it appears in “Nonstandard Semileptonic Hyperon Decays,” Hsi-Ming Chang, Martin González-Alonso and Jorge Martín Camalich, Phys. Rev. Lett. **114**, 161802 (2015) [arXiv:1412.8484 [hep-ph]], of which I was a co-author.

Appendix A

Bag Model Wave Function in Momentum Space

We collect simplified expressions for the bag model wave function in momentum space and the functions ϕ_n needed for the PY projection. Several of these results were already obtained in Ref. [37]. The Fourier transform of the wave function is

$$\begin{aligned}\tilde{\Psi}_m(\mathbf{k}) &= \int d^3\mathbf{x} e^{i\mathbf{k}\cdot\mathbf{x}} \Psi_m(\mathbf{x}) \\ &= \frac{2\pi\Omega R^{3/2}}{\sqrt{\Omega^2 - \sin^2 \Omega}} \begin{pmatrix} s_1(\kappa) \chi_m \\ s_2(\kappa) \hat{\mathbf{k}} \cdot \boldsymbol{\sigma} \chi_m \end{pmatrix},\end{aligned}\tag{A.1}$$

where $\kappa = |\mathbf{k}|R$ and

$$\begin{aligned}s_1(\kappa) &= \frac{1}{\kappa} \left[\frac{\sin(\kappa - \Omega)}{\kappa - \Omega} - \frac{\sin(\kappa + \Omega)}{\kappa + \Omega} \right], \\ s_2(\kappa) &= 2j_0(\Omega)j_1(\kappa) - \frac{\kappa}{\Omega} s_1(\kappa),\end{aligned}\tag{A.2}$$

and χ_m is defined in Eq. (2.5). For the unpolarized and longitudinally polarized single PDFs this leads to

$$\begin{aligned}\bar{\tilde{\Psi}}_m \frac{\vec{\eta}}{2} \tilde{\Psi}_m &= \frac{\pi R^3 \Omega^2}{2(\Omega^2 - \sin^2 \Omega)} (s_1^2 + s_2^2 + 2s_1 s_2 \hat{k}_z), \\ \bar{\tilde{\Psi}}_m \frac{\vec{\eta}}{2} \gamma_5 \tilde{\Psi}_m &= (-1)^{m+3/2} \frac{\pi R^3 \Omega^2}{2(\Omega^2 - \sin^2 \Omega)} \\ &\quad \times [s_1^2 + s_2^2 (1 - 2\hat{k}_\perp^2) + 2s_1 s_2 \hat{k}_z].\end{aligned}\tag{A.3}$$

For the transversely polarized PDF we need

$$\begin{aligned}\bar{\tilde{\Psi}}_\uparrow \frac{\vec{\eta}}{2} \gamma_\perp^1 \gamma_5 \tilde{\Psi}_\downarrow + \bar{\tilde{\Psi}}_\downarrow \frac{\vec{\eta}}{2} \gamma_\perp^1 \gamma_5 \tilde{\Psi}_\uparrow \\ = \frac{\pi R^3 \Omega^2}{\Omega^2 - \sin^2 \Omega} [s_1^2 + s_2^2 (1 - 2\hat{k}_x^2) + 2s_1 s_2 \hat{k}_z].\end{aligned}\tag{A.4}$$

The functions ϕ_n , used in the PY projection, are

$$|\phi_n(\mathbf{p})|^2 = \frac{2^{4-n} \pi R^3 \Omega^{n-2}}{\kappa(\Omega^2 - \sin^2 \Omega)^n} \int_0^\Omega \frac{dv}{v^{n-1}} \sin \frac{2\kappa v}{\Omega} T^n(v),\tag{A.5}$$

with

$$\begin{aligned}T(v) &= \left(\Omega - \frac{1 - \cos 2\Omega}{2\Omega} - v \right) \sin 2v - \left(\frac{1}{2} + \frac{\sin 2\Omega}{2\Omega} \right) \cos 2v \\ &\quad + \frac{1}{2} + \frac{\sin 2\Omega}{2\Omega} - \frac{1 - \cos 2\Omega}{2\Omega^2} v^2.\end{aligned}\tag{A.6}$$

Appendix B

Relationship between the dPDFs \mathcal{F} and F

The relationship between the dPDFs \mathcal{F} and F defined in Sec. 2.2.3 is

$$\begin{aligned}
\mathcal{F}_{q_1\delta q_2}(x_1, x_2, \mathbf{k}_\perp) &= -\frac{iM^2}{\mathbf{k}_\perp^2} \int d\mathbf{z}_\perp e^{i\mathbf{k}_\perp \cdot \mathbf{z}_\perp} (\mathbf{k}_\perp \cdot \mathbf{z}_\perp) \\
&\quad \times F_{q_1\delta q_2}(x_1, x_2, \mathbf{z}_\perp), \\
\mathcal{F}_{\Delta q_1\delta q_2}(x_1, x_2, \mathbf{k}_\perp) &= -\frac{iM^2}{\mathbf{k}_\perp^2} \int d\mathbf{z}_\perp e^{i\mathbf{k}_\perp \cdot \mathbf{z}_\perp} (\mathbf{k}_\perp \cdot \mathbf{z}_\perp) \\
&\quad \times F_{\Delta q_1\delta q_2}(x_1, x_2, \mathbf{z}_\perp), \\
\mathcal{F}_{\delta q_1\delta q_2}^t(x_1, x_2, \mathbf{k}_\perp) &= \frac{M^4}{|\mathbf{k}_\perp|^4} \int d\mathbf{z}_\perp e^{i\mathbf{k}_\perp \cdot \mathbf{z}_\perp} [2(\mathbf{k}_\perp \cdot \mathbf{z}_\perp)^2 - \mathbf{k}_\perp^2 \mathbf{z}_\perp^2] \\
&\quad \times F_{\delta q_1\delta q_2}^t(x_1, x_2, \mathbf{z}_\perp). \tag{B.1}
\end{aligned}$$

The factors of $\mathbf{k} \cdot \mathbf{z}$ arise because $q_1\delta q_2$ and $\Delta q_1\delta q_2$ have \perp angular momentum one, and $\delta q_1\delta q_2^t$ has \perp angular momentum two. The other spin structures are not affected when switching to momentum space, so $F_{q_1q_2}(x_1, x_2, \mathbf{k}_\perp)$ is the Fourier transform of $F_{q_1q_2}(x_1, x_2, \mathbf{z}_\perp)$, etc.

Appendix C

Resummation

For the NLL' distribution in Eq. (4.50), we need expressions for the evolution kernels. Apart from the non-perturbative parameter g_1^L , the evolution kernels are the same between calorimeter thrust and track thrust, and governed by the relevant RGEs given in Sec. 4.5.

The RGE for the hard function in Eq. (4.30) leads to the evolution

$$\begin{aligned} H(Q^2, \mu) &= H(Q^2, \mu_0) U_H(Q^2, \mu_0, \mu), \\ U_H(Q^2, \mu_0, \mu) &= e^{K_H(\mu_0, \mu)} \left(\frac{Q^2}{\mu_0^2} \right)^{\eta_H(\mu_0, \mu)}, \\ K_H(\mu_0, \mu) &= -4K_\Gamma(\mu_0, \mu) + K_{\gamma_H}(\mu_0, \mu), \\ \eta_H(\mu_0, \mu) &= 2\eta_\Gamma(\mu_0, \mu), \end{aligned} \tag{C.1}$$

where $K_\Gamma(\mu_0, \mu)$, $\eta_\Gamma(\mu_0, \mu)$ and K_γ are given below in Eq. (C.4). Similarly, the RGE for the jet function in Eq. (4.49) leads to the evolution

$$\begin{aligned} \bar{J}(\bar{s}, x, \mu) &= \int_0^{\bar{s}} d\bar{s}' U_{\bar{J}}(\bar{s} - \bar{s}', \mu_0, \mu) \bar{J}(\bar{s}', x, \mu_0), \\ U_{\bar{J}}(\bar{s}, \mu_0, \mu) &= \frac{e^{K_{\bar{J}} - \gamma_E \eta_{\bar{J}}}}{\Gamma(1 + \eta_{\bar{J}})} \left[\frac{\eta_{\bar{J}}}{\mu_0^2} \mathcal{L}^{\eta_{\bar{J}}} \left(\frac{\bar{s}}{\mu_0^2} \right) + \delta(\bar{s}) \right], \\ K_{\bar{J}}(\mu_0, \mu) &= 4K_\Gamma(\mu_0, \mu) + K_{\gamma_{\bar{J}}}(\mu_0, \mu), \end{aligned}$$

$$\eta_{\bar{J}}(\mu_0, \mu) = -2\eta_\Gamma(\mu_0, \mu). \quad (\text{C.2})$$

The function $K_{\gamma_{\bar{J}}}$ contains the contribution from the non-perturbative parameter g_1^L to the non-cusp anomalous dimension $\gamma_{\bar{J}}[\alpha_s]$. Finally, the RGE for the soft function in Eq. (4.35) leads to the evolution

$$\begin{aligned} \bar{S}(\bar{k}, \mu) &= \int_0^{\bar{k}} d\bar{k}' U_{\bar{S}}(\bar{k} - \bar{k}', \mu_0, \mu) \bar{S}(\bar{k}', \mu_0), \\ U_{\bar{S}}(\bar{k}, \mu_0, \mu) &= \frac{e^{K_{\bar{S}} - \gamma_E \eta_{\bar{S}}}}{\Gamma(1 + \eta_{\bar{S}})} \left[\frac{\eta_{\bar{S}}}{\mu_0} \mathcal{L}^{\eta_{\bar{S}}} \left(\frac{\bar{k}}{\mu_0} \right) + \delta(\bar{k}) \right], \\ K_{\bar{S}}(\mu_0, \mu) &= -4K_\Gamma(\mu_0, \mu) + K_{\gamma_{\bar{S}}}(\mu_0, \mu), \\ \eta_{\bar{S}}(\mu_0, \mu) &= 4\eta_\Gamma(\mu_0, \mu). \end{aligned} \quad (\text{C.3})$$

Here, $K_{\gamma_{\bar{S}}}$ contains the contribution from g_1^L to $\gamma_{\bar{S}}[\alpha_s]$.

The functions $K_\Gamma(\mu_0, \mu)$, $\eta_\Gamma(\mu_0, \mu)$, and $K_{\gamma_x}(\mu_0, \mu)$ in the above RGE solutions are defined as

$$\begin{aligned} K_\Gamma^i(\mu_0, \mu) &= \int_{\alpha_s(\mu_0)}^{\alpha_s(\mu)} \frac{d\alpha_s}{\beta(\alpha_s)} \Gamma_{\text{cusp}}^i(\alpha_s) \int_{\alpha_s(\mu_0)}^{\alpha_s} \frac{d\alpha'_s}{\beta(\alpha'_s)}, \\ \eta_\Gamma^i(\mu_0, \mu) &= \int_{\alpha_s(\mu_0)}^{\alpha_s(\mu)} \frac{d\alpha_s}{\beta(\alpha_s)} \Gamma_{\text{cusp}}^i(\alpha_s), \\ K_{\gamma_x}(\mu_0, \mu) &= \int_{\alpha_s(\mu_0)}^{\alpha_s(\mu)} \frac{d\alpha_s}{\beta(\alpha_s)} \gamma_x(\alpha_s), \end{aligned} \quad (\text{C.4})$$

and their explicit expressions at NLL order are

$$\begin{aligned} K_\Gamma(\mu_0, \mu) &= -\frac{\Gamma_0}{4\beta_0^2} \left\{ \frac{4\pi}{\alpha_s(\mu_0)} \left(1 - \frac{1}{r} - \ln r \right) \right. \\ &\quad \left. + \left(\frac{\Gamma_1}{\Gamma_0} - \frac{\beta_1}{\beta_0} \right) (1 - r + \ln r) + \frac{\beta_1}{2\beta_0} \ln^2 r \right\}, \\ \eta_\Gamma(\mu_0, \mu) &= -\frac{\Gamma_0}{2\beta_0} \left[\ln r + \frac{\alpha_s(\mu_0)}{4\pi} \left(\frac{\Gamma_1}{\Gamma_0} - \frac{\beta_1}{\beta_0} \right) (r - 1) \right], \\ K_{\gamma_x}(\mu_0, \mu) &= -\frac{\gamma_{x,0}}{2\beta_0} \ln r. \end{aligned} \quad (\text{C.5})$$

Here $r = \alpha_s(\mu)/\alpha_s(\mu_0)$, and β_i , Γ_i , and $\gamma_{x,i}$ are the coefficients of the β -function, the cusp, and the non-cusp anomalous dimensions in their α_s expansion,

$$\begin{aligned}\beta(\alpha_s) &= -2\alpha_s \sum_{n=0}^{\infty} \beta_n \left(\frac{\alpha_s}{4\pi} \right)^{n+1}, \\ \Gamma_{\text{cusp}}(\alpha_s) &= \sum_{n=0}^{\infty} \Gamma_n \left(\frac{\alpha_s}{4\pi} \right)^{n+1}, \\ \gamma_x(\alpha_s) &= \sum_{n=0}^{\infty} \gamma_{x,n} \left(\frac{\alpha_s}{4\pi} \right)^{n+1}. \end{aligned} \quad (\text{C.6})$$

At NLL' order, we only need the first two coefficients of $\beta(\alpha_s)$ and $\Gamma_{\text{cusp}}(\alpha_s)$, which are

$$\begin{aligned}\beta_0 &= \frac{11}{3} C_A - \frac{4}{3} T_F n_f, \\ \beta_1 &= \frac{34}{3} C_A^2 - \left(\frac{20}{3} C_A + 4C_F \right) T_F n_f, \\ \Gamma_0 &= 4C_F, \\ \Gamma_1 &= 4C_F \left[\left(\frac{67}{9} - \frac{\pi^2}{3} \right) C_A - \frac{20}{9} T_F n_f \right]. \end{aligned} \quad (\text{C.7})$$

For the non-cusp anomalous dimension $\gamma_x(\alpha_s)$ we only need the first coefficient, given in Eqs. (4.30), (4.35), and (4.49).

Appendix D

Profile Functions

The optimal choice of RG scales depends on the value of τ , so we use profile functions to smoothly interpolate between the small τ and large τ regions.

Our choice of running scales is adopted from Ref. [93] with some modifications:

$$\begin{aligned} \mu_H &= e_H Q, \\ \mu_J(\tau) &= \left[1 + e_J \theta(\tau_3 - \tau) \left(1 - \frac{\tau}{\tau_3} \right)^2 \right] \sqrt{\mu_H \mu_{\text{run}}(\tau, \mu_H)}, \\ \mu_S(\tau) &= \left[1 + e_S \theta(\tau_3 - \tau) \left(1 - \frac{\tau}{\tau_3} \right)^2 \right] \mu_{\text{run}}(\tau, \mu_H), \end{aligned} \quad (\text{D.1})$$

where μ_{run} is given by

$$\begin{aligned} \mu_{\text{run}}(\tau, \mu) &= \begin{cases} \mu_0 + a \tau^2 / \tau_1 & \tau \leq \tau_1, \\ 2a \tau + b & \tau_1 \leq \tau \leq \tau_2, \\ \mu - a(\tau - \tau_3)^2 / (\tau_3 - \tau_2) & \tau_2 \leq \tau \leq \tau_3, \\ \mu & \tau > \tau_3, \end{cases} \\ a &= \frac{\mu_0 - \mu}{\tau_1 - \tau_2 - \tau_3}, \quad b = \frac{\mu \tau_1 - \mu_0(\tau_2 + \tau_3)}{\tau_1 - \tau_2 - \tau_3}. \end{aligned} \quad (\text{D.2})$$

The expressions for a and b follow from demanding that μ_{run} is continuous and has

a continuous derivative. The value of μ_0 determines the scales at $\tau = 0$, while $\tau_{1,2,3}$ determine the transition between the peak, tail, and far-tail regions discussed in Sec. 4.5. For $\tau > \tau_3$, our choice for μ_{run} ensures that the resummation of logarithms of τ turns off.

The parameters for the central curve are

$$\begin{aligned} e_H &= 1, & e_B = e_S &= 0, & \mu_0 &= 2 \text{ GeV}, \\ \tau_1 &= \frac{2 \text{ GeV}}{Q}, & \tau_2 &= 0.15, & \tau_3 &= 0.33. \end{aligned} \quad (\text{D.3})$$

The scale uncertainty bands are obtained by taking the envelope of the following scale variations:

$$\begin{aligned} a) \quad &e_H = 2^{\pm 1}, & e_J = e_S &= 0, \\ b) \quad &e_H = 1, & e_J &= \pm 0.5, & e_S &= 0, \\ c) \quad &e_H = 1, & e_J &= 0, & e_S &= \pm 0.5. \end{aligned} \quad (\text{D.4})$$

Appendix E

Plus Distributions

The standard plus distribution for some function $g(x)$ is defined as

$$[\theta(x)g(x)]_+ = \lim_{\beta \rightarrow 0} \frac{d}{dx} [\theta(x - \beta) G(x)] \quad (\text{E.1})$$

with

$$G(x) = \int_1^x dx' g(x'). \quad (\text{E.2})$$

This satisfies the boundary condition $\int_0^1 dx [\theta(x)g(x)]_+ = 0$. The two special cases we need in this chapter are

$$\begin{aligned} \mathcal{L}_n(x) &\equiv \left[\frac{\theta(x) \ln^n x}{x} \right]_+ = \lim_{\beta \rightarrow 0} \left[\frac{\theta(x - \beta) \ln^n x}{x} + \delta(x - \beta) \frac{\ln^{n+1} \beta}{n+1} \right] \\ \mathcal{L}^\eta(x) &\equiv \left[\frac{\theta(x)}{x^{1-\eta}} \right]_+ = \lim_{\beta \rightarrow 0} \left[\frac{\theta(x - \beta)}{x^{1-\eta}} + \delta(x - \beta) \frac{x^\eta - 1}{\eta} \right]. \end{aligned} \quad (\text{E.3})$$

In our calculations, we use the plus distribution identities appearing in appendix B of Ref. [105]. In particular, we utilize the following rescaling identity for a constant λ ,

$$\lambda \mathcal{L}_n(\lambda x) = \frac{\ln^{n+1}(\lambda)}{n+1} \delta(x) + \sum_{k=0}^n \binom{n}{k} \ln^{n-k}(\lambda) \mathcal{L}_k(x). \quad (\text{E.4})$$

Appendix F

Operator Relations and Custodial Symmetry

Refs. [119, 118] split the $Q^{qqq\ell}$ operator into two operators

$$\begin{aligned} Q_{prst}^{qqq\ell(1)} &= \epsilon_{\alpha\beta\gamma}\epsilon_{ij}\epsilon_{kl}(q_p^{i\alpha}Cq_r^{j\beta})(q_s^{\gamma k}Cl_t^l), \\ Q_{prst}^{qqq\ell(3)} &= \epsilon_{\alpha\beta\gamma}(\tau^I\epsilon)_{ij}(\tau^I\epsilon)_{kl}(q_p^{i\alpha}Cq_r^{j\beta})(q_s^{\gamma k}Cl_t^l), \end{aligned} \quad (\text{F.1})$$

where τ^I is an $SU(2)_L$ generator. These operators can be written in terms of $Q_{prst}^{qqq\ell}$ [121]

$$\begin{aligned} Q_{prst}^{qqq\ell(1)} &= -(Q_{prst}^{qqq\ell} + Q_{rpst}^{qqq\ell}), \\ Q_{prst}^{qqq\ell(3)} &= -(Q_{prst}^{qqq\ell} - Q_{rpst}^{qqq\ell}), \end{aligned} \quad (\text{F.2})$$

$Q_{prst}^{qqq\ell(1)}$ and $Q_{prst}^{qqq\ell(3)}$ are symmetric and antisymmetric in the first two flavor indices, respectively, and transform as symmetric plus mixed, and antisymmetric plus mixed representations under permutation of the three q indices. Since there is only one mixed symmetry tensor in $Q^{qqq\ell}$ by Eq. (5.10), the mixed symmetry tensors in $Q^{qqq\ell(1,3)}$ are the same, and the two operators are not independent.

The custodial $SU(2)_L \times SU(2)_R$ symmetry is preserved in the SM for $g_1 \rightarrow 0$ and $Y_{u(N)} \rightarrow Y_{d(e)}$. It can be implemented in the BNV operators by arranging the right-

handed fermions in doublets, $q_R = (u_R, d_R)^T$ and $\ell_R = (N_R, e_R)^T$. By construction, $Q^{qqq\ell}$ is already custodial invariant and the five remaining operators are grouped into the custodial $SU(2)$ invariant combinations

$$\begin{aligned} \epsilon_{ij}\epsilon_{kl}(q_{Rp}^i C q_{Rr}^j)(q_s^k C \ell_t^l) &= -Q_{prst}^{duq\ell} - Q_{rpst}^{duq\ell}, \\ \epsilon_{ij}\epsilon_{kl}(q_p^i C q_r^j)(q_{Rs}^k C \ell_{Rt}^l) &= Q_{prst}^{qque} - Q_{prst}^{qqdN}, \\ \epsilon_{ij}\epsilon_{kl}(q_{Rp}^i C q_{Rr}^j)(q_{Rs}^k C \ell_{Rt}^l) &= -Q_{prst}^{uddN} - Q_{rpst}^{uddN} \\ &\quad - Q_{prst}^{duee} - Q_{rpst}^{duee}, \end{aligned} \tag{F.3}$$

where color indices are implicit. The component fields of q_R and ℓ_R have different hypercharges, but the custodial invariant operators *are* $U(1)_Y$ invariant. The above equations imply extra relations for the operator coefficients

$$\begin{aligned} C_{prst}^{duq\ell} &= C_{rpst}^{duq\ell}, & C_{prst}^{qque} &= -C_{prst}^{qqdN}, \\ C_{prst}^{duee} &= C_{rpst}^{duee}, & C_{prst}^{duee} &= C_{prst}^{uddN}, \end{aligned} \tag{F.4}$$

in the custodial $SU(2)$ limit.

Bibliography

- [1] T. Sjostrand, S. Mrenna, and P. Z. Skands, *PYTHIA 6.4 Physics and Manual*, *JHEP* **05** (2006) 026, [hep-ph/0603175].
- [2] T. Sjostrand, S. Mrenna, and P. Z. Skands, *A Brief Introduction to PYTHIA 8.1*, *Comput. Phys. Commun.* **178** (2008) 852–867, [arXiv:0710.3820].
- [3] H.-M. Chang, M. Procura, J. Thaler, and W. J. Waalewijn, *Calculating Track-Based Observables for the LHC*, *Phys. Rev. Lett.* **111** (2013) 102002, [arXiv:1303.6637].
- [4] E. Fermi, *Quantum Theory of Radiation*, *Rev.Mod.Phys.* **4** (1932) 87–132.
- [5] F. Close, *The infinity puzzle: Quantum field theory and the hunt for an orderly universe*, 2011.
- [6] V. Gribov and L. Lipatov, *Deep inelastic e p scattering in perturbation theory*, *Sov. J. Nucl. Phys.* **15** (1972) 438–450.
- [7] G. Altarelli and G. Parisi, *Asymptotic Freedom in Parton Language*, *Nucl. Phys.* **B126** (1977) 298.
- [8] Y. L. Dokshitzer, *Calculation of the Structure Functions for Deep Inelastic Scattering and $e^+ e^-$ Annihilation by Perturbation Theory in Quantum Chromodynamics.*, *Sov. Phys. JETP* **46** (1977) 641–653.
- [9] N. H. Christ, B. Hasslacher, and A. H. Mueller, *Light cone behavior of perturbation theory*, *Phys. Rev.* **D6** (1972) 3543.
- [10] H. Georgi and H. D. Politzer, *Electroproduction scaling in an asymptotically free theory of strong interactions*, *Phys. Rev.* **D9** (1974) 416–420.
- [11] D. Gross and F. Wilczek, *Asymptotically Free Gauge Theories. 2.*, *Phys. Rev.* **D9** (1974) 980–993.
- [12] E. E. Jenkins, A. V. Manohar, and M. Trott, *Renormalization Group Evolution of the Standard Model Dimension Six Operators I: Formalism and lambda Dependence*, *JHEP* **1310** (2013) 087, [arXiv:1308.2627].

- [13] E. E. Jenkins, A. V. Manohar, and M. Trott, *Renormalization Group Evolution of the Standard Model Dimension Six Operators II: Yukawa Dependence*, *JHEP* **1401** (2014) 035, [arXiv:1310.4838].
- [14] R. Alonso, E. E. Jenkins, A. V. Manohar, and M. Trott, *Renormalization Group Evolution of the Standard Model Dimension Six Operators III: Gauge Coupling Dependence and Phenomenology*, *JHEP* **04** (2014) 159, [arXiv:1312.2014].
- [15] A. Kulesza and W. Stirling, *Like sign W boson production at the LHC as a probe of double parton scattering*, *Phys. Lett.* **B475** (2000) 168–175, [hep-ph/9912232].
- [16] E. Cattaruzza, A. Del Fabbro, and D. Treleani, *Fractional momentum correlations in multiple production of W bosons and of $b\bar{b}$ pairs in high energy pp collisions*, *Phys. Rev.* **D72** (2005) 034022, [hep-ph/0507052].
- [17] E. Maina, *Multiple Parton Interactions in Z+4j, $W^\pm W^\pm + 0/2j$ and $W^+ W^- + 2j$ production at the LHC*, *JHEP* **0909** (2009) 081, [arXiv:0909.1586].
- [18] J. R. Gaunt, C.-H. Kom, A. Kulesza, and W. Stirling, *Same-sign W pair production as a probe of double parton scattering at the LHC*, *Eur. Phys. J.* **C69** (2010) 53–65, [arXiv:1003.3953].
- [19] A. Del Fabbro and D. Treleani, *A Double Parton Scattering Background to Higgs Boson Production at the LHC*, *Phys. Rev.* **D61** (2000) 077502, [hep-ph/9911358].
- [20] M. Hussein, *A Double parton scattering background to associate WH and ZH production at the LHC*, *Nucl. Phys. Proc. Suppl.* **174** (2007) 55–58, [hep-ph/0610207].
- [21] D. Bandurin, G. Golovanov, and N. Skachkov, *Double parton interactions as a background to associated HW production at the Tevatron*, *JHEP* **1104** (2011) 054, [arXiv:1011.2186].
- [22] E. L. Berger, C. Jackson, S. Quackenbush, and G. Shaughnessy, *Calculation of $W b \bar{b}$ Production via Double Parton Scattering at the LHC*, *Phys. Rev.* **D84** (2011) 074021, [arXiv:1107.3150].
- [23] ATLAS Collaboration, *A measurement of hard double-partonic interactions in $w \rightarrow \ell\nu + 2$ jet events*, Tech. Rep. ATLAS-CONF-2011-160, CERN, Geneva, Dec, 2011.
- [24] N. Paver and D. Treleani, *Multi-Quark Scattering and Large p_T Jet Production in Hadronic Collisions*, *Nuovo Cim.* **A70** (1982) 215.
- [25] M. Mekhfi, *Correlations in Color and Spin in Multiparton Processes*, *Phys. Rev.* **D32** (1985) 2380.

- [26] M. Diehl and A. Schafer, *Theoretical considerations on multiparton interactions in QCD*, *Phys. Lett.* **B698** (2011) 389–402, [arXiv:1102.3081].
- [27] M. Diehl, D. Ostermeier, and A. Schafer, *Elements of a theory for multiparton interactions in QCD*, *JHEP* **1203** (2012) 089, [arXiv:1111.0910].
- [28] A. V. Manohar and W. J. Waalewijn, *A QCD Analysis of Double Parton Scattering: Color Correlations, Interference Effects and Evolution*, *Phys. Rev.* **D85** (2012) 114009, [arXiv:1202.3794].
- [29] R. Kirschner, *Generalized Lipatov-Altarelli-Parisi Equations and Jet Calculus Rules*, *Phys. Lett.* **B84** (1979) 266.
- [30] V. Shelest, A. Snigirev, and G. Zinovjev, *The Multiparton Distribution Equations in QCD*, *Phys. Lett.* **B113** (1982) 325.
- [31] A. V. Manohar and W. J. Waalewijn, *What is Double Parton Scattering?*, *Phys. Lett.* **B713** (2012) 196–201, [arXiv:1202.5034].
- [32] M. Mekhfi and X. Artru, *Sudakov Suppression of Color Correlations in Multiparton Scattering*, *Phys. Rev.* **D37** (1988) 2618–2622.
- [33] T. Kasemets and M. Diehl, *Angular correlations in the double Drell-Yan process*, *JHEP* **01** (2013) 121, [arXiv:1210.5434].
- [34] A. Chodos, R. Jaffe, K. Johnson, and C. B. Thorn, *Baryon Structure in the Bag Theory*, *Phys. Rev.* **D10** (1974) 2599.
- [35] R. Jaffe, *Deep Inelastic Structure Functions in an Approximation to the Bag Theory*, *Phys. Rev.* **D11** (1975) 1953.
- [36] C. Benesh and G. Miller, *Deep Inelastic Structure Functions in the MIT Bag Model*, *Phys. Rev.* **D36** (1987) 1344–1349.
- [37] A. W. Schreiber, A. Signal, and A. W. Thomas, *Structure functions in the bag model*, *Phys. Rev.* **D44** (1991) 2653–2662.
- [38] X.-M. Wang, X.-T. Song, and P.-C. Yin, *The Hadron Structure Functions in the Bag Model and their Modifications*, *Hadronic J.* **6** (1983) 985.
- [39] J. R. Gaunt and W. J. Stirling, *Double Parton Distributions Incorporating Perturbative QCD Evolution and Momentum and Quark Number Sum Rules*, *JHEP* **03** (2010) 005, [arXiv:0910.4347].
- [40] A. Snigirev, *Asymptotic behavior of double parton distribution functions*, *Phys. Rev.* **D83** (2011) 034028, [arXiv:1010.4874].

- [41] A. V. Manohar, *Bosonic operator methods for the quark model*, *Phys. Rev.* **D70** (2004) 014004, [hep-ph/0404122].
- [42] R. Peierls and J. Yoccoz, *The Collective model of nuclear motion*, *Proc. Phys. Soc.* **A70** (1957) 381–387.
- [43] F. E. Close and A. W. Thomas, *The Spin and Flavor Dependence of Parton Distribution Functions*, *Phys. Lett.* **B212** (1988) 227.
- [44] I. Barnhill, Maurice V., *Bag Model Electromagnetic Form-Factors*, *Phys. Rev.* **D20** (1979) 723.
- [45] M. Betz and R. Goldflam, *Boosting the Bag*, *Phys. Rev.* **D28** (1983) 2848.
- [46] D.-H. Lu, A. W. Thomas, and A. G. Williams, *Electromagnetic form-factors of the nucleon in an improved quark model*, *Phys. Rev.* **C57** (1998) 2628–2637, [nucl-th/9706019].
- [47] G. A. Miller, *Light front cloudy bag model: Nucleon electromagnetic form-factors*, *Phys. Rev.* **C66** (2002) 032201, [nucl-th/0207007].
- [48] T. Hahn, *CUBA: A Library for multidimensional numerical integration*, *Comput. Phys. Commun.* **168** (2005) 78–95, [hep-ph/0404043].
- [49] G. P. Salam, *Towards Jetography*, *Eur. Phys. J.* **C67** (2010) 637–686, [arXiv:0906.1833].
- [50] M. Cacciari and G. P. Salam, *Pileup subtraction using jet areas*, *Phys. Lett.* **B659** (2008) 119–126, [arXiv:0707.1378].
- [51] D. Krohn, J. Thaler, and L.-T. Wang, *Jet Trimming*, *JHEP* **02** (2010) 084, [arXiv:0912.1342].
- [52] S. D. Ellis, C. K. Vermilion, and J. R. Walsh, *Recombination Algorithms and Jet Substructure: Pruning as a Tool for Heavy Particle Searches*, *Phys. Rev.* **D81** (2010) 094023, [arXiv:0912.0033].
- [53] R. Alon, E. Duchovni, G. Perez, A. P. Pranko, and P. K. Sinervo, *A Data-driven method of pile-up correction for the substructure of massive jets*, *Phys. Rev.* **D84** (2011) 114025, [arXiv:1101.3002].
- [54] G. Soyez, G. P. Salam, J. Kim, S. Dutta, and M. Cacciari, *Pileup subtraction for jet shapes*, *Phys. Rev. Lett.* **110** (2013), no. 16 162001, [arXiv:1211.2811].
- [55] A. Abdesselam, E. B. Kuutmann, U. Bitenc, G. Brooijmans, J. Butterworth, P. B. de Renstrom, D. B. Franzosi, R. Buckingham, B. Chapleau, M. Dasgupta, A. Davison, J. Dolen, S. Ellis, F. Fassi, J. F. M. Frandsen, J. Frost, T. Gadfort,

- N. Glover, A. Haas, E. Halkiadakis, K. Hamilton, C. Hays, C. Hill, J. Jackson, C. Issever, M. Karagoz, A. Katz, L. Kreczko, D. Krohn, A. Lewis, S. Livermore, P. Loch, P. Maksimovic, J. March-Russell, A. Martin, N. McCubbin, D. Newbold, J. Ott, G. Perez, A. Policchio, S. Rappoccio, A. Raklev, P. Richardson, G. Salam, F. Sannino, J. Santiago, A. Schwartzman, C. Shepherd-Themistocleous, P. Sinervo, J. Sjoelin, M. Son, M. Spannowsky, E. Strauss, M. Takeuchi, J. Tseng, B. Tweedie, C. Vermilion, J. Voigt, M. Vos, J. Wacker, J. Wagner-Kuhr, and M. Wilson, *Boosted objects: A Probe of beyond the Standard Model physics*, *Eur. Phys. J.* **C71** (2011) 1661, [arXiv:1012.5412].
- [56] A. Altheimer, S. Arora, L. Asquith, G. Brooijmans, J. Butterworth, M. Campanelli, B. Chapleau, A. E. Cholakian, J. P. Chou, M. Dasgupta, A. Davison, J. Dolen, S. D. Ellis, R. Essig, J. J. Fan, R. Field, A. Fregoso, J. Gallicchio, Y. Gershtein, A. Gomes, A. Haas, E. Halkiadakis, V. Halyo, S. Hoeche, A. Hook, A. Hornig, P. Huang, E. Izaguirre, M. Jankowiak, G. Kribs, D. Krohn, A. J. Larkoski, A. Lath, C. Lee, S. J. Lee, P. Loch, P. Maksimovic, M. Martinez, D. W. Miller, T. Plehn, K. Prokofiev, R. Rahmat, S. Rappoccio, A. Safonov, G. P. Salam, S. Schumann, M. D. Schwartz, A. Schwartzman, M. Seymour, J. Shao, P. Sinervo, M. Son, D. E. Soper, M. Spannowsky, I. W. Stewart, M. Strassler, E. Strauss, M. Takeuchi, J. Thaler, S. Thomas, B. Tweedie, R. V. Sierra, C. K. Vermilion, M. Villapiana, M. Vos, J. Wacker, D. Walker, J. R. Walsh, L.-T. Wang, S. Wilbur, and W. Zhu, *Jet Substructure at the Tevatron and LHC: New results, new tools, new benchmarks*, *J. Phys.* **G39** (2012) 063001, [arXiv:1201.0008].
- [57] D. Krohn, M. D. Schwartz, T. Lin, and W. J. Waalewijn, *Jet Charge at the LHC*, *Phys. Rev. Lett.* **110** (2013), no. 21 212001, [arXiv:1209.2421].
- [58] W. J. Waalewijn, *Calculating the Charge of a Jet*, *Phys. Rev.* **D86** (2012) 094030, [arXiv:1209.3019].
- [59] T. Kinoshita, *Mass singularities of Feynman amplitudes*, *J. Math. Phys.* **3** (1962) 650–677.
- [60] T. Lee and M. Nauenberg, *Degenerate Systems and Mass Singularities*, *Phys. Rev.* **133** (1964) B1549–B1562.
- [61] F. A. Berends and W. Giele, *Recursive Calculations for Processes with n Gluons*, *Nucl. Phys.* **B306** (1988) 759.
- [62] M. L. Mangano and S. J. Parke, *Multiparton amplitudes in gauge theories*, *Phys. Rept.* **200** (1991) 301–367, [hep-th/0509223].
- [63] D. A. Kosower, *All order collinear behavior in gauge theories*, *Nucl. Phys.* **B552** (1999) 319–336, [hep-ph/9901201].

- [64] M. Cacciari, G. P. Salam, and G. Soyez, *The Anti- $k(t)$ jet clustering algorithm*, *JHEP* **0804** (2008) 063, [arXiv:0802.1189].
- [65] M. Cacciari, G. P. Salam, and G. Soyez, *FastJet user manual*, *Eur. Phys. J.* **C72** (2012) 1896, [arXiv:1111.6097].
- [66] CMS Coll. Report, *Commissioning of TrackJets in pp Collisions at 7 TeV*, *CMS-PAS-JME-10-006* (2010).
- [67] J. C. Collins and D. E. Soper, *Back-To-Back Jets in QCD*, *Nucl. Phys.* **B193** (1981) 381.
- [68] J. C. Collins and D. E. Soper, *Parton Distribution and Decay Functions*, *Nucl. Phys.* **B194** (1982) 445.
- [69] H.-M. Chang, M. Procura, J. Thaler, and W. J. Waalewijn, *Calculating Track Thrust with Track Functions*, *Phys. Rev.* **D88** (2013) 034030, [arXiv:1306.6630].
- [70] S. D. Ellis, C. K. Vermilion, J. R. Walsh, A. Hornig, and C. Lee, *Jet Shapes and Jet Algorithms in SCET*, *JHEP* **1011** (2010) 101, [arXiv:1001.0014].
- [71] M. Procura and W. J. Waalewijn, *Fragmentation in Jets: Cone and Threshold Effects*, *Phys. Rev.* **D85** (2012) 114041, [arXiv:1111.6605].
- [72] M. Procura and I. W. Stewart, *Quark Fragmentation within an Identified Jet*, *Phys. Rev.* **D81** (2010) 074009, [arXiv:0911.4980].
- [73] A. Jain, M. Procura, and W. J. Waalewijn, *Parton Fragmentation within an Identified Jet at NNLL*, *JHEP* **1105** (2011) 035, [arXiv:1101.4953].
- [74] G. Salam and D. Wicke, *Hadron masses and power corrections to event shapes*, *JHEP* **0105** (2001) 061, [hep-ph/0102343].
- [75] B. Andersson, G. Gustafson, G. Ingelman, and T. Sjöstrand, *Parton Fragmentation and String Dynamics*, *Phys. Rept.* **97** (1983) 31–145.
- [76] Y. L. Dokshitzer and B. Webber, *Power corrections to event shape distributions*, *Phys. Lett.* **B404** (1997) 321–327, [hep-ph/9704298].
- [77] C. Lee and G. F. Sterman, *Momentum Flow Correlations from Event Shapes: Factorized Soft Gluons and Soft-Collinear Effective Theory*, *Phys. Rev.* **D75** (2007) 014022, [hep-ph/0611061].
- [78] V. Mateu, I. W. Stewart, and J. Thaler, *Power Corrections to Event Shapes with Mass-Dependent Operators*, *Phys. Rev.* **D87** (2013) 014025, [arXiv:1209.3781].
- [79] J. Thaler and K. Van Tilburg, *Identifying Boosted Objects with N-subjettiness*, *JHEP* **1103** (2011) 015, [arXiv:1011.2268].

- [80] S. Catani and M. Seymour, *A General algorithm for calculating jet cross-sections in NLO QCD*, *Nucl. Phys.* **B485** (1997) 291–419, [hep-ph/9605323].
- [81] ALEPH Collaboration, D. Buskulic, D. Decamp, C. Goy, J. Lees, M. Minard, B. Mours, R. Alemany, F. Ariztizabal, P. Comas, J. Crespo, M. Delfino, E. Fernandez, V. Gaitan, L. Garrido, L. Mir, A. Pacheco, A. Pascual, D. Creanza, M. de Palma, A. Farilla, G. Iaselli, G. Maggi, M. Maggi, S. Natali, S. Nuzzo, M. Quattromini, A. Ranieri, G. Raso, F. Romano, F. Ruggieri, G. Selvaggi, L. Silvestris, P. Tempesta, G. Zito, Y. Gao, H. Hu, D. Huang, X. Huang, J. Lin, J. Lou, C. Qiao, T. Wang, Y. Xie, D. Xu, R. Xu, J. Zhang, W. Zhao, W. Atwood, L. Bauerdick, E. Blucher, G. Bonvicini, F. Bossi, J. Boudreau, T. Burnett, H. Drevermann, R. Forty, R. Hagelberg, J. Harvey, S. Haywood, J. Hilgart, R. Jacobsen, B. Jost, J. Knobloch, E. Lancon, I. Lehraus, T. Lohse, A. Lusiani, M. Martinez, P. Mato, T. Mattison, H. Meinhard, S. R. Menary, T. Meyer, A. Minten, A. Miotto, R. Miquel, H. Moser, J. Nash, P. Palazzi, J. Perlas, F. Ranjard, G. Redlinger, G. Rolandi, A. Roth, J. Rothberg, T. Ruan, M. Saich, D. Schlatter, M. Schmelling, F. Sefkow, W. Tejessy, H. Wachsmuth, W. Wiedenmann, T. Wildish, W. Witzeling, J. Wotschack, Z. Ajaltouni, F. Badaud, M. Bardadin-Otwinowska, A. Bencheikh, R. E. Fellous, A. Falvard, P. Gay, C. Guicheney, P. Henrard, J. Jousset, B. Michel, J. Montret, D. Pallin, P. Perret, B. Pietrzyk, J. Proriol, F. Prulhiere, G. Stimpfl, T. Fearnley, J. Hansen, J. Hansen, P. Hansen, R. Mollerud, B. Nilsson, I. Efthymiopoulos, A. Kyriakis, E. Simopoulou, A. Vayaki, K. Zachariadou, J. Badier, A. Blondel, G. Bonneau, J. Brient, G. Fouque, A. Gamess, S. Orteu, A. Rosowsky, A. Rouge, M. Rumpf, R. Tanaka, H. Videau, D. Candlin, M. Parsons, E. Veitch, L. Moneta, G. Parrini, M. Corden, C. Georgopoulos, M. Ikeda, J. Lannutti, D. Levinthal, M. Mermikides, L. Sawyer, S. Wasserbaech, A. Antonelli, R. Baldini, G. Bencivenni, G. Bologna, P. Campana, G. Capon, F. Cerutti, V. Chiarella, B. D. Piazzoli, G. Felici, P. Laurelli, G. Mannocchi, F. Murtas, G. Murtas, L. Passalacqua, M. Pepe-Altarelli, P. Picchi, B. Altoon, O. Boyle, P. Colrain, I. ten Have, J. Lynch, W. Maitland, W. Morton, C. Raine, J. Scarr, K. Smith, A. Thompson, R. Turnbull, B. Brandl, O. Braun, R. Geiges, C. Geweniger, P. Hanke, V. Hepp, E. Kluge, Y. Maumary, A. Putzer, B. Rensch, A. Stahl, K. Tittel, M. Wunsch, A. Belk, R. Beuselinck, D. Binne, W. Cameron, M. Cattaneo, D. Colling, P. Dornan, S. Dugeay, A. Greene, J. Hassard, N. Lieske, S. Patton, D. Payne, M. Phillips, J. Sedgbeer, I. Tomalin, A. Wright, E. Kneringer, D. Kuhn, G. Rudolph, C. Bowdery, T. Brodbeck, A. Finch, F. Foster, G. Hughes, D. Jackson, N. Keemer, M. Nuttall, A. Patel, T. Sloan, S. Snow, E. Whelan, T. Barczewski, K. Kleinknecht, J. Raab, B. Renk, S. Roehn, H. Sander, H. Schmidt, F. Steeg, S. Walther, B. Wolf, J. Aubert, C. Benchouk, V. Bernard, A. Bonissent, J. Carr, P. Coyle, J. Drinkard, F. Etienne, S. Papalexiou, P. Payre, Z. Qian, D. Rousseau, P. Schwemling, M. Talby, S. Adlung, H. Becker, W. Blum, D. N. Brown, P. Cattaneo, G. Cowan, B. Dehning, H. Dielt, F. Dydak, M. Fernandez-Bosman, M. Frank, A. Halley, T. Hansl-Kozanecki,

J. Lauber, G. Lutjens, G. Lutz, W. Manner, Y. Pan, R. Richter, H. Rotscheidt, J. Schroder, A. S. Schwarz, R. Settles, U. Stierlin, U. Stiegler, R. D. S. Denis, M. Takashima, J. Thomas, G. Wolf, V. Bertin, J. Boucrot, O. Callot, X. Chen, A. Cordier, M. Davier, J. Grivaz, P. Heusse, P. Janot, D. Kim, F. L. Diberder, J. Lefrancois, A. Lutz, M. Schune, J. Veillet, I. Videau, Z. Zhang, F. Zomer, D. Abbaneo, S. Amendolia, G. Bagliesi, G. Batignani, L. Bosisio, U. Bottigli, C. Bradaschia, M. Carpinelli, M. Ciocci, R. Dell'Orso, I. Ferrante, F. Fidecaro, L. Foa, E. Focardi, F. Forti, A. Giassi, M. Giorgi, F. Ligabue, E. Mannelli, P. Marrocchesi, A. Messineo, F. Palla, G. Rizzo, G. Sanguinetti, J. Steinberger, R. Tenchini, G. Tonelli, G. Triggiani, C. Vannini, A. Venturi, P. Verdini, J. Walsh, J. Carter, M. Green, P. March, T. Medcalf, I. Quazi, J. Strong, L. West, D. Botterill, R. Cliff, T. Edgecock, M. Edwards, S. Fisher, T. Jones, P. Norton, D. Salmon, J. Thompson, B. Bloch-Devaux, P. Colas, W. Kozanecki, M. Lemaire, E. Locci, S. Loucatos, E. Monnier, P. Perez, F. Perrier, J. Rander, J. Renardy, A. Roussarie, J. Schuller, J. Schwindling, D. S. Mohand, B. Vallage, R. Johnson, A. Litke, G. Taylor, J. Wear, J. Ashman, W. Babbage, C. Booth, C. Buttar, R. Carney, S. Cartwright, F. Combley, F. Hatfield, P. Reeves, L. Thompson, E. Barbiero, S. Brandt, C. Grupen, L. Mirabito, U. Schafer, H. Seywerd, G. Ganis, G. Giannini, B. Gobbo, F. Ragusa, L. Bellantoni, D. Cinabro, J. Conway, D. Cowen, Z. Feng, D. Ferguson, Y. Gao, J. Grahl, J. L. Harton, R. Jared, B. LeClaire, C. Lishka, Y. Pan, J. Pater, Y. Saadi, V. Sharma, M. Schmitt, Z. Shi, Y. sTang, A. Walsh, F. Weber, M. Whitney, S. Wu, X. Wu, and G. Zobernig, *Properties of hadronic Z decays and test of QCD generators*, *Z. Phys.* **C55** (1992) 209–234.

- [82] DELPHI Collaboration, P. Abreu, W. Adam, T. Adye, I. Azhinenko, G. Alekseev, R. Alemany, P. Allport, S. Almehed, U. Amaldi, S. Amato, A. Andreazza, M. Andrieux, P. Antilogus, W. Apel, B. Asman, J. Augustin, A. Augustinus, P. Baillon, P. Bambade, F. Barao, R. Barate, M. Barbi, D. Bardin, A. Baroncelli, O. Barrig, J. Barrio, W. Bartl, M. Bates, M. Battaglia, M. Baubillier, J. Baudot, K. Becks, M. Begalli, P. Beilliere, Y. Belokopytov, K. Belous, A. Benvenuti, M. Berggren, D. Bertini, D. Bertrand, M. Besancon, F. Bianchi, M. Bigi, M. S. Bilenky, P. Billoir, D. Bloch, M. Blume, T. Bolognese, M. Bonesini, W. Bonivento, P. Booth, C. Bosio, O. Botner, E. Boudinov, B. Bouquet, C. Bourdarios, T. Bowcock, M. Bozzo, P. Branchini, K. Brand, T. Brenke, R. Brenner, C. Bricman, R. Brown, P. Bruckman, J. Brunet, L. Bugge, T. Buran, T. Burgsmueller, P. Buschmann, A. Buys, S. Cabrera, M. Caccia, M. Calvi, A. C. Rozas, T. Camporesi, V. Canale, M. Canepa, K. Cankocak, F. Cao, F. Carena, L. Carroll, C. Caso, M. C. Gimenez, A. Cattai, F. Cavallo, V. Chabaud, P. Charpentier, L. Chaussard, P. Checchia, G. Chelkov, M. Chen, R. Chierici, P. Chliapnikov, P. Chochula, V. Chorowicz, J. Chudoba, V. Cindro, P. Collins, J. Contreras, R. Contri, E. Cortina, G. Cosme, F. Cosutti, J. Cowell, H. Crawley, D. Crennell, G. Crosetti, J. C. Maestro, S. Czellar, E. Dahl-Jensen, J. Dahm, B. Dalmagne, M. Dam, G. Damgaard, P. D. Dauncey, M. Davenport, W. D. Silva, C. Defoix, A. Deghorain, G. D. Ricca, P. Delpierre,

N. Demaria, A. D. Angelis, W. D. Boer, S. D. Brabandere, C. D. Clercq, C. de la Vaissiere, B. D. Lotto, A. D. Min, L. D. Paula, C. D. Saint-Jean, H. Dijkstra, L. D. Ciaccio, A. D. Diodato, F. Djama, J. Dolbeau, M. Donszelmann, K. Doroba, M. Dracos, J. Drees, K. Drees, M. Dris, J. Durand, D. Edsall, R. Ehret, G. Eigen, T. Ekelof, G. Ekspong, M. Elsing, J. Engel, B. Erzen, M. E. Santo, E. F. Harris, D. Fassouliotis, M. Feindt, A. Ferrer, S. Fichet, T. Filippas, A. Firestone, P. Fischer, H. Foeth, E. Fokitis, F. Fontanelli, F. Formenti, B. Franek, P. Frenkiel, D. Fries, A. Frodesen, R. Fruhwirth, F. Fulda-Quenzer, J. Fuster, A. Galloni, D. Gamba, M. Gandelman, C. Garcia, J. Garcia, C. Gaspar, U. Gasparini, P. Gavillet, E. Gazis, D. Gele, J. Gerber, R. Gokieli, B. Golob, G. Gopal, L. Gorn, M. Gorski, Y. Gouz, V. Gracco, E. Graziani, C. Green, A. Grefrath, P. Gris, G. Grosdidier, K. Grzelak, S. Gumenyuk, P. Gunnarsson, M. Gunther, J. Guy, F. Hahn, S. Hahn, Z. Hajduk, A. Hallgren, K. Hamacher, F. Harris, V. Hedberg, R. Henriques, J. Hernandez, P. Herquet, H. Herr, T. Hessing, E. Higon, H. Hilke, T. Hill, S. Holmgren, P. Holt, D. Holthuizen, S. Hoorelbeke, M. Houlden, J. Hrubec, K. Huet, K. Hultqvist, J. N. Jackson, R. Jacobsson, P. Jalocha, R. Janik, C. Jarlskog, G. Jarlskog, P. Jarry, B. Jean-Marie, E. K. Johansson, L. Jonsson, P. Jonsson, C. Joram, P. Juillot, M. Kaiser, F. Kapusta, K. Karafasoulis, M. Karlsson, E. Karvelas, S. Katsanevas, E. Katsoufis, R. Keranen, Y. Khokhlov, B. Khomenko, N. Khovansky, B. King, N. Kjaer, O. Klapp, H. Klein, A. Kloving, P. Kluit, B. Koene, P. Kokkinias, M. Kortzinos, K. Korcyl, V. Kostioukhine, C. Kourkoumelis, O. Kouznetsov, C. Kreuter, I. Kronkvist, Z. Krumshtein, W. Krupinski, P. Kubinec, W. Kucewicz, K. Kurvinen, C. Lacasta, I. Laktineh, J. Lamsa, L. Lanceri, D. Lane, P. Langefeld, V. Lapin, J. Laugier, R. Lauhakangas, G. Leder, F. Ledroit, V. Lefebure, C. Legan, R. Leitner, J. Lemonne, G. Lenzen, V. Lepeltier, T. Lesiak, J. Libby, D. Liko, R. Lindner, A. Lipniacka, I. Lippi, B. Loerstad, J. Loken, J. Lopez, D. Loukas, P. Lutz, L. Lyons, J. MacNaughton, G. Maehlum, J. Mahon, A. Maio, T. Malmgren, V. Mal'ychev, F. Mandl, J. Marco, R. Marco, B. Marechal, M. Margoni, J. Marin, C. Mariotti, A. Markou, C. Martinez-Rivero, F. Martinez-Vidal, S. M. i Garcia, J. Masik, F. Matorras, C. Matteuzzi, G. Matthiae, M. Mazzucato, M. McCubbin, R. McKay, R. McNulty, J. Medbo, M. Merk, C. Meroni, S. Meyer, W. Meyer, A. Myagkov, M. Michelotto, E. Migliore, L. Mirabito, W. Mitaroff, U. Mjornmark, T. Moa, R. Moller, K. Monig, M. Monge, P. Morettini, H. Mueller, M. Mulders, L. Mundim, W. Murray, B. Muryn, G. Myatt, F. Naraghi, F. Navarria, S. Navas, K. Nawrocki, P. Negri, W. Neumann, N. Neumeister, R. Nicolaidou, B. Nielsen, M. Nieuwenhuizen, V. Nikolaenko, P. Niss, A. Nomerotski, A. Normand, W. Oberschulte-Beckmann, V. Obraztsov, A. Olshevsky, A. Onofre, R. Orava, K. Osterberg, A. Ouraou, P. Paganini, M. Paganoni, P. Pages, R. Pain, H. Palka, T. Papadopoulou, K. Papageorgiou, L. Pape, C. Parkes, F. Parodi, A. Passeri, M. Pegoraro, L. Peralta, H. Pernegger, M. Pernicka, A. Perrotta, C. Petridou, A. Petrolini, M. Petrovyck, H. Phillips, G. Piana, F. Pierre, S. Plaszczynski, O. Podobrin, M. Pol, G. Polok, P. Poropat, V. Pozdniakov, P. Privitera, N. Pukhaeva, A. Pullia, D. Radojicic, S. Ragazzi, H. Rahmani, J. Rames, P. Ratoff, A. L. Read, M. Reale, P. Rebec-

chi, N. G. Redaelli, M. Regler, D. Reid, P. Renton, L. Resvanis, F. Richard, J. Richardson, J. Ridky, G. Rinaudo, I. Ripp-Baudot, A. Romero, I. Roncaglione, P. Ronchese, L. Roos, E. Rosenberg, E. Rosso, P. Roudeau, T. Rovelli, W. Ruckstuhl, V. Ruhmann-Kleider, A. Ruiz, K. Rybicki, H. Saarikko, Y. Sacquin, A. Sadovsky, O. Sahr, G. Sajot, J. Salt, J. Sanchez, M. Sannino, M. Schimelpfennig, H. Schneider, U. Schwickerath, M. Schyns, G. Sciolla, F. Scuri, P. Seager, Y. Sedykh, A. Segar, A. Seitz, R. Sekulin, L. Serbelloni, R. Shellard, I. Siccama, P. Siegrist, R. Silvestre, S. Simonetti, F. Simonetto, A. Sisakian, B. Sitar, T. Skaali, G. Smadja, N. Smirnov, O. Smirnova, G. Smith, A. Sokolov, R. Sosnowski, D. Souza-Santos, T. Spassov, E. Spiriti, P. Sponholz, S. Squarcia, C. Stanescu, S. Stapnes, I. Stavitski, K. Stevenson, F. Stichelbaut, A. Stocchi, J. Strauss, R. Strub, B. Stugu, M. Szczekowski, M. Szeptycka, T. Tabarelli, J. Tavernet, O. Chikilev, J. Thomas, A. Tilquin, J. Timmermans, L. Tkachev, T. Todorov, S. Todorova, D. Toet, A. Tomaradze, B. Tome, A. Tonazzo, L. Tortora, G. Transtromer, D. Treille, W. Trischuk, G. Tristram, A. Trombini, C. Troncon, A. Tsirou, M. Turluer, I. Tyapkin, M. Tyndel, S. Tzamarias, B. Uberschar, O. Ullaland, V. Uvarov, G. Valenti, E. Vallazza, G. V. Apeldoorn, P. V. Dam, J. V. Eldik, N. Vassilopoulos, G. Vegni, L. Ventura, W. Venus, F. Verbeure, M. Verlato, L. Vertogradov, D. Vilanova, P. Vincent, L. Vitale, E. Vlasov, A. Vodopianov, V. Vrba, H. Wahlen, C. Walck, F. Waldner, M. Weierstall, P. Weilhammer, C. Weiser, A. Wetherell, D. Wicke, J. Wickens, M. Wielers, G. Wilkinson, W. Williams, M. Winter, M. Witek, K. Woschnagg, K. Yip, O. Yushchenko, F. Zach, A. Zaitsev, A. Zalewska, P. Zalewski, D. Zavrtanik, E. Zevgolatakos, N. Zimine, M. Zito, D. Zontar, G. Zucchelli, and G. Zumerle, *Tuning and test of fragmentation models based on identified particles and precision event shape data*, *Z. Phys.* **C73** (1996) 11–60.

- [83] M. Dasgupta and G. P. Salam, *Event shapes in $e^+ e^-$ annihilation and deep inelastic scattering*, *J. Phys.* **G30** (2004) R143, [hep-ph/0312283].
- [84] ALEPH Collaboration, A. Heister, S. Schael, R. Barate, R. Bruneliere, I. D. Bonis, D. Decamp, C. Goy, S. Jezequel, J. Lees, F. Martin, E. Merle, M. Minard, B. Pietrzyk, B. Trocmé, S. Bravo, M. Casado, M. Chmeissani, J. Crespo, E. Fernandez, M. Fernandez-Bosman, L. Garrido, M. Martinez, A. Pacheco, H. Ruiz, A. Colaleo, D. Creanza, N. D. Filippis, M. D. Palma, G. Iaselli, G. Maggi, M. Maggi, S. Nuzzo, A. Ranieri, G. Raso, F. Ruggieri, G. Selvaggi, L. Silvestris, P. Tempesta, A. Tricomi, G. Zito, X. Huang, J. Lin, Q. Ouyang, T. Wang, Y. Xie, R. Xu, S. Xue, J. Zhang, L. Zhang, W. Zhao, D. Abbaneo, T. Barklow, O. Buchmuller, M. Cattaneo, B. Clerbaux, H. Drevermann, R. Forty, M. Frank, F. Gianotti, J. Hansen, J. Harvey, D. Hutchcroft, P. Janot, B. Jost, M. Kado, P. Mato, A. Moutoussi, F. Ranjard, G. Rolandi, D. Schlatter, G. Sguazzoni, F. Teubert, A. Valassi, I. Videau, F. Badaud, S. Dessagne, A. Falvard, D. Fayolle, P. Gay, J. Jousset, B. Michel, S. Monteil, D. Pallin, J. Pascolo, P. Perret,

J. Hansen, J. Hansen, P. Hansen, A. Kraan, B. Nilsson, A. Kyriakis, C. Markou, E. Simopoulou, A. Vayaki, K. Zachariadou, A. Blondel, J. Brient, F. Machefer, A. Rouge, H. Videau, V. Ciulli, E. Focardi, G. Parrini, A. Antonelli, M. Antonelli, G. Bencivenni, F. Bossi, G. Capon, F. Cerutti, V. Chiarella, P. Laurelli, G. Mannocchi, G. Murtas, L. Passalacqua, J. Kennedy, J. Lynch, P. Negus, V. O’Shea, A. Thompson, S. Wasserbaech, R. Cavanaugh, S. Dhamotharan, C. Geweniger, P. Hanke, V. Hepp, E. Kluge, A. Putzer, H. Stenzel, K. Tittel, M. Wunsch, R. Beuselinck, W. Cameron, G. Davies, P. Dornan, M. Girone, R. Hill, N. Marinelli, J. Nowell, S. Rutherford, J. Sedgbeer, J. Thompson, R. White, V. Ghete, P. Girtler, E. Kneringer, D. Kuhn, G. Rudolph, E. Bouhova-Thacker, C. Bowdery, D. Clarke, G. Ellis, A. Finch, F. Foster, G. Hughes, R. Jones, M. Pearson, N. Robertson, M. Smizanska, O. van der Aa, C. Delaere, G. Leibenguth, V. Lemaitre, U. Blumschein, F. Hollendorfer, K. Jakobs, F. Kayser, K. Kleinknecht, A. Muller, B. Renk, H. Sander, S. Schmeling, H. Wachsmuth, C. Zeitnitz, T. Ziegler, A. Bonissent, P. Coyle, C. Curti, A. Ealet, D. Fouchez, P. Payre, A. Tilquin, F. Ragusa, A. David, H. Dietl, G. Ganis, K. Huttmann, G. Lutjens, W. Manner, H. Moser, R. Settles, M. Villegas, G. Wolf, J. Boucrot, O. Callot, M. Davier, L. Duflot, J. Grivaz, P. Heusse, A. Jacholkowska, L. Serin, J. Veillet, P. Azzurri, G. Bagliesi, T. Boccali, L. Foa, A. Giannanco, A. Giassi, F. Ligabue, A. Messineo, F. Palla, G. Sanguinetti, A. Sciaba, P. Spagnolo, R. Tenchini, A. Venturi, P. Verdini, O. Awunor, G. Blair, G. Cowan, A. Garcia-Bellido, M. Green, T. Medcalf, A. Misiejuk, J. Strong, P. Teixeira-Dias, R. Clifft, T. Edgecock, P. Norton, I. Tomalin, J. Ward, B. Bloch-Devaux, D. Boumediene, P. Colas, B. Fabbro, E. Lancon, M. Lemaire, E. Locci, P. Perez, J. Rander, B. Tuchming, B. Vallage, A. Litke, G. Taylor, C. Booth, S. Cartwright, F. Combley, P. Hodgson, M. Lehto, L. Thompson, A. Boehrer, S. Brandt, C. Grupen, J. Hess, A. Ngac, G. Prange, C. Borean, G. Giannini, H. He, J. Putz, J. Rothberg, S. Armstrong, K. Berkelman, K. Cranmer, D. Ferguson, Y. Gao, S. Gonzalez, O. Hayes, H. Hu, S. Jin, J. Kile, P. McNamara, J. Nielsen, Y. Pan, J. von Wimmersperg-Toeller, W. Wiedenmann, J. Wu, S. Wu, X. Wu, G. Zobernig, and G. Dissertori, *Studies of QCD at $e^+ e^-$ centre-of-mass energies between 91-GeV and 209-GeV*, *Eur. Phys. J.* **C35** (2004) 457–486.

- [85] DELPHI Collaboration, J. Abdallah, P. Abreu, W. Adam, P. Adzic, T. Albrecht, T. Alderweireld, R. Alemany-Fernandez, T. Allmendinger, P. Allport, U. Amaldi, N. Amapane, S. Amato, E. Anashkin, A. Andreazza, S. Andringa, N. Anjos, P. Antilogus, W. Apel, Y. Arnoud, S. Ask, B. Asman, J. Augustin, A. Augustinus, P. Baillon, A. Ballestrero, P. Bambade, R. Barbier, D. Bardin, G. Barker, A. Baroncelli, M. Battaglia, M. Baubillier, K. Becks, M. Begalli, A. Behrmann, E. Ben-Haim, N. Benekos, A. Benvenuti, C. Berat, M. Berggren, L. Berntzon, D. Bertrand, M. Besancon, N. Besson, D. Bloch, M. Blom, M. Bluj, M. Bonesini, M. Boonekamp, P. Booth, G. Borisov, O. Botner, B. Bouquet, T. Bowcock, I. Boyko, M. Bracko, R. Brenner, E. Brodet, P. Bruckman, J. Brunet, L. Bugge, P. Buschmann, M. Calvi, T. Camporesi, V. Canale, F. Carena, N. F. Castro, F. Cavallo, M. Chapkin, P. Char-

pentier, P. Checchia, R. Chierici, P. Chliapnikov, J. Chudoba, S. Chung, K. Cieslik, P. Collins, R. Contri, G. Cosme, F. Cossutti, M. Costa, B. Crawley, D. Crennell, J. Cuevas, J. D'Hondt, J. Dalmau, T. da Silva, W. D. Silva, G. D. Ricca, A. D. Angelis, W. D. Boer, C. D. Clercq, B. D. Lotto, N. D. Maria, A. D. Min, L. de Paula, L. D. Ciaccio, A. D. Simone, K. Doroba, J. Drees, M. Dris, G. Eigen, T. Ekelof, M. Ellert, M. Elsing, M. E. Santo, G. Fanourakis, D. Fassouliotis, M. Feindt, J. Fernandez, A. Ferrer, F. Ferro, U. Flagmeyer, H. Foeth, E. Fokitis, F. Fulda-Quenzer, J. Fuster, M. Gandelman, C. Garcia, P. Gavillet, E. Gazis, R. Gokieli, B. Golob, G. Gomez-Ceballos, P. Goncalves, E. Graziani, G. Grosdidier, K. Grzelak, J. Guy, C. Haag, A. Hallgren, K. Hamacher, K. Hamilton, J. Hansen, S. Haug, F. Hauler, V. Hedberg, M. Hennecke, H. Herr, J. Hoffman, S. Holmgren, P. Holt, M. Houlden, K. Hultqvist, J. N. Jackson, G. Jarlskog, P. Jarry, D. Jeans, E. K. Johansson, P. Johansson, P. Jonsson, C. Joram, L. Jungermann, F. Kapusta, S. Katsanevas, E. Katsoufis, G. Kernel, B. Kersevan, A. Kiiskinen, B. King, N. Kjaer, P. Kluit, P. Kokkinias, C. Kourkoumelis, O. Kouznetsov, Z. Krumstein, M. Kucharczyk, J. Lamsa, G. Leder, F. Ledroit, L. Leinonen, R. Leitner, J. Lemonne, V. Lepeltier, T. Lesiak, W. Liebig, D. Liko, A. Lipniacka, J. Lopes, J. Lopez, D. Loukas, P. Lutz, L. Lyons, J. MacNaughton, A. Malek, S. Maltezos, F. Mandl, J. Marco, R. Marco, B. Marechal, M. Margoni, J. Marin, C. Mariotti, A. Markou, C. Martinez-Rivero, J. Masik, N. Mastroyiannopoulos, F. Matorras, C. Matteuzzi, F. Mazzucato, M. Mazzucato, R. McNulty, C. Meroni, W. Meyer, E. Migliore, W. Mitaroff, U. Mjoernmark, T. Moa, M. Moch, K. Monig, R. Monge, J. Montenegro, D. Moraes, S. Moreno, P. Morettini, U. Mueller, K. Muenich, M. Mulders, L. Mundim, W. Murray, B. Muryn, G. Myatt, T. Myklebust, M. Nassiakou, F. Navarria, K. Nawrocki, R. Nicolaïdou, M. Nikolenko, A. Oblakowska-Mucha, V. Obraztsov, A. Olshevski, A. Onofre, R. Orava, K. Osterberg, A. Ouraou, A. Oyanguren, M. Paganoni, S. Paiano, J. Palacios, H. Palka, T. Papadopoulou, L. Pape, C. Parkes, F. Parodi, U. Parzefall, A. Passeri, O. Passon, L. Peralta, V. Perepelitsa, A. Perrotta, A. Petrolini, J. Piedra, L. Pieri, F. Pierre, M. Pimenta, E. Piotto, T. Podobnik, V. Poireau, M. Pol, G. Polok, P. Poropat, V. Pozdniakov, N. Pukhaeva, A. Pullia, J. Rames, L. Ramler, A. L. Read, P. Rebecchi, J. Rehn, D. Reid, R. Reinhardt, P. Renton, F. Richard, J. Ridky, M. Rivero, D. Rodriguez, A. Romero, P. Ronchese, E. Rosenberg, P. Roudeau, T. Rovelli, V. Ruhlmann-Kleider, D. Ryabtchikov, A. Sadovsky, L. Salmi, J. Salt, A. Savoy-Navarro, U. Schwickerath, A. Segar, R. Sekulin, M. Siebel, A. Sisakian, G. Smadja, O. Smirnova, A. Sokolov, A. Sopczak, R. Sosnowski, T. Spassov, M. Stanitzki, A. Stocchi, J. Strauss, B. Stugu, M. Szczekowski, M. Szeptycka, T. Szumlak, T. Tabarelli, A. Taffard, F. Tegenfeldt, J. Timmermans, L. Tkatchev, M. Tobin, S. Todorovova, B. Tome, A. Tonazzo, P. Tortosa, P. Travnicek, D. Treille, G. Tristram, M. Trochimczuk, C. Troncon, M. Turluer, I. Tyapkin, P. Tyapkin, S. Tzamarias, V. Uvarov, G. Valenti, P. V. Dam, J. V. Eldik, A. V. Lysebetten, N. van Remortel, I. V. Vulpen, G. Vegni, F. Veloso, W. Venus, F. Verbeure, P. Verdier, V. Verzi, D. Vilanova, L. Vitale, V. Vrba, H. Wahlen, A. Washbrook, C. Weiser,

- D. Wicke, J. Wickens, G. Wilkinson, M. Winter, M. Witek, O. Yushchenko, A. Zalewska, P. Zalewski, D. Zavrtanik, V. Zhuravlov, N. Zimine, A. Zintchenko, and M. Zupan, *A Study of the energy evolution of event shape distributions and their means with the DELPHI detector at LEP*, *Eur. Phys. J.* **C29** (2003) 285–312, [hep-ex/0307048].
- [86] L3 Collaboration, P. Achard, O. Adriani, M. Aguilar-Benitez, J. Alcaraz, G. Alemanni, J. Allaby, A. Aloisio, M. Alviggi, H. Anderhub, V. P. Andreev, F. Anselmo, A. Arefev, T. Azemoon, T. Aziz, P. Bagnaia, A. Bajo, G. Baksay, L. Baksay, S. Baldew, S. Banerjee, S. Banerjee, A. Barczyk, R. Barillere, P. Bartalini, M. Basile, N. Batalova, R. Battiston, A. Bay, F. Becattini, U. Becker, F. Behner, L. Bellucci, R. Berbeco, J. Berdugo, P. Berges, B. Bertucci, B. Betev, M. Biasini, M. Biglietti, A. Biland, J. Blaising, S. Blyth, G. Bobbink, A. Bohm, L. Boldizsar, B. Borgia, S. Bottai, D. Bourilkov, M. Bourquin, S. Braccini, J. Branson, F. Brochu, J. Burger, W. Burger, X. Cai, M. Capell, G. Romeo, G. Carlino, A. Cartacci, J. Casaus, F. Cavallari, N. Cavallo, C. Cecchi, M. Cerrada, M. Chamizo, Y. Chang, M. Chemarin, A. Chen, G. Chen, G. Chen, H. Chen, H. Chen, G. Chiefari, L. Cifarelli, F. Cindolo, I. Clare, R. Clare, G. Coignet, N. Colino, S. Costantini, B. de la Cruz, S. Cucciarelli, J. van Dalen, R. de Asmundis, P. Deglon, J. Debreczeni, A. Degre, K. Dehmelt, K. Deiters, D. della Volpe, E. Delmeire, P. Denes, F. DeNotaristefani, A. D. Salvo, M. Diemoz, M. Dierckxsens, C. Dionisi, M. Dittmar, A. Doria, M. Dova, D. Duchesneau, M. Duda, B. Echenard, A. Eline, A. E. Hage, H. E. Mamouni, A. Engler, F. Eppling, P. Extermann, M. Falagan, S. Falciano, A. Favara, J. Fay, O. Fedin, M. Felcini, T. Ferguson, H. Fesefeldt, E. Fiandrini, J. Field, F. Filthaut, P. Fisher, W. Fisher, I. Fisk, G. Forconi, K. Freudenreich, C. Furetta, I. Galaktionov, S. Ganguli, P. Garcia-Abia, M. Gataullin, S. Gentile, S. Giagu, Z. Gong, G. J. Grenier, O. Grimm, M. Gruenewald, M. Guida, V. Gupta, A. Gurtu, L. Gutay, D. Haas, D. Hatzifotiadou, T. Hebbeker, A. Herve, J. Hirschfelder, H. Hofer, M. Hohlmann, G. Holzner, S. Hou, Y. Hu, B. Jin, L. W. Jones, P. de Jong, I. Josa-Mutuberria, M. Kaur, M. Kienzle-Focacci, J. Kim, J. Kirkby, W. Kittel, A. Klimentov, A. Konig, M. Kopal, V. Koutsenko, M. Kraber, R. Kraemer, A. Kruger, A. Kunin, P. L. de Guevara, I. Laktineh, G. Landi, M. Lebeau, A. Lebedev, P. Lebrun, P. Lecomte, P. Lecoq, P. L. Coultre, J. L. Goff, R. Leiste, M. Levchenko, P. Levchenko, C. Li, S. Likhoded, C. Lin, W. Lin, F. Linde, L. Lista, Z. Liu, W. Lohmann, E. Longo, Y. Lu, C. Luci, L. Luminari, W. Lustermann, W. Ma, L. Malgeri, A. Malinin, C. Mana, D. Mangeol, J. Mans, J. Martin, F. Marzano, K. Mazumdar, R. McNeil, S. Mele, L. Merola, M. Meschini, W. Metzger, A. Mihul, H. Milcent, G. Mirabelli, J. Mnich, G. Mohanty, G. Muanza, A. Muijs, B. Musicar, M. Musy, S. Nagy, S. Natale, M. Napolitano, F. Nessi-Tedaldi, H. Newman, A. Nisati, T. Novak, H. Kluge, R. Ofierzynski, G. Organini, I. Pal, C. Palomares, P. Paolucci, R. Paramatti, G. Passaleva, S. Patricelli, T. C. Paul, M. Pauluzzi, C. Paus, F. Pauss, M. Pedace, S. Pensotti, D. Perret-Gallix, B. Petersen, D. Piccolo, F. Pierella, M. Pioppi, P. Piroue, E. Pistolesi, V. Plyaskin,

- M. Pohl, V. Pojidaev, J. Pothier, D. Prokofev, J. Quartieri, G. Rahal-Callot, M. A. Rahaman, P. Raics, N. Raja, R. Ramelli, P. Rancoita, R. Ranieri, A. Raspereza, P. Razis, D. Ren, M. Rescigno, S. Reucroft, S. Riemann, K. Riles, B. Roe, L. Romero, A. Rosca, C. Rosemann, C. Rosenbleck, S. Rosier-Lees, S. Roth, J. Rubio, G. Ruggiero, H. Rykaczewski, A. Sakharov, S. Saremi, S. Sarkar, J. Salicio, E. Sanchez, C. Schafer, V. Schegelsky, H. Schopper, D. Schotanus, C. Sciacca, L. Servoli, S. Shevchenko, N. Shivarov, V. Shoutko, E. Shumilov, A. Shvorob, D. Son, C. Souga, P. Spillantini, M. Steuer, D. Stickland, B. Stoyanov, A. Straessner, K. Sudhakar, G. Sultanov, L. Sun, S. Sushkov, H. Suter, J. Swain, Z. Szillasi, X. Tang, P. Tarjan, L. Tauscher, L. Taylor, B. Tellili, D. Teyssier, C. Timmermans, S. C. Ting, S. Ting, S. Tonwar, J. Toth, C. Tully, K. Tung, J. Ulbricht, E. Valente, R. V. de Walle, R. Vasquez, V. Veszpremi, G. Vesztregombi, I. Vetlitsky, D. Vicinanza, G. Viertel, S. Villa, M. Vivargent, S. Vlachos, I. Vodopianov, H. Vogel, H. Vogt, I. Vorobev, A. Vorobyov, M. Wadhwa, Q. Wang, X. Wang, Z. Wang, M. Weber, H. Wilkens, S. Wynhoff, L. Xia, Z. Xu, J. Yamamoto, B. Yang, C. Yang, H. Yang, M. Yang, S. Yeh, A. Zalite, Y. Zalite, Z. Zhang, J. Zhao, G. Zhu, R. Zhu, H. Zhuang, A. Zichichi, B. Zimmermann, and M. Zoller, *Studies of hadronic event structure in e^+e^- annihilation from 30-GeV to 209-GeV with the L3 detector*, *Phys.Rept.* **399** (2004) 71–174, [[hep-ex/0406049](#)].
- [87] OPAL Collaboration, G. Abbiendi, C. Ainsley, P. Akesson, G. Alexander, J. Allison, P. Amaral, G. Anagnostou, K. Anderson, S. Asai, D. Axen, I. Bailey, E. Barberio, T. Barillari, R. Barlow, R. Batley, P. Bechtle, T. Behnke, K. W. Bell, P. Bell, G. Bella, A. Bellerive, G. Benelli, S. Bethke, O. Biebel, O. Boeriu, P. Bock, M. Boutemeur, S. Braibant, R. M. Brown, H. Burckhart, S. Campana, R. Carnegie, A. Carter, J. Carter, C. Chang, D. Charlton, C. Ciocca, A. Csilling, M. Cuffiani, S. Dado, A. Roeck, E. Wolf, K. Desch, B. Dienes, M. Donkers, J. Dubbert, E. Duchovni, G. Duckeck, I. Duerdorff, E. Etzion, F. Fabbri, A. Fanfani, P. Ferrari, F. Fiedler, I. Fleck, M. Ford, A. Frey, P. Gagnon, J. W. Gary, C. Geich-Gimbel, G. Giacomelli, P. Giacomelli, M. Giunta, J. Goldberg, E. Gross, J. Grunhaus, M. Gruwe, P. Gunther, A. Gupta, C. Hajdu, M. Hamann, G. Hanson, A. Harel, M. Hauschild, C. Hawkes, R. Hawkings, R. Hemingway, G. Herten, R. Heuer, J. Hill, K. D. Hoffman, D. Horvath, P. Igo-Kemenes, K. Ishii, H. Jeremie, P. Jojanovic, T. Junk, J. Kanzaki, D. Karlen, K. Kawagoe, T. Kawamoto, R. Keeler, R. Kellogg, B. Kennedy, S. Kluth, T. Kobayashi, M. Kobel, S. Komamiya, T. Kramer, P. Krieger, J. Krogh, T. Kuhl, M. Kupper, G. Lafferty, H. Landsman, D. Lanske, D. Lellouch, J. Lettso, L. Levinson, J. Lillich, S. Lloyd, F. Loebinger, J. Lu, A. Ludwig, J. Ludwig, W. Mader, S. Marcellini, A. Martin, G. Masetti, T. Mashimo, P. Mattig, J. McKenna, R. McPherson, F. Meijers, W. Menges, F. Merritt, H. Mes, N. T. Meyer, A. Michelini, S. Mihara, G. Mikenberg, D. Miller, W. Mohr, A. Montanari, T. Mori, A. Mutter, K. Nagai, I. Nakamura, H. Nanjo, H. Neal, R. Nisius, S. O’Neale, A. Oh, M. Oreglia, S. Orito, C. Pahl, G. Pasztor, J. Pater, J. Pilcher, J. Pinfold, D. E. Plane, O. Pooth, M. Przybycien, A. Quadt,

- K. Rabbertz, C. Rembser, P. Renkel, J. Roney, Y. Rozen, K. Runge, K. Sachs, T. Saeki, E. Sarkisyan, A. Schaile, O. Schaile, P. Scharff-Hansen, J. Schieck, T. Schorner-Sadenius, M. Schroder, M. Schumacher, R. Seuster, T. Shears, B. Shen, P. Sherwood, A. Skuja, A. Smith, R. Sobie, S. Soldner-Rembold, F. Spano, A. Stahl, D. M. Strom, R. Strohmer, S. Tarem, M. Tasevsky, R. Teuscher, M. Thomson, E. Torrence, D. Toya, P. Tran, I. Trigger, Z. Trocsanyi, E. Tsur, M. Turner-Watson, I. Ueda, B. Ujvari, C. Vollmer, P. Vannerem, R. Vertesi, M. Verzocchi, H. Voss, J. Vossebeld, C. Ward, D. Ward, P. Watkins, A. Watson, N. Watson, P. Wells, T. Wengler, N. Wermes, G. Wilson, J. Wilson, G. Wolf, T. Wyatt, S. Yamashita, D. Zer-Zion, and L. Zivkovic, *Measurement of event shape distributions and moments in $e^+ e^- \rightarrow \text{hadrons}$ at 91-GeV - 209-GeV and a determination of alpha(s)*, *Eur.Phys.J.* **C40** (2005) 287–316, [hep-ex/0503051].
- [88] C. W. Bauer, S. Fleming, and M. E. Luke, *Summing Sudakov logarithms in $B \rightarrow X_s \gamma$ in effective field theory*, *Phys. Rev. D* **63** (2000) 014006, [hep-ph/0005275].
 - [89] C. W. Bauer, S. Fleming, D. Pirjol, and I. W. Stewart, *An effective field theory for collinear and soft gluons: Heavy to light decays*, *Phys. Rev. D* **63** (2001) 114020, [hep-ph/0011336].
 - [90] C. W. Bauer and I. W. Stewart, *Invariant operators in collinear effective theory*, *Phys. Lett. B* **516** (2001) 134–142, [hep-ph/0107001].
 - [91] C. W. Bauer, D. Pirjol, and I. W. Stewart, *Soft-collinear factorization in effective field theory*, *Phys. Rev. D* **65** (2002) 054022, [hep-ph/0109045].
 - [92] E. Farhi, *A QCD Test for Jets*, *Phys. Rev. Lett.* **39** (1977) 1587–1588.
 - [93] R. Abbate, M. Fickinger, A. H. Hoang, V. Mateu, and I. W. Stewart, *Thrust at N^3LL with Power Corrections and a Precision Global Fit for alphas(mZ)*, *Phys. Rev. D* **83** (2011) 074021, [arXiv:1006.3080].
 - [94] S. Catani, L. Trentadue, G. Turnock, and B. R. Webber, *Resummation of large logarithms in e^+e^- event shape distributions*, *Nucl. Phys.* **B407** (1993) 3–42.
 - [95] G. P. Korchemsky and G. F. Sterman, *Power corrections to event shapes and factorization*, *Nucl. Phys.* **B555** (1999) 335–351, [hep-ph/9902341].
 - [96] S. Fleming, A. H. Hoang, S. Mantry, and I. W. Stewart, *Jets from massive unstable particles: Top-mass determination*, *Phys. Rev. D* **77** (2008) 074010, [hep-ph/0703207].
 - [97] M. D. Schwartz, *Resummation and NLO Matching of Event Shapes with Effective Field Theory*, *Phys. Rev. D* **77** (2008) 014026, [arXiv:0709.2709].

- [98] S. Fleming, A. H. Hoang, S. Mantry, and I. W. Stewart, *Top Jets in the Peak Region: Factorization Analysis with NLL Resummation*, *Phys. Rev.* **D77** (2008) 114003, [arXiv:0711.2079].
- [99] A. V. Manohar and M. B. Wise, *Power suppressed corrections to hadronic event shapes*, *Phys. Lett.* **B344** (1995) 407–412, [hep-ph/9406392].
- [100] B. Webber, *Estimation of power corrections to hadronic event shapes*, *Phys. Lett.* **B339** (1994) 148–150, [hep-ph/9408222].
- [101] G. P. Korchemsky and G. F. Sterman, *Nonperturbative corrections in resummed cross-sections*, *Nucl. Phys.* **B437** (1995) 415–432, [hep-ph/9411211].
- [102] Y. L. Dokshitzer and B. Webber, *Calculation of power corrections to hadronic event shapes*, *Phys. Lett.* **B352** (1995) 451–455, [hep-ph/9504219].
- [103] G. Korchemsky and S. Tafat, *On power corrections to the event shape distributions in QCD*, *JHEP* **0010** (2000) 010, [hep-ph/0007005].
- [104] A. H. Hoang and I. W. Stewart, *Designing gapped soft functions for jet production*, *Phys. Lett.* **B660** (2008) 483–493, [arXiv:0709.3519].
- [105] Z. Ligeti, I. W. Stewart, and F. J. Tackmann, *Treating the b quark distribution function with reliable uncertainties*, *Phys. Rev.* **D78** (2008) 114014, [arXiv:0807.1926].
- [106] R. Akhoury and V. I. Zakharov, *On the universality of the leading, 1/Q power corrections in QCD*, *Phys. Lett.* **B357** (1995) 646–652, [hep-ph/9504248].
- [107] X. Liu, *SCET approach to top quark decay*, *Phys. Lett.* **B699** (2011) 87–92, [arXiv:1011.3872].
- [108] T. Becher and M. D. Schwartz, *A Precise determination of α_s from LEP thrust data using effective field theory*, *JHEP* **0807** (2008) 034, [arXiv:0803.0342].
- [109] J. Thaler and K. Van Tilburg, *Maximizing Boosted Top Identification by Minimizing N-subjettiness*, *JHEP* **1202** (2012) 093, [arXiv:1108.2701].
- [110] A. J. Larkoski, G. P. Salam, and J. Thaler, *Energy Correlation Functions for Jet Substructure*, *JHEP* **06** (2013) 108, [arXiv:1305.0007].
- [111] G. 't Hooft, *Symmetry Breaking Through Bell-Jackiw Anomalies*, *Phys.Rev.Lett.* **37** (1976) 8–11.
- [112] H. Georgi and S. Glashow, *Unity of All Elementary Particle Forces*, *Phys.Rev.Lett.* **32** (1974) 438–441.
- [113] H. Fritzsch and P. Minkowski, *Unified Interactions of Leptons and Hadrons*, *Annals Phys.* **93** (1975) 193–266.

- [114] J. C. Pati and A. Salam, *Lepton Number as the Fourth Color*, *Phys.Rev.* **D10** (1974) 275–289.
- [115] Super-Kamiokande Collaboration, H. Nishino, S. Clark, K. Abe, Y. Hayato, T. Iida, M. Ikeda, J. Kameda, K. Kobayashi, Y. Koshio, M. Miura, S. Moriyama, M. Nakahata, S. Nakayama, Y. Obayashi, H. Ogawa, H. Sekiya, M. Shiozawa, Y. Suzuki, A. Takeda, Y. Takenaga, Y. Takeuchi, K. Ueno, K. Ueshima, H. Watanabe, S. Yamada, S. Hazama, I. Higuchi, C. Ishihara, T. Kajita, K. Kaneyuki, G. Mitsuka, K. Okumura, N. Tanimoto, M. Vagins, F. Dufour, E. Kearns, M. Litos, J. Raaf, J. Stone, L. Sulak, W. Wang, M. Goldhaber, S. Dazeley, R. Svoboda, K. Bays, D. Casper, J. Cravens, W. Kropp, S. Mine, C. Regis, M. Smy, H. Sobel, K. Ganezer, J. Hill, W. Keig, J. Jang, J. Kim, I. Lim, M. Fechner, K. Scholberg, C. Walter, R. Wendell, S. Tasaka, J. Learned, S. Matsuno, Y. Watanabe, T. Hasegawa, T. Ishida, T. Ishii, T. Kobayashi, T. Nakadaira, K. Nakamura, K. Nishikawa, Y. Oyama, K. Sakashita, T. Sekiguchi, T. Tsukamoto, A. Suzuki, A. Minamino, T. Nakaya, M. Yokoyama, Y. Fukuda, Y. Itow, T. Tanaka, C. Jung, G. Lopez, C. McGrew, R. Terri, C. Yanagisawa, N. Tamura, Y. Idehara, M. Sakuda, Y. Kuno, M. Yoshida, S. Kim, B. Yang, T. Ishizuka, H. Okazawa, Y. Choi, H. Seo, Y. Furuse, K. Nishijima, Y. Yokosawa, M. Koshiba, Y. Totsuka, S. Chen, Y. Heng, Z. Yang, H. Zhang, D. Kielczewska, E. Thrane, and R. Wilkes, *Search for Proton Decay via $p \rightarrow e^+ \pi^0$ and $p \rightarrow \mu^+ \pi^0$ in a Large Water Cherenkov Detector*, *Phys.Rev.Lett.* **102** (2009) 141801, [arXiv:0903.0676].
- [116] Super-Kamiokande, H. Nishino, K. Abe, Y. Hayato, T. Iida, M. Ikeda, J. Kameda, Y. Koshio, M. Miura, S. Moriyama, M. Nakahata, S. Nakayama, Y. Obayashi, H. Sekiya, M. Shiozawa, Y. Suzuki, A. Takeda, Y. Takenaga, Y. Takeuchi, K. Ueno, K. Ueshima, H. Watanabe, S. Yamada, S. Hazama, I. Higuchi, C. Ishihara, H. Kaji, T. Kajita, K. Kaneyuki, G. Mitsuka, K. Okumura, N. Tanimoto, F. Dufour, E. Kearns, M. Litos, J. Raaf, J. Stone, L. Sulak, M. Goldhaber, K. Bays, J. Cravens, W. Kropp, S. Mine, C. Regis, M. Smy, H. Sobel, K. Ganezer, J. Hill, W. Keig, J. Jang, J. Kim, I. Lim, J. Albert, K. Scholberg, C. Walter, R. Wendell, T. Ishizuka, S. Tasaka, J. Learned, S. Matsuno, Y. Watanabe, T. Hasegawa, T. Ishida, T. Ishii, T. Kobayashi, T. Nakadaira, K. Nakamura, K. Nishikawa, Y. Oyama, K. Sakashita, T. Sekiguchi, T. Tsukamoto, A. Suzuki, A. Minamino, T. Nakaya, M. Yokoyama, Y. Fukuda, Y. Itow, T. Tanaka, C. Jung, G. Lopez, C. McGrew, C. Yanagisawa, N. Tamura, Y. Idehara, M. Sakuda, Y. Kuno, M. Yoshida, S. Kim, B. Yang, H. Okazawa, Y. Choi, H. Seo, Y. Furuse, K. Nishijima, Y. Yokosawa, M. Koshiba, Y. Totsuka, M. Vagins, S. Chen, Y. Heng, J. Liu, Z. Yang, H. Zhang, D. Kielczewska, K. Connolly, E. Thrane, and R. Wilkes, *Search for Nucleon Decay into Charged Anti-lepton plus Meson in Super-Kamiokande I and II*, *Phys.Rev.* **D85** (2012) 112001, [arXiv:1203.4030].
- [117] W. Buchmuller and D. Wyler, *Effective Lagrangian Analysis of New Interactions and Flavor Conservation*, *Nucl.Phys.* **B268** (1986) 621–653.

- [118] B. Grzadkowski, M. Iskrzynski, M. Misiak, and J. Rosiek, *Dimension-Six Terms in the Standard Model Lagrangian*, *JHEP* **1010** (2010) 085, [arXiv:1008.4884].
- [119] S. Weinberg, *Baryon and Lepton Nonconserving Processes*, *Phys.Rev.Lett.* **43** (1979) 1566–1570.
- [120] F. Wilczek and A. Zee, *Operator Analysis of Nucleon Decay*, *Phys.Rev.Lett.* **43** (1979) 1571–1573.
- [121] L. Abbott and M. B. Wise, *The Effective Hamiltonian for Nucleon Decay*, *Phys.Rev.* **D22** (1980) 2208.
- [122] C. Grojean, E. E. Jenkins, A. V. Manohar, and M. Trott, *Renormalization Group Scaling of Higgs Operators and $\Gamma(h \rightarrow \gamma\gamma)$* , *JHEP* **1304** (2013) 016, [arXiv:1301.2588].
- [123] P. Minkowski, $\mu \rightarrow e\gamma$ at a Rate of One Out of 10^9 Muon Decays?, *Phys.Lett.* **B67** (1977) 421.
- [124] M. Gell-Mann, P. Ramond, and R. Slansky, *Complex Spinors and Unified Theories*, *Conf.Proc.* **C790927** (1979) 315–321, [arXiv:1306.4669].
- [125] R. N. Mohapatra and G. Senjanovic, *Neutrino Mass and Spontaneous Parity Violation*, *Phys.Rev.Lett.* **44** (1980) 912.
- [126] J. Schechter and J. W. F. Valle, *Neutrino Masses in $SU(2) \times U(1)$ Theories*, *Phys. Rev.* **D22** (1980) 2227.
- [127] M. Blennow and E. Fernandez-Martinez, *Parametrization of Seesaw Models and Light Sterile Neutrinos*, *Phys.Lett.* **B704** (2011) 223–229, [arXiv:1107.3992].
- [128] B. S. Chivukula and H. Georgi, *Composite-technicolor standard model*, *Physics Letters B* **188** (1987) 99–104.
- [129] G. D’Ambrosio, G. Giudice, G. Isidori, and A. Strumia, *Minimal flavor violation: An Effective field theory approach*, *Nucl.Phys.* **B645** (2002) 155–187, [hep-ph/0207036].
- [130] V. Cirigliano, B. Grinstein, G. Isidori, and M. B. Wise, *Minimal flavor violation in the lepton sector*, *Nucl.Phys.* **B728** (2005) 121–134, [hep-ph/0507001].
- [131] S. Davidson and F. Palorini, *Various definitions of Minimal Flavour Violation for Leptons*, *Phys.Lett.* **B642** (2006) 72–80, [hep-ph/0607329].
- [132] R. Alonso, G. Isidori, L. Merlo, L. A. Munoz, and E. Nardi, *Minimal flavour violation extensions of the seesaw*, *JHEP* **1106** (2011) 037, [arXiv:1103.5461].

- [133] E. Nikolidakis and C. Smith, *Minimal Flavor Violation, Seesaw, and R-parity*, *Phys. Rev.* **D77** (2008) 015021, [arXiv:0710.3129].
- [134] R. Alonso, M. Gavela, L. Merlo, and S. Rigolin, *On the scalar potential of minimal flavour violation*, *JHEP* **1107** (2011) 012, [arXiv:1103.2915].
- [135] B. Grinstein, V. Cirigliano, G. Isidori, and M. B. Wise, *Grand Unification and the Principle of Minimal Flavor Violation*, *Nucl.Phys.* **B763** (2007) 35–48, [hep-ph/0608123].
- [136] N. Sakai and T. Yanagida, *Proton Decay in a Class of Supersymmetric Grand Unified Models*, *Nucl.Phys.* **B197** (1982) 533.
- [137] S. Dimopoulos, S. Raby, and F. Wilczek, *Proton Decay in Supersymmetric Models*, *Phys.Lett.* **B112** (1982) 133.
- [138] S. Weinberg, *Supersymmetry at Ordinary Energies. I. Masses and Conservation Laws*, *Phys.Rev.* **D26** (1982) 287.
- [139] J. Bernon and C. Smith, *Baryonic R-parity violation and its running*, *JHEP* **07** (2014) 038, [arXiv:1404.5496].
- [140] BaBar Collaboration, P. del Amo Sanchez, J. Lees, V. Poireau, E. Prencipe, V. Tisserand, J. G. Tico, E. Grauges, M. Martinelli, D. Milanes, A. Palano, M. Papagallo, G. Eigen, B. Stugu, L. Sun, D. N. Brown, L. Kerth, Y. Kolomensky, G. Lynch, I. Osipenkov, H. Koch, T. Schroeder, D. Asgeirsson, C. Hearty, T. Mattison, J. McKenna, A. Khan, V. Blinov, A. Buzykaev, V. Druzhinin, V. Golubev, E. Kravchenko, A. Onuchin, S. Serednyakov, Y. Skovpen, E. Solodov, K. Todyshev, A. Yushkov, M. Bondioli, S. Curry, D. Kirkby, A. Lankford, M. Mandelkern, E. Martin, D. Stoker, H. Atmacan, J. Gary, F. Liu, O. Long, G. Vitug, C. Campagnari, T. Hong, D. Kovalskyi, J. Richman, C. West, A. Eisner, C. Heusch, J. Kroeseberg, W. Lockman, A. Martinez, T. Schalk, B. Schumm, A. Seiden, L. Winstrom, C. Cheng, D. Doll, B. Echenard, D. Hitlin, P. Ongmongkolkul, F. Porter, A. Rakitin, R. Andreassen, M. Dubrovin, B. Meadows, M. Sokoloff, P. Bloom, W. Ford, A. Gaz, M. Nagel, U. Nauenberg, J. Smith, S. Wagner, R. Ayad, W. Toki, H. Jasper, A. Petzold, B. Spaan, M. Kobel, K. Schubert, R. Schwierz, D. Bernard, M. Verderi, P. Clark, S. Playfer, J. Watson, M. Andreotti, D. Bettoni, C. Bozzi, R. Calabrese, A. Cecchi, G. Cibinetto, E. Fioravanti, P. Franchini, I. Garzia, E. Luppi, M. Munerato, M. Negrini, A. Petrella, L. Piemontese, R. Baldini-Ferroli, A. Calcaterra, R. de Sangro, G. Finocchiaro, M. Nicolaci, S. Pacetti, P. Patteri, I. Peruzzi, M. Piccolo, M. Rama, A. Zallo, R. Contri, E. Guido, M. L. Vetere, M. Monge, S. Passaggio, C. Patrignani, E. Robutti, B. Bhuyan, V. Prasad, C. Lee, M. Morii, A. Edwards, A. Adametz, J. Marks, U. Uwer, F. Bernlochner, M. Ebert, H. Lacker, T. Lueck, A. Volk, P. Dauncey, M. Tibbetts, P. Behera, U. Mallik, C. Chen, J. Cochran, H. Crawley, W. Meyer, S. Prell, E. Rosenberg, A. Rubin, A. Gritsan, Z. Guo,

N. Arnaud, M. Davier, D. Derkach, J. F. da Costa, G. Grosdidier, F. L. Diberder, A. Lutz, B. Malaescu, A. Perez, P. Roudeau, M. Schune, J. Serrano, V. Sordini, A. Stocchi, L. Wang, G. Wormser, D. Lange, D. Wright, I. Bingham, C. Chavez, J. Coleman, J. Fry, E. Gabathuler, D. Hutchcroft, D. Payne, C. Touramanis, A. Bevan, F. D. Lodovico, R. Sacco, M. Sigamani, G. Cowan, S. Paramesvaran, A. Wren, D. N. Brown, C. Davis, A. Denig, M. Fritsch, W. Gradl, A. Hafner, K. Alwyn, D. Bailey, R. Barlow, G. Jackson, G. Lafferty, J. Anderson, R. Cenci, A. Jawahery, D. Roberts, G. Simi, J. Tuggle, C. Dallapiccola, E. Salvati, R. Cowan, D. Dujmic, G. Sciolla, M. Zhao, D. Lindemann, P. Patel, S. Robertson, M. Schram, P. Biassoni, A. Lazzaro, V. Lombardo, F. Palombo, S. Stracka, L. Cremaldi, R. Godang, R. Kroeger, P. Sonnek, D. Summers, X. Nguyen, M. Simard, P. Taras, G. D. Nardo, D. Monorchio, G. Onorato, C. Sciacca, G. Raven, H. Snoek, C. Jessop, K. Knoepfel, J. LoSecco, W. Wang, L. Corwin, K. Honscheid, R. Kass, N. Blount, J. Brau, R. Frey, O. Igolkina, J. Kolb, R. Rahmat, N. Sinev, D. Strom, J. Strube, E. Torrence, G. Castelli, E. Feltresi, N. Gagliardi, M. Margoni, M. Morandin, M. Posocco, M. Rotondo, F. Simonetto, R. Stroili, E. Ben-Haim, M. Bomben, G. Bonneaud, H. Briand, G. Calderini, J. Chauveau, O. Hamon, P. Leruste, G. Marchiori, J. Ocariz, J. Prendki, S. Sitt, M. Biasini, E. Manoni, A. Rossi, C. Angelini, G. Batignani, S. Bettarini, M. Carpinelli, G. Casarosa, A. Cervelli, F. Forti, M. Giorgi, A. Lusiani, N. Neri, E. Paoloni, G. Rizzo, J. Walsh, D. L. Pegna, C. Lu, J. Olsen, A. Smith, A. Telnov, F. Anulli, E. Baracchini, G. Cavoto, R. Faccini, F. Ferrarotto, F. Ferroni, M. Gaspero, L. L. Gioi, M. Mazzoni, G. Piredda, F. Renga, C. Buenger, T. Hartmann, T. Leddig, H. Schroder, R. Waldi, T. Adye, E. Olaiya, F. Wilson, S. Emery, G. H. de Monchenault, G. Vasseur, C. Yeche, M. Allen, D. Aston, D. Bard, R. Bartoldus, J. Benitez, C. Cartaro, M. Convery, J. Dorfan, G. Dubois-Felsmann, W. Dunwoodie, R. Field, M. F. Sevilla, B. Fulsom, A. Gabareen, M. Graham, P. Grenier, C. Hast, W. Innes, M. Kelsey, H. Kim, P. Kim, M. Kocian, D. Leith, P. Lewis, S. Li, B. Lindquist, S. Luitz, V. Luth, H. Lynch, D. MacFarlane, D. Muller, H. Neal, S. Nelson, C. O'Grady, I. Ofte, M. Perl, T. Pulliam, B. Ratcliff, A. Roodman, A. Salnikov, V. Santoro, R. Schindler, J. Schwiening, A. Snyder, D. Su, M. Sullivan, S. Sun, K. Suzuki, J. Thompson, J. Va'vra, A. Wagner, M. Weaver, W. Wisniewski, M. Wittgen, D. Wright, H. Wulsin, A. Yarritu, C. Young, V. Ziegler, X. Chen, W. Park, M. Purohit, R. White, J. Wilson, A. Randle-Conde, S. Sekula, M. Bellis, P. Burchart, T. Miyashita, S. Ahmed, M. Alam, J. Ernst, B. Pan, M. Saeed, S. Zain, N. Guttman, A. Soffer, P. Lund, S. Spanier, R. Eckmann, J. Ritchie, A. Ruland, C. Schilling, R. Schwitters, B. Wray, J. Izen, X. Lou, F. Bianchi, D. Gamba, M. Pelliccioni, L. Lanceri, L. Vitale, N. Lopez-March, F. Martinez-Vidal, A. Oyanguren, H. Ahmed, J. Albert, S. Banerjee, H. Choi, K. Hamano, G. King, R. Kowalewski, M. Lewczuk, C. Lindsay, I. Nugent, J. Roney, R. Sobie, T. Gershon, P. Harrison, T. Latham, E. Puccio, H. Band, S. Dasu, K. Flood, Y. Pan, R. Prepost, C. Vuosalo, and S. Wu, *Searches for the baryon- and lepton-number violating decays $B^0 \rightarrow \Lambda_c^+ \ell^-$, $B^- \rightarrow \Lambda \ell^-$, and $B^- \rightarrow \bar{\Lambda} \ell^-$* , *Phys.Rev.* **D83** (2011) 091101,

[arXiv:1101.3830].

- [141] CMS Collaboration, S. Chatrchyan, V. Khachatryan, A. M. Sirunyan, A. Tumasyan, W. Adam, T. Bergauer, M. Dragicevic, J. Erö, C. Fabjan, M. Friedl, R. Fruehwirth, V. M. Ghete, N. Hörmann, J. Hrubec, M. Jeitler, W. Kiesenhofer, V. Knünz, M. Krammer, I. Krätschmer, D. Liko, I. Mikulec, D. Rabady, B. Rahbaran, C. Rohringer, H. Rohringer, R. Schöfbeck, J. Strauss, A. Taurok, W. Treberer-Treberspurg, W. Waltenberger, C.-E. Wulz, V. Mossolov, N. Shumeiko, J. S. Gonzalez, S. Alderweireldt, M. Bansal, S. Bansal, T. Cornelis, E. A. D. Wolf, X. Janssen, A. Knutsson, S. Luyckx, L. Mucibello, S. Ochesanu, B. Roland, R. Rougny, Z. Staykova, H. V. Haevermaet, P. V. Mechelen, N. V. Remortel, A. V. Spilbeeck, F. Blekman, S. Blyweert, J. D'Hondt, A. Kalogeropoulos, J. Keaveney, S. Lowette, M. Maes, A. Olbrechts, S. Tavernier, W. V. Doninck, P. V. Mulders, G. P. V. Onsem, I. Villella, C. Caillol, B. Clerbaux, G. D. Lentdecker, L. Favart, A. Gay, T. Hreus, A. Léonard, P. E. Marage, A. Mohammadi, L. Perniè, T. Reis, T. Seva, L. Thomas, C. V. Velde, P. Vanlaer, J. Wang, V. Adler, K. Beernaert, L. Benucci, A. Cimmino, S. Costantini, S. Dildick, G. Garcia, B. Klein, J. Lelouch, A. Marinov, J. Mccartin, A. A. O. Rios, D. Ryckbosch, M. Sigamani, N. Strobbe, F. Thyssen, M. Tytgat, S. Walsh, E. Yazgan, N. Zaganidis, S. Basegmez, C. Beluffi, G. Bruno, R. Castello, A. Caudron, L. Ceard, G. G. D. Silveira, C. Delaere, T. D. Pree, D. Favart, L. Forthomme, A. Giannanco, J. Hollar, P. Jez, V. Lemaitre, J. Liao, O. Militaru, C. Nuttens, D. Pagano, A. Pin, K. Piotrkowski, A. Popov, M. Selvaggi, M. V. Marono, J. M. V. Garcia, N. Beliy, T. Caebergs, E. Daubie, G. H. Hammad, G. Alves, M. C. M. Junior, T. Martins, M. E. Pol, M. H. G. E. Souza, W. L. A. Júnior, W. Carvalho, J. Chinellato, A. Custódio, E. M. D. Costa, D. D. J. Damiao, C. D. O. Martins, S. F. D. Souza, H. Malbouisson, M. Malek, D. M. Figueiredo, L. Mundim, H. Nogima, W. L. P. D. Silva, A. Santoro, A. Sznajder, E. J. T. Manganote, A. V. Pereira, C. A. Bernardes, F. D. A. Dias, T. Tomei, E. D. M. Gregores, C. Lagana, P. G. Mercadante, S. F. Novaes, S. Padula, V. Genchev, P. Iaydjiev, S. Piperov, M. Rodozov, G. Sultanov, M. Vutova, A. Dimitrov, R. Hadjiiska, V. Kozhuharov, L. Litov, B. Pavlov, P. Petkov, J.-G. Bian, G.-M. Chen, H.-S. Chen, C.-H. Jiang, D. Liang, S. Liang, X. Meng, J. Tao, X. Wang, Z. Wang, C. Asawatangtrakuldee, Y. Ban, Y. Guo, Q. Li, W. Li, S. Liu, Y. Mao, S.-J. Qian, D. Wang, L. Zhang, W. Zou, C. Avila, C. A. C. Montoya, L. F. C. Sierra, J. P. Gomez, B. G. Moreno, J. C. Sanabria, N. Godinovic, D. Lelas, R. Plestina, D. Polic, I. Puljak, Z. Antunovic, M. Kovac, V. Brigljevic, K. Kadija, J. Luetic, D. Mekterovic, S. Morovic, L. Tikvica, A. Attikis, G. Mavromanolakis, J. Mousa, C. Nicolaou, F. Ptochos, P. A. Razis, M. Finger, M. F. Jr, A. A. Abdelalim, Y. Assran, S. Elgammal, A. E. Kamel, M. Mahmoud, A. Radi, M. Kadastik, M. Müntel, M. Murumaa, M. Raidal, L. Rebane, A. Tiko, P. Eerola, G. Fedi, M. Voutilainen, J. Härkönen, V. Karimäki, R. Kinnunen, M. J. Kortelainen, T. Lampén, K. Lassila-Perini, S. Lehti, T. Lindén, P.-R. Luukka, T. Mäenpää, T. Peltola, E. Tuominen, J. Tuominiemi, E. Tuovinen, L. Wendland, T. Tuuva,

M. Besancon, F. Couderc, M. Dejardin, D. Denegri, B. Fabbro, J.-L. Faure, F. Ferri, S. Ganjour, A. Givernaud, P. Gras, G. H. de Monchenault, P. Jarry, E. Locci, J. Malcles, L. Millischer, A. Nayak, J. Rander, A. Rosowsky, M. Titov, S. Baffioni, F. Beaudette, L. Benhabib, M. Bluj, P. Busson, C. Charlot, N. Daci, T. Dahms, M. Dalchenko, L. Dobrzynski, A. Florent, R. G. de Cassagnac, M. Haguenauer, P. Miné, C. Mironov, I. N. Naranjo, M. Nguyen, C. Ochando, P. Paganini, D. Sabes, R. Salerno, Y. Sirois, C. Veelken, A. Zabi, J.-L. Agram, J. Andrea, D. Bloch, J.-M. Brom, E. C. Chabert, C. Collard, E. Conte, F. Drouhin, J.-C. Fontaine, D. Gelé, U. Goerlach, C. Goetzmann, P. Juillot, A.-C. L. Bihan, P. V. Hove, S. Gadrat, S. Beauceron, N. Beaupere, G. Boudoul, S. Brochet, J. Chasserat, R. Chierici, D. Contardo, P. Depasse, H. E. Mamouni, J. Fan, J. Fay, S. Gascon, M. Gouzevitch, B. Ille, T. Kurca, M. Lethuillier, L. Mirabito, S. Perries, L. Sgandurra, V. Sordini, M. V. Donckt, P. Verdier, S. Viret, H. Xiao, Z. Tsamalaidze, C. Autermann, S. Beranek, M. Bontenackels, B. Calpas, M. Edelhoff, L. Feld, N. Heracleous, O. Hindrichs, K. Klein, A. Ostapchuk, A. Perieanu, F. Raupach, J. Sammet, S. Schael, D. Sprenger, H. Weber, B. Wittmer, V. Zhukov, M. Ata, J. Caudron, E. Dietz-Laursonn, D. Duchardt, M. Erdmann, R. Fischer, A. Güth, T. Hebbeker, C. Heidemann, K. Hoepfner, D. Klingebiel, S. Knutzen, P. Kreuzer, M. Merschmeyer, A. Meyer, M. Olschewski, K. Padéken, P. Papacz, H. Pieta, H. Reithler, S. A. Schmitz, L. Sonnenschein, J. Steggemann, D. Teyssier, S. Thüer, M. Weber, V. Cherepanov, Y. Erdogan, G. Flügge, H. Geenen, M. Geisler, W. H. Ahmad, F. Hoehle, B. Kargoll, T. Kress, Y. Kuessel, J. Lingemann, A. Nowack, I. M. Nugent, L. Perchalla, O. Pooth, A. Stahl, I. Asin, N. Bartosik, J. Behr, W. Behrenhoff, U. Behrens, A. J. Bell, M. Bergholz, A. Bethani, K. Borras, A. Burgmeier, A. Cakir, L. Calligaris, A. Campbell, S. Choudhury, F. Costanza, C. D. Pardos, S. Dooling, T. Dorland, G. Eckerlin, D. Eckstein, G. Flucke, A. Geiser, I. Glushkov, A. Grebenyuk, P. Gunnellini, S. Habib, J. Hauk, G. Hellwig, D. Horton, H. Jung, M. Kasemann, P. Katsas, C. Kleinwort, H. Kluge, M. Krämer, D. Krücker, E. Kuznetsova, W. Lange, J. Leonard, K. Lipka, W. Lohmann, B. Lutz, R. Mankel, I. Marfin, I.-A. Melzer-Pellmann, A. B. Meyer, J. Mnich, A. Mussgiller, S. Naumann-Emme, O. Novgorodova, F. Nowak, J. Olzem, H. Perrey, A. Petrukhin, D. Pitzl, R. Placakyte, A. Raspereza, P. M. R. Cipriano, C. Riedl, E. Ron, M. Özgür Sahin, J. Salfeld-Nebgen, R. Schmidt, T. Schoerner-Sadenius, N. Sen, M. Stein, R. Walsh, C. Wissing, M. A. Martin, V. Blobel, H. Enderle, J. Erfle, E. Garutti, U. Gebbert, M. Görner, M. Gosselink, J. Haller, K. Heine, R. S. Höing, G. Kaussen, H. Kirschenmann, R. Klanner, R. Kogler, J. Lange, I. Marchesini, T. Peiffer, N. Pietsch, D. Rathjens, C. Sander, H. Schettler, P. Schleper, E. Schlieckau, A. Schmidt, M. Schröder, T. Schum, M. Seidel, J. Sibille, V. Sola, H. Stadie, G. Steinbrück, J. Thomsen, D. Troendle, E. Usai, L. Vanelderden, C. Barth, C. Baus, J. Berger, C. Böser, E. Butz, T. Chwalek, W. D. Boer, A. Descroix, A. Dierlamm, M. Feindt, M. Guthoff, F. Hartmann, T. Hauth, H. Held, K.-H. Hoffmann, U. Husemann, I. Katkov, J. R. Komaragiri, A. Kornmayer, P. L. Pardo, D. Martschei, M. U. Mozer, T. Müller, M. Niegel, A. Nürnberg, O. Oberst, J. Ott, G. Quast, K. Rab-

bertz, F. Ratnikov, S. Röcker, F.-P. Schilling, G. Schott, H.-J. Simonis, F.-M. H. Stober, R. Ulrich, J. Wagner-Kuhr, S. Wayand, T. Weiler, M. Zeise, G. Anagnostou, G. Daskalakis, T. Geralis, S. Kesisoglou, A. Kyriakis, D. Loukas, A. Markou, C. Markou, E. Ntomari, I. Topsis-giotis, L. Gouskos, A. Panagiotou, N. Saoulidou, E. Stiliaris, X. Aslanoglou, I. Evangelou, G. Flouris, C. Foudas, P. Kokkas, N. Manthos, I. Papadopoulos, E. Paradas, G. Bencze, C. Hajdu, P. Hidas, D. Horvath, F. Sikler, V. Veszpremi, G. Vesztergombi, A. J. Zsigmond, N. Beni, S. Czellar, J. Molnar, J. Palinkas, Z. Szillasi, J. Karancsi, P. Raics, Z. L. Trocsanyi, B. Ujvari, S. K. Swain, S. B. Beri, V. Bhatnagar, N. Dhingra, R. Gupta, M. Kaur, M. Z. Mehta, M. Mittal, N. Nishu, A. Sharma, J. Singh, A. Kumar, A. Kumar, S. Ahuja, A. Bhardwaj, B. C. Choudhary, A. Kumar, S. Malhotra, M. Naimuddin, K. Ranjan, P. Saxena, V. Sharma, R. K. Shivpuri, S. Banerjee, S. Bhattacharya, K. Chatterjee, S. Dutta, B. Gomber, S. Jain, S. Jain, R. Khurana, A. Modak, S. Mukherjee, D. Roy, S. Sarkar, M. Sharan, A. Singh, A. Abdulsalam, D. Dutta, S. Kailas, V. Kumar, A. K. Mohanty, L. M. Pant, P. Shukla, A. Topkar, T. Aziz, R. M. Chatterjee, S. Ganguly, S. Ghosh, M. Guchait, A. Gurtu, G. Kole, S. Kumar, M. Maity, G. Majumder, K. Mazumdar, G. B. Mohanty, B. Parida, K. Sudhakar, N. Wickramage, S. Banerjee, S. Dugad, H. Arfaei, H. Bakhshiansohi, S. M. Etesami, A. Fahim, A. Jafari, M. Khakzad, M. M. Najafabadi, S. P. Mehdiabadi, B. Safarzadeh, M. Zeinali, M. Grunewald, M. Abbrescia, L. Barbone, C. Calabria, S. S. Chhibra, A. Colaleo, D. Creanza, N. D. Filippis, M. D. Palma, L. Fiore, G. Iaselli, G. Maggi, M. Maggi, B. Marangelli, S. My, S. Nuzzo, N. Pacifico, A. Pompili, G. Pugliese, G. Selvaggi, L. Silvestris, G. Singh, R. Venditti, P. Verwilligen, G. Zito, G. Abbiendi, A. Benvenuti, D. Bonacorsi, S. Braibant-Giacomelli, L. Brigliadori, R. Campanini, P. Capiluppi, A. Castro, F. R. Cavallo, G. Codispoti, M. Cuffiani, G.-M. Dallavalle, F. Fabbri, A. Fanfani, D. Fasanella, P. Giacomelli, C. Grandi, L. Guiducci, S. Marcellini, G. Masetti, M. Meneghelli, A. Montanari, F. Navarria, F. Odorici, A. Perrotta, F. Primavera, A. Rossi, T. Rovelli, G. P. Siroli, N. Tosi, R. Travaglini, S. Albergo, G. Cappello, M. Chiorboli, S. Costa, F. Giordano, R. Potenza, A. Tricomi, C. Tuve, G. Barbagli, V. Ciulli, C. Civinini, R. D'Alessandro, E. Focardi, S. Frosali, E. Gallo, S. Gonzi, V. Gori, P. Lenzi, M. Meschini, S. Paoletti, G. Sguazzoni, A. Tropiano, L. Benussi, S. Bianco, F. Fabbri, D. Piccolo, P. Fabbricatore, R. Ferretti, F. Ferro, M. L. Vetere, R. Musenich, E. Robutti, S. Tosi, A. Benaglia, M. E. Dinardo, S. Fiorendi, S. Gennai, A. Ghezzi, P. Govoni, M. T. Lucchini, S. Malvezzi, R. A. Manzoni, A. Martelli, D. Menasce, L. Moroni, M. Paganoni, D. Pedrini, S. Ragazzi, N. Redaelli, T. T. de Fatis, S. Buontempo, N. Cavallo, A. D. Cosa, F. Fabozzi, A. O. M. Iorio, L. Lista, S. Meola, M. Merola, P. Paolucci, P. Azzi, N. Bacchetta, D. Bisello, A. Branca, R. Carlin, P. Checchia, T. Dorigo, F. Fanzago, M. Galanti, F. Gasparini, U. Gasparini, P. Giubilato, F. Gonella, A. Gozzelino, K. Kanishchev, S. Lacaprara, I. Lazzizzera, M. Margoni, A. T. Meneguzzo, M. Passaseo, J. Pazzini, N. Pozzobon, P. Ronchese, F. Simonetto, E. Torassa, M. Tosi, A. Triossi, P. Zotto, A. Zucchetta, G. Zumerle, M. Gabusi, S. P. Ratti, C. Riccardi, P. Vitulo, M. Biasini, G. M. Bilei, L. Fanò, P. Lariccia, G. Mantovani,

M. Menichelli, A. Nappi, F. Romeo, A. Saha, A. Santocchia, A. Spiezia, K. Androssov, P. Azzurri, G. Bagliesi, J. Bernardini, T. Boccali, G. Broccolo, R. Castaldi, M. A. Ciocci, R. T. D'Agnolo, R. Dell'Orso, F. Fiori, L. Foà, A. Giassi, M. T. Grippo, A. Kraan, F. Ligabue, T. Lomtadze, L. Martini, A. Messineo, C.-S. Moon, F. Palla, A. Rizzi, A. Savoy-Navarro, A. T. Serban, P. Spagnolo, P. Squillaciotti, R. Tenchini, G. Tonelli, A. Venturi, P. G. Verdini, C. Vernieri, L. Barone, F. Cavallari, D. D. Re, M. Diemoz, M. Grassi, E. Longo, F. Margaroli, P. Meridiani, F. Micheli, S. Nourbakhsh, G. Organtini, R. Paramatti, S. Rahatlou, C. Rovelli, L. Soffi, N. Amapane, R. Arcidiacono, S. Argiro, M. Arneodo, R. Bellan, C. Biino, N. Cartiglia, S. Casasso, M. Costa, A. Degano, N. Demaria, C. Mariotti, S. Maselli, E. Migliore, V. Monaco, M. Musich, M. M. Obertino, N. Pastrone, M. Pelliccioni, A. Potenza, A. Romero, M. Ruspa, R. Sacchi, A. Solano, A. Staiano, U. Tamponi, S. Belforte, V. Candelise, M. Casarsa, F. Cossutti, G. D. Ricca, B. Gobbo, C. L. Licata, M. Marone, D. Montanino, A. Penzo, A. Schizzi, A. Zanetti, S. Chang, T. Y. Kim, S.-K. Nam, D. H. Kim, G. N. Kim, J. E. Kim, D. J. Kong, S. Lee, Y. D. Oh, H. Park, D.-C. Son, J. Y. Kim, Z. J. Kim, S. Song, S. Choi, D. Gyun, B.-S. Hong, M. Jo, H. Kim, T. J. Kim, K. S. Lee, S. K. Park, Y. Roh, M. Choi, J. H. Kim, C. Park, I. Park, S. Park, G. Ryu, Y.-I. Choi, Y. K. Choi, J. Goh, M. S. Kim, E. Kwon, B. Lee, J. Lee, S. Lee, H. Seo, I. Yu, I. Grigelionis, A. Juodagalvis, H. Castilla-Valdez, E. D. L. Cruz-Burelo, I. H. de La Cruz, R. Lopez-Fernandez, J. Martínez-Ortega, A. S. Hernández, L. M. Villasenor-Cendejas, S. C. Moreno, F. V. Valencia, H. A. S. Ibarguen, E. C. Linares, A. M. Pineda, M. A. Reyes-Santos, D. Kroccheck, P. H. Butler, R. Doesburg, S. Reucroft, H. Silverwood, M. Ahmad, M. I. Asghar, J. Butt, H. R. Hoorani, S. Khalid, W. A. Khan, T. Khurshid, S. Qazi, M. A. Shah, M. Shoaib, H. Bialkowska, B. Boimska, T. Frueboes, M. Górski, M. Kazana, K. Nawrocki, K. Romanowska-Rybinska, M. Szleper, G. Wrochna, P. Zalewski, G. Brona, K. Bunkowski, M. Cwiok, W. Dominik, K. Doroba, A. Kalinowski, M. Konecki, J. Krolikowski, M. Misiura, W. Wolszczak, N. Almeida, P. Bargassa, C. B. D. C. E. Silva, P. Faccioli, P. G. F. Parracho, M. Gallinaro, F. Nguyen, J. R. Antunes, J. Seixas, J. Varela, P. Vischia, S. Afanasiev, P. Bunin, M. Gavrilenko, I. Golutvin, I. Gorbunov, A. Kamenev, V. Karjavin, V. Konoplyanikov, A. Lanev, A. Malakhov, V. Matveev, P. Moisenz, V. Palichik, V. Perelygin, S. Shmatov, N. Skatchkov, V. Smirnov, A. Zarubin, S. Evstyukhin, V. Golovtsov, Y. Ivanov, V. Kim, P. Levchenko, V. Murzin, V. Oreshkin, I. Smirnov, V. Sulimov, L. Uvarov, S. Vavilov, A. Vorobyev, A. Vorobyev, Y. Andreev, A. Dermenev, S. Glinenko, N. Golubev, M. Kirsanov, N. Krasnikov, A. Pashenkov, D. Tlisov, A. Toropin, V. Epshteyn, M. Erofeeva, V. Gavrilov, N. Lychkovskaya, V. Popov, G. Safronov, S. Semenov, A. Spiridonov, V. Stolin, E. Vlasov, A. Zhokin, V. Andreev, M. Azarkin, I. Dremin, M. Kirakosyan, A. Leonidov, G. Mesyats, S. V. Rusakov, A. Vinogradov, A. Belyaev, E. Boos, M. Dubinin, L. Dudko, A. Ershov, A. Gribushin, V. Klyukhin, O. Kodolova, I. Loktin, A. Markina, S. Obraztsov, S. Petrushanko, V. Savrin, A. Snigirev, I. Azhgirey, I. Bayshev, S. Bitioukov, V. Kachanov, A. Kalinin, D. Konstantinov, V. Krychkine, V. Petrov, R. Ryutin,

A. Sobol, L. Tourtchanovitch, S. Troshin, N. Tyurin, A. Uzunian, A. Volkov, P. Adzic, M. Djordjevic, M. Ekmedzic, J. Milosevic, M. Aguilar-Benitez, J. A. Maestre, C. Battilana, E. Calvo, M. Cerrada, M. C. Llatas, N. Colino, B. D. L. Cruz, A. D. Peris, D. D. Vázquez, C. F. Bedoya, J. P. F. Ramos, A. Ferrando, J. Flix, M. C. Fouz, P. Garcia-Abia, O. G. Lopez, S. G. Lopez, J. M. Hernandez, M. I. Josa, G. Merino, E. N. D. Martino, J. P. Pelayo, A. Q. Olmeda, I. Redondo, L. Romero, J. Santaolalla, M. S. Soares, C. Willmott, C. Albajar, J. F. de Trocóniz, H. Brun, J. Cuevas, J. F. Menendez, S. Folgueras, I. G. Caballero, L. L. Iglesias, J. P. Gomez, J. A. B. Cifuentes, I. J. Cabrillo, A. Calderon, S.-H. Chuang, J. D. Campderros, M. Fernandez, G. Gomez, J. G. Sanchez, A. Graziano, C. Jordà, A. L. Virto, J. Marco, R. Marco, C. M. Rivero, F. Matorras, F. J. M. Sanchez, T. Rodrigo, A. Y. Rodríguez-Marrero, A. Ruiz-Jimeno, L. Scodellaro, I. Vila, R. V. Cortabitarte, D. Abbaneo, E. Auffray, G. Auzinger, M. Bachtis, P. Baillon, A. Ball, D. Barney, J. Bendavid, J. F. Benitez, C. Bernet, G. Bianchi, P. Bloch, A. Bocci, A. Bonato, O. Bondu, C. Botta, H. Breuker, T. Camporesi, G. Cerminara, T. Christiansen, J. A. C. Perez, S. Colafranceschi, M. D'Alfonso, D. D'Enterria, A. Dabrowski, A. D. T. Mendes, F. D. Guio, A. D. Roeck, S. D. Visscher, S. D. Guida, M. Dobson, N. Dupont-Sagorin, A. Elliott-Peisert, J. Eugster, G. Franzoni, W. Funk, G. Georgiou, M. Giffels, D. Gigi, K. Gill, D. Giordano, M. Girone, M. Giunta, F. Glege, R. G.-R. Garrido, S. Gowdy, R. Guida, J. Hammer, M. Hansen, P. Harris, C. Hartl, A. Hinzmann, V. Innocente, P. Janot, E. Karavakis, K. Kousouris, K. Krajczar, P. Lecoq, Y.-J. Lee, C. Lourenco, N. Magini, L. Malgeri, M. Mannelli, L. Masetti, F. Meijers, S. Mersi, E. Meschi, R. Moser, M. Mulders, P. Musella, E. Nesvold, L. Orsini, E. P. Cortezon, E. Perez, L. Perrozzi, A. Petrilli, A. Pfeiffer, M. Pierini, M. Pimiä, D. Piparo, M. Plagge, L. Quertenmont, A. Racz, W. Reece, G. Rolandi, M. Rovere, H. Sakulin, F. Santanastasio, C. Schäfer, C. Schwick, S. Sekmen, A. Sharma, P. Siegrist, P. Silva, M. Simon, P. Sphicas, D. Spiga, B. Stieger, M. Stoye, A. Tsirou, G. I. Veres, J.-R. Vlimant, H. K. Wöhri, S. Worm, W. D. Zeuner, W. Bertl, K. Deiters, W. Erdmann, K. Gabathuler, R. Horisberger, Q. Ingram, H.-C. Kaestli, S. König, D. Kotlinski, U. Langenegger, D. Renker, T. Rohe, F. Bachmair, L. Bäni, L. Bianchini, P. Bortignon, M.-A. Buchmann, B. Casal, N. Chanon, A. Deisher, G. Dissertori, M. Dittmar, M. Donegà, M. Dünser, P. Eller, K. Freudenreich, C. Grab, D. Hits, P. Lecomte, W. Lustermann, B. Mangano, A. C. Marini, P. M. R. del Arbol, D. Meister, N. Mohr, F. Moortgat, C. Nägeli, P. Nef, F. Nessi-Tedaldi, F. Pandolfi, L. Pape, F. Pauss, M. Peruzzi, M. Quittnat, F. J. Ronga, M. Rossini, L. Sala, A. K. Sanchez, A. Starodumov, M. Takahashi, L. Tauscher, A. Thea, K. Theofilatos, D. Treille, C. Urscheler, R. Wallny, H. A. Weber, C. Amsler, V. Chiochia, C. Favaro, M. I. Rikova, B. Kilminster, B. M. Mejias, P. Robmann, H. Snoek, S. Taroni, M. Verzetti, Y. Yang, M. Cardaci, K.-H. Chen, C. Ferro, C.-M. Kuo, S.-W. Li, W. Lin, Y.-J. Lu, R. Volpe, S.-S. Yu, P. Bartalini, P. Chang, Y.-H. Chang, Y.-W. Chang, Y. Chao, K.-F. Chen, C. Dietz, U. Grundler, G. W.-S. Hou, Y. Hsiung, K.-Y. Kao, Y.-J. Lei, R.-S. Lu, D. Majumder, E. Petrakou, X. Shi, J.-G. Shiu, Y.-M. Tzeng, M. Wang, B. Asavapibhop, N. Suwonjandee,

A. Adiguzel, M. N. Bakirci, S. Cerci, C. Dozen, I. Dumanoglu, E. Eskut, S. Girgis, G. Gokbulut, E. Gurpinar, I. Hos, E. E. Kangal, A. K. Topaksu, G. Onengut, K. Ozdemir, S. Ozturk, A. Polatoz, K. Sogut, D. S. Cerci, B. Tali, H. Topakli, M. Vergili, I. V. Akin, T. Aliev, B. Bilin, S. Bilmis, M. Deniz, H. Gamsizkan, A. M. Guler, G. Karapinar, K. Ocalan, A. Ozpineci, M. Serin, R. Sever, U. E. Surat, M. Yalvac, M. Zeyrek, E. Gülmek, B. Isildak, M. Kaya, O. Kaya, S. Ozkorucuklu, N. Sonmez, H. Bahtiyar, E. Barlas, K. Cankocak, Y. O. Günaydin, F. I. Vardarli, M. Yücel, L. Levchuk, P. Sorokin, J. J. Brooke, E. Clement, D. Cussans, H. Flacher, R. Frazier, J. Goldstein, M. Grimes, G. P. Heath, H. F. Heath, L. Kreczko, C. Lucas, Z. Meng, S. Metson, D. M. Newbold, K. Nirunpong, S. Paramesvaran, A. Poll, S. Senkin, V. J. Smith, T. Williams, K. W. Bell, A. Belyaev, C. Brew, R. M. Brown, D. J. Cockerill, J. A. Coughlan, K. Harder, S. Harper, J. Ilic, E. Olaiya, D. Petyt, B. C. Radburn-Smith, C. Shepherd-Themistocleous, I. R. Tomalin, W. J. Womersley, R. Bainbridge, O. Buchmuller, D. Burton, D. Colling, N. Cripps, M. Cutajar, P. Dauncey, G. Davies, M. D. Negra, W. Ferguson, J. Fulcher, D. Futyan, A. Gilbert, A. G. Bryer, G. Hall, Z. Hatherell, J. Hays, G. Iles, M. Jarvis, G. Karapostoli, M. Kenzie, R. Lane, R. Lucas, L. Lyons, A.-M. Magnan, J. Marrouche, B. Mathias, R. Nandi, J. Nash, A. Nikitenko, J. Pela, M. Pesaresi, K. Petridis, M. Pioppi, D. M. Raymond, S. Rogerson, A. Rose, C. Seez, P. Sharp, A. Sparrow, A. Tapper, M. V. Acosta, T. Virdee, S. Wakefield, N. Wardle, M. Chadwick, J. Cole, P. R. Hobson, A. Khan, P. Kyberd, D. Leggat, D. Leslie, W. Martin, I. Reid, P. Symonds, L. Teodorescu, M. Turner, J. Dittmann, K. Hatakeyama, A. Kasmi, H. Liu, T. Scarborough, O. Charaf, S. Cooper, C. Henderson, P. Rumerio, A. Avetisyan, T. Bose, C. Fantasia, A. Heister, P. Lawson, D. Lazic, J. Rohlf, D. Sperka, J. S. John, L. Sulak, J. Alimena, S. Bhattacharya, G. Christopher, D. Cutts, Z. Demiragli, A. Ferapontov, A. Garabedian, U. Heintz, S. Jabeen, G. Kukartsev, E. Laird, G. Landsberg, M. Luk, M. Narain, M. Segala, T. Sinthuprasith, T. Speer, R. Breeden, G. Breto, M. C. D. L. B. Sanchez, S. Chauhan, M. Chertok, J. Conway, R. Conway, P. T. Cox, R. Erbacher, M. Gardner, R. Houtz, W. Ko, A. Kopecky, R. Lander, T. Miceli, D. Pellett, J. Pilot, F. Ricci-Tam, B. Rutherford, M. Searle, J. Smith, M. Squires, M. Tripathi, S. Wilbur, R. Yohay, V. Andreev, D. Cline, R. Cousins, S. Erhan, P. Everaerts, C. Farrell, M. Felcini, J. Hauser, M. Ignatenko, C. Jarvis, G. Rakness, P. Schlein, E. Takasugi, P. Traczyk, V. Valuev, M. Weber, J. Babb, R. Clare, J. A. Ellison, J. W. Gary, G. Hanson, J. Heilman, P. Jandir, H. Liu, O. R. Long, A. Luthra, M. Malberti, H. Nguyen, A. Shrinivas, J. Sturdy, S. Sumowidagdo, R. Wilken, S. Wimpenny, W. Andrews, J. G. Branson, G. B. Cerati, S. Cittolin, D. Evans, A. Holzner, R. Kelley, M. Lebourgeois, J. Letts, I. Macneill, S. Padhi, C. Palmer, G. Petrucciani, M. Pieri, M. Sani, V. Sharma, S. Simon, E. Sudano, M. Tadel, Y. Tu, A. Vartak, S. Wasserbaech, F. Würthwein, A. Yagil, J. Yoo, D. Barge, C. Campagnari, T. Danielson, K. Flowers, P. Geffert, C. George, F. Golf, J. Incandela, C. Justus, D. Kovalskyi, V. Krutelyov, R. M. Villalba, N. Mccoll, V. Pavlunin, J. Richman, R. Rossin, D. Stuart, W. To, C. West, A. Apresyan, A. Bornheim, J. Bunn, Y. Chen, E. D. Marco, J. Duarte, D. Kcira,

Y. Ma, A. Mott, H. B. Newman, C. Pena, C. Rogan, M. Spiropulu, V. Timciuc, J. Veerka, R. Wilkinson, S. Xie, R.-Y. Zhu, V. Azzolini, A. Calamba, R. Carroll, T. Ferguson, Y. Iiyama, D. W. Jang, Y.-F. Liu, M. Paulini, J. Russ, H. Vogel, I. Vorobiev, J. P. Cumalat, B. R. Drell, W. T. Ford, A. Gaz, E. L. Lopez, U. Nauenberg, J. Smith, K. Stenson, K. Ulmer, S. R. Wagner, J. Alexander, A. Chatterjee, N. Eggert, L. K. Gibbons, W. Hopkins, A. Khukhunaishvili, B. Kreis, N. Mirman, G. N. Kaufman, J. R. Patterson, A. Ryd, E. Salvati, W. Sun, W. D. Teo, J. Thom, J. Thompson, J. Tucker, Y. Weng, L. Winstrom, P. Wittich, D. Winn, S. Abdullin, M. Albrow, J. Anderson, G. Apollinari, L. A. Bauerdiick, A. Beretvas, J. Berryhill, P. C. Bhat, K. Burkett, J. N. Butler, V. Chetluru, H. Cheung, F. Chlebana, S. Ci-hangir, V. D. Elvira, I. Fisk, J. Freeman, Y. Gao, E. Gottschalk, L. Gray, D. Green, O. Gutsche, D. Hare, R. M. Harris, J. Hirschauer, B. Hooberman, S. Jindariani, M. Johnson, U. Joshi, K. Kaadze, B. Klima, S. Kunori, S. Kwan, J. Linacre, D. Lincoln, R. Lipton, J. Lykken, K. Maeshima, J. M. Marraffino, V. I. M. Outschoorn, S. Maruyama, D. Mason, P. McBride, K. Mishra, S. Mrenna, Y. Musienko, C. Newman-Holmes, V. O'Dell, O. Prokofyev, N. Ratnikova, E. Sexton-Kennedy, S. Sharma, W. J. Spalding, L. Spiegel, L. Taylor, S. Tkaczyk, N. V. Tran, L. Uplegger, E. W. Vaandering, R. Vidal, J. Whitmore, W. Wu, F. Yang, J. C. Yun, D. Acosta, P. Avery, D. Bourilkov, M. Chen, T. Cheng, S. Das, M. D. Gruttola, G. P. D. Giovanni, D. Dobur, A. Drozdetskiy, R. D. Field, M. Fisher, Y. Fu, I.-K. Furic, J. Hugon, B. Kim, J. Konigsberg, A. Korytov, A. Kropivnitskaya, T. Kypreos, J. F. Low, K. Matchev, P. Milenovic, G. Mitselmakher, L. Muniz, R. Remington, A. Rinkevicius, N. Skhirtladze, M. Snowball, J. Yelton, M. Zakaria, V. Gaultney, S. Hewamanage, S. Linn, P. Markowitz, G. Martinez, J. L. Rodriguez, T. Adams, A. Askew, J. Bochenek, J. Chen, B. Diamond, J. Haas, S. Hagopian, V. Hagopian, K. F. Johnson, H. Prosper, V. Veeraraghavan, M. Weinberg, M. M. Baarmann, B. Dorney, M. Hohlmann, H. Kalakhety, F. Yumiceva, M. R. Adams, L. Apanasevich, V. E. Bazterra, R. R. Betts, I. Bucinskaite, J. Callner, R. Cavanaugh, O. Evdokimov, L. Gauthier, C. E. Gerber, D. J. Hofman, S. Khalatyan, P. Kurt, F. Lacroix, D. H. Moon, C. O'Brien, C. Silkworth, D. Strom, P. Turner, N. Varelas, U. Akgun, E. A. Albayrak, B. Bilki, W. Clarida, K. Dilsiz, F. Duru, S. Griffiths, J.-P. Merlo, H. Mermerkaya, A. Mestvirishvili, A. Moeller, J. Nachtmann, C. R. Newsom, H. Ogul, Y. Onel, F. Ozok, S. Sen, P. Tan, E. Tiras, J. Wetzel, T. Yetkin, K. Yi, B. A. Barnett, B. Blumenfeld, S. Bolognesi, G. Giurgiu, A. Gritsan, G. Hu, P. Maksimovic, C. Martin, M. Swartz, A. Whitbeck, P. Baringer, A. Bean, G. Benelli, R. P. K. III, M. Murray, D. Noonan, S. Sanders, R. Stringer, J. S. Wood, A.-F. Barfuss, I. Chakaberia, A. Ivanov, S. Khalil, M. Makouski, Y. Maravin, L. K. Saini, S. Shrestha, I. Svintradze, J. Gronberg, D. Lange, F. Rebassoo, D. Wright, D. Baden, B. Calvert, S. C. Eno, J. Gomez, N. J. Hadley, R. G. Kellogg, T. Kolberg, Y. Lu, M. Marionneau, A. Mignerey, K. Pedro, A. Peterman, A. Skuja, J. Temple, M. Tonjes, S. C. Tonwar, A. Apyan, G. Bauer, W. Busza, I. A. Cali, M. Chan, L. D. Matteo, V. Dutta, G. G. Ceballos, M. Goncharov, D. Gulhan, Y. Kim, M. Klute, Y. S. Lai, A. Levin, P. D. Luckey, T. Ma, S. Nahn,

C. Paus, D. Ralph, C. Roland, G. Roland, G. Stephans, F. Stöckli, K. Sumorok, D. Velicanu, R. Wolf, B. Wyslouch, M. Yang, Y. Yilmaz, S. Yoon, M. Zanetti, V. Zhukova, B. Dahmes, A. D. Benedetti, A. Gude, J. Haupt, S.-C. Kao, K. Klapoetke, Y. Kubota, J. Mans, N. Pastika, R. Rusack, M. Sasseville, A. Singovsky, N. Tambe, J. Turkewitz, J. G. Acosta, L. M. Cremaldi, R. Kroeger, S. Oliveros, L. Perera, R. Rahmat, D. A. Sanders, D. Summers, E. Avdeeva, K. Bloom, S. Bose, D. R. Claes, A. Dominguez, M. Eads, R. G. Suarez, J. Keller, I. Kravchenko, J. Lazo-Flores, S. Malik, F. Meier, G. R. Snow, J. Dolen, A. Godshalk, I. Iashvili, S. Jain, A. Kharchilava, A. Kumar, S. Rappoccio, Z. Wan, G. Alverson, E. Barberis, D. Baumgartel, M. Chasco, J. Haley, A. Massironi, D. Nash, T. Orimoto, D. Trocino, D. Wood, J. Zhang, A. Anastassov, K. A. Hahn, A. Kubik, L. Lusito, N. Mucia, N. Odell, B. Pollack, A. Pozdnyakov, M. H. Schmitt, S. Stoynev, K. Sung, M. Velasco, S. Won, D. Berry, A. Brinkerhoff, K. M. Chan, M. Hildreth, C. Jessop, D. J. Karmgard, J. Kolb, K. Lannon, W. Luo, S. Lynch, N. Marinelli, D. M. Morse, T. Pearson, M. Planer, R. Ruchti, J. Slaunwhite, N. Valls, M. Wayne, M. Wolf, L. Antonelli, B. Bylsma, L. S. Durkin, S. Flowers, C. Hill, R. Hughes, K. Kotov, T.-Y. Ling, D. Puigh, M. Rodenburg, G. Smith, C. Vuosalo, B. L. Winer, H. Wolfe, E. Berry, P. Elmer, V. Halyo, P. Hebda, J. Hegeman, A. Hunt, P. Jindal, S. A. Koay, P. Lujan, D. Marlow, T. Medvedeva, M. Mooney, J. Olsen, P. Piroué, X. Quan, A. Raval, H. Saka, D. Stickland, C. Tully, J. S. Werner, S. C. Zenz, A. Zuranski, E. Brownson, A. Lopez, H. Mendez, J. E. R. Vargas, E. Alagoz, D. Benedetti, G. Bolla, D. Bortoletto, M. D. Mattia, A. Everett, Z. Hu, M. Jones, K. Jung, O. Koybasi, M. Kress, N. Leonardo, D. L. Pegna, V. Maroussov, P. Merkel, D. H. Miller, N. Neumeister, I. Shipsey, D. Silvers, A. Svyatkovskiy, F. Wang, W. Xie, L. Xu, H. D. Yoo, J. Zablocki, Y. Zheng, N. Parashar, A. Adair, B. Akgun, K. M. Ecklund, F. J. Geurts, W. Li, B. Michlin, B. P. Padley, R. Redjimi, J. Roberts, J. Zabel, B. Betchart, A. Bodek, R. Covarelli, P. de Barbaro, R. Demina, Y. Eshaq, T. Ferbel, A. Garcia-Bellido, P. Goldenzweig, J. Han, A. Harel, D. C. Miner, G. Petrillo, D. Vishnevskiy, M. Zielinski, A. Bhatti, R. Ciesielski, L. Demortier, K. Goulian, G. Lungu, S. Malik, C. Mesropian, S. Arora, A. Barker, J. P. Chou, C. Contreras-Campana, E. Contreras-Campana, D. Duggan, D. Ferencek, Y. Gershstein, R. Gray, E. Halkiadakis, D. Hidas, A. Lath, S. Panwalkar, M. Park, R. Patel, V. Rekovic, J. Robles, S. Salur, S. Schnetzer, C. Seitz, S. Somalwar, R. Stone, S. Thomas, P. Thomassen, M. Walker, G. Cerizza, M. Hollingsworth, K. Rose, S. Spanier, Z.-C. Yang, A. York, O. Bouhali, R. Eusebi, W. Flanagan, J. Gilmore, T. Kamon, V. Khotilovich, R. Montalvo, I. Osipenkov, Y. Pakhotin, A. Perloff, J. Roe, A. Safonov, T. Sakuma, I. Suarez, A. Tatarinov, D. Toback, N. Akchurin, C. Cowden, J. Damgov, C. Dragoiu, P. R. Dudero, K. Kovitanggoon, S. W. Lee, T. Libeiro, I. Volobouev, E. Appelt, A. G. Delannoy, S. Greene, A. Gurrola, W. Johns, C. Maguire, Y. Mao, A. Melo, M. Sharma, P. Sheldon, B. Snook, S. Tuo, J. Velkovska, M. W. Arenton, S. Boutle, B. Cox, B. Francis, J. Goodell, R. Hirosky, A. Ledovskoy, C. Lin, C. Neu, J. Wood, S. Gollapinni, R. Harr, P. E. Karchin, C. K. K. Don, P. Lamichhane, A. Sakharov, D. Belknap, L. Borrello, D. Carlsmith,

- M. Cepeda, S. Dasu, S. Duric, E. Friis, M. Grothe, R. Hall-Wilton, M. Herndon, A. Hervé, P. Klabbers, J. Klukas, A. Lanaro, R. Loveless, A. Mohapatra, I. Ojalvo, T. Perry, G. A. Pierro, G. Polese, I. Ross, T. Sarangi, A. Savin, W. H. Smith, and J. Swanson, *Search for baryon number violation in top-quark decays*, *Phys.Lett.* **B731** (2014) 173, [arXiv:1310.1618].
- [142] D. E. Morrissey, T. M. P. Tait, and C. E. M. Wagner, *Proton lifetime and baryon number violating signatures at the CERN LHC in gauge extended models*, *Phys. Rev.* **D72** (2005) 095003, [hep-ph/0508123].
- [143] W.-S. Hou, M. Nagashima, and A. Soddu, *Baryon number violation involving higher generations*, *Phys.Rev.* **D72** (2005) 095001, [hep-ph/0509006].
- [144] Z. Dong, G. Durieux, J.-M. Gerard, T. Han, and F. Maltoni, *Baryon number violation at the LHC: the top option*, *Phys. Rev.* **D85** (2012) 016006, [arXiv:1107.3805].
- [145] S. Weinberg, *V-A was the key*, *J. Phys. Conf. Ser.* **196** (2009) 012002.
- [146] N. Cabibbo, *Unitary Symmetry and Leptonic Decays*, *Phys. Rev. Lett.* **10** (1963) 531–533.
- [147] V. Cirigliano, J. Jenkins, and M. Gonzalez-Alonso, *Semileptonic decays of light quarks beyond the Standard Model*, *Nucl. Phys.* **B830** (2010) 95–115, [arXiv:0908.1754].
- [148] P. Herczeg, *Beta decay beyond the standard model*, *Prog. Part. Nucl. Phys.* **46** (2001) 413–457.
- [149] N. Severijns, M. Beck, and O. Naviliat-Cuncic, *Tests of the standard electroweak model in beta decay*, *Rev. Mod. Phys.* **78** (2006) 991–1040, [nucl-ex/0605029].
- [150] T. Bhattacharya, V. Cirigliano, S. D. Cohen, A. Filipuzzi, M. Gonzalez-Alonso, M. L. Graesser, R. Gupta, and H.-W. Lin, *Probing Novel Scalar and Tensor Interactions from (Ultra)Cold Neutrons to the LHC*, *Phys. Rev.* **D85** (2012) 054512, [arXiv:1110.6448].
- [151] V. Cirigliano, S. Gardner, and B. Holstein, *Beta Decays and Non-Standard Interactions in the LHC Era*, *Prog. Part. Nucl. Phys.* **71** (2013) 93–118, [arXiv:1303.6953].
- [152] O. Naviliat-Cuncic and M. González-Alonso, *Prospects for precision measurements in nuclear β decay at the LHC era*, *Annalen Phys.* **525** (2013) 600–619, [arXiv:1304.1759].
- [153] M. González-Alonso and J. Martin Camalich, *Isospin breaking in the nucleon mass and the sensitivity of β decays to new physics*, *Phys. Rev. Lett.* **112** (2014), no. 4 042501, [arXiv:1309.4434].

- [154] P. Herczeg, *On the question of a tensor interaction in $\pi \rightarrow e\nu_e\gamma$ decay*, *Phys. Rev.* **D49** (1994) 247–253.
- [155] B. A. Campbell and D. W. Maybury, *Constraints on scalar couplings from $\pi^\pm \rightarrow l^\pm \nu_l$* , *Nucl. Phys.* **B709** (2005) 419–439, [hep-ph/0303046].
- [156] V. Cirigliano, M. Gonzalez-Alonso, and M. L. Graesser, *Non-standard Charged Current Interactions: beta decays versus the LHC*, *JHEP* **02** (2013) 046, [arXiv:1210.4553].
- [157] V. Cirigliano, G. Ecker, H. Neufeld, A. Pich, and J. Portoles, *Kaon Decays in the Standard Model*, *Rev. Mod. Phys.* **84** (2012) 399, [arXiv:1107.6001].
- [158] V. Bernard, M. Oertel, E. Passemar, and J. Stern, *$K(\mu\nu 3)^{**}L$ decay: A Stringent test of right-handed quark currents*, *Phys. Lett.* **B638** (2006) 480–486, [hep-ph/0603202].
- [159] V. Bernard, M. Oertel, E. Passemar, and J. Stern, *Tests of non-standard electroweak couplings of right-handed quarks*, *JHEP* **01** (2008) 015, [arXiv:0707.4194].
- [160] O. Yushchenko, S. Akimenko, G. Britvich, K. Datsko, A. Filin, A. Inyakin, A. Konstantinov, V. Konstantinov, I. Korolkov, V. K. V. Leontiev, V. Novikov, V. Obraztsov, V. Polyakov, V. Romanovsky, V. Ronjin, V. Shelikhov, N. Smirnov, O. Tchikilev, V. Uvarov, V. Bolotov, S. Laptev, and A. Polyarush, *High statistic measurement of the $K^- \rightarrow \pi^0 e^- \nu$ decay form-factors*, *Phys. Lett.* **B589** (2004) 111–117, [hep-ex/0404030].
- [161] M. Antonelli, D. M. Asner, D. A. Bauer, T. G. Becher, M. Beneke, A. J. Bevan, M. Blanke, C. Bloise, M. Bona, A. E. Bondar, C. Bozzi, J. Brod, A. J. Buras, N. Cabibbo, A. Carbone, G. Cavoto, V. Cirigliano, M. Ciuchini, J. P. Coleman, D. P. Cronin-Hennessy, J. Dalseno, C. Davies, F. D. Lodovico, J. C. Dingfelder, Z. Dolezal, S. Donati, W. Dungel, U. Egede, G. Eigen, R. Faccini, T. Feldmann, F. Ferroni, J. M. Flynn, E. Franco, M. Fujikawa, I. K. Furic, P. Gambino, E. Gardi, T. J. Gershon, S. Giagu, E. Golowich, T. Goto, C. Greub, C. Grojean, D. Guadagnoli, U. Haisch, R. F. Harr, A. H. Hoang, T. Hurth, G. Isidori, D. Jaffe, A. Juttner, S. Jager, A. Khodjamirian, P. S. Koppenburg, R. V. Kowalewski, P. Krokovny, A. S. Kronfeld, J. Laiho, G. Lanfranchi, T. E. Latham, J. F. Libby, A. Limosani, D. L. Pegna, C.-D. Lu, V. Lubicz, E. Lunghi, V. G. Luth, K. Maltman, W. J. Marciano, E. C. M. Martin, G. Martinelli, F. Martinez-Vidal, A. Masiero, V. Mateu, F. Mescia, G. B. Mohanty, M. Moulson, M. Neubert, H. Neufeld, S. Nishida, N. Offen, M. Palutan, P. Paradisi, Z. Parsa, E. Passemar, M. Patel, B. Pecjak, A. A. Petrov, A. Pich, M. Pierini, B. Plaster, B. A. Powell, S. A. Prell, J. Rademaker, M. Rescigno, S. Ricciardi, P. Robbe, E. Rodrigues, M. Rotondo, R. Sacco, C. J. Schilling, O. Schneider, E. E. Scholz, B. A. Schumm, C. Schwanda, A. J. Schwartz, B. Sciascia, J. Serrano, J. Shigemitsu, I. P. Shipsey, A. Sibidanov, L. Silvestrini,

- F. Simonetto, S. Simula, C. Smith, A. Soni, L. Sonnenschein, V. Sordini, M. S. Sozzi, T. Spadaro, P. M. Spradlin, A. Stocchi, N. Tantalo, C. Tarantino, A. V. Telnov, D. Tonelli, I. Towner, K. Trabelsi, P. Urquijo, R. V. de Water, R. J. V. Kooten, J. Virto, G. Volpi, R. Wanke, S. Westhoff, G. Wilkinson, M. B. Wingate, Y. Xie, and J. Zupan, *Flavor Physics in the Quark Sector*, *Phys. Rept.* **494** (2010) 197–414, [arXiv:0907.5386].
- [162] M. Carpentier and S. Davidson, *Constraints on two-lepton, two quark operators*, *Eur. Phys. J.* **C70** (2010) 1071–1090, [arXiv:1008.0280].
- [163] FlaviaNet Working Group on Kaon Decays, M. Antonelli, E. D. Lucia, P. D. Simone, P. Franzini, S. Glazov, E. Goudzovski, M. Moulson, V. Obraztsov, M. Palutan, M. Piccini, G. Ruggiero, B. Sciascia, T. Spadaro, M. Veltri, R. Wanke, A. Winhart, O. Yushchenko, M. Sozzi, J. Bijnens, V. Cirigliano, J. Gasser, C. Gatti, R. Hill, G. Isidori, F. Mescia, E. Passemar, and J. Stern, *Precision tests of the Standard Model with leptonic and semileptonic kaon decays*, in *PHIPSI08, proceedings of the International Workshop on e^+e^- Collisions from phi to psi, Frascati (Rome) Italy, 7-10 April 2008*, 2008. [arXiv:0801.1817].
- [164] J. M. Gaillard and G. Sauvage, *Hyperon Beta Decays*, *Ann. Rev. Nucl. Part. Sci.* **34** (1984) 351–402.
- [165] A. Garcia, *The Beta Decay of Hyperons*, *Lect. Notes Phys.* **222** (1985) 1–173.
- [166] N. Cabibbo, E. C. Swallow, and R. Winston, *Semileptonic hyperon decays*, *Ann. Rev. Nucl. Part. Sci.* **53** (2003) 39–75, [hep-ph/0307298].
- [167] A. Kadeer, J. G. Korner, and U. Moosbrugger, *Helicity analysis of semileptonic hyperon decays including lepton mass effects*, *Eur. Phys. J.* **C59** (2009) 27–47, [hep-ph/0511019].
- [168] KTeV E832/E799 Collaboration, A. A. Affolder, A. Alavi-Harati, I. Albuquerque, T. Alexopoulos, M. Arenton, K. Arisaka, S. Averitte, A. Barker, L. Bellantoni, A. Bellavance, J. Belz, R. Ben-David, D. Bergman, E. Blucher, G. Bock, C. Bown, S. Bright, E. Cheu, S. Childress, R. Coleman, M. Corcoran, G. Corti, B. Cox, M. Crisler, A. Erwin, R. Ford, A. Golossanov, G. Graham, J. Graham, K. Hagan, E. Halkiadakis, K. Hanagaki, S. Hidaka, Y. Hsiung, V. Jejer, J. Jennings, D. Jensen, R. Kessler, H. Kobrak, J. LaDue, A. Lath, A. Ledovskoy, P. McBride, A. McManus, P. Mikelsons, E. Monnier, T. Nakaya, U. Nauenberg, K. Nelson, H. Nguyen, V. O’Dell, M. Pang, R. Pordes, V. Prasad, C. Qiao, B. Quinn, E. Ramberg, R. Ray, A. Roodman, M. Sadamoto, S. Schnetzer, K. Senyo, P. Shanahan, P. Shawhan, W. Slater, N. Solomey, S. Somalwar, R. Stone, I. Suzuki, E. Swallow, R. Swanson, S. Taegar, R. Tesarek, G. Thomson, P. Toale, A. Tripathi, R. Tschirhart, Y. Wah, J. Wang, H. White, J. Whitmore, B. Winstein, R. Winston, J. Wu, T. Yamanaka, and E. Zimmerman, *Observation of the decay $\Xi^0 \rightarrow \Sigma^+ e^- \bar{\nu}_e$* , *Phys. Rev. Lett.* **82** (1999) 3751–3754.

- [169] KTeV Collaboration, A. Alavi-Harati, T. Alexopoulos, M. Areton, K. Arisaka, S. Averitte, R. Barbosa, A. Barker, M. Barrio, L. Bellantoni, A. Bellavance, J. Belz, R. Ben-David, D. Bergman, E. Blucher, G. Bock, C. Bown, S. Bright, E. Cheu, S. Childress, R. Coleman, M. Corcoran, G. Corti, B. Cox, M. Crisler, A. Erwin, R. Ford, A. Glazov, A. Golossanov, G. Graham, J. Graham, K. Hagan, E. Halkiadakis, J. Hamm, K. Hanagaki, S. Hidaka, Y. Hsiung, V. Jejer, D. Jensen, R. Kessler, H. Kobrak, J. LaDue, A. Lath, A. Ledovskoy, P. McBride, P. Mikelsons, E. Monnier, T. Nakaya, K. Nelson, H. Nguyen, V. O'Dell, M. Pang, R. Pordes, V. Prasad, X. Qi, B. Quinn, E. Ramberg, R. Ray, A. Roodman, M. Sadamoto, S. Schnetzer, K. Senyo, P. Shanahan, P. Shawhan, J. Shields, W. Slater, N. Solomey, S. Somalwar, R. Stone, E. Swallow, S. Taegar, R. Tesarek, G. Thomson, P. Toale, A. Tripathi, R. Tschirhart, S. Turner, Y. Wah, J. Wang, H. White, J. Whitmore, B. Weinstein, R. Winston, T. Yamanaka, and E. Zimmerman, *First measurement of form-factors of the decay $\Xi^0 \rightarrow \Sigma^+ e^- \bar{\nu}_e$* , *Phys. Rev. Lett.* **87** (2001) 132001, [hep-ex/0105016].
- [170] KTeV Collaboration, E. Abouzaid, T. Alexopoulos, M. Areton, R. Barbosa, A. Barker, L. Bellantoni, A. Bellavance, E. Blucher, G. Bock, E. Cheu, R. Coleman, M. Corcoran, B. Cox, A. Erwin, C. Escobar, A. Glazov, A. Golossanov, R. Gomes, P. Gouffon, K. Hanagaki, Y. Hsiung, H. Huang, D. Jensen, R. Kessler, K. Kotera, J. LaDue, A. Ledovskoy, P. McBride, E. Monnier, K. Nelson, H. Nguyen, R. Niclasen, H. Ping, V. Prasad, X. Qi, E. Ramberg, R. Ray, M. Ronquest, E. Santos, J. Shields, W. Slater, D. Smith, N. Solomey, E. Swallow, P. Toale, R. Tschirhart, C. Velissaris, Y. Wah, J. Wang, H. White, J. Whitmore, M. Wilking, B. Weinstein, R. Winston, E. Worcester, M. Worcester, T. Yamanaka, E. Zimmerman, and R. Zukanovich, *Observation of the decay $\Xi^0 \rightarrow \Sigma^+ \mu^- \bar{\nu}_\mu$* , *Phys. Rev. Lett.* **95** (2005) 081801, [hep-ex/0504055].
- [171] NA48/I Collaboration, J. Batley, G. Kalmus, C. Lazzeroni, D. Munday, M. Patel, M. Slater, S. Wotton, R. Arcidiacono, G. Bocquet, A. Ceccucci, D. Cundy, N. Doble, V. Falaleev, L. Gatignon, A. Gonidec, P. Grafstrom, W. Kubischta, F. Marchetto, I. Mikulec, A. Norton, B. Panzer-Steindel, P. Rubin, H. Wahl, E. Goudzovski, P. Hristov, V. Kekelidze, L. Litov, D. Madigozhin, N. Molokanova, Y. Potrebenikov, S. Stoynev, A. Zinchenko, E. Monnier, E. Swallow, R. Winston, R. Sacco, A. Walker, W. Baldini, P. Dalpiaz, P. Frabetti, A. Gianoli, M. Martini, F. Petrucci, M. Scarpa, M. Savrie, A. Bizzeti, M. Calvetti, G. Collazuol, E. Iacopini, M. Lenti, G. Ruggiero, M. Veltri, M. Behler, K. Eppard, M. Eppard, A. Hirstius, K. Kleinknecht, U. Koch, L. Masetti, P. Marouelli, U. Moosbrugger, C. M. Morales, A. Peters, R. Wanke, A. Winhart, A. Dabrowski, T. F. Martin, M. Velasco, G. Anzivino, P. Cenci, E. Imbergamo, G. Lamanna, P. Lubrano, A. Michetti, A. Nappi, M. Pepe, M. Petrucci, M. Piccini, M. Valdata, C. Cerri, F. Costantini, R. Fantechi, L. Fiorini, S. Giudici, I. Mannelli, G. Pierazzini, M. Sozzi, C. Cheshkov, J. Cheze, M. D. Beer, P. Debu, G. Gouge, G. Marel,

- E. Mazzucato, B. Peyaud, B. Vallage, M. Holder, A. Maier, M. Ziolkowski, C. Biino, N. Cartiglia, M. Clemencic, S. G. Lopez, E. A. Menichetti, N. Pastrone, W. Wislicki, H. Dibon, M. Jeitler, M. Markytan, G. Neuhofer, and L. Widhalm, *Measurement of the branching ratios of the decays $\Xi^0 \rightarrow \Sigma^+ e^- \bar{\nu}_e$ and $\Xi^0 \rightarrow \Sigma^+ e^+ \nu_e$* , *Phys. Lett.* **B645** (2007) 36–46, [hep-ex/0612043].
- [172] NA48/1 Collaboration, J. Batley, G. Kalmus, C. Lazzeroni, D. Munday, M. Patel, M. Slater, S. Wotton, R. Arcidiacono, G. Bocquet, A. Ceccucci, D. Cundy, N. Doble, V. Falaleev, L. Gatignon, A. Gonidec, P. Grafstrom, W. Kubischta, F. Marchetto, I. Mikulec, A. Norton, B. Panzer-Steindel, P. Rubin, H. Wahl, E. Goudzovski, P. Hristov, V. Kekelidze, V. Kozuharov, L. Litov, D. Madigozhin, N. Molokanova, Y. Potrebenikov, S. Stoynev, A. Zinchenko, E. Monnier, E. Swallow, R. Winston, R. Sacco, A. Walker, W. Baldini, P. Dalpiaz, P. Frabetti, A. Gianoli, M. Martini, F. Petrucci, M. Scarpa, M. Savrie, A. Bizzeti, M. Calvetti, G. Collazuol, E. Iacopini, M. Lenti, G. Ruggiero, M. Veltri, M. Behler, K. Eppard, M. Eppard, A. Hirstius, K. Kleinknecht, U. Koch, L. Masetti, P. Marouelli, U. Moosbrugger, C. M. Morales, A. Peters, R. Wanke, A. Winhart, A. Dabrowski, T. F. Martin, M. Velasco, G. Anzivino, P. Cenci, E. Imbergamo, G. Lamanna, P. Lubrano, A. Michetti, A. Nappi, M. Pepe, M. Petrucci, M. Piccini, M. Valdata, C. Cerri, F. Costantini, R. Fantechi, L. Fiorini, S. Giudici, I. Mannelli, G. Pierazzini, M. Sozzi, C. Cheshkov, J. Cheze, M. D. Beer, P. Debu, G. Gouge, G. Marek, E. Mazzucato, B. Peyaud, B. Vallage, M. Holder, A. Maier, M. Ziolkowski, S. Bifani, C. Biino, N. Cartiglia, M. Clemencic, S. G. Lopez, E. Menichetti, N. Pastrone, W. Wislicki, H. Dibon, M. Jeitler, M. Markytan, G. Neuhofer, and L. Widhalm, *Measurement of the branching ratio of the decay $\Xi^0 \rightarrow \Sigma^+ \mu^- \bar{\nu}_\mu$* , *Phys. Lett.* **B720** (2013) 105–110, [arXiv:1212.3131].
- [173] Particle Data Group, K. Olive, K. Agashe, C. Amsler, M. Antonelli, J.-F. Arguin, D. Asner, H. Baer, H. Band, R. Barnett, T. Basaglia, C. Bauer, J. Beatty, V. Belousov, J. Beringer, G. Bernardi, S. Bethke, H. Bichsel, O. Biebel, E. Blucher, S. Blusk, G. Brooijmans, O. Buchmueller, V. Burkert, M. Bychkov, R. Cahn, M. Carena, A. Ceccucci, A. Cerri, D. Chakraborty, M.-C. Chen, R. Chivukula, K. Copic, G. Cowan, O. Dahl, G. D'Ambrosio, T. Damour, D. de Florian, A. de Gouvea, T. DeGrand, P. de Jong, G. Dissertori, B. Dobrescu, M. Doser, M. Drees, H. Dreiner, D. Edwards, S. Eidelman, J. Erler, V. Ezhela, W. Fetscher, B. Fields, B. Foster, A. Freitas, T. Gaisser, H. Gallagher, L. Garren, H.-J. Gerber, G. Gerbier, T. Gershon, T. Gherghetta, S. Golwala, M. Goodman, C. Grab, A. Gritsan, C. Grojen, D. Groom, M. Grunewald, A. Gurtu, T. Gutsche, H. Haber, K. Hagiwara, C. Hanhart, S. Hashimoto, Y. Hayato, K. Hayes, M. Heffner, B. Heltsley, J. Hernandez-Rey, K. Hikasa, A. Hocker, J. Holder, A. Holtkamp, J. Huston, J. Jackson, K. Johnson, T. Junk, M. Kado, D. Karlen, U. Katz, S. Klein, E. Klempert, R. Kowalewski, F. Krauss, M. Kreps, B. Krusche, Y. Kuyanov, Y. Kwon, O. Lahav, J. Laiho, P. Langacker, A. Liddle, Z. Ligeti, C.-J. Lin, T. Liss, L. Littenberg, K. Lu-

- govsky, S. Lugovsky, F. Maltoni, T. Mannel, A. Manohar, W. Marciano, A. Martin, A. Masoni, J. Matthews, D. Milstead, P. Molaro, K. Munig, F. Moortgat, M. Mortonson, H. Murayama, K. Nakamura, M. Narain, P. Nason, S. Navas, M. Neubert, P. Nevski, Y. Nir, L. Pape, J. Parsons, C. Patrignani, J. Peacock, M. Pennington, S. Petcov, A. Piepke, A. Pomarol, A. Quadt, S. Raby, J. Rademacker, G. Rafelt, B. Ratcliff, P. Richardson, A. Ringwald, S. Roesler, S. Rolli, A. Romaniouk, L. Rosenberg, J. Rosner, G. Rybka, C. Sachrajda, Y. Sakai, G. Salam, S. Sarkar, F. Sauli, O. Schneider, K. Scholberg, D. Scott, V. Sharma, S. Sharpe, M. Silari, T. Sjostrand, P. Skands, J. Smith, G. Smoot, S. Spanier, H. Spieler, C. Spiering, A. Stahl, T. Stanev, S. Stone, T. Sumiyoshi, M. Syphers, F. Takahashi, M. Tanabashi, J. Terning, L. Tiator, M. Titov, N. Tkachenko, N. Tornqvist, D. Tovey, G. Valencia, G. Venanzoni, M. Vincter, P. Vogel, A. Vogt, S. Wakely, W. Walkowiak, C. Walter, D. Ward, G. Weiglein, D. Weinberg, E. Weinberg, M. White, L. Wiencke, C. Wohl, L. Wolfenstein, J. Womersley, C. Woody, R. Workman, A. Yamamoto, W.-M. Yao, G. Zeller, O. Zenin, J. Zhang, R.-Y. Zhu, F. Zimmermann, P. Zyla, G. Harper, V. Lugovsky, and P. Schaffner, *Review of Particle Physics*, *Chin. Phys. C* **38** (2014) 090001.
- [174] PANDA Collaboration, K. Schönning and E. Thomé, *Antihyperon-hyperon production in antiproton-proton annihilations with PANDA*, *J. Phys. Conf. Ser.* **503** (2014) 012013.
- [175] J-PARC P40 Collaboration, K. Miwa, R. Honda, Y. Matsumoto, H. Kanda, H. Tamura, and M. Ieiri, *Experimental plan of Sigma p scatterings at J-PARC*, *EPJ Web Conf.* **20** (2012) 05001.
- [176] R. Alonso, H.-M. Chang, E. E. Jenkins, A. V. Manohar, and B. Shotwell, *Renormalization group evolution of dimension-six baryon number violating operators*, *Phys. Lett.* **B734** (2014) 302–307, [arXiv:1405.0486].
- [177] S. Davidson and S. Descotes-Genon, *Minimal Flavour Violation for Leptoquarks*, *JHEP* **11** (2010) 073, [arXiv:1009.1998].
- [178] S. Weinberg, *Charge symmetry of weak interactions*, *Phys. Rev.* **112** (1958) 1375–1379.
- [179] H. Georgi, *Lie Algebras in Particle Physics. From Isospin to Unified Theories*, *Front. Phys.* **54** (1982) 1–255.
- [180] A. Krause, *Baryon Matrix Elements of the Vector Current in Chiral Perturbation Theory*, *Helv. Phys. Acta* **63** (1990) 3–70.
- [181] E. E. Jenkins and A. V. Manohar, *Baryon chiral perturbation theory using a heavy fermion Lagrangian*, *Phys. Lett.* **B255** (1991) 558–562.

- [182] L. S. Geng, J. Martin Camalich, L. Alvarez-Ruso, and M. J. Vicente Vacas, *Leading $SU(3)$ -breaking corrections to the baryon magnetic moments in Chiral Perturbation Theory*, *Phys. Rev. Lett.* **101** (2008) 222002, [arXiv:0805.1419].
- [183] T. Ledwig, J. Martin Camalich, L. S. Geng, and M. J. Vicente Vacas, *Octet-baryon axial-vector charges and $SU(3)$ -breaking effects in the semileptonic hyperon decays*, *Phys. Rev.* **D90** (2014), no. 5 054502, [arXiv:1405.5456].
- [184] L. Geng, *Recent developments in $SU(3)$ covariant baryon chiral perturbation theory*, *Front. Phys. China* **8** (2013) 328–348, [arXiv:1301.6815].
- [185] D. Guadagnoli, V. Lubicz, M. Papinutto, and S. Simula, *First Lattice QCD Study of the $\Sigma^- \rightarrow n$ Axial and Vector Form Factors with $SU(3)$ Breaking Corrections*, *Nucl. Phys.* **B761** (2007) 63–91, [hep-ph/0606181].
- [186] S. Sasaki and T. Yamazaki, *Lattice study of flavor $SU(3)$ breaking in hyperon beta decay*, *Phys. Rev.* **D79** (2009) 074508, [arXiv:0811.1406].
- [187] S. Sasaki, *Hyperon vector form factor from 2+1 flavor lattice QCD*, *Phys. Rev.* **D86** (2012) 114502, [arXiv:1209.6115].
- [188] G. Ecker, J. Gasser, H. Leutwyler, A. Pich, and E. de Rafael, *Chiral Lagrangians for Massive Spin 1 Fields*, *Phys. Lett.* **B223** (1989) 425.
- [189] P. Masjuan, E. Ruiz Arriola, and W. Broniowski, *Meson dominance of hadron form factors and large- N_c phenomenology*, *Phys. Rev.* **D87** (2013), no. 1 014005, [arXiv:1210.0760].
- [190] R. Flores-Mendieta, A. Garcia, A. Martinez, and J. J. Torres, *Radiative corrections to the semileptonic Dalitz plot with angular correlation between polarized decaying and emitted hyperons*, *Phys. Rev.* **D55** (1997) 5702–5718.
- [191] QCDSF/UKQCD Collaboration, M. Gockeler, P. Hagler, R. Horsley, Y. Nakamura, D. Pleiter, P. E. L. Rakow, A. Schafer, G. Schierholz, H. Stuben, and J. M. Zanotti, *Baryon Axial Charges and Momentum Fractions with $N_f = 2 + 1$ Dynamical Fermions*, *Pos LATTICE2010* (2010) 163, [arXiv:1102.3407].
- [192] J. Green, *Hadron Structure from Lattice QCD*, in *11th Conference on Quark Confinement and the Hadron Spectrum (Confinement XI) St. Petersburg, Russia, September 8-12, 2014*, 2014. [arXiv:1412.4637].
- [193] T. Ledwig, A. Silva, and H.-C. Kim, *Tensor charges and form factors of $SU(3)$ baryons in the self-consistent $SU(3)$ chiral quark-soliton model*, *Phys. Rev.* **D82** (2010) 034022, [arXiv:1004.3612].

- [194] J. R. Green, J. W. Negele, A. V. Pochinsky, S. N. Syritsyn, M. Engelhardt, and S. Krieg, *Nucleon Scalar and Tensor Charges from Lattice QCD with Light Wilson Quarks*, *Phys. Rev.* **D86** (2012) 114509, [arXiv:1206.4527].
- [195] T. Bhattacharya, S. D. Cohen, R. Gupta, A. Joseph, H.-W. Lin, and B. Yoon, *Nucleon Charges and Electromagnetic Form Factors from 2+1+1-Flavor Lattice QCD*, *Phys. Rev.* **D89** (2014), no. 9 094502, [arXiv:1306.5435].
- [196] G. S. Bali, S. Collins, B. Glässle, M. Göckeler, J. Najjar, R. H. Rödl, A. Schäfer, R. W. Schiel, W. Söldner, and A. Sternbeck, *Nucleon isovector couplings from $N_f = 2$ lattice QCD*, *Phys. Rev.* **D91** (2015), no. 5 054501, [arXiv:1412.7336].
- [197] D. J. Broadhurst and A. G. Grozin, *Matching QCD and HQET heavy - light currents at two loops and beyond*, *Phys. Rev.* **D52** (1995) 4082–4098, [hep-ph/9410240].
- [198] CMS Collaboration, V. Khachatryan, A. M. Sirunyan, A. Tumasyan, W. Adam, T. Bergauer, M. Dragicevic, J. Erö, C. Fabjan, M. Friedl, R. Fruehwirth, V. M. Ghete, C. Hartl, N. Hörmann, J. Hrubec, M. Jeitler, W. Kiesenhofer, V. Knünz, M. Krammer, I. Krätschmer, D. Liko, I. Mikulec, D. Rabady, B. Rahbaran, H. Rohringer, R. Schöfbeck, J. Strauss, A. Taurok, W. Treberer-Treberspurg, W. Waltenberger, C.-E. Wulz, V. Mossolov, N. Shumeiko, J. S. Gonzalez, S. Alderweireldt, M. Bansal, S. Bansal, T. Cornelis, E. A. D. Wolf, X. Janssen, A. Knutsson, S. Luyckx, S. Ochesanu, B. Roland, R. Rougny, M. V. D. Klundert, H. V. Haevermaet, P. V. Mechelen, N. V. Remortel, A. V. Spilbeeck, F. Blekman, S. Blyweert, J. D'Hondt, N. Daci, N. Heracleous, A. Kalogeropoulos, J. Keaveney, T. J. Kim, S. Lowette, M. Maes, A. Olbrechts, Q. Python, D. Strom, S. Tavernier, W. V. Doninck, P. V. Mulders, G. P. V. Onsem, I. Villella, C. Caillol, B. Clerbaux, G. D. Lentdecker, D. Dobur, L. Favart, A. Gay, A. Grebenyuk, A. Léonard, A. Mohammadi, L. Perniè, T. Reis, T. Seva, L. Thomas, C. V. Velde, P. Vanlaer, J. Wang, V. Adler, K. Beernaert, L. Benucci, A. Cimmino, S. Costantini, S. Crucy, S. Dildick, A. Fagot, G. Garcia, J. Mccartin, A. A. O. Rios, D. Ryckbosch, S. S. Diblen, M. Sigamani, N. Strobbe, F. Thyssen, M. Tytgat, E. Yazgan, N. Zaganidis, S. Basegmez, C. Beluffi, G. Bruno, R. Castello, A. Caudron, L. Ceard, G. G. D. Silveira, C. Delaere, T. D. Pree, D. Favart, L. Forthomme, A. Giannanco, J. Hollar, P. Jez, M. Komm, V. Lemaitre, J. Liao, C. Nuttens, D. Pagano, L. Perrini, A. Pin, K. Piotrzkowski, A. Popov, L. Quertenmont, M. Selvaggi, M. V. Marono, J. M. V. Garcia, N. Belyi, T. Caebergs, E. Daubie, G. H. Hammad, W. L. A. Júnior, G. Alves, M. C. M. Junior, T. D. R. Martins, M. E. Pol, W. Carvalho, J. Chinellato, A. Custódio, E. M. D. Costa, D. D. J. Damiao, C. D. O. Martins, S. F. D. Souza, H. Malbouisson, M. Malek, D. M. Figueiredo, L. Mundim, H. Nogima, W. L. P. D. Silva, J. Santaolalla, A. Santoro, A. Sznajder, E. J. T. Manganote, A. V. Pereira, C. A. Bernardes, F. D. A. Dias, T. Tomei, E. D. M. Gregores, P. G. Mercadante, S. F. Novaes, S. Padula, A. Aleksandrov, V. Genchev,

P. Iaydjiev, A. Marinov, S. Piperov, M. Rodozov, G. Sultanov, M. Vutova, A. Dimitrov, I. Glushkov, R. Hadjiiska, V. Kozhuharov, L. Litov, B. Pavlov, P. Petkov, J.-G. Bian, G.-M. Chen, H.-S. Chen, M. Chen, R. Du, C.-H. Jiang, D. Liang, S. Liang, R. Plestina, J. Tao, X. Wang, Z. Wang, C. Asawatangtrakuldee, Y. Ban, Y. Guo, Q. Li, W. Li, S. Liu, Y. Mao, S.-J. Qian, D. Wang, L. Zhang, W. Zou, C. Avila, L. F. C. Sierra, C. Florez, J. P. Gomez, B. G. Moreno, J. C. Sanabria, N. Godinovic, D. Lelas, D. Polic, I. Puljak, Z. Antunovic, M. Kovac, V. Brigljevic, K. Kadija, J. Luetic, D. Mekterovic, L. Sudic, A. Attikis, G. Mavromanolakis, J. Mousa, C. Nicolaou, F. Ptochos, P. A. Razis, M. Bodlak, M. Finger, M. F. Jr, Y. Assran, S. Elgammal, M. Mahmoud, A. Radi, M. Kadastik, M. Murumaa, M. Raidal, A. Tiko, P. Eerola, G. Fedi, M. Voutilainen, J. Häkkinen, V. Karimäki, R. Kinnunen, M. J. Kortelainen, T. Lampén, K. Lassila-Perini, S. Lehti, T. Lindén, P.-R. Luukka, T. Mäenpää, T. Peltola, E. Tuominen, J. Tuominiemi, E. Tuovinen, L. Wendland, T. Tuuva, M. Besancon, F. Couderc, M. Dejardin, D. Denegri, B. Fabbro, J.-L. Faure, C. Favaro, F. Ferri, S. Ganjour, A. Givernaud, P. Gras, G. H. de Monchenault, P. Jarry, E. Locci, J. Malcles, J. Rander, A. Rosowsky, M. Titov, S. Baffioni, F. Beaudette, P. Busson, C. Charlot, T. Dahms, M. Dalchenko, L. Dobrzynski, N. Filipovic, A. Florent, R. G. de Cassagnac, L. Mastrolorenzo, P. Miné, C. Mironov, I. N. Naranjo, M. Nguyen, C. Ochando, P. Paganini, R. Salerno, J.-B. Sauvan, Y. Sirois, C. Veelken, Y. Yilmaz, A. Zabi, J.-L. Agram, J. Andrea, A. Aubin, D. Bloch, J.-M. Brom, E. C. Chabert, C. Collard, E. Conte, J.-C. Fontaine, D. Gelé, U. Goerlach, C. Goetzmann, A.-C. L. Bihan, P. V. Hove, S. Gadrat, S. Beauceron, N. Beaupere, G. Boudoul, S. Brochet, C. A. C. Montoya, J. Chasserat, R. Chierici, D. Contardo, P. Depasse, H. E. Mamouni, J. Fan, J. Fay, S. Gascon, M. Gouzevitch, B. Ille, T. Kurca, M. Lethuillier, L. Mirabito, S. Perries, J. D. R. Alvarez, D. Sabes, L. Sgandurra, V. Sordini, M. V. Donckt, P. Verdier, S. Viret, H. Xiao, Z. Tsamalaidze, C. Autermann, S. Beranek, M. Bontenackels, M. Edelhoff, L. Feld, O. Hindrichs, K. Klein, A. Ostapchuk, A. Perieanu, F. Raupach, J. Sammet, S. Schael, H. Weber, B. Wittmer, V. Zhukov, M. Ata, E. Dietz-Laursonn, D. Duchardt, M. Erdmann, S. Erdweg, R. Fischer, A. Güth, T. Hebbeker, C. Heidemann, K. Hoepfner, D. Klingebiel, S. Knutzen, P. Kreuzer, M. Merschmeyer, A. Meyer, P. Millet, M. Olschewski, K. Padeken, P. Papacz, H. Reithler, S. A. Schmitz, L. Sonnenschein, D. Teyssier, S. Thüer, M. Weber, V. Cherepanov, Y. Erdogan, G. Flügge, H. Geenen, M. Geisler, W. H. Ahmad, F. Hoehle, B. Kargoll, T. Kress, Y. Kuessel, J. Lingemann, A. Nowack, I. M. Nugent, L. Perchalla, O. Pooth, A. Stahl, I. Asin, N. Bartosik, J. Behr, W. Behrenhoff, U. Behrens, A. J. Bell, M. Bergholz, A. Bethani, K. Borras, A. Burgmeier, A. Cakir, L. Calligaris, A. Campbell, S. Choudhury, F. Costanza, C. D. Pardos, S. Dooling, T. Dorland, G. Eckerlin, D. Eckstein, T. Eichhorn, G. Flucke, J. G. Garcia, A. Geiser, P. Gunnellini, J. Hauk, G. Hellwig, M. Hempel, D. Horton, H. Jung, M. Kasemann, P. Katsas, J. Kieseler, C. Kleinwort, D. Krücker, W. Lange, J. Leonard, K. Lipka, A. Lobanov, W. Lohmann, B. Lutz, R. Mankel, I. Marfin, I.-A. Melzer-Pellmann, A. B. Meyer, J. Mnich, A. Mussgiller, S. Naumann-

Emme, A. Nayak, O. Novgorodova, F. Nowak, E. Ntomari, H. Perrey, D. Pitzl, R. Placakyte, A. Raspereza, P. M. R. Cipriano, E. Ron, M. Özgür Sahin, J. Salfeld-Nebgen, P. Saxena, R. Schmidt, T. Schoerner-Sadenius, M. Schröder, S. Spannagel, A. D. R. V. Trevino, R. Walsh, C. Wissing, M. A. Martin, V. Blobel, M. C. Vignali, J. Erfle, E. Garutti, K. Goebel, M. Görner, J. Haller, M. Hoffmann, R. S. Höing, H. Kirschenmann, R. Klanner, R. Kogler, J. Lange, T. Lapsien, T. Lenz, I. Marchesini, J. Ott, T. Peiffer, N. Pietsch, D. Rathjens, C. Sander, H. Schettler, P. Schleper, E. Schlieckau, A. Schmidt, M. Seidel, J. Poehlsen, V. Sola, H. Stadie, G. Steinbrück, D. Troendle, E. Usai, L. Vanelder, C. Barth, C. Baus, J. Berger, C. Böser, E. Butz, T. Chwalek, W. D. Boer, A. Descroix, A. Dierlamm, M. Feindt, F. Fensch, M. Giffels, F. Hartmann, T. Hauth, U. Husemann, I. Katkov, A. Kornmayer, E. Kuznetsova, P. L. Pardo, M. U. Mozer, T. Müller, A. Nürnberg, G. Quast, K. Rabbertz, F. Ratnikov, S. Röcker, H.-J. Simonis, F.-M. H. Stober, R. Ulrich, J. Wagner-Kuhr, S. Wayand, T. Weiler, R. Wolf, G. Anagnostou, G. Daskalakis, T. Geralis, V. A. Giakoumopoulou, A. Kyriakis, D. Loukas, A. Markou, C. Markou, A. Psallidas, I. Topsis-Giotis, A. Panagiotou, N. Saoulidou, E. Stiliaris, X. Aslanoglou, I. Evangelou, G. Flouris, C. Foudas, P. Kokkas, N. Manthos, I. Papadopoulos, E. Paradas, G. Bencze, C. Hajdu, P. Hidas, D. Horvath, F. Sikler, V. Veszpremi, G. Vesztregombi, A. J. Zsigmond, N. Beni, S. Czellar, J. Karancsi, J. Molnar, J. Palinkas, Z. Szillasi, P. Raics, Z. L. Trocsanyi, B. Ujvari, S. K. Swain, S. B. Beri, V. Bhatnagar, N. Dhingra, R. Gupta, B. Bhawandeep, A. K. Kalsi, M. Kaur, M. Mittal, N. Nishu, J. Singh, A. Kumar, A. Kumar, S. Ahuja, A. Bhardwaj, B. C. Choudhary, A. Kumar, S. Malhotra, M. Naimuddin, K. Ranjan, V. Sharma, S. Banerjee, S. Bhattacharya, K. Chatterjee, S. Dutta, B. Gomber, S. Jain, S. Jain, R. Khurana, A. Modak, S. Mukherjee, D. Roy, S. Sarkar, M. Sharan, A. Abdulsalam, D. Dutta, S. Kailas, V. Kumar, A. K. Mohanty, L. M. Pant, P. Shukla, A. Topkar, T. Aziz, S. Banerjee, R. M. Chatterjee, R. K. Dewanjee, S. Dugad, S. Ganguly, S. Ghosh, M. Guchait, A. Gurtu, G. Kole, S. Kumar, M. Maity, G. Majumder, K. Mazumdar, G. B. Mohanty, B. Parida, K. Sudhakar, N. Wickramage, H. Bakhshiansohi, H. Behnamian, S. M. Etesami, A. Fahim, R. Goldouzian, A. Jafari, M. Khakzad, M. M. Najafabadi, M. Naseri, S. P. Mehdiabadi, B. Safarzadeh, M. Zeinali, M. Felcini, M. Grunewald, M. Abbrescia, L. Barbone, C. Calabria, S. S. Chhibra, A. Colaleo, D. Creanza, N. D. Filippis, M. D. Palma, L. Fiore, G. Iaselli, G. Maggi, M. Maggi, S. My, S. Nuzzo, A. Pompili, G. Pugliese, R. Radogna, G. Selvaggi, L. Silvestris, G. Singh, R. Venditti, P. Verwilligen, G. Zito, G. Abbiendi, A. Benvenuti, D. Bonacorsi, S. Braibant-Giacomelli, L. Brigliadori, R. Campanini, P. Capiluppi, A. Castro, F. R. Cavallo, G. Codispoti, M. Cuffiani, G.-M. Dallavalle, F. Fabbri, A. Fanfani, D. Fasanella, P. Giacomelli, C. Grandi, L. Guiducci, S. Marcellini, G. Masetti, A. Montanari, F. Navarria, A. Perrotta, F. Primavera, A. Rossi, T. Rovelli, G. P. Siroli, N. Tosi, R. Travaglini, S. Albergo, G. Cappello, M. Chiorboli, S. Costa, F. Giordano, R. Potenza, A. Tricomi, C. Tuve, G. Barbagli, V. Ciulli, C. Civinini, R. D'Alessandro, E. Focardi, E. Gallo, S. Gonzi, V. Gori, P. Lenzi, M. Meschini, S. Paoletti, G. Sguazzoni, A. Tropiano, L. Be-

nussi, S. Bianco, F. Fabbri, D. Piccolo, F. Ferro, M. L. Vetere, E. Robutti, S. Tosi, M. E. Dinardo, S. Fiorendi, S. Gennai, R. Gerosa, A. Ghezzi, P. Govoni, M. T. Lucchini, S. Malvezzi, R. A. Manzoni, A. Martelli, B. Marzocchi, D. Menasce, L. Moroni, M. Paganoni, D. Pedrini, S. Ragazzi, N. Redaelli, T. T. de Fatis, S. Buontempo, N. Cavallo, S. D. Guida, F. Fabozzi, A. O. M. Iorio, L. Lista, S. Meola, M. Merola, P. Paolucci, P. Azzi, N. Bacchetta, D. Bisello, A. Branca, R. Carlin, P. Checchia, M. Dall'Osso, T. Dorigo, S. Fantinel, M. Galanti, F. Gasparini, U. Gasparini, P. Giubilato, A. Gozzelino, K. Kanishchev, S. Lacaprara, M. Margoni, A. T. Meneguzzo, J. Pazzini, N. Pozzobon, P. Ronchese, F. Simonetto, E. Torassa, M. Tosi, P. Zotto, A. Zucchetta, G. Zumerle, M. Gabusi, S. P. Ratti, C. Riccardi, P. Salvini, P. Vitulo, M. Biasini, G. M. Bilei, D. Ciangottini, L. Fanò, P. Lariccia, G. Mantovani, M. Menichelli, F. Romeo, A. Saha, A. Santochia, A. Spiezia, K. Androsov, P. Azzurri, G. Bagliesi, J. Bernardini, T. Boccali, G. Broccolo, R. Castaldi, M. A. Ciocci, R. Dell'Orso, S. Donato, F. Fiori, L. Foà, A. Giassi, M. T. Grippo, F. Ligabue, T. Lomtadze, L. Martini, A. Messineo, C.-S. Moon, F. Palla, A. Rizzi, A. Savoy-Navarro, A. T. Serban, P. Spagnolo, P. Squilaciotti, R. Tenchini, G. Tonelli, A. Venturi, P. G. Verdini, C. Vernieri, L. Barone, F. Cavallari, D. D. Re, M. Diemoz, M. Grassi, C. Jorda, E. Longo, F. Margaroli, P. Meridiani, F. Micheli, S. Nourbakhsh, G. Organtini, R. Paramatti, S. Rahatlou, C. Rovelli, F. Santanastasio, L. Soffi, P. Traczyk, N. Amapane, R. Arcidiacono, S. Argiro, M. Arneodo, R. Bellan, C. Biino, N. Cartiglia, S. Casasso, M. Costa, A. Degano, N. Demaria, L. Finco, C. Mariotti, S. Maselli, E. Migliore, V. Monaco, M. Musich, M. M. Obertino, G. Ortona, L. Pacher, N. Pastrone, M. Pelliccioni, G. L. P. Angioni, A. Potenza, A. Romero, M. Ruspa, R. Sacchi, A. Solano, A. Staiano, U. Tamponi, S. Belforte, V. Candelise, M. Casarsa, F. Cossutti, G. D. Ricca, B. Gobbo, C. L. Licata, M. Marone, D. Montanino, A. Schizzi, T. Umer, A. Zanetti, S. Chang, A. Kropivnitskaya, S.-K. Nam, D. H. Kim, G. N. Kim, M. S. Kim, D. J. Kong, S. Lee, Y. D. Oh, H. Park, A. Sakharov, D.-C. Son, J. Y. Kim, S. Song, S. Choi, D. Gyun, B.-S. Hong, M. Jo, H. Kim, Y. Kim, B. Lee, K. S. Lee, S. K. Park, Y. Roh, M. Choi, J. H. Kim, I. Park, S. Park, G. Ryu, M. S. Ryu, Y.-I. Choi, Y. K. Choi, J. Goh, E. Kwon, J. Lee, H. Seo, I. Yu, A. Juodagalvis, J. R. Komaragiri, H. Castilla-Valdez, E. D. L. Cruz-Burelo, I. H. de La Cruz, R. Lopez-Fernandez, A. S. Hernández, S. C. Moreno, F. V. Valencia, I. Pedraza, H. A. S. Ibarguen, E. C. Linares, A. M. Pineda, D. Krofcheck, P. H. Butler, S. Reucroft, A. Ahmad, M. Ahmad, Q. Hassan, H. R. Hoorani, S. Khalid, W. A. Khan, T. Khurshid, M. A. Shah, M. Shoaib, H. Bialkowska, M. Bluj, B. Boimska, T. Frueboes, M. Górski, M. Kazana, K. Nawrocki, K. Romanowska-Rybinska, M. Szleper, P. Zalewski, G. Brona, K. Bunkowski, M. Cwiok, W. Dominik, K. Doroba, A. Kalinowski, M. Konecki, J. Krolkowski, M. Misiura, M. Olzewski, W. Wolszczak, P. Bargassa, C. B. D. C. E. Silva, P. Faccioli, P. G. F. Parracho, M. Gallinaro, F. Nguyen, J. R. Antunes, J. Seixas, J. Varela, P. Vischia, P. Bunin, M. Gavrilenko, I. Golutvin, A. Kamenev, V. Karjavin, V. Konoplyanikov, A. Lanev, A. Malakhov, V. Matveev, P. Moisenz, V. Palichik, V. Pere-

lygin, M. Savina, S. Shmatov, S. Shulha, N. Skatchkov, V. Smirnov, A. Zarubin, V. Golovtsov, Y. Ivanov, V. Kim, P. Levchenko, V. Murzin, V. Oreshkin, I. Smirnov, V. Sulimov, L. Uvarov, S. Vavilov, A. Vorobyev, A. Vorobyev, Y. Andreev, A. Dermenev, S. Glinenko, N. Golubev, M. Kirsanov, N. Krasnikov, A. Pashenkov, D. Tlisov, A. Toropin, V. Epshteyn, V. Gavrilov, N. Lychkovskaya, V. Popov, G. Safronov, S. Semenov, A. Spiridonov, V. Stolin, E. Vlasov, A. Zhokin, V. Andreev, M. Azarkin, I. Dremin, M. Kirakosyan, A. Leonidov, G. Mesyats, S. V. Rusakov, A. Vinogradov, A. Belyaev, E. Boos, V. Bunichev, M. Dubinin, L. Dudko, A. Ershov, A. Gribushin, V. Klyukhin, O. Kodolova, I. Loktin, S. Obraztsov, M. Perfilov, V. Savrin, I. Azhgirey, I. Bayshev, S. Bitioukov, V. Kachanov, A. Kalinin, D. Konstantinov, V. Krychkine, V. Petrov, R. Ryutin, A. Sobol, L. Tourtchanovitch, S. Troshin, N. Tyurin, A. Uzunian, A. Volkov, P. Adzic, M. Dordevic, M. Ekmedzic, J. Milosevic, J. A. Maestre, C. Battilana, E. Calvo, M. Cerrada, M. C. Llatas, N. Colino, B. D. L. Cruz, A. D. Peris, D. D. Vázquez, A. E. D. Valle, C. F. Bedoya, J. P. F. Ramos, J. Flix, M. C. Fouz, P. Garcia-Abia, O. G. Lopez, S. G. Lopez, J. M. Hernandez, M. I. Josa, G. Merino, E. N. D. Martino, A. M. P. C. Yzquierdo, J. P. Pelayo, A. Q. Olmeda, I. Redondo, L. Romero, M. S. Soares, C. Albajar, J. F. de Trocóniz, M. Missiroli, H. Brun, J. Cuevas, J. F. Menendez, S. Folgueras, I. G. Caballero, L. L. Iglesias, J. A. B. Cifuentes, I. J. Cabrillo, A. Calderon, J. D. Campderros, M. Fernandez, G. Gomez, A. Graziano, A. L. Virto, J. Marco, R. Marco, C. M. Rivero, F. Matorras, F. J. M. Sanchez, J. P. Gomez, T. Rodrigo, A. Y. Rodríguez-Marrero, A. Ruiz-Jimeno, L. Scodellaro, I. Vila, R. V. Cortabitarte, D. Abbaneo, E. Auffray, G. Auzinger, M. Bachtis, P. Baillon, A. Ball, D. Barney, A. Benaglia, J. Bendavid, L. Benhabib, J. F. Benitez, C. Bernet, G. Bianchi, P. Bloch, A. Bocci, A. Bonato, O. Bondu, C. Botta, H. Breuker, T. Camporesi, G. Cerminara, S. Colafranceschi, M. D'Alfonso, D. D'Enterria, A. Dabrowski, A. D. T. Mendes, F. D. Guio, A. D. Roeck, S. D. Visscher, M. Dobson, N. Dupont-Sagorin, A. Elliott-Peisert, J. Eugster, G. Franzoni, W. Funk, D. Gigi, K. Gill, D. Giordano, M. Girone, F. Gleje, R. Guida, S. Gundacker, M. Guthoff, J. Hammer, M. Hansen, P. Harris, J. Hege-man, V. Innocente, P. Janot, K. Kousouris, K. Krajczar, P. Lecoq, C. Lourenco, N. Magini, L. Malgeri, M. Mannelli, J. Marrouche, L. Masetti, F. Meijers, S. Mersi, E. Meschi, F. Moortgat, S. Morovic, M. Mulders, P. Musella, L. Orsini, L. Pape, E. Perez, L. Perrozzi, A. Petrilli, G. Petrucciani, A. Pfeiffer, M. Pierini, M. Pimiä, D. Piparo, M. Plagge, A. Racz, G. Rolandi, M. Rovere, H. Sakulin, C. Schäfer, C. Schwick, S. Sekmen, A. Sharma, P. Siegrist, P. Silva, M. Simon, P. Sphicas, D. Spiga, J. Steggemann, B. Stieger, M. Stoye, D. Treille, A. Tsirou, G. I. Veres, J.-R. Vlimant, N. Wardle, H. K. Wöhri, W. D. Zeuner, W. Bertl, K. Deiters, W. Erdmann, R. Horisberger, Q. Ingram, H.-C. Kaestli, S. König, D. Kotlinski, U. Langenegger, D. Renker, T. Rohe, F. Bachmair, L. Bäni, L. Bianchini, P. Bortignon, M.-A. Buchmann, B. Casal, N. Chanon, A. Deisher, G. Dissertori, M. Dittmar, M. Donegà, M. Dünser, P. Eller, C. Grab, D. Hits, W. Lustermann, B. Mangano, A. C. Marini, P. M. R. del Arbol, D. Meister, N. Mohr, C. Näheli,

P. Nef, F. Nessi-Tedaldi, F. Pandolfi, F. Pauss, M. Peruzzi, M. Quittnat, L. Rebane, M. Rossini, A. Starodumov, M. Takahashi, K. Theofilatos, R. Wallny, H. A. Weber, C. Amsler, M. F. Canelli, V. Chiochia, A. D. Cosa, A. Hinzmann, T. Hreus, B. Kilminster, B. M. Mejias, J. Ngadiuba, P. Robmann, F. J. Ronga, H. Snoek, S. Taroni, M. Verzetti, Y. Yang, M. Cardaci, K.-H. Chen, C. Ferro, C.-M. Kuo, W. Lin, Y.-J. Lu, R. Volpe, S.-S. Yu, P. Chang, Y.-H. Chang, Y.-W. Chang, Y. Chao, K.-F. Chen, P.-H. Chen, C. Dietz, U. Grundler, G. W.-S. Hou, K.-Y. Kao, Y.-J. Lei, Y.-F. Liu, R.-S. Lu, D. Majumder, E. Petrakou, Y.-M. Tzeng, R. Wilken, B. Asavapibhop, N. Sriamanobhas, N. Suwonjandee, A. Adiguzel, M. N. Bakirci, S. Cerci, C. Dozen, I. Dumanoglu, E. Eskut, S. Girgis, G. Gokbulut, E. Gurpinar, I. Hos, E. E. Kangal, A. K. Topaksu, G. Onengut, K. Ozdemir, S. Ozturk, A. Polatoz, K. Sogut, D. S. Cerci, B. Tali, H. Topakli, M. Vergili, I. V. Akin, B. Bilin, S. Bilmis, H. Gamsizkan, G. Karapinar, K. Ocalan, U. E. Surat, M. Yalvac, M. Zeyrek, E. Gülmek, B. Isildak, M. Kaya, O. Kaya, H. Bahtiyar, E. Barlas, K. Cankocak, F. I. Vardarlı, M. Yücel, L. Levchuk, P. Sorokin, J. J. Brooke, E. Clement, D. Cussans, H. Flacher, R. Frazier, J. Goldstein, M. Grimes, G. P. Heath, H. F. Heath, J. Jacob, L. Kreczko, C. Lucas, Z. Meng, D. M. Newbold, S. Paramesvaran, A. Poll, S. Senkin, V. J. Smith, T. Williams, K. W. Bell, A. Belyaev, C. Brew, R. M. Brown, D. J. Cockerill, J. A. Coughlan, K. Harder, S. Harper, E. Olaiya, D. Petyt, C. Shepherd-Themistocleous, A. Thea, I. R. Tomalin, W. J. Womersley, S. Worm, M. Baber, R. Bainbridge, O. Buchmuller, D. Burton, D. Colling, N. Cripps, M. Cutajar, P. Dauncey, G. Davies, M. D. Negra, P. Dunne, W. Ferguson, J. Fulcher, D. Futyan, A. Gilbert, G. Hall, G. Iles, M. Jarvis, G. Karapostoli, M. Kenzie, R. Lane, R. Lucas, L. Lyons, A.-M. Magnan, S. Malik, B. Mathias, J. Nash, A. Nikitenko, J. Pela, M. Pesaresi, K. Petridis, D. M. Raymond, S. Rogerson, A. Rose, C. Seez, P. Sharp, A. Tapper, M. V. Acosta, T. Virdee, J. Cole, P. R. Hobson, A. Khan, P. Kyberd, D. Leggat, D. Leslie, W. Martin, I. Reid, P. Symonds, L. Teodorescu, M. Turner, J. Dittmann, K. Hatakeyama, A. Kasmi, H. Liu, T. Scarborough, O. Charaf, S. Cooper, C. Henderson, P. Rumerio, A. Avetisyan, T. Bose, C. Fantasia, A. Heister, P. Lawson, C. Richardson, J. Rohlf, D. Sperka, J. S. John, L. Sulak, J. Alimena, S. Bhattacharya, G. Christopher, D. Cutts, Z. Demiragli, A. Ferapontov, A. Garabedian, U. Heintz, S. Jabeen, G. Kukartsev, E. Laird, G. Landsberg, M. Luk, M. Narain, M. Segala, T. Sinhuprasith, T. Speer, J. Swanson, R. Breedon, G. Breto, M. C. D. L. B. Sanchez, S. Chauhan, M. Chertok, J. Conway, R. Conway, P. T. Cox, R. Erbacher, M. Gardner, W. Ko, R. Lander, T. Miceli, M. Mulhearn, D. Pellett, J. Pilot, F. Ricci-Tam, M. Searle, S. Shalhout, J. Smith, M. Squires, D. Stolp, M. Tripathi, S. Wilbur, R. Yohay, R. Cousins, P. Eversaerts, C. Farrell, J. Hauser, M. Ignatenko, G. Rakness, E. Takasugi, V. Valuev, M. Weber, J. Babb, R. Clare, J. A. Ellison, J. W. Gary, G. Hanson, J. Heilman, M. I. Rikova, P. Jandir, E. Kennedy, F. Lacroix, H. Liu, O. R. Long, A. Luthra, M. Malberti, H. Nguyen, A. Shrinivas, S. Sumowidagdo, S. Wimpenny, W. Andrews, J. G. Branson, G. B. Cerati, S. Cittolin, R. T. D'Agnolo, D. Evans, A. Holzner, R. Kelley, D. Klein, M. Lebourgeois, J. Letts, I. Macneill, D. Olivito, S. Padhi,

C. Palmer, M. Pieri, M. Sani, V. Sharma, S. Simon, E. Sudano, M. Tadel, Y. Tu, A. Vartak, C. Welke, F. Würthwein, A. Yagil, J. Yoo, D. Barge, J. Bradmiller-Feld, C. Campagnari, T. Danielson, A. Dishaw, K. Flowers, M. F. Sevilla, P. Geffert, C. George, F. Golf, L. Gouskos, J. Incandela, C. Justus, N. Mccoll, J. Richman, D. Stuart, W. To, C. West, A. Apresyan, A. Bornheim, J. Bunn, Y. Chen, E. D. Marco, J. Duarte, A. Mott, H. B. Newman, C. Pena, C. Rogan, M. Spiropulu, V. Timciuc, R. Wilkinson, S. Xie, R.-Y. Zhu, V. Azzolini, A. Calamba, T. Ferguson, Y. Iiyama, M. Paulini, J. Russ, H. Vogel, I. Vorobiev, J. P. Cumalat, B. R. Drell, W. T. Ford, A. Gaz, E. L. Lopez, U. Nauenberg, J. Smith, K. Stenson, K. Ulmer, S. R. Wagner, J. Alexander, A. Chatterjee, J. Chu, S. Dittmer, N. Eggert, N. Mirman, G. N. Kaufman, J. R. Patterson, A. Ryd, E. Salvati, L. Skinnari, W. Sun, W. D. Teo, J. Thom, J. Thompson, J. Tucker, Y. Weng, L. Winstrom, P. Wittich, D. Winn, S. Abdullin, M. Albrow, J. Anderson, G. Apollinari, L. A. Bauerdick, A. Beretvas, J. Berryhill, P. C. Bhat, K. Burkett, J. N. Butler, H. Cheung, F. Chlebana, S. Cihangir, V. D. Elvira, I. Fisk, J. Freeman, Y. Gao, E. Gottschalk, L. Gray, D. Green, S. Grünendahl, O. Gutsche, J. Hanlon, D. Hare, R. M. Harris, J. Hirschauer, B. Hooberman, S. Jindariani, M. Johnson, U. Joshi, K. Kaadze, B. Klima, B. Kreis, S. Kwan, J. Linacre, D. Lincoln, R. Lipton, T. Liu, J. Lykken, K. Maeshima, J. M. Marraffino, V. I. M. Outschoorn, S. Maruyama, D. Mason, P. McBride, K. Mishra, S. Mrenna, Y. Musienko, S. Nahn, C. Newman-Holmes, V. O'Dell, O. Prokofyev, E. Sexton-Kennedy, S. Sharma, A. Soha, W. J. Spalding, L. Spiegel, L. Taylor, S. Tkaczyk, N. V. Tran, L. Uplegger, E. W. Vaandering, R. Vidal, A. Whitbeck, J. Whitmore, F. Yang, D. Acosta, P. Avery, D. Bourilkov, M. Carver, T. Cheng, D. Curry, S. Das, M. D. Gruttola, G. P. D. Giovanni, R. D. Field, M. Fisher, I.-K. Furic, J. Hugon, J. Konigsberg, A. Korytov, T. Kypreos, J. F. Low, K. Matchev, P. Milenovic, G. Mitselmakher, L. Muniz, A. Rinkevicius, L. Shchutska, N. Skhirtladze, M. Snowball, J. Yelton, M. Zakaria, S. Hewamanage, S. Linn, P. Markowitz, G. Martinez, J. L. Rodriguez, T. Adams, A. Askew, J. Bochenek, B. Diamond, J. Haas, S. Hagopian, V. Hagopian, K. F. Johnson, H. Prosper, V. Veeraraghavan, M. Weinberg, M. M. Baarmand, M. Hohlmann, H. Kalakhety, F. Yumiceva, M. R. Adams, L. Apanasevich, V. E. Bazterra, D. Berry, R. R. Betts, I. Bucinskaite, R. Cavanaugh, O. Evdokimov, L. Gauthier, C. E. Gerber, D. J. Hofman, S. Khalatyan, P. Kurt, D. H. Moon, C. O'Brien, C. Silkworth, P. Turner, N. Varelas, E. A. Albayrak, B. Bilki, W. Clarida, K. Dilsiz, F. Duru, M. Haytmyradov, J.-P. Merlo, H. Mermerkaya, A. Mestvirishvili, A. Moeller, J. Nachtman, H. Ogul, Y. Onel, F. Ozok, A. Penzo, R. Rahmat, S. Sen, P. Tan, E. Tiras, J. Wetzel, T. Yetkin, K. Yi, B. A. Barnett, B. Blumenfeld, S. Bolognesi, D. Fehling, A. Gritsan, P. Maksimovic, C. Martin, M. Swartz, P. Baringer, A. Bean, G. Benelli, C. Bruner, J. Gray, R. P. K. III, M. Murray, D. Noonan, S. Sanders, J. Sekaric, R. Stringer, Q. Wang, J. S. Wood, A.-F. Barfuss, I. Chakaberia, A. Ivanov, S. Khalil, M. Makouski, Y. Maravin, L. K. Saini, S. Shrestha, I. Svintradze, J. Gronberg, D. Lange, F. Rebassoo, D. Wright, D. Baden, A. Belloni, B. Calvert, S. C. Eno, J. Gomez, N. J. Hadley, R. G. Kellogg, T. Kolberg, Y. Lu, M. Marionneau, A. Mignerey, K. Pedro,

A. Skuja, M. Tonjes, S. C. Tonwar, A. Apyan, R. Barbieri, G. Bauer, W. Busza, I. A. Cali, M. Chan, L. D. Matteo, V. Dutta, G. G. Ceballos, M. Goncharov, D. Gulhan, M. Klute, Y. S. Lai, Y.-J. Lee, A. Levin, P. D. Luckey, T. Ma, C. Paus, D. Ralph, C. Roland, G. Roland, G. Stephans, F. Stöckli, K. Sumorok, D. Velicanu, J. Veverka, B. Wyslouch, M. Yang, M. Zanetti, V. Zhukova, B. Dahmes, A. Gude, S.-C. Kao, K. Klapoetke, Y. Kubota, J. Mans, N. Pastika, R. Rusack, A. Singovsky, N. Tambe, J. Turkewitz, J. G. Acosta, S. Oliveros, E. Avdeeva, K. Bloom, S. Bose, D. R. Claes, A. Dominguez, R. G. Suarez, J. Keller, D. Knowlton, I. Kravchenko, J. Lazo-Flores, S. Malik, F. Meier, G. R. Snow, J. Dolen, A. Godshalk, I. Iashvili, A. Kharchilava, A. Kumar, S. Rappoccio, G. Alverson, E. Barberis, D. Baumgartel, M. Chasco, J. Haley, A. Massironi, D. M. Morse, D. Nash, T. Orimoto, D. Trocino, R.-J. Wang, D. Wood, J. Zhang, K. A. Hahn, A. Kubik, N. Mucia, N. Odell, B. Pollack, A. Pozdnyakov, M. H. Schmitt, S. Stoynev, K. Sung, M. Velasco, S. Won, A. Brinkerhoff, K. M. Chan, A. Drozdetskiy, M. Hildreth, C. Jessop, D. J. Karmgard, N. Kellams, K. Lannon, W. Luo, S. Lynch, N. Marinelli, T. Pearson, M. Planer, R. Ruchti, N. Valls, M. Wayne, M. Wolf, A. Woodard, L. Antonelli, J. Brinson, B. Bylsma, L. S. Durkin, S. Flowers, C. Hill, R. Hughes, K. Kotov, T.-Y. Ling, D. Puigh, M. Rodenburg, G. Smith, C. Vuosalo, B. L. Winer, H. Wolfe, H. W. Wulsin, E. Berry, O. Driga, P. Elmer, P. Hebda, A. Hunt, S. A. Koay, P. Lujan, D. Marlow, T. Medvedeva, M. Mooney, J. Olsen, P. Piroué, X. Quan, H. Saka, D. Stickland, C. Tully, J. S. Werner, S. C. Zenz, A. Zuranski, E. Brownson, H. Mendez, J. E. R. Vargas, E. Alagoz, V. E. Barnes, D. Benedetti, G. Bolla, D. Bortoletto, M. D. Mattia, Z. Hu, M. Jha, M. Jones, K. Jung, M. Kress, N. Leonardo, D. L. Pegna, V. Maroussov, P. Merkel, D. H. Miller, N. Neumeister, B. C. Radburn-Smith, X. Shi, I. Shipsey, D. Silvers, A. Svyatkovskiy, F. Wang, W. Xie, L. Xu, H. D. Yoo, J. Zablocki, Y. Zheng, N. Parashar, J. Stupak, A. Adair, B. Akgun, K. M. Ecklund, F. J. Geurts, W. Li, B. Michlin, B. P. Padley, R. Redjimi, J. Roberts, J. Zabel, B. Betchart, A. Bodek, R. Covarelli, P. de Barbaro, R. Demina, Y. Eshaq, T. Ferbel, A. Garcia-Bellido, P. Goldenzweig, J. Han, A. Harel, A. Khukhunaishvili, D. C. Miner, G. Petrillo, D. Vishnevskiy, R. Ciesielski, L. Demortier, K. Goulianatos, G. Lungu, C. Mesropian, S. Arora, A. Barker, J. P. Chou, C. Contreras-Campana, E. Contreras-Campana, D. Duggan, D. Ferencek, Y. Gershtein, R. Gray, E. Halkiadakis, D. Hidas, A. Lath, S. Panwalkar, M. Park, R. Patel, V. Rekovic, S. Salur, S. Schnetzer, C. Seitz, S. Somalwar, R. Stone, S. Thomas, P. Thomassen, M. Walker, K. Rose, S. Spanier, A. York, O. Bouhali, R. Eusebi, W. Flanagan, J. Gilmore, T. Kamon, V. Khotilovich, V. Krutelyov, R. Montalvo, I. Osipenkov, Y. Pakhotin, A. Perloff, J. Roe, A. Rose, A. Safonov, T. Sakuma, I. Suarez, A. Tatarinov, N. Akchurin, C. Cowden, J. Damgov, C. Dragoiu, P. R. Dudero, J. Faulkner, K. Kovitanggoon, S. Kunori, S. W. Lee, T. Libeiro, I. Volobouev, E. Appelt, A. G. Delannoy, S. Greene, A. Gurrola, W. Johns, C. Maguire, Y. Mao, A. Melo, M. Sharma, P. Sheldon, B. Snook, S. Tuo, J. Velkovska, M. W. Arenton, S. Boutle, B. Cox, B. Francis, J. Goodell, R. Hirosky, A. Ledovskoy, H. Li, C. Lin, C. Neu, J. Wood, S. Gollapinni, R. Harr, P. E. Karchin,

- C. K. K. Don, P. Lamichhane, J. Sturdy, D. Belknap, D. Carlsmith, M. Cepeda, S. Dasu, S. Duric, E. Friis, R. Hall-Wilton, M. Herndon, A. Hervé, P. Klabbers, A. Lanaro, C. Lazaridis, A. Levine, R. Loveless, A. Mohapatra, I. Ojalvo, T. Perry, G. A. Pierro, G. Polese, I. Ross, T. Sarangi, A. Savin, W. H. Smith, and N. Woods, *Search for physics beyond the standard model in final states with a lepton and missing transverse energy in proton-proton collisions at $\sqrt{s} = 8 \text{ TeV}$* , *Phys. Rev.* **D91** (2015), no. 9 092005, [arXiv:1408.2745].
- [199] CMS Collaboration, S. Chatrchyan, V. Khachatryan, A. M. Sirunyan, A. Tumasyan, W. Adam, T. Bergauer, M. Dragicevic, J. Erö, C. Fabjan, M. Friedl, R. Fruehwirth, V. M. Ghete, J. Hammer, N. Hörmann, J. Hrubec, M. Jeitler, W. Kiesenhofer, V. Knünz, M. Krammer, D. Liko, I. Mikulec, M. Pernicka, B. Rahbaran, C. Rohringer, H. Rohringer, R. Schöfbeck, J. Strauss, A. Taurok, F. Teischinger, P. Wagner, W. Waltenberger, G. Walzel, E. Widl, C.-E. Wulz, V. Mossolov, N. Shumeiko, J. S. Gonzalez, S. Bansal, K. Cerny, T. Cornelis, E. A. D. Wolf, X. Janssen, S. Luyckx, T. Maes, L. Mucibello, S. Ochesanu, B. Roland, R. Rougny, M. Selvaggi, H. V. Haevermaet, P. V. Mechelen, N. V. Remortel, A. V. Spilbeeck, F. Blekman, S. Blyweert, J. D'Hondt, R. G. Suarez, A. Kalogeropoulos, M. Maes, A. Olbrechts, W. V. Doninck, P. V. Mulders, G. P. V. Onsem, I. Villella, O. Charaf, B. Clerbaux, G. D. Lentdecker, V. Dero, A. Gay, T. Hreus, A. Léonard, P. E. Marage, T. Reis, L. Thomas, C. V. Velde, P. Vanlaer, V. Adler, K. Beernaert, A. Cimmino, S. Costantini, G. Garcia, M. Grunewald, B. Klein, J. Lellouch, A. Marinov, J. Mccartin, A. A. O. Rios, D. Ryckbosch, N. Strobbe, F. Thyssen, M. Tytgat, L. Vanelderen, P. Verwilligen, S. Walsh, E. Yazgan, N. Zaganidis, S. Basegmez, G. Bruno, L. Ceard, C. Delaere, T. D. Pree, D. Favart, L. Forthomme, A. Giammancio, J. Hollar, V. Lemaitre, J. Liao, O. Militaru, C. Nuttens, D. Pagano, A. Pin, K. Piotrzkowski, N. Schul, N. Beliy, T. Caebergs, E. Daubie, G. H. Hammad, G. Alves, M. C. M. Junior, D. D. J. Damiao, T. Martins, M. E. Pol, M. H. G. E. Souza, W. L. A. Júnior, W. Carvalho, A. Custódio, E. M. D. Costa, C. D. O. Martins, S. F. D. Souza, D. M. Figueiredo, L. Mundim, H. Nogima, V. Oguri, W. L. P. D. Silva, A. Santoro, S. M. S. D. Amaral, L. S. Jorge, A. Sznajder, T. S. D. Anjos, C. A. Bernardes, F. D. A. Dias, T. Tomei, E. D. M. Gregores, C. Lagana, F. D. C. Marinho, P. G. Mercadante, S. F. Novaes, S. Padula, V. Genchev, P. Iaydjiev, S. Piperov, M. Rodozov, S. Stoykova, G. Sultanov, V. Tcholakov, R. Trayanov, M. Vutova, A. Dimitrov, R. Hadjiiska, V. Kozuharov, L. Litov, B. Pavlov, P. Petkov, J.-G. Bian, G.-M. Chen, H.-S. Chen, C.-H. Jiang, D. Liang, S. Liang, X. Meng, J. Tao, J. Wang, J. Wang, X. Wang, Z. Wang, H. Xiao, M. Xu, J. Zang, Z. Zhang, C. Asawatangtrakuldee, Y. Ban, S. Guo, Y. Guo, W. Li, S. Liu, Y. Mao, S.-J. Qian, H. Teng, S. Wang, B. Zhu, W. Zou, C. Avila, B. G. Moreno, A. F. O. Oliveros, J. C. Sanabria, N. Godinovic, D. Lelas, R. Plestina, D. Polic, I. Puljak, Z. Antunovic, M. Dzelalija, M. Kovac, V. Brigljevic, S. Duric, K. Kadija, J. Luetic, S. Morovic, A. Attikis, M. Galanti, G. Mavromanolakis, J. Mousa, C. Nicolaou, F. Ptochos, P. A. Razis, M. Fin-

ger, M. F. Jr, Y. Assran, S. Elgammal, A. E. Kamel, S. Khalil, M. Mahmoud, A. Radi, M. Kadastik, M. Müntel, M. Raidal, L. Rebane, A. Tiko, V. Azzolini, P. Eerola, G. Fedi, M. Voutilainen, J. Härkönen, M. A. Heikkinen, V. Karimäki, R. Kinnunen, M. J. Kortelainen, T. Lampén, K. Lassila-Perini, S. Lehti, T. Lindén, P.-R. Luukka, T. Mäenpää, T. Peltola, E. Tuominen, J. Tuominiemi, E. Tuovinen, D. Ungaro, L. Wendland, K. Banzuzi, A. Korpela, T. Tuuva, M. Besancon, S. Choudhury, M. Dejardin, D. Denegri, B. Fabbro, J.-L. Faure, F. Ferri, S. Gajjour, A. Givernaud, P. Gras, G. H. de Monchenault, P. Jarry, E. Locci, J. Malcles, L. Millischer, A. Nayak, J. Rander, A. Rosowsky, I. Shreyber, M. Titov, S. Baffioni, F. Beaudette, L. Benhabib, L. Bianchini, M. Bluj, C. Broutin, P. Busson, C. Charlotte, N. Daci, T. Dahms, L. Dobrzynski, R. G. de Cassagnac, M. Haguenauer, P. Miné, C. Mironov, C. Ochando, P. Paganini, D. Sabes, R. Salerno, Y. Sirois, C. Veelken, A. Zabi, J.-L. Agram, J. Andrea, D. Bloch, D. Bodin, J.-M. Brom, M. Cardaci, E. C. Chabert, C. Collard, E. Conte, F. Drouhin, C. Ferro, J.-C. Fontaine, D. Gelé, U. Goerlach, P. Juillot, M. Karim, A.-C. L. Bihan, P. V. Hove, F. Fassi, D. Mercier, S. Beauceron, N. Beaupere, O. Bondu, G. Boudoul, H. Brun, J. Chasserat, R. Chierici, D. Contardo, P. Depasse, H. E. Mamouni, J. Fay, S. Gascon, M. Gouzevitch, B. Ille, T. Kurca, M. Lethuillier, L. Mirabito, S. Perries, V. Sordini, S. Tosi, Y. Tschudi, P. Verdier, S. Viret, Z. Tsamalaidze, G. Anagnostou, S. Beranek, M. Edelhoff, L. Feld, N. Heracleous, O. Hindrichs, R. Jussen, K. Klein, J. Merz, A. Ostapchuk, A. Perieanu, F. Raupach, J. Sammet, S. Schael, D. Sprenger, H. Weber, B. Wittmer, V. Zhukov, M. Ata, J. Caudron, E. Dietz-Lauronn, D. Duchardt, M. Erdmann, A. Güth, T. Hebbeker, C. Heidemann, K. Hoepfner, T. Klimkovich, D. Klingebiel, P. Kreuzer, D. Lanske, J. Lingemann, C. Magass, M. Merschmeyer, A. Meyer, M. Olszewski, P. Papacz, H. Pieta, H. Reithler, S. A. Schmitz, J. frederik Schulte, L. Sonnenschein, J. Steggemann, D. Teyssier, S. Thüer, M. Weber, M. Bontenackels, V. Cherepanov, M. Davids, G. Flügge, H. Geenen, M. Geisler, W. H. Ahmad, F. Hoehle, B. Kargoll, T. Kress, Y. Kuessel, A. Linn, A. Nowack, L. Perchalla, O. Pooth, J. Rennefeld, P. Sauerland, A. Stahl, M. A. Martin, J. Behr, W. Behrenhoff, U. Behrens, M. Bergholz, A. Bethani, K. Borras, A. Burgmeier, A. Cakir, L. Calligaris, A. Campbell, E. Castro, F. Costanza, D. Dammann, G. Eckerlin, D. Eckstein, D. Fischer, G. Flucke, A. Geiser, I. Glushkov, S. Habib, J. Hauk, H. Jung, M. Kasemann, P. Katsas, C. Kleinwort, H. Kluge, A. Knutsson, M. Krämer, D. Krücker, E. Kuznetsova, W. Lange, W. Lohmann, B. Lutz, R. Mankel, I. Marfin, M. Marienfeld, I.-A. Melzer-Pellmann, A. B. Meyer, J. Mnich, A. Mussgiller, S. Naumann-Emme, J. Olzem, H. Perrey, A. Petrukhin, D. Pitzl, A. Raspereza, P. M. R. Cipriano, C. Riedl, M. Rosin, J. Salfeld-Nebgen, R. Schmidt, T. Schoerner-Sadenius, N. Sen, A. Spiridonov, M. Stein, R. Walsh, C. Wissing, C. Autermann, V. Blobel, S. Bobrovskyi, J. Draeger, H. Enderle, J. Erfle, U. Gebbert, M. Görner, T. Hermanns, R. S. Höing, K. Kaschube, G. Kaussen, H. Kirschenmann, R. Klanner, J. Lange, B. Mura, F. Nowak, N. Pietsch, D. Rathjens, C. Sander, H. Schettler, P. Schleper, E. Schlieckau, A. Schmidt, M. Schröder, T. Schum, M. Seidel, H. Stadie, G. Stein-

brück, J. Thomsen, C. Barth, J. Berger, T. Chwalek, W. D. Boer, A. Dierlamm, M. Feindt, M. Guthoff, C. Hackstein, F. Hartmann, M. Heinrich, H. Held, K.-H. Hoffmann, S. Honc, I. Katkov, J. R. Komaragiri, D. Martschei, S. Mueller, T. Müller, M. Niegel, A. Nürnberg, O. Oberst, A. Oehler, J. Ott, T. Peiffer, G. Quast, K. Rabbertz, F. Ratnikov, N. Ratnikova, S. Röcker, C. Saout, A. Scheurer, F.-P. Schilling, M. Schmanau, G. Schott, H.-J. Simonis, F.-M. H. Stober, D. Troendle, R. Ulrich, J. Wagner-Kuhr, T. Weiler, M. Zeise, E. B. Ziebarth, G. Daskalakis, T. Geralis, S. Kesisoglou, A. Kyriakis, D. Loukas, I. Manolakos, A. Markou, C. Markou, C. Mavrommatis, E. Ntomari, L. Gouskos, T. Mertzimekis, A. Panagiotou, N. Saoulidou, I. Evangelou, C. Foudas, P. Kokkas, N. Manthos, I. Papadopoulos, V. Patras, G. Bencze, C. Hajdu, P. Hidas, D. Horvath, K. Krajczar, B. Radics, F. Sikler, V. Veszpremi, G. Vesztregombi, N. Beni, S. Czellar, J. Molnar, J. Palinkas, Z. Szillasi, J. Karancsi, P. Raics, Z. L. Trocsanyi, B. Ujvari, S. B. Beri, V. Bhatnagar, N. Dhingra, R. Gupta, M. Jindal, M. Kaur, J. M. Kohli, M. Z. Mehta, N. Nishu, L. K. Saini, A. Sharma, J. Singh, S. P. Singh, S. Ahuja, A. Bhardwaj, B. C. Choudhary, A. Kumar, A. Kumar, S. Malhotra, M. Naimuddin, K. Ranjan, V. Sharma, R. K. Shivpuri, S. Banerjee, S. Bhattacharya, S. Dutta, B. Gomber, S. Jain, S. Jain, R. Khurana, S. Sarkar, A. Abdulsalam, R. K. Choudhury, D. Dutta, S. Kailas, V. Kumar, A. K. Mohanty, L. M. Pant, P. Shukla, T. Aziz, S. Ganguly, M. Guchait, A. Gurtu, M. Maity, G. Majumder, K. Mazumdar, G. B. Mohanty, B. Parida, K. Sudhakar, N. Wickramage, S. Banerjee, S. Dugad, H. Arfaei, H. Bakhshiansohi, S. M. Etesami, A. Fahim, M. Hashemi, H. Hesari, A. Jafari, M. Khakzad, A. Mohammadi, M. M. Najafabadi, S. P. Mehdiabadi, B. Safarzadeh, M. Zeinali, M. Abbrescia, L. Barbone, C. Calabria, S. S. Chhibra, A. Colaleo, D. Creanza, N. D. Filippis, M. D. Palma, L. Fiore, G. Iaselli, L. Lusito, G. Maggi, M. Maggi, B. Marangelli, S. My, S. Nuzzo, N. Pacifico, A. Pompili, G. Pugliese, G. Selvaggi, L. Silvestris, G. Singh, G. Zito, G. Abbiendi, A. Benvenuti, D. Bonacorsi, S. Braibant-Giacomelli, L. Brigliadori, P. Capiluppi, A. Castro, F. R. Cavallo, M. Cuffiani, G.-M. Dallavalle, F. Fabbri, A. Fanfani, D. Fasanella, P. Giacomelli, C. Grandi, L. Guiducci, S. Marcellini, G. Masetti, M. Meneghelli, A. Montanari, F. Navarria, F. Odorici, A. Perrotta, F. Primavera, A. Rossi, T. Rovelli, G. Siroli, R. Travaglini, S. Albergo, G. Cappello, M. Chiorboli, S. Costa, R. Potenza, A. Tricomi, C. Tuve, G. Barbagli, V. Ciulli, C. Civinini, R. D'Alessandro, E. Focardi, S. Frosali, E. Gallo, S. Gonzi, M. Meschini, S. Paoletti, G. Sguazzoni, A. Tropiano, L. Benussi, S. Bianco, S. Colafranceschi, F. Fabbri, D. Piccolo, P. Fabbricatore, R. Musenich, A. Benaglia, F. D. Guio, L. D. Matteo, S. Fiorendi, S. Gennai, A. Ghezzi, S. Malvezzi, R. A. Manzoni, A. Martelli, A. Massironi, D. Menasce, L. Moroni, M. Paganoni, D. Pedrini, S. Ragazzi, N. Redaelli, S. Sala, T. T. de Fatis, S. Buontempo, C. A. C. Montoya, N. Cavallo, A. D. Cosa, O. Dogangun, F. Fabozzi, A. O. M. Iorio, L. Lista, S. Meola, M. Merola, P. Paolucci, P. Azzi, N. Bacchetta, P. Bellan, D. Bisello, A. Branca, R. Carlin, P. Checchia, T. Dorigo, U. Dosselli, F. Gasparini, A. Gozzelino, K. Kanishchev, S. Lacaprara, I. Lazzizzera, M. Margoni, A. T. Meneguzzo, L. Perrozzi, N. Pozzobon, P. Ronch-

ese, F. Simonetto, E. Torassa, M. Tosi, S. Vanini, P. Zotto, G. Zumerle, M. Gabusi, S. P. Ratti, C. Riccardi, P. Torre, P. Vitulo, G. M. Bilei, L. Fanò, P. Lariccia, A. Lucaroni, G. Mantovani, M. Menichelli, A. Nappi, F. Romeo, A. Saha, A. Santocchia, S. Taroni, P. Azzurri, G. Bagliesi, T. Boccali, G. Broccolo, R. Castaldi, R. T. D'Agnolo, R. Dell'Orso, F. Fiori, L. Foà, A. Giassi, A. Kraan, F. Ligabue, T. Lomtadze, L. Martini, A. Messineo, F. Palla, F. Palmonari, A. Rizzi, A. T. Serban, P. Spagnolo, P. Squillacioti, R. Tenchini, G. Tonelli, A. Venturi, P. G. Verdini, L. Barone, F. Cavallari, D. D. Re, M. Diemoz, C. Fanelli, M. Grassi, E. Longo, P. Meridiani, F. Micheli, S. Nourbakhsh, G. Organtini, F. Pandolfi, R. Paramatti, S. Rahatlou, M. Sigamani, L. Soffi, N. Amapane, R. Arcidiacono, S. Argiro, M. Arneodo, C. Biino, C. Botta, N. Cartiglia, R. Castello, M. Costa, N. Demaria, A. Graziano, C. Mariotti, S. Maselli, E. Migliore, V. Monaco, M. Musich, M. M. Obertino, N. Pastrone, M. Pelliccioni, A. Potenza, A. Romero, M. Ruspa, R. Sacchi, V. Sola, A. Solano, A. Staiano, A. V. Pereira, S. Belforte, F. Cossutti, G. D. Ricca, B. Gobbo, M. Marone, D. Montanino, A. Penzo, A. Schizzi, S. G. Heo, T. Y. Kim, S.-K. Nam, S. Chang, J. H. Chung, D. H. Kim, G. N. Kim, D. J. Kong, H. Park, S.-R. Ro, D.-C. Son, T. Son, J. Y. Kim, Z. J. Kim, S. Song, H. Y. Jo, S. Choi, D. Gyun, B.-S. Hong, M. Jo, H. Kim, T. J. Kim, K. S. Lee, D. H. Moon, S. K. Park, E. Seo, M. Choi, S. Kang, H. Kim, J. H. Kim, C. Park, I. Park, S. Park, G. Ryu, Y. Cho, Y.-I. Choi, Y. K. Choi, J. Goh, M. S. Kim, E. Kwon, B. Lee, J. Lee, S. Lee, H. Seo, I. Yu, M. J. Bilinskas, I. Grigelionis, M. Janulis, A. Juodagalvis, H. Castilla-Valdez, E. D. L. Cruz-Burelo, I. H. de La Cruz, R. Lopez-Fernandez, R. M. Villalba, J. Martínez-Ortega, A. Sánchez-Hernández, L. M. Villasenor-Cendejas, S. C. Moreno, F. V. Valencia, H. A. S. Ibarguen, E. C. Linares, A. M. Pineda, M. A. Reyes-Santos, D. Krofcheck, A. J. Bell, P. H. Butler, R. Doesburg, S. Reucroft, H. Silverwood, M. Ahmad, M. I. Asghar, H. R. Hoorani, S. Khalid, W. A. Khan, T. Khurshid, S. Qazi, M. A. Shah, M. Shoaib, G. Brona, K. Bunkowski, M. Cwiok, W. Dominik, K. Doroba, A. Kalinowski, M. Konecki, J. Krolkowski, H. Bialkowska, B. Boimska, T. Frueboes, R. Gokieli, M. Górski, M. Kazana, K. Nawrocki, K. Romanowska-Rybinska, M. Szleper, G. Wrochna, P. Zalewski, N. Almeida, P. Bargassa, A. D. T. Mendes, P. Faccioli, P. G. F. Parracho, M. Gallinaro, P. Musella, J. Seixas, J. Varela, P. Vischia, I. Belotelov, M. Gavrilenko, I. Golutvin, I. Gorbunov, A. Kamenev, V. Karjavin, G. Kozlov, A. Lanev, A. Malakhov, P. Moisenz, V. Palichik, V. Perelygin, M. Savina, S. Shmatov, V. Smirnov, A. Volodko, A. Zarubin, S. Evstyukhin, V. Golovtsov, Y. Ivanov, V. Kim, P. Levchenko, V. Murzin, V. Oreshkin, I. Smirnov, V. Sulimov, L. Uvarov, S. Vavilov, A. Vorobyev, A. Vorobyev, Y. Andreev, A. Dermenev, S. Gninenko, N. Golubev, M. Kirsanov, N. Krasnikov, V. Matveev, A. Pashenkov, D. Tlisov, A. Toropin, V. Epshteyn, M. Erofeeva, V. Gavrilov, M. Kossov, N. Lychkovskaya, V. Popov, G. Safronov, S. Semenov, V. Stolin, E. Vlasov, A. Zhokin, A. Belyaev, E. Boos, V. Bunichev, M. Dubinin, L. Dudko, A. Ershov, A. Gribushin, V. Klyukhin, O. Kodolova, I. Loktin, A. Markina, S. Obraztsov, M. Perfilov, S. Petrushanko, A. Popov, L. Sarycheva, V. Savrin,

V. Andreev, M. Azarkin, I. Dremin, M. Kirakosyan, A. Leonidov, G. Mesyats, S. V. Rusakov, A. Vinogradov, I. Azhgirey, I. Bayshev, S. Bitioukov, V. Grishin, V. Kachanov, D. Konstantinov, A. Korablev, V. Krychkine, V. Petrov, R. Ryutin, A. Sobol, L. Tourtchanovitch, S. Troshin, N. Tyurin, A. Uzunian, A. Volkov, P. Adzic, M. Djordjevic, M. Ekmedzic, D. Krpic, J. Milosevic, M. Aguilar-Benitez, J. A. Maestre, P. Arce, C. Battilana, E. Calvo, M. Cerrada, M. C. Llatas, N. Colino, B. D. L. Cruz, A. D. Peris, C. D. Pardos, D. D. Vázquez, C. F. Bedoya, J. P. F. Ramos, A. Ferrando, J. Flix, M. C. Fouz, P. Garcia-Abia, O. G. Lopez, S. G. Lopez, J. M. Hernandez, M. I. Josa, G. Merino, J. P. Pelayo, I. Redondo, L. Romero, J. Santaolalla, M. S. Soares, C. Willmott, C. Albajar, G. Codispoti, J. F. de Trocóniz, J. Cuevas, J. F. Menendez, S. Folgueras, I. G. Caballero, L. L. Iglesias, J. P. Gomez, J. M. V. Garcia, J. A. B. Cifuentes, I. J. Cabrillo, A. Calderon, S.-H. Chuang, J. D. Campderros, M. Felcini, M. Fernandez, G. Gomez, J. G. Sanchez, C. Jorda, P. L. Pardo, A. L. Virto, J. Marco, R. Marco, C. M. Rivero, F. Matorras, F. J. M. Sanchez, T. Rodrigo, A. Y. Rodríguez-Marrero, A. Ruiz-Jimeno, L. Scodellaro, M. S. Sanudo, I. Vila, R. V. Cortabitarte, D. Abbaneo, E. Auffray, G. Auzinger, P. Baillon, A. Ball, D. Barney, C. Bernet, G. Bianchi, P. Bloch, A. Bocci, A. Bonato, H. Breuker, T. Camporesi, G. Cerminara, T. Christiansen, J. A. C. Perez, D. D'Enterria, A. D. Roeck, S. D. Guida, M. Dobson, N. Dupont-Sagorin, A. Elliott-Peisert, B. Frisch, W. Funk, G. Georgiou, M. Giffels, D. Gigi, K. Gill, D. Giordano, M. Giunta, F. Glege, R. G.-R. Garrido, P. Govoni, S. Gowdy, R. Guida, M. Hansen, P. Harris, C. Hartl, J. Harvey, B. Hegner, A. Hinzmann, V. Innocente, P. Janot, K. Kaadze, E. Karavakis, K. Kousouris, P. Lecoq, P. Lenzi, C. Lourenco, T. Maki, M. Malberti, L. Malgeri, M. Mannelli, L. Masetti, F. Meijers, S. Mersi, E. Meschi, R. Moser, M. U. Mozer, M. Mulders, E. Nesvold, M. Nguyen, T. Orimoto, L. Orsini, E. P. Cortezon, E. Perez, A. Petrilli, A. Pfeiffer, M. Pierini, M. Pimiä, D. Piparo, G. Polese, L. Quertenmont, A. Racz, W. Reece, J. R. Antunes, G. Rolandi, T. Rommerskirchen, C. Rovelli, M. Rovere, H. Sakulin, F. Santanastasio, C. Schäfer, C. Schwick, I. Segoni, S. Sekmen, A. Sharma, P. Siegrist, P. Silva, M. Simon, P. Sphicas, D. Spiga, M. Spiropulu, M. Stoye, A. Tsirou, G. I. Veres, J.-R. Vlimant, H. K. Wöhri, S. Worm, W. D. Zeuner, W. Bertl, K. Deiters, W. Erdmann, K. Gabathuler, R. Horisberger, Q. Ingram, H.-C. Kaestli, S. König, D. Kotlinski, U. Langenegger, F. Meier, D. Renker, T. Rohe, J. Sibille, L. Bäni, P. Bortignon, M.-A. Buchmann, B. Casal, N. Chanon, Z. Chen, A. Deisher, G. Dissertori, M. Dittmar, M. Dünser, J. Eugster, K. Freudreich, C. Grab, P. Lecomte, W. Lustermann, A. C. Marini, P. M. R. del Arbol, N. Mohr, F. Moortgat, C. Nägeli, P. Nef, F. Nessi-Tedaldi, L. Pape, F. Pauss, M. Peruzzi, F. J. Ronga, M. Rossini, L. Sala, A. K. Sanchez, A. Starodumov, B. Stieger, M. Takahashi, L. Tauscher, A. Thea, K. Theofilatos, D. Treille, C. Urscheler, R. Wallny, H. A. Weber, L. Wehrli, E. Aguiro, C. Amsler, V. Chiochia, S. D. Visscher, C. Favaro, M. I. Rikova, B. M. Mejias, P. Otiougova, P. Robmann, H. Snoek, S. Tupputi, M. Verzetti, Y.-H. Chang, K.-H. Chen, A. Go, C.-M. Kuo, S.-W. Li, W. Lin, Z.-K. Liu, Y.-J. Lu, D. Mekterovic, A. Singh, R. Volpe, S.-S. Yu,

P. Bartalini, P. Chang, Y.-H. Chang, Y.-W. Chang, Y. Chao, K.-F. Chen, C. Dietz, U. Grundler, G. W.-S. Hou, Y. Hsiung, K.-Y. Kao, Y.-J. Lei, R.-S. Lu, D. Majumder, E. Petrakou, X. Shi, J.-G. Shiu, Y.-M. Tzeng, M. Wang, A. Adiguzel, M. N. Bakirci, S. Cerci, C. Dozen, I. Dumanoglu, E. Eskut, S. Girgis, G. Gokbulut, I. Hos, E. E. Kangal, G. Karapinar, A. K. Topaksu, G. Onengut, K. Ozdemir, S. Ozturk, A. Polatoz, K. Sogut, D. S. Cerci, B. Tali, H. Topakli, L. N. Vergili, M. Vergili, I. V. Akin, T. Aliev, B. Bilin, S. Bilmis, M. Deniz, H. Gamsizkan, A. M. Guler, K. Ocalan, A. Ozpineci, M. Serin, R. Sever, U. E. Surat, M. Yalvac, E. Yildirim, M. Zeyrek, M. Deliomeroglu, E. Glmez, B. Isildak, M. Kaya, O. Kaya, S. Ozkorucuklu, N. Sonmez, K. Cankocak, L. Levchuk, F. Bostock, J. J. Brooke, E. Clement, D. Cussans, H. Flacher, R. Frazier, J. Goldstein, M. Grimes, G. P. Heath, H. F. Heath, L. Kreczko, S. Metson, D. M. Newbold, K. Nirunpong, A. Poll, S. Senkin, V. J. Smith, T. Williams, L. Bass, K. W. Bell, A. Belyaev, C. Brew, R. M. Brown, D. J. Cockerill, J. A. Coughlan, K. Harder, S. Harper, J. Jackson, B. W. Kennedy, E. Olaiya, D. Petyt, B. C. Radburn-Smith, C. Shepherd-Themistocleous, I. R. Tomalin, W. J. Womersley, R. Bainbridge, G. Ball, R. Beuselinck, O. Buchmuller, D. Colling, N. Cripps, M. Cutajar, P. Dauncey, G. Davies, M. D. Negra, W. Ferguson, J. Fulcher, D. Futyan, A. Gilbert, A. G. Bryer, G. Hall, Z. Hatherell, J. Hays, G. Iles, M. Jarvis, G. Karapostoli, L. Lyons, A.-M. Magnan, J. Marrouche, B. Mathias, R. Nandi, J. Nash, A. Nikitenko, A. Papageorgiou, J. Pela, M. Pesaresi, K. Petridis, M. Pioppi, D. M. Raymond, S. Rogerson, N. Rompotis, A. Rose, M. J. Ryan, C. Seez, P. Sharp, A. Sparrow, A. Tapper, M. V. Acosta, T. Virdee, S. Wakefield, N. Wardle, T. Whyntie, M. Barrett, M. Chadwick, J. Cole, P. R. Hobson, A. Khan, P. Kyberd, D. Leggat, D. Leslie, W. Martin, I. Reid, P. Symonds, L. Teodorescu, M. Turner, K. Hatakeyama, H. Liu, T. Scarborough, C. Henderson, P. Rumerio, A. Avetisyan, T. Bose, C. Fantasia, A. Heister, J. S. John, P. Lawson, D. Lazic, J. Rohlf, D. Sperka, L. Sulak, J. Alimena, S. Bhattacharya, D. Cutts, A. Ferapontov, U. Heintz, S. Jabeen, G. Kukartsev, G. Landsberg, M. Luk, M. Narain, D. Nguyen, M. Segala, T. Sinthuprasith, T. Speer, K. V. Tsang, R. Breedon, G. Breto, M. C. D. L. B. Sanchez, S. Chauhan, M. Chertok, J. Conway, R. Conway, P. T. Cox, J. Dolen, R. Erbacher, M. Gardner, R. Houtz, W. Ko, A. Kopecky, R. Lander, O. Mall, T. Miceli, R. Nelson, D. Pellett, B. Rutherford, M. Searle, J. Smith, M. Squires, M. Tripathi, R. V. Sierra, V. Andreev, D. Cline, R. Cousins, J. Duris, S. Erhan, P. Everaerts, C. Farrell, J. Hauser, M. Ignatenko, C. Plager, G. Rakness, P. Schlein, J. Tucker, V. Valuev, M. Weber, J. Babb, R. Clare, M. E. Dinardo, J. A. Ellison, J. W. Gary, F. Giordano, G. Hansson, G.-Y. Jeng, H. Liu, O. R. Long, A. Luthra, H. Nguyen, S. Paramesvaran, J. Sturdy, S. Sumowidagdo, R. Wilken, S. Wimpenny, W. Andrews, J. G. Branson, G. B. Cerati, S. Cittolin, D. Evans, F. Golf, A. Holzner, R. Kelley, M. Lebourgeois, J. Letts, I. Macneill, B. Mangano, J. Muelmenstaedt, S. Padhi, C. Palmer, G. Petrucciani, M. Pieri, R. Ranieri, M. Sani, V. Sharma, S. Simon, E. Sudano, M. Tadel, Y. Tu, A. Vartak, S. Wasserbaech, F. Wrthwein, A. Yagil, J. Yoo, D. Barge, R. Bellan, C. Campagnari, M. D'Alfonso, T. Danielson, K. Flowers, P. Geffert,

J. Incandela, C. Justus, P. Kalavase, S. A. Koay, D. Kovalskyi, V. Krutelyov, S. Lowette, N. Mccoll, V. Pavlunin, F. Rebassoo, J. Ribnik, J. Richman, R. Rossin, D. Stuart, W. To, C. West, A. Apresyan, A. Bornheim, Y. Chen, E. D. Marco, J. Duarte, M. Gataullin, Y. Ma, A. Mott, H. B. Newman, C. Rogan, V. Timciuc, P. Traczyk, J. Veverka, R. Wilkinson, Y. Yang, R.-Y. Zhu, B. Akgun, R. Carroll, T. Ferguson, Y. Iiyama, D. W. Jang, Y.-F. Liu, M. Paulini, H. Vogel, I. Vorobiev, J. P. Cumalat, B. R. Drell, C. Edelmaier, W. T. Ford, A. Gaz, B. Heyburn, E. L. Lopez, J. Smith, K. Stenson, K. Ulmer, S. R. Wagner, L. Agostino, J. Alexander, A. Chatterjee, N. Eggert, L. K. Gibbons, B. Heltsley, W. Hopkins, A. Khukhunaishvili, B. Kreis, N. Mirman, G. N. Kaufman, J. R. Patterson, A. Ryd, E. Salvati, W. Sun, W. D. Teo, J. Thom, J. Thompson, J. Vaughan, Y. Weng, L. Winstrom, P. Wittich, D. Winn, S. Abdullin, M. Albrow, J. Anderson, L. A. Bauerdick, A. Beretvas, J. Berryhill, P. C. Bhat, I. Bloch, K. Burkett, J. N. Butler, V. Chetluru, H. Cheung, F. Chlebana, V. D. Elvira, I. Fisk, J. Freeman, Y. Gao, D. Green, O. Gutsche, A. Hahn, J. Hanlon, R. M. Harris, J. Hirschauer, B. Hoberman, S. Jindariani, M. Johnson, U. Joshi, B. Kilminster, B. Klima, S. Kunori, S. Kwan, C. Leonidopoulos, D. Lincoln, R. Lipton, L. Lueking, J. Lykken, K. Maeshima, J. M. Marrafino, S. Maruyama, D. Mason, P. McBride, K. Mishra, S. Mrenna, Y. Musienko, C. Newman-Holmes, V. O'Dell, O. Prokofyev, E. Sexton-Kennedy, S. Sharma, W. J. Spalding, L. Spiegel, P. Tan, L. Taylor, S. Tkaczyk, N. V. Tran, L. Uplegger, E. W. Vaandering, R. Vidal, J. Whitmore, W. Wu, F. Yang, F. Yumiceva, J. C. Yun, D. Acosta, P. Avery, D. Bourilkov, M. Chen, S. Das, M. D. Gruttola, G. P. D. Giovanni, D. Dobur, A. Drozdetskiy, R. D. Field, M. Fisher, Y. Fu, I.-K. Furic, J. Gartner, J. Hugon, B. Kim, J. Konigsberg, A. Korytov, A. Kropivnitskaya, T. Kypreos, J. F. Low, K. Matchev, P. Milenovic, G. Mitselmakher, L. Muniz, R. Remington, A. Rinkevicius, P. Sellers, N. Skhirtladze, M. Snowball, J. Yelton, M. Zakaria, V. Gaultney, L. M. Lebolo, S. Linn, P. Markowitz, G. Martinez, J. L. Rodriguez, T. Adams, A. Askew, J. Bochenek, J. Chen, B. Diamond, S. V. Gleyzer, J. Haas, S. Hagopian, V. Hagopian, M. Jenkins, K. F. Johnson, H. Prosper, V. Veeraraghavan, M. Weinberg, M. M. Baarmand, B. Dorney, M. Hohlmann, H. Kalakhety, I. Vodopiyanov, M. R. Adams, I. M. Anghel, L. Apanasevich, Y. Bai, V. E. Bazterra, R. R. Betts, J. Callner, R. Cavanaugh, C. Dragoiu, O. Evdokimov, E. J. Garcia-Solis, L. Gauthier, C. E. Gerber, D. J. Hofman, S. Khalatyan, F. Lacroix, M. Malek, C. O'Brien, C. Silkworth, D. Strom, N. Varelas, U. Akgun, E. A. Albayrak, B. Bilki, K. Chung, W. Clarida, F. Duru, S. Griffiths, C. K. Lae, J.-P. Merlo, H. Mermekaya, A. Mestvirishvili, A. Moeller, J. Nachtman, C. R. Newsom, E. Norbeck, J. Olson, Y. Onel, F. Ozok, S. Sen, E. Tiras, J. Wetzel, T. Yetkin, K. Yi, B. A. Barnett, B. Blumenfeld, S. Bolognesi, D. Fehling, G. Giurgiu, A. Gritsan, Z. Guo, G. Hu, P. Maksimovic, S. Rappoccio, M. Swartz, A. Whitbeck, P. Baringer, A. Bean, G. Benelli, O. Grachov, R. P. K. Iii, M. Murray, D. Noonan, V. Radicci, S. Sanders, R. Stringer, G. Tinti, J. S. Wood, V. Zhukova, A.-F. Barfuss, T. Bolton, I. Chakaberia, A. Ivanov, S. Khalil, M. Makouski, Y. Marvin, S. Shrestha, I. Svintradze, J. Gronberg, D. Lange, D. Wright, D. Baden,

M. Boutemeur, B. Calvert, S. C. Eno, J. Gomez, N. J. Hadley, R. G. Kellogg, M. Kirn, T. Kolberg, Y. Lu, M. Marionneau, A. Mignerey, A. Peterman, K. Rossato, A. Skuja, J. Temple, M. Tonjes, S. C. Tonwar, E. Twedt, G. Bauer, J. Bendavid, W. Busza, E. Butz, I. A. Cali, M. Chan, V. Dutta, G. G. Ceballos, M. Goncharov, K. A. Hahn, Y. Kim, M. Klute, Y.-J. Lee, W. Li, P. D. Luckey, T. Ma, S. Nahn, C. Paus, D. Ralph, C. Roland, G. Roland, M. Rudolph, G. Stephans, F. Stöckli, K. Sumorok, K. Sung, D. Velicanu, E. A. Wenger, R. Wolf, B. Wyslouch, S. Xie, M. Yang, Y. Yilmaz, S. Yoon, M. Zanetti, S. Cooper, P. Cushman, B. Dahmes, A. D. Benedetti, G. Franzoni, A. Gude, J. Haupt, S.-C. Kao, K. Klapoetke, Y. Kubota, J. Mans, N. Pastika, R. Rusack, M. Sasseville, A. Singovsky, N. Tambe, J. Turkewitz, L. M. Cremaldi, R. Kroeger, L. Perera, R. Rahmat, D. A. Sanders, E. Avdeeva, K. Bloom, S. Bose, J. Butt, D. R. Claes, A. Dominguez, M. Eads, P. Jindal, J. Keller, I. Kravchenko, J. Lazo-Flores, H. Malbouisson, S. Malik, G. R. Snow, U. Baur, A. Godshalk, I. Iashvili, S. Jain, A. Kharchilava, A. Kumar, S. P. Shipkowski, K. Smith, G. Alverson, E. Barberis, D. Baumgartel, M. Chasco, J. Haley, D. Trocino, D. Wood, J. Zhang, A. Anastassov, A. Kubik, N. Mucia, N. Odell, R. A. Ofierzynski, B. Pollack, A. Pozdnyakov, M. H. Schmitt, S. Stoynev, M. Velasco, S. Won, L. Antonelli, D. Berry, A. Brinkerhoff, M. Hildreth, C. Jessop, D. J. Karmgard, J. Kolb, K. Lannon, W. Luo, S. Lynch, N. Marinelli, D. M. Morse, T. Pearson, R. Ruchti, J. Slaunwhite, N. Valls, J. Warchol, M. Wayne, M. Wolf, J. Ziegler, B. Bylsma, L. S. Durkin, C. Hill, R. Hughes, P. Killewald, K. Kotov, T.-Y. Ling, D. Puigh, M. Rodenburg, C. Vuosalo, G. Williams, B. L. Winer, N. Adam, E. Berry, P. Elmer, D. Gerbaudo, V. Halyo, P. Hebda, J. Hegeman, A. Hunt, E. Laird, D. L. Pegna, P. Lujan, D. Marlow, T. Medvedeva, M. Mooney, J. Olsen, P. Piroué, X. Quan, A. Raval, H. Saka, D. Stickland, C. Tully, J. S. Werner, A. Zurenski, J. G. Acosta, E. Brownson, X. T. Huang, A. Lopez, H. Mendez, S. Oliveros, J. E. R. Vargas, A. Zatserklyaniy, E. Alagoz, V. E. Barnes, D. Benedetti, G. Bolla, D. Bortoletto, M. D. Mattia, A. Everett, Z. Hu, M. Jones, O. Koybasi, M. Kress, A. T. Laasanen, N. Leonardo, V. Maroussov, P. Merkel, D. H. Miller, N. Neumeister, I. Shipsey, D. Silvers, A. Svyatkovskiy, M. V. Marono, H. D. Yoo, J. Zablocki, Y. Zheng, S. Guragain, N. Parashar, A. Adair, C. Boulahouache, V. Culpov, K. M. Ecklund, F. J. Geurts, B. P. Padley, R. Redjimi, J. Roberts, J. Zabel, B. Betchart, A. Bodek, Y. S. Chung, R. Covarelli, P. de Barbaro, R. Demina, Y. Es-haq, A. Garcia-Bellido, P. Goldenzweig, Y. Gotra, J. Han, A. Harel, S. Korjenevski, D. C. Miner, D. Vishnevskiy, M. Zielinski, A. Bhatti, R. Ciesielski, L. Demortier, K. Goulianios, G. Lungu, S. Malik, C. Mesropian, S. Arora, A. Barker, J. P. Chou, C. Contreras-Campana, E. Contreras-Campana, D. Duggan, D. Ferencek, Y. Gershstein, R. Gray, E. Halkiadakis, D. Hidas, D. Hits, C. Kilic, A. Lath, S. Panwalkar, M. Park, R. Patel, V. Rekovic, A. Richards, J. Robles, K. Rose, S. Salur, S. Schnetzer, C. Seitz, S. Somalwar, R. Stone, S. Thomas, G. Cerizza, M. Hollingsworth, S. Spanier, Z.-C. Yang, A. York, R. Eusebi, W. Flanagan, J. Gilmore, T. Kamon, V. Khotilovich, R. Montalvo, I. Osipenkov, Y. Pakhotin, A. Perloff, J. Roe, A. Safonov, T. Sakuma, S. Sengupta, I. Suarez, A. Tatarinov, D. Toback, N. Akchurin,

- J. Damgov, P. R. Dudero, C. Jeong, K. Kovitanggoon, S. W. Lee, T. Libeiro, Y. Roh, I. Volobouev, E. Appelt, D. Engh, C. Florez, S. Greene, A. Gurrola, W. Johns, P. Kurt, C. Maguire, A. Melo, P. Sheldon, B. Snook, S. Tuo, J. Velkovska, M. W. Arenton, M. Balazs, S. Boutle, B. Cox, B. Francis, J. Goodell, R. Hirosky, A. Ledovskoy, C. Lin, C. Neu, J. Wood, R. Yohay, S. Gollapinni, R. Harr, P. E. Karchin, C. K. K. Don, P. Lamichhane, A. Sakharov, M. Anderson, M. Bachtis, D. Belknap, L. Borrello, D. Carlsmith, M. Cepeda, S. Dasu, L. Gray, K. S. Grogg, M. Grothe, R. Hall-Wilton, M. Herndon, A. Hervé, P. Klabbers, J. Klukas, A. Lanaro, C. Lazaridis, J. Leonard, R. Loveless, A. Mohapatra, I. Ojalvo, G. A. Pierro, I. Ross, A. Savin, W. H. Smith, and J. Swanson, *Search for leptonic decays of W' bosons in pp collisions at $\sqrt{s} = 7$ TeV*, *JHEP* **08** (2012) 023, [arXiv:1204.4764].
- [200] A. D. Martin, W. J. Stirling, R. S. Thorne, and G. Watt, *Parton distributions for the LHC*, *Eur. Phys. J.* **C63** (2009) 189–285, [arXiv:0901.0002].
- [201] HyperCP Collaboration, C. White, *Results from the HyperCP experiment (FNAL E871)*, *AIP Conf. Proc.* **917** (2007) 330–337.